Connecting Common Ratio and Common Consequence Preferences*

Christina McGranaghan Kirby Nielsen Ted O'Donoghue
Jason Somerville Charles D. Sprenger

February 13, 2026

Abstract

Common ratio and common consequence effects are two foundational deviations from expected utility (EU). Most non-EU models treat them as global preference features, yet there has been little experimental exploration of parameters. Moreover, the two effects are typically analyzed independently despite their natural link through mixture attitudes. We empirically characterize combinations of preferences across the parameter space, documenting new regularities that are inconsistent with leading non-EU models. Finding no prominent model that can explain these regularities, we propose a model of "upside potential" motivated by our results.

*McGranaghan: Department of Applied Economics and Statistics, University of Delaware, email: cmcgran@udel.edu; Nielsen: Division of the Humanities and Social Sciences, California Institute of Technology, email: kirby@caltech.edu; O'Donoghue: Department of Economics, Cornell University, email: edo1@cornell.edu; Somerville: University of California Santa Barbara, email: jasonsomerville@ucsb.edu; Sprenger: Division of the Humanities and Social Sciences, California Institute of Technology, email: sprenger@caltech.edu. For helpful comments and suggestions, we thank Doug Bernheim, Drew Fudenberg, Shengwu Li, and seminar participants at Chapman University, University of Zurich, University of Pittsburgh, Lehigh University, Stanford University, University of California at Berkeley, University of California at Davis, University of California at Los Angeles, University of California at Santa Barbara, University of Southern California, Ohio State University, the Max Planck Institute for Research on Collective Goods, the 2023 Stanford Institute for Theoretical Economics, the 2023 North American Meeting of the Economic Science Association, and the 2023 Spring Behavioral & Experimental Economics Research Conference. Supporting analysis and additional design details can be found in the Online Appendix. The experiment reported in this paper was preregistered in the AEA RCT Registry in August 2022, under the ID AEARCTR-0009974. The experiment was reviewed and granted an exemption by the Institutional Review Board at the California Institute of Technology under protocol number IR21-2073.

1 Introduction

The common ratio effect (CRE) and the common consequence effect (CCE) are two prominent deviations from expected utility (EU). These effects were first proposed as thought experiments by Allais (1953) and served as important counterexamples against EU as a positive model of behavior. They were later popularized by Kahneman and Tversky (1979), who broadened their scope by treating them as foundational features of preferences that motivate the shape of the probability weighting function in prospect theory. Subsequent work found empirical support for both effects, and researchers have developed many non-EU models of decision-making to accommodate them.

Despite the widespread acceptance of the CRE and CCE as stylized facts, the existing evidence suffers from two major limitations. First, while behavioral theories often assume these effects represent global features of preferences, the experimental evidence for each comes from a narrow set of experimental parameters, and thus there is little empirical justification for such global assumptions. Second, previous studies have almost always analyzed the CRE and CCE independently. However, there is a natural connection between them that links both to a third property of risk preferences that has been studied in the literature: attitudes toward probabilistic mixtures of lotteries. Examining these three features of preferences together through connected problems provides a more complete picture of risk attitudes and an improved empirical base for assessing models of risk preferences.

In this paper, we examine connected common ratio (CR), common consequence (CC), and mixture (MX) problems across a broad range of experimental parameters, including many not previously explored in the literature. For parameters close to those in the canonical CR and CC problems, we observe a CRE and a CCE, consistent with conventional findings. However, across much of the parameter space, we find a modest CRE, a pronounced *reverse* CCE, and a robust attraction to probabilistic mixtures. This prominent new regularity in risk attitudes is inconsistent with both EU and leading non-EU models. Because our empirical results conflict sharply with existing models, we propose a theoretical model of "upside potential" that is motivated by our results.

In Section 2, we formally demonstrate the natural connection between CR, CC, and MX problems and how it can yield insight for models of risk preferences. We then leverage this connection to summarize and reanalyze the existing experimental literature. Allais (1953) first introduced the CR problem, but the canonical version comes from Kahneman and Tversky (1979) and presents individuals with the following pair of choice tasks:[1]

***AB* Choice**: Lottery A: 100 percent chance of \$3000 vs. Lottery B: 80 percent chance of \$4000

***CD* Choice**: Lottery C: 25 percent chance of \$3000 vs. Lottery D: 20 percent chance of \$4000

[1]Throughout the paper, we suppress the probability of \$0. For instance, in Lottery B, the remaining probability of 20 percent is on a \$0 outcome.

In this example, lotteries C and D are constructed from lotteries A and B by scaling down the probabilities of the non-zero outcomes by a *common ratio* of 0.25. The canonical version of the CCE is from Allais (1953) and presents participants with the following pair of choice tasks:

$\boldsymbol{AB'}$ **Choice**:	Lottery A:	100 percent chance of \$1M	vs.	Lottery B':	89 percent chance of \$1M 10 percent chance of \$5M
$\boldsymbol{CD}$ **Choice**:	Lottery C:	11 percent chance of \$1M	vs.	Lottery D:	10 percent chance of \$5M

Lotteries C and D are constructed from lotteries A and B' by changing the *common consequence* of an 89 percent chance of \$1M into an 89 percent chance of \$0.

EU predicts that CR and CC manipulations cannot reverse an individual's preference. In contrast, the CRE and CCE describe systematic empirical patterns of people appearing more risk-tolerant in the CD problems relative to the AB and AB' problems, respectively. As a result, the aggregate share of individuals choosing A is larger than the share choosing C in both problems.

The prior literature contains many experiments on the CRE and CCE. Two recent meta-studies by Blavatskyy et al. (2023) on the CRE and Blavatskyy et al. (2022) on the CCE report a total of 224 experiments (143 CRE and 81 CCE) across 48 studies. They document that both effects are sensitive to various design choices, including experimental parameters. We leverage their data to highlight two further points. First, these experiments cover a limited set of experimental parameters that are dominated by the canonical examples in Kahneman and Tversky (1979) and Allais (1953). Second, these experiments have almost always studied the CRE and CCE as independent phenomena—indeed, of the 48 studies, only 10 contain both CRE and CCE experiments, and virtually all of these study the two problems separately.

By studying the CRE and CCE as independent phenomena, the prior literature has neglected a natural connection between them that can provide a more complete picture of the underlying nature of risk attitudes and an improved empirical base for assessing models of risk preferences. While this connection was noted in early theoretical work by Chew and MacCrimmon (1979) and both theoretically and experimentally by Chew and Waller (1986), it remains largely absent from the CRE and CCE literature. To illustrate this connection, consider the following three choice tasks:

$\boldsymbol{AB}$ **Choice**:	Lottery A:	100 percent chance of \$27	vs.	Lottery B:	90 percent chance of \$35
$\boldsymbol{AB'}$ **Choice**:	Lottery A:	100 percent chance of \$27	vs.	Lottery B':	9 percent chance of \$35 90 percent chance of \$27
$\boldsymbol{CD}$ **Choice**:	Lottery C:	10 percent chance of \$27	vs.	Lottery D:	9 percent chance of \$35

The combination of the AB and CD choices constitutes a CR problem while the combination of

the AB' and CD choices constitutes a CC problem. Thus, three tasks are sufficient to study both problems. This formulation also highlights a third comparison: AB versus AB'. Since B' is a probabilistic mixture of lotteries A and B (in this case 90 percent A and 10 percent B), this third comparison reveals attitudes toward probabilistic mixtures. We refer to the combination of the AB and AB' choices as a *mixture (MX)* problem, where EU predicts that people should be neutral to mixtures. We refer to a finding of people appearing more risk-tolerant in the AB' problem relative to the AB problem as a mixture effect (MXE). In other words, the MXE pattern suggests that individuals prefer the probabilistic mixture of A and B to both A and B individually.[2]

We refer to the combination of an AB task, an AB' task, and a CD task as a *connected CR-CC-MX problem*. We characterize such problems with two parameters. The first is the probability of the non-zero outcome in lottery B, which we denote by p (0.9 in the example above). The second parameter, which we denote by r, is both the common ratio that converts A and B into C and D and the mixing weight that generates B' from A and B (0.1 in the example above).[3]

Each connected CR-CC-MX problem allows us to simultaneously identify three features of underlying preferences for a given (p, r) parameter combination: whether people have a *common ratio preference (CRP)*, a *common consequence preference (CCP)*, and a *mixture preference (MXP)*. In each case, a person might have that preference, its reverse (which we label RCRP, RCCP, or RMXP), or be neutral to the manipulation (which we label ⃠CRP, ⃠CCP, and ⃠MXP).[4] Existing models of risk preferences make predictions for the empirical patterns we ought to observe. EU implies neutrality to all three manipulations and therefore pattern ⃠CRP-⃠CCP-⃠MXP. In Section 2.2, we delineate the predictions from several leading parameterized non-EU models. Under each model's common assumptions, all predict a CRP and a CCP, and most further predict either an RMXP or an ⃠MXP; that is, people either dislike or are neutral to mixtures. Furthermore, in most cases these models predict these patterns apply globally and are independent of (p, r). We can test these predictions using connected CR-CC-MX problems.

While it is possible to study CR, CC, and MX problems using binary choice tasks like those above—as most of the prior literature, including Chew and Waller (1986), does—this approach can yield biased conclusions in the presence of choice noise. In McGranaghan et al. (2024), we build on prior work highlighting this potential bias in CRE experiments and demonstrate how paired valuation tasks can provide unbiased inference under these circumstances. Therefore, our primary analysis focuses on valuation tasks in the form of stated indifference points implemented using multiple price

[2]The MX problem relates to tests of betweenness and to work on deliberate randomization; we discuss these literatures in Section 2.4. We also highlight that our connected problems examine one specific type of MX problem in which a binary lottery is mixed with a certain lottery, and thus our analysis will not provide a full characterization of people's attitudes toward mixtures.

[3]The canonical version of the CRE uses $p = 0.8$ and $r = 0.25$, and the canonical version of the CCE uses $p = 10/11$ and $r = 0.11$.

[4]We adopt the "reverse" terminology from the literature, which dates at least to Blavatskyy (2010).

lists. For example, in a CD valuation task analogous to the CD choice task above, a participant selects the amount to be received with a 9 percent chance that makes them indifferent to a 10 percent chance of \$27. To complement the primary analysis, we conduct a secondary analysis using carefully selected choice tasks. Both methods yield the same conclusions about average behavior across the parameter space.[5] Moreover, we document strong links between valuations and choices, indicating that the patterns we find meaningfully reflect underlying preferences.

In Section 3, we describe the details of our experimental design. We recruit 2,102 participants through Prolific for an online experiment. In stage 1 of the experiment, we elicit a series of valuations. Each participant provides AB, AB', and CD valuations for four different (p, r) combinations. Across all of our participants, we implement 20 different (p, r) combinations covering a wide range of the parameter space. In stage 2, the same participants complete binary choice tasks linked to their stage 1 valuation tasks, facilitating direct comparison between the patterns of behavior emerging in valuations and choices.

Section 4 describes our main results. We first study aggregate behavior by analyzing mean valuations across all participants. We find that the three features of preferences react differently to changes in the experimental parameters. CRP is highly sensitive to the common ratio r: It increases as r decreases, and disappears entirely for the two largest values of r in our design. In contrast, CCP is highly sensitive to the high-prize probability p: It decreases as p decreases, transitioning from a small CCP for large p to a substantial RCCP for small p. Finally, we find a robust MXP that increases as either r or p decreases. Taken together, these results yield two striking regularities in the combinations of CR-CC-MX preferences. On one hand, for parameters close to the canonical CR and CC examples (large p and small r), we find CRP and CCP with limited MXP, consistent with the conventional wisdom. On the other hand, across much of the parameter space, we find a robust pattern of CRP-RCCP-MXP, which is inconsistent with both EU and leading non-EU models. The exact same patterns emerge when analyzing the aggregate paired binary choice data, albeit with more noise.

We next analyze behavior at the individual level. Using our valuation data, we examine the distribution of behavior across the 27 possible combinations of CR-CC-MX patterns, where a person might exhibit the effect, its reverse, or no effect for each. We find that mean behavior masks substantial heterogeneity. The modal individual pattern aligns with the CRP-RCCP-MXP combination that frequently appears in mean preferences, but it accounts for only 15 percent of observations. Of

[5]While not the main focus of this paper, we describe in Section 2.5 how the inference problem described in McGranaghan et al. (2024) becomes even more severe when comparing three binary choice tasks, as in a connected CR-CC-MX problem. Section 4.2 presents empirical evidence for the relevance of these biased inference problems for our CR, CC, and MX choice tasks. At the same time, we describe in Sections 4.2 and 4.5 why our choice data yield the same conclusions as our valuations data despite the potential inference problems: Based on pilot data, we were able to select experimental parameters that produced a set of paired choice problems that mitigate aggregate bias by balancing instances in which choice noise would lead to positive and negative bias.

course, some of this variability in behavior at the individual level is likely due to noise. Because our design elicits multiple measures of the same valuation within subject, we can structurally decompose the variability in valuations into an underlying preference component and a noise component. We estimate that roughly half of the variability in valuations is due to preference heterogeneity. The resulting distribution of preferences still yields a modal pattern of CRP-RCCP-MXP, but also involves substantial heterogeneity. Finally, we show that heterogeneity in preferences measured from valuations strongly predicts choice behavior, suggesting that choices and valuations capture some common information about the underlying preferences of interest.

Taken together, our experimental results pose an important challenge to existing models of risk preferences. In simple terms, our results confirm some earlier results that suggest the CRE and CCE are not global phenomena, whereas prominent models of risk preferences either assume or imply that they are. More unique to our data is the prevalence of the pattern CRP-RCCP-MXP, which cannot be accommodated by any of the leading parameterized non-EU models.

Because our experimental results are so at odds with existing models, in Section 5 we attempt to develop a model to rationalize our data. Our approach is motivated by our finding that people have a robust attraction to probabilistic mixtures between a certain payment and a binary lottery with a higher expected value. This finding suggests that, compared to having the certain amount, people prefer to mix in some, but not all, of the binary lottery. To accommodate this preference, we posit that people value lotteries according to their "upside potential," trading off the total probability of winning something against an expected valuation of those winnings—which turns out to be a previously unstudied version of quadratic utility (Machina, 1982; Chew et al., 1991). Encouragingly, this approach to accommodating MXP also explains the modal CRP-RCCP-MXP pattern we observe, and successfully predicts some more nuanced patterns in our data. Expanding beyond our data, we derive more general predictions of the model for indifference curves in a Marschak-Machina triangle—which offers additional testable implications for future research—and show how the model is consistent with the reliable finding of risk tolerance for small probabilities and risk aversion for large probabilities when eliciting certainty equivalents for binary lotteries (as in Tversky and Kahneman, 1992). Though the psychology of upside potential appears a promising way to organize our data, we also discuss the limitations of the model, and hope that future work can expand and improve upon the initial ideas we propose.

Finally, in Section 6 we discuss some broader implications of our analysis, including connections between our results and the recent literature on deliberate randomization and the underlying mechanisms for such phenomena (Cerreia-Vioglio et al., 2015; Agranov and Ortoleva, 2017; Dwenger et al., 2018; Feldman and Rehbeck, 2022; Agranov and Ortoleva, 2023; Agranov et al., 2023).

Our exploration of the connections between CRP, CCP, and MXP is similar in spirit to exercises by Dean and Ortoleva (2019), Chapman et al. (2023), and Stango and Zinman (2023), who study the

correlations between decision-making phenomena across a range of domains including risk, ambiguity, updating, and intertemporal choice. However, our contribution differs in two important ways. First, our work is motivated by structural connections between the three features of risk preferences, and these connections provide a framework for using the empirical patterns that emerge to assess models of risk preferences. In contrast, the correlational analyses above are challenging to interpret because it is unclear how a link between, say, present bias and ambiguity aversion might relate to specific models of choice. Second, one of our primary goals is to study how the three features of risk preferences vary across the parameter space, which is crucial to assessing the performance of different models. In contrast, the papers cited above use a limited number of measures for each phenomena, often at canonical parameterizations. For example, Dean and Ortoleva (2019) have a single measure of the CRE and a single measure of the CCE, each at its canonical parameter values. While such exercises are valuable for documenting broad correlations in classic phenomena across many domains, this approach provides limited information for assessing different models.

Finally, we note the potential benefits of broader exploration of parameter spaces in other domains and the richer appreciation of preferences that might emerge from these exercises. Within the domain of risky choice, our exploration yields a new empirical foundation upon which to theorize. We hope such explorations in other domains will be similarly useful.

2 Background and Prior Literature

The prior literature has almost always studied the CRE and CCE as separate problems, and for each problem, it has focused on a limited set of parameters. In contrast, we study connected problems for a broad set of parameters. In this section, we formalize the connection and highlight the value of investigating connected problems, which is reminiscent of—but expands upon—the exercise in Chew and MacCrimmon (1979) and Chew and Waller (1986). We then describe in detail the limitations of the prior literature.

2.1 Connected CR-CC-MX Problems

For fixed prizes $H > M > 0$, consider three binary choice tasks parameterized by the vector (p, r), where $p, r \in (0, 1)$:

AB Choice Task: choose Lottery $A \equiv (M, 1)$ or Lottery $B \equiv (H, p)$

AB' Choice Task: choose Lottery $A \equiv (M, 1)$ or Lottery $B' \equiv (H, pr; M, 1 - r)$

CD Choice Task: choose Lottery $C \equiv (M, r)$ or Lottery $D \equiv (H, pr)$

The combination of an AB task and a CD task represents a CR Problem. According to EU, scaling down the probabilities of the non-zero outcomes by the common ratio r should leave preferences unchanged: Anyone who prefers A over B should also prefer C over D, and anyone who prefers B over A should also prefer D over C. In contrast, the CRE pattern involves choosing lotteries A and D; that is, people are more risk-tolerant in the CD task than in the AB task.

The combination of an AB' task and a CD task represents a CC Problem. According to EU, shifting the common consequence of a $1-r$ chance of $\$M$ into a $1-r$ chance of \$0 should leave preferences unchanged: Anyone who prefers A over B' should also prefer C over D, and anyone who prefers B' over A should also prefer D over C. In contrast, the CCE pattern involves choosing lotteries A and D; that is, people are more risk-tolerant in the CD task than in the AB' task.

Hence, for a given H and M, each (p, r) generates a connected pair of CR and CC problems. Panel A of Figure 1 illustrates one such connected pair by plotting the five lotteries in a Marschak-Machina probability triangle for a particular (p, r). Each problem separately involves comparing two choice sets on parallel line segments. Connecting the problems involves placing the AB and AB' choice sets on the same line and using the same CD choice for both problems.

Panel A also highlights that lottery B' is a probabilistic mixture of lotteries A and B, with weights $(1-r)$ and r, and suggests a third comparison of two parallel choice sets: AB versus AB'. This comparison reveals people's attitudes toward probabilistic mixtures of a binary lottery and a certain lottery, and thus we refer to the combination of the AB and AB' choices as a *mixture (MX)* problem. According to EU, people should be neutral to probabilistic mixtures, and thus the expected utility of a probabilistic mixture of A and B should be in between the expected utilities of A and B. Hence, anyone who prefers A over B should also prefer A over B', and anyone who prefers B over A should also prefer B' over A. In contrast, we refer to the pattern of choosing A over B and B' over A as a mixture effect (MXE) since people are appearing more risk-tolerant in the AB' problem relative to the AB problem—i.e., they appear to like the probabilistic mixture.

Hence, for a given (p, r), we refer to the combination of an AB task, an AB' task, and a CD task as a *connected CR-CC-MX problem*.

2.2 Why Study Connected Problems?

Studying connected problems allows researchers to obtain richer quantitative data that provide a stronger empirical base for assessing models of risk preferences. In particular, it reveals patterns in how people simultaneously react to CR, CC, and MX manipulations, allowing us to jointly study three key characteristics of underlying preferences.

To formalize these preferences, if we assume monotonicity, then for a fixed (p, r, M) there exist three underlying indifference values h^*_{AB}, $h^*_{AB'}$, and h^*_{CD} that satisfy:

Figure 1: Connected Problems and Parameter Coverage in the Prior CR and CC Literature

Panel A: CR, CC, and MX in a MM Triangle

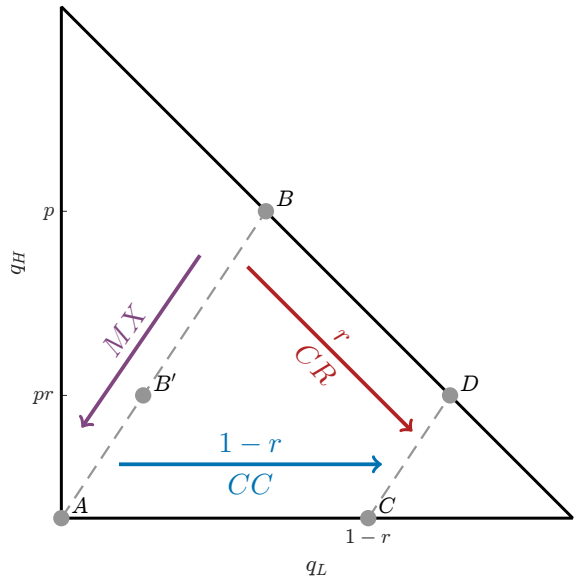

Panel B: CR and CC Parameter Coverage

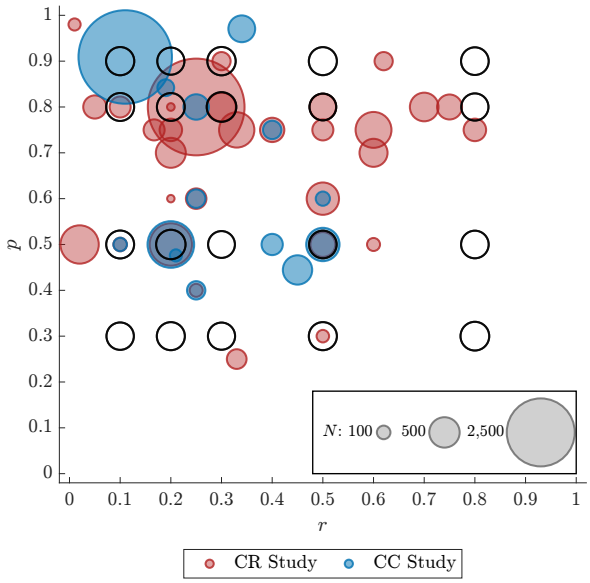

Note: Panel A depicts a Marschak-Machina (MM) triangle for lotteries with outcomes H, M, and 0 and associated probabilities q_H, q_M, and q_L. Paired binary choices $A \equiv (M, 1)$ vs. $B \equiv (H, p)$ and $C \equiv (M, r)$ vs. $D \equiv (H, pr)$ represent a common ratio (CR) problem. Paired binary choices A vs. $B' \equiv (H, pr; M, 1-r)$ and C vs. D represent a common consequence (CC) problem. Paired binary choices A vs. B and A vs. B' represent a mixture (MX) problem. Panel B depicts the experimental parameters (p, r) used in the prior literature and our paired-choice experiments. Red dots denote the CR experiments reported in Blavatskyy et al. (2023). Blue dots denote the CC experiments reported in Blavatskyy et al. (2022). Black open circles denote paired-choice parameters in stage 2 of our study. The size of each circle reflects the total number of participants who completed a paired choice task with that parameter.

- Prefer A over B if and only if $H < h^*_{AB}$,
- Prefer A over B' if and only if $H < h^*_{AB'}$, and
- Prefer C over D if and only if $H < h^*_{CD}$.

Note that, for each, a smaller h^* implies increased risk tolerance.

A person's reaction to a CR manipulation is captured by $\Delta^*_{CR} \equiv h^*_{AB} - h^*_{CD}$, and their reaction to a CC manipulation is captured by $\Delta^*_{CC} \equiv h^*_{AB'} - h^*_{CD}$. The standard effects suggest greater risk tolerance in the CD choice than in either the AB or AB' choice, which implies $\Delta^*_{CR} > 0$ and $\Delta^*_{CC} > 0$. We label these two features of preferences *common ratio preference (CRP)* and *common consequence preference (CCP)*. We label $\Delta^*_{CR} < 0$ and $\Delta^*_{CC} < 0$ as *reverse common ratio preference (RCRP)* and *reverse common consequence preference (RCCP)*. A person's attitudes toward probabilistic mixtures are captured by $\Delta^*_{MX} \equiv h^*_{AB} - h^*_{AB'}$. If a person likes mixtures, they will have $\Delta^*_{MX} > 0$, which we label a *mixture preference (MXP)*. If they dislike mixtures, they will have $\Delta^*_{MX} < 0$, which we label a *reverse mixture preference (RMXP)*.[6]

[6]Building on our comment in footnote 2, we note that Δ^*_{MX} only captures attitudes towards mixtures in which a binary lottery is mixed with a certain lottery. The decision-theory literature often considers global mixture attitudes,

With this notation, EU implies $\Delta^*_{CR} = \Delta^*_{CC} = \Delta^*_{MX} = 0$. Over the years, researchers have developed various non-EU models, and these models make predictions for Δ^*_{CR}, Δ^*_{CC}, and Δ^*_{MX}. In Appendix B, we derive these predictions for several prominent parameterized models. In Table 1, we summarize the predictions from each model as a function of the model's key parameter, and also highlight the focal range for that parameter (i.e., the range in which that parameter is typically assumed to lie).

Table 1: Predictions of Leading Non-EU Models for Δ^*_{CR}, Δ^*_{CC}, and Δ^*_{MX}

Model and Structure	Parameter Range	Predictions
Original Prospect Theory (Kahneman and Tversky, 1979) with $\pi(q) = q^\delta / \left[q^\delta + (1-q)^\delta\right]^{\frac{1}{\delta}}$ $U(B) = \pi(p)v(H)$	$\delta \in (0.279, 1)^\dagger$	$\Delta^*_{CR} > 0,\ \Delta^*_{CC} > 0,\ \Delta^*_{MX} \gtreqless 0$
	$\delta > 1$	$\Delta^*_{CR} < 0,\ \Delta^*_{CC} > 0,\ \Delta^*_{MX} < 0$
Cumulative Prospect Theory (Tversky and Kahneman, 1992) with $\pi(q) = q^\delta / \left[q^\delta + (1-q)^\delta\right]^{\frac{1}{\delta}}$ $U(B) = \pi(p)v(H)$	$\delta \in (0.279, 1)^\dagger$	$\Delta^*_{CR} > 0,\ \Delta^*_{CC} > 0,\ \Delta^*_{MX} \gtreqless 0$
	$\delta > 1$	$\Delta^*_{CR} < 0,\ \Delta^*_{CC} \gtreqless 0,\ \Delta^*_{MX} \gtreqless 0$
Loss Aversion under CPE (Kőszegi and Rabin, 2007)	$\Lambda \in (0, 1)^\dagger$	$\Delta^*_{CR} > 0,\ \Delta^*_{CC} > 0,\ \Delta^*_{MX} < 0$
$U(B) = pu(H) - p(1-p)\Lambda u(H)$	$\Lambda \in (-1, 0)$	$\Delta^*_{CR} < 0,\ \Delta^*_{CC} < 0,\ \Delta^*_{MX} > 0$
Disappointment Aversion (Bell, 1985)	$\beta \in (0, 1)^\dagger$	$\Delta^*_{CR} > 0,\ \Delta^*_{CC} > 0,\ \Delta^*_{MX} < 0$
$U(B) = pu(H) - p(1-p)\beta u(H)$	$\beta \in (-1, 0)$	$\Delta^*_{CR} < 0,\ \Delta^*_{CC} < 0,\ \Delta^*_{MX} > 0$
Disappointment Aversion (Gul, 1991)	$\beta > 0^\dagger$	$\Delta^*_{CR} = \Delta^*_{CC} > 0,\ \Delta^*_{MX} = 0$
$U(B) = \dfrac{p}{1 + \beta(1-p)} u(H)$	$\beta \in (-1, 0)$	$\Delta^*_{CR} = \Delta^*_{CC} < 0,\ \Delta^*_{MX} = 0$

Notes: Table presents predictions of each model for the sign of Δ^*_{CR}, Δ^*_{CC}, and Δ^*_{MX}; see Appendix B for formal derivations. To give a sense of the parametric structure of each model, the first column provides the utility from lottery $B \equiv (H, p)$. For each model, the sign predictions are independent of the utility for outcomes ($v(x)$ or $u(x)$), and thus depend on the single listed parameter. Focal ranges for a model's key parameter are indicated by †, but the table also reports predictions for other ranges where the model is still well-defined but reflects a different psychology. All predictions hold for all $(p, r) \in (0, 1)^2$, except $\gtreqless$ indicates cases where the predictions depend on (p, r). Note that original prospect theory and cumulative prospect theory differ only for lottery B' among our set of five lotteries, and the same applies for Kőszegi-Rabin loss aversion under CPE (Choice-Acclimating Personal Equilibrium) and Bell disappointment aversion.

Table 1 demonstrates how connected CR-CC-MX problems can be used to assess models of non-EU risk preferences. In particular, it reveals three important features. First, each model predicts a CRP and CCP for the focal range of its key parameter. This commonality reflects that the CRE and CCE are typically seen as stylized facts that either motivate non-EU models or serve as a litmus test

using the label "quasi-convex preferences" to refer to preferences with an attraction to mixtures of any two lotteries. Note, then, that while quasi-convex preferences imply an MXP (i.e., $\Delta^*_{MX} > 0$), an MXP does not imply a person has quasi-convex preferences.

for those models. Second, the models differ in their predictions for mixture preferences. However, for the focal range of each model's key parameter, the prediction is either mixture neutrality or RMXP, except for the two variants of prospect theory where the prediction can go either way depending on the specific (p, r) combination. Third, when we also consider cases where the models' key parameters lie outside their focal ranges, the set of predicted patterns expands, but none of the models permit the pattern CRP, RCCP, and MXP that features prominently in our data.[7]

Two final observations are relevant for linking our data on connected CR-CC-MX problems to non-EU models. First, with a few noted exceptions, the directional predictions in Table 1 hold for any (p, r) combination—that is, these models predict preference patterns that are invariant to (p, r).[8] Second, of the models covered by Table 1, the two prospect theory models have some scope to expand their predictions by permitting alternative functional forms for the probability weighting function $\pi(q)$. We assess in Appendix G whether that additional flexibility can explain the patterns in our data.

2.3 Limitations of the Prior Literature on the CRE and CCE

There is a large empirical literature on both the CRE and CCE (and also a smaller empirical literature on the MXE that we discuss in Section 2.4). To illustrate the limitations of the prior evidence on the CRE and CCE, we reanalyze the literature in terms of the (p, r) combinations that researchers have used. Specifically, we merge data from two recent meta-studies: Blavatskyy et al. (2023) identify 143 CR experiments drawn from 39 studies and Blavatskyy et al. (2022) identify 81 CC experiments drawn from 29 studies. We combine the datasets from these meta-studies while converting the probabilities into our (p, r) framework. The resulting dataset yields several insights.

First, the prior literature has almost always studied the CRE and CCE independently. Of the CR and CC studies covered in the two meta-studies, only 10 contain both CR and CC experiments. Among those, only four collected observations for CR and CC problems at the same parameters for the same participants, and only two intentionally studied the connection between the two problems to better understand the nature of risk preferences.[9]

[7] Table 1 focuses on parameterized non-EU models that make predictions as a function of parameters for any choice set. There are additional non-parameterized models based on axioms that make predictions for one or more of the three features of preferences. Two recent models make predictions for all three: Cautious expected utility (Cerreia-Vioglio et al., 2015) predicts $\Delta^*_{CR} = \Delta^*_{CC} > 0$ and $\Delta^*_{MX} = 0$, and simplicity preferences (Puri, 2025) predict $\Delta^*_{CR} > 0$, $\Delta^*_{CC} > 0$, and $\Delta^*_{MX} < 0$ (see Appendix B.6 and B.7). There is also a class of models that impose or satisfy the betweenness axiom, which implies $\Delta^*_{MX} = 0$; this class includes the Gul (1991) model in Table 1 and also models of weighted utility (Chew, 1983; Dekel, 1986). These models are thus inconsistent with the CRP-RCCP-MXP pattern that is prominent in our data.

[8] Beyond the predictions for the pattern of preferences, these models also make predictions about the sensitivities of Δ^*_{CR}, Δ^*_{CC}, and Δ^*_{MX} to p and r. For probability-weighting models, the comparative statics are often non-monotone at leading parameter values, contrary to our data. For loss aversion and disappointment aversion models, the comparative statics are often directionally opposed to what we observe in our data.

[9] Burke et al. (1996) and Loomes and Sugden (1998) have connected CR-CC-MX problems, but this appears incidental. Burke et al. focus on whether the CCE differs for real versus hypothetical incentives; they do not mention that

Second, for each problem, the prior literature has used a limited set of parameters. Panel B of Figure 1 illustrates the (p, r) configurations used in this literature: Red circles denote CR experiments, while blue circles denote CC experiments. For each type of experiment, there is a large concentration at the canonical parameters. Of the 143 prior CR experiments, 48 (34%) use the Kahneman and Tversky (1979) values of $(p, r) = (0.80, 0.25)$, depicted by the large red dot in Panel B. Similarly, of the 81 prior CC experiments, 34 (42%) use the Allais (1953) values of $(p, r) = (0.91, 0.11)$, depicted by the large blue dot in Panel B. While there is some variation among the other experiments, Panel B reveals that a substantial portion of the parameter space remains unexplored.

This limited coverage would be of little consequence if the direction of the observed effects were broadly invariant to parameter choices. Indeed, all prominent parametrized non-EU models that we summarize in Table 1 predict, for their focal parameter range, that people have both a CRP and a CCP for all (p, r). However, Blavatskyy et al. (2023) and Blavatskyy et al. (2022) show that both the CRE and CCE are sensitive to parameter choices. Specifically, they find that a CRE is more likely to occur in experiments with smaller r, while the choice of p has no significant impact. Conversely, they find that the RCCE pattern becomes more likely for smaller p (their specification does not include r).[10]

In Table 2, we further explore the sensitivity of these effects to the choice of experimental parameters. We use the following continuous measures as our primary outcome variables:[11]

$$CRE - RCRE \equiv \widehat{\Pr}(A|AB) - \widehat{\Pr}(C|CD)$$
$$CCE - RCCE \equiv \widehat{\Pr}(A|AB') - \widehat{\Pr}(C|CD)$$

In Panel A of Table 2, we estimate OLS regressions with these measures as dependent variables. We replicate the qualitative findings from Blavatskyy et al. (2023) and Blavatskyy et al. (2022) and additionally find that CRE and CCE are differentially sensitive to p and r. This result suggests that what we learn about each effect and their connection is contingent on the parameters of the experiment.

their study includes a connected CR-CC-MX experiment. Loomes and Sugden compare three stochastic specifications of EU, collecting data on roughly 50 binary choices that include five connected CR-CC-MX problems. However, they make no special use of these connected problems, and do not discuss CCE or MXE. Bateman and Munro (2005) and Chew and Waller (1986) intentionally study connected CR-CC-MX problems. Bateman and Munro examine whether couples' joint decision making differs from individual decision making in terms of the CRE, CCE, and MXE, using several connected CR-CC-MX problems. As emphasized in the Introduction, Chew and Waller explicitly highlight how connected CR-CC-MX problems can provide more information about risk preferences. However, both of these papers only cover a small set of parameter configurations.

[10] Blavatskyy et al. (2023) and Blavatskyy et al. (2022) focus much of their analysis on the effects of other features of experiments such as real versus hypothetical stakes, the ratio of high to middle outcomes, and whether lotteries are presented as a probability distributions versus in compound form.

[11] We use $\widehat{\Pr}(X|YZ)$ to denote the share of participants in an experiment that chooses option X from the choice set YZ. Note that $CRE - RCRE$ is equivalent to the share choosing combination A and D minus the share choosing B and C in a CR problem, and $CCE - RCCE$ is equivalent to the share choosing combination A and D minus the share choosing B' and C in a CC problem.

In Panel B of Table 2, we divide prior CRE and CCE experiments into two categories: those conducted at the canonical (p, r) values and those conducted at alternative (p, r) values. We find a sizable CRE and CCE for the experiments at their respective canonical parameter values. In contrast, both effect sizes are significantly smaller in magnitude for experiments conducted at non-canonical values. Strikingly, CC experiments conducted away from the canonical (p, r) configuration exhibit an average RCCE.

Table 2: Sensitivity of Results to Experimental Parameters in the Prior Literature

Panel A. Sensitivity to Experimental Parameters

	(1) CR Study	(2) CC Study
H Probability: p	12.44	50.70
	(11.59)	(14.01)
Common Ratio: r	−61.14	−45.16
	(8.23)	(19.10)
Sample	Blavatskyy et al. (2023)	Blavatskyy et al. (2022)
Outcome Mean	19.25	8.64
Observations	143	81

Panel B. Canonical vs. Non-Canonical

	(3) Canonical	(4) Other	(5) Difference
	(i): KT Parameters		
CRE − RCRE	30.48	19.00	−11.48
	(15.38)	(24.04)	[−3.03]
Experiments	48	95	143
	(ii): Allais Parameters		
CCE − RCCE	17.40	−3.05	−20.46
	(17.34)	(22.95)	[−4.55]
Experiments	34	47	81

Notes: Panel A presents linear regressions that assess the sensitivity of experimental results from CR or CC studies based on the probability of the high outcome (p) and the common ratio (r). Column (1) presents the results for the 143 experiments reported in Blavatskyy et al. (2023), where the outcome is the net share of participants displaying a CRE relative to an RCRE, $CRE - RCRE$. Column (2) presents the results for the 81 experiments reported in Blavatskyy et al. (2022), where the outcome is the net share of participants displaying a CCE relative to an RCCE, $CCE - RCCE$. Specifications also include the value of the high outcome (H), the relative stakes ($M/(pH)$), and a dummy for whether the experiment had real stakes. Standard errors are in parentheses. Panel B presents the average of these outcomes based on whether the experiments reported in Blavatskyy et al. (2023) and Blavatskyy et al. (2022) were conducted at the canonical parameters in Kahneman and Tversky (1979) (KT; $p = 0.8$, $r = 0.25$) or Allais (1953) ($p = 0.91$, $r = 0.11$), respectively. Standard deviations are in parentheses, and t-statistics are in brackets. All experiments are weighted by the number of participants that took part in a given study.

Recent work has shown that researcher decisions related to experimental design, data processing, and empirical analysis can have a substantial impact on the results (Steegen et al., 2016; Simonsohn et al., 2020; Huber et al., 2023; Menkveld et al., 2024). Table 2 reinforces this point for CR and CC studies—the choices of p and r, along with other design parameters, are critical researcher decisions that can play a large role in determining the outcome. This further highlights the need for broad exploration of the parameter space when analyzing patterns of CR-CC-MX preferences.

This sort of broad exploration is largely absent from the prior literature. Most prior studies have not focused on testing whether the CRE and CCE are robust to the choice of experimental parameters, in part because many do not have these effects as their main object of interest. Of the 39 CRE studies identified by Blavatskyy et al. (2023), 21 (53%) use only one or two parameter configurations, and the average number of parameter configurations per study is less than four. Of

the 29 CCE studies identified by Blavatskyy et al. (2022), 18 (62%) use only one or two parameter configurations, and the average number of parameter configurations per study is less than three. The limited use of parameters within and across prior studies highlights a need for more scrutiny in establishing whether CRE and CCE reflect global features of preferences.[12]

2.4 Prior Literature on Mixture Preferences

Separate from the literature on the CRE and CCE, two distinct strands of work speak to mixture preferences. The first is a small literature from the 1980s through the early 2000s on direct tests of the betweenness axiom. Two papers provide nice reviews of this literature: Camerer and Ho (1994) summarize and contribute to the early literature on betweenness, and Blavatskyy (2006) provides an update. Both papers conclude that individuals frequently violate betweenness, but the evidence is mixed on the direction of violation, with some studies finding more mixture loving and others finding more mixture aversion. These tests of betweenness are almost never in the context of connected CR-CC-MX problems.

Second, there is an emerging literature on deliberate randomization (see, for example, Agranov and Ortoleva, 2017; Dwenger et al., 2018; Feldman and Rehbeck, 2022; Agranov et al., 2023; Agranov and Ortoleva, 2023). These studies typically present individuals with the same decision problem repeated multiple times, either interspersed throughout the study or explicitly repeated in a row. Evidence from these studies suggests that individuals often prefer to generate mixtures through randomization across task repetitions. However, this type of design does not allow for the measurement of *aversion* to randomization (i.e., RMXP). We discuss in Section 6 how our analysis relates to this literature.

We emphasize that our goal is not to investigate mixture preferences in isolation; if it were, connected problems would be unnecessary, and designs more directly connected to the work surveyed by Camerer and Ho (1994) and Blavatskyy (2006) would be better suited. Rather, our goal is to identify combinations of CR, CC, and MX preferences, providing the richer data required for a more holistic model assessment.

2.5 Choices and Valuations

The prior literatures on the CRE, CCE, and MXE have relied almost exclusively on paired binary choice tasks of the form described in Section 2.1.[13] If there is decision noise, however, then even if responses to individual binary choice tasks are unbiased noisy reflections of underlying preferences,

[12] There are a few recent papers that feature broader parameter coverage, including Kobayashi and Lucia (2023), Jain and Nielsen (2024), Lucia (2024), and McGranaghan et al. (2024).

[13] All 224 experiments from the two meta-studies by Blavatskyy et al. (2022) and Blavatskyy et al. (2023) use paired choices. In McGranaghan et al. (2024), we identified only 10 CRE experiments across four studies that instead use valuations.

a comparison of responses across a pair of binary choice tasks can yield biased conclusions. McGranaghan et al. (2024) build on prior work to demonstrate this issue in the context of the CRE, and show how analogous paired *valuation tasks* can avoid the problem.

Motivated by McGranaghan et al. (2024), our primary analysis focuses on three valuation tasks:

$$\begin{array}{lllll} \textbf{\textit{AB}} \textbf{ Valuation Task}: & \text{state an } h_{AB} \text{ such that} & (M,1) & \sim & (h_{AB},p), \\ \textbf{\textit{AB}}' \textbf{ Valuation Task}: & \text{state an } h_{AB'} \text{ such that} & (M,1) & \sim & (h_{AB'},pr;M,1-r), \\ \textbf{\textit{CD}} \textbf{ Valuation Task}: & \text{state an } h_{CD} \text{ such that} & (M,r) & \sim & (h_{CD},pr). \end{array}$$

To see how such valuation tasks can yield unbiased conclusions, consider a person who reports valuations with noise. Specifically, for a fixed (p, r, M), the person has underlying indifference values h^*_{AB}, $h^*_{AB'}$, and h^*_{CD} as defined in Section 2.2, but reports valuations $h_{AB} = h^*_{AB} + \varepsilon_{AB}$, $h_{AB'} = h^*_{AB'} + \varepsilon_{AB'}$, and $h_{CD} = h^*_{CD} + \varepsilon_{CD}$, where ε_{AB}, $\varepsilon_{AB'}$, and ε_{CD} are random variables that reflect noise. The person's empirically measured preferences are then

$$\begin{aligned} \Delta_{CR} &\equiv h_{AB} - h_{CD} &&= \Delta^*_{CR} + \varepsilon_{AB} - \varepsilon_{CD}, \\ \Delta_{CC} &\equiv h_{AB'} - h_{CD} &&= \Delta^*_{CC} + \varepsilon_{AB'} - \varepsilon_{CD}, \\ \Delta_{MX} &\equiv h_{AB} - h_{AB'} &&= \Delta^*_{MX} + \varepsilon_{AB} - \varepsilon_{AB'}. \end{aligned}$$

As long as $E[\varepsilon_{AB}] = E[\varepsilon_{AB'}] = E[\varepsilon_{CD}] = 0$, Δ_{CR}, Δ_{CC}, and Δ_{MX} are unbiased measures of the three objects of interest Δ^*_{CR}, Δ^*_{CC}, and Δ^*_{MX}.[14]

In contrast to comparing behavior across valuation tasks, comparing behavior across binary choice tasks can lead to biased inference. To illustrate, consider an EU maximizer with no CRP who faces a CR paired choice task. If the parameters of the problem are such that EU preferences favor A and C (e.g., for small H), then with unbiased choice noise, they will choose both A and C with probabilities greater than 1/2. However, if the noise has a differential impact on the two choice tasks, then the two choice probabilities will not be the same. In particular, if the noise has a larger impact on the CD choice task, then we would predict $1 > \Pr(A|AB) > \Pr(C|CD) > 1/2$; that is, we would predict $CRE - RCRE > 0$.[15] An analogous argument applies when the parameters are such that EU preferences favor B and D (e.g., for large H): If the noise has a larger impact on the CD choice task, then we would predict $1/2 > \Pr(C|CD) > \Pr(A|AB) > 0$; that is, we would predict $CRE - RCRE < 0$. Hence, the bias can be upward or downward depending on the choice of the experimental parameter H. Further, aggregating across heterogeneous EU individuals with different preferred alternatives can easily generate aggregate choice proportions $Pr(A|AB) > 1/2 > Pr(C|CD)$

[14] In McGranaghan et al. (2024), we also demonstrate that for some formulations of non-mean-zero noise—in particular, noise expressed in terms of utility—one can still test the null of $\Delta^*_{CR} = 0$ using a sign test. In Appendix C.1, we develop an analogous argument in the context of connected CR-CC-MX problems, and we conduct both means and sign tests in Section 4.

[15] We use $\Pr(A|AB)$ to denote the theoretical prediction for the observed $\widehat{\Pr}(A|AB)$.

or the reverse.

In McGranaghan et al. (2024), we formalize these arguments in more detail in the context of CR problems. In Appendix C.2, we provide the analogous formal argument for the three tasks that constitute a connected CR-CC-MX problem. We further demonstrate that the potential for misleading conclusions is even greater when attempting to identify preference patterns by comparing behavior across three binary choices.

Given the shortcomings of comparing behavior across binary choice tasks, our primary analysis focuses on identifying patterns of Δ^*_{CR}, Δ^*_{CC}, and Δ^*_{MX} using valuation tasks. An additional benefit of valuation tasks is that Δ_{CR}, Δ_{CC}, and Δ_{MX} provide direct measures of the *magnitudes* of their corresponding underlying preferences Δ^*_{CR}, Δ^*_{CC}, and Δ^*_{MX}. In contrast, with binary choice tasks, we only observe $\widehat{\Pr}(A|AB) - \widehat{\Pr}(C|CD)$, $\widehat{\Pr}(A|AB') - \widehat{\Pr}(C|CD)$, and $\widehat{\Pr}(A|AB) - \widehat{\Pr}(A|AB')$. Even if the signs of these differences were unbiased, their magnitudes have no clear interpretation because they represent a combination of the magnitude of the underlying Δ^*_{CR}, Δ^*_{CC}, and Δ^*_{MX} and the magnitude of the differential noise.

While our discussion above (and in McGranaghan et al., 2024) assumes that individual (as opposed to paired) valuation and choice tasks both provide unbiased measures of underlying preferences, some researchers (e.g., Brown and Healy, 2018 and Freeman et al., 2019) have argued that individual valuation tasks might themselves be biased—for example, due to menu effects that draw individuals toward the middle of a multiple price list.[16] Given this potential concern, our experiment also conducts binary choice tasks that are linked to the valuation tasks. In fact, the analysis in McGranaghan et al. (2024) points to an approach for mitigating the potential bias when comparing behavior across choice tasks: select multiple payment values—in this case, multiple values for H—such that upward and downward biases roughly offset. Hence, in our paired binary choice tasks, we intentionally select values of the high payment H based on pilot data to accomplish this balance. Given this approach, the main empirical patterns that we document below are the same for both our valuation and choice data.

3 Experimental Methodology

We study connected CR-CC-MX problems using both paired valuation tasks and paired choice tasks at 20 different (p, r) combinations.[17] We consider four possible values of $p \in \{0.3, 0.5, 0.8, 0.9\}$ and five possible values of $r \in \{0.1, 0.2, 0.3, 0.5, 0.8\}$. These values cover a wide range of (p, r) configurations while still including some of the most popular parameter choices in the prior literature. Open circles

[16] In our design, each of our three key measures Δ_{CR}, Δ_{CC}, and Δ_{MX} represents a *difference* in responses across two valuation tasks with the same menu. Hence, even if menu effects distort valuation levels, they may not distort valuation differences.

[17] We conducted the experiment in October 2022 and preregistered it in the AEA RCT Registry under the ID AEARCTR-0009974 prior to data collection.

in Panel B of Figure 1 indicate our choice of (p, r) combinations.

Figure 2 provides an overview of the experiment timeline. The experiment consists of two stages. In stage 1, we randomly assign each participant to four of our 20 (p, r) combinations, and each participant then completes 20 valuation tasks. Each valuation task fixes M and uses a multiple price list to elicit the value of H that makes the participant indifferent between two lotteries. In stage 2, the same participant completes 24 binary choice tasks for the same four (p, r) combinations as in stage 1. Participants complete all 20 valuations before the 24 binary choices, and we randomize the order of questions within each stage.

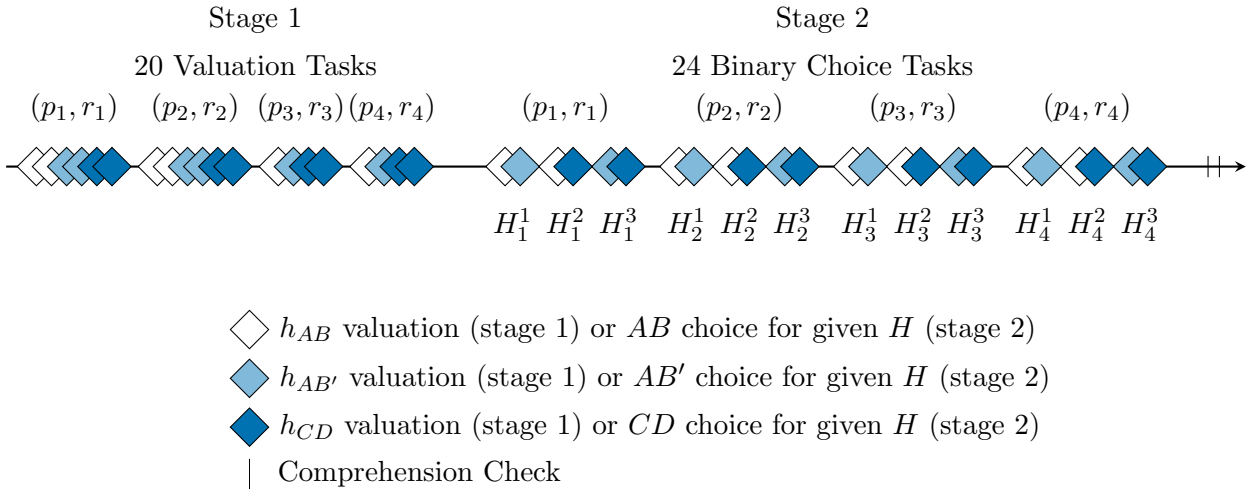

Figure 2: Experiment Timeline

3.1 Stage 1: Valuation Tasks

In stage 1, each participant completes 20 valuation tasks across four randomly drawn combinations of (p, r). We draw the values of p without replacement so that each participant sees all four possible values of p. Conversely, we draw the values of r with replacement, so a participant might face the same r across multiple values of p.[18]

For each (p, r) combination, we elicit the following indifference points:

$$\begin{aligned} h_{AB} \quad &\text{such that} : (M, 1) \sim (h_{AB}, p) \\ h_{AB'} \quad &\text{such that} : (M, 1) \sim (h_{AB'}, pr; M, 1-r) \\ h_{CD} \quad &\text{such that} : (M, r) \sim (h_{CD}, pr) \end{aligned}$$

We fix $M = \$(p \cdot 30)$ and elicit the relevant valuations using a multiple price list.[19] The left-hand

[18] We draw p without replacement to avoid duplicate elicitations of the same AB task, since the AB task does not depend on r.

[19] We set M in this way for practical reasons. We did not want M to be too large when $p = 0.3$ to avoid very

option in each price list is fixed at either lottery $(M, 1)$ or (M, r). The right-hand option is either lottery (H, p), $(H, pr; M, 1-r)$, or (H, pr), with H varying in \$1 increments from $\$M$ to $\$(M+50)$. For example, for $p = 0.3$, we fix $M = \$9$ and vary H from \$9 to \$59. We take the average value of H at the switching rows as our measure of the indifference valuation.[20]

For each price list, we enforce a single switching point. Clicking a row in the left column selects the left-hand option in that row and all rows above; clicking a row in the right column selects the right-hand option in that row and all rows below. Participants can adjust their selections as much as they want before submitting their final choices for that valuation task. Appendix Figures H.1 to H.3 provide example screenshots of all three variants of the valuation task.

For two randomly drawn (p, r) combinations that a given participant sees, we elicit each valuation twice, generating observations $\{h_{AB}, h'_{AB}, h_{AB'}, h'_{AB'}, h_{CD}, h'_{CD}\}$ where the repeat elicitations are denoted by h'. For the remaining two (p, r) combinations, we only elicit the CD valuation twice, generating observations $\{h_{AB}, h_{AB'}, h_{CD}, h'_{CD}\}$.[21] Therefore, we have duplicate observations for all CD valuations but only half of AB and AB' valuations. We discuss the purpose of collecting multiple elicitations of the same valuation in Section 4. In total, participants complete 20 valuation tasks: six valuations each for two (p, r) combinations and four valuations each for the remaining two (p, r) combinations. We randomize the order of valuation tasks subject to the constraint that repeat elicitations of the same valuation are separated from each other by at least three other valuation tasks.

3.2 Stage 2: Paired Choice Tasks

In stage 2, each participant completes 24 binary choices across the same four (p, r) combinations they saw in stage 1. These 24 binary choices comprise 12 paired choice tasks, three for each (p, r) combination: a CR pair (an AB choice and a CD choice), a CC pair (an AB' choice and a CD choice), and an MX pair (an AB choice and an AB' choice). Appendix Figures H.4 to H.6 present examples of each type of binary choice task.

Each binary choice that a participant sees in stage 2 is equivalent to a single row from one of the price lists they saw in stage 1. Specifically, for each (p, r) combination, we again fix $M = \$(p \cdot 30)$. For each of the three types of paired choice tasks, we then draw a random value of H from the relevant

large H values at indifference. We also did not want M to be too small when $p = 0.9$ to avoid being unable to detect preference variations given our \$1 increments in the price list. Our approach means that a risk neutral person would choose $H = \$30$ for all price lists.

[20] In prior work, we also implement m-valuation tasks in which we hold H fixed and elicit the M that makes participants indifferent between two lotteries (McGranaghan et al., 2024). For AB' valuations, varying M would lead to changes in both columns of the price list, which adds a layer of complexity to the valuation process. For this reason, we focus on h-valuation tasks in this paper.

[21] For each participant and (p, r) pair, we randomly label one of the two elicitations h_{XY} and the other h'_{XY} for $XY \in \{AB, AB', CD\}$. In other words, the superscript prime does not indicate the order in which the valuations were elicited.

row in Table 3 without replacement. Hence, for a given (p, r) combination, we conduct three paired choice tasks (CR, CC, or MX) with a different value of H for each pair (but with the same H for both choices within a given pair). We randomize the order in which these choices appear, with no restrictions on the order. The values of H in Table 3 were selected based on pilot data to roughly balance the number of cases with upward versus downward bias (see our discussion in Section 2.5). Specifically, the goal was to have three smaller values intended to produce a majority that prefer A over B, A over B', and C over D, and three larger values where the majority exhibits the opposite pattern.

Table 3: Stage 2 H Parameter Values by p

	(1)	(2)	(3)	(4)	(5)	(6)
$p = 0.9$	31	36	41	46	51	56
$p = 0.8$	29	34	39	44	49	54
$p = 0.5$	28	33	38	43	48	53
$p = 0.3$	27	32	37	42	47	52

Notes: Table presents values of H used in stage 2 for each p. For each (p, r) that a participant saw, they are presented with three paired choice tasks (one CR, one CC, and one MX); we randomly selected three of the six H values for the relevant p, and assigned one to each of these paired choice tasks.

It is useful to benchmark the scale of our stage 2 paired choice tasks relative to the prior CR and CC literature. We can view stage 2 as conducting many paired-choice "experiments," where one experiment consists of responses from multiple participants for a fixed set of parameters (p, r, H). With 20 (p, r) combinations and six values of H for each, we effectively run 120 CR experiments, 120 CC experiments, and 120 MX experiments, with a total of 8,408 observations for each type of experiment. In comparison, the two meta-studies discussed in Section 2.3 report 143 CR experiments with 14,794 total observations and 81 CC experiments with 8,947 observations.

3.3 Additional Design Details

Before stage 1, participants complete an unincentivized attention check and a quiz about the payment mechanism. After completing stage 2, they complete two incentivized comprehension checks to gauge their understanding of the multiple price list format and the binary choice tasks. The first tests whether individuals can correctly fill out a price list given a specified indifference value. The second tests whether participants can correctly answer a binary choice question when given another person's responses to a multiple price list. Appendix Figures H.7 and H.8 provide example screenshots of these comprehension checks.[22] Finally, to break up the tasks and reduce fatigue, we present participants

[22]For the first comprehension check, 85 percent of participants answer correctly, and for the second, 79 percent answer correctly. See Appendix Table A.1. The qualitative patterns in Figure 3 are unchanged if we restrict the sample to those who pass both comprehension checks.

with an unincentivized visual puzzle after every fifth question in both experiment stages. Appendix Figure H.9 provides an example of one of these puzzles.

3.4 Recruiting

We recruited 2,102 participants through Prolific who met the following eligibility criteria: at least a high school education; between the ages of 18 and 31; living in the United States or Western Europe; minimum Prolific approval rating of 99 percent; fluent in English; and 50 to 1,000 previous Prolific submissions. We targeted this group of participants to approximate the typical undergraduate sample recruited in prior CC and CR studies. We also recruited a gender-balanced sample with an even split of male and female participants. Appendix Table A.1 presents summary statistics for our sample.

We paid each participant a fixed $5 fee for completing the experiment. In addition, we randomly selected one in five participants to receive a bonus based on their responses. Specifically, we randomly chose one of their 46 decisions (20 valuations, 24 choices, and two incentivized comprehension checks) to be the decision that counts. If the decision that counts was a valuation task, then we randomly selected one row of the price list and paid the participant according to their choice in that row. If the decision that counts was a binary choice task, then we paid the participant based on the option they selected. If the decision that counts was a comprehension-check question, then we paid the participant $5 if they answered correctly. The average completion time was 24 minutes and 27 seconds, and the average bonus payment for selected participants was $15.76.

4 Results

4.1 Aggregate Behavior in Valuation Tasks

We first study aggregate behavior across all participants using the AB, AB', and CD valuations collected in stage 1 to measure CR, CC, and MX preferences—that is, to measure Δ^*_{CR}, Δ^*_{CC}, and Δ^*_{MX}.[23]

As described in Section 3.1, we collect some valuations twice and randomly label them h_{XY} and h'_{XY} for $XY \in \{AB, AB', CD\}$.[24] We collect repeat valuations for three main reasons. First, we use the repeat valuations to get an initial assessment of the reliability of the stage 1 data. We compute the correlation between repeated elicitations of the same valuation—e.g., h_{CD} and h'_{CD}—for each (p, r). Appendix Table A.3 reports these correlations; all are positive, ranging from 0.389 to 0.731. Given that the repeat elicitations are separated from each other by at least three other tasks, these strong

[23] We pre-registered the construction of our experimental outcomes and the analyses that we describe throughout Section 4 in our pre-analysis plan. We note any deviations and additional exploratory analyses.

[24] Appendix Table A.2 reports the means for all six valuations $(h_{AB}, h'_{AB}, h_{AB'}, h'_{AB'}, h_{CD}, h'_{CD})$ for each (p, r) combination.

correlations suggest that our valuation data capture meaningful information about the underlying preferences of interest.

Second, we use the repeat valuations to construct independent measures of our three main outcomes of interest. Specifically, we define the following measures:

$\Delta_{CR} \equiv h_{AB} - h_{CD}$, a (noisy) measure of an individual's CRP, Δ^*_{CR},

$\Delta_{CC} \equiv h_{AB'} - h'_{CD}$, a (noisy) measure of an individual's CCP, Δ^*_{CC}, and

$\Delta_{MX} \equiv h'_{AB} - h'_{AB'}$, a (noisy) measure of an individual's MXP, Δ^*_{MX}.

If we had only a single elicitation for each valuation, then measurement error in the valuations would induce mechanical correlations between Δ_{CR}, Δ_{CC}, and Δ_{MX}. For example, using the same measure h_{CD} to construct both Δ_{CR} and Δ_{CC} would create a mechanical positive correlation between Δ_{CR} and Δ_{CC} if there is any measurement error in h_{CD}. By eliciting valuations twice and using independent observations to construct our difference measures, we avoid this problem.[25]

Third, we use the repeat valuations to disentangle noise from preferences, which we describe in detail in Section 4.4.

To investigate aggregate behavior, we analyze the mean values of Δ_{CR}, Δ_{CC}, and Δ_{MX} across all participants for each (p, r) combination. Figure 3 presents these quantities by p, separately for each r. EU predicts all of these values to be zero, while many non-EU models predict a systematic $\Delta_{CR} > 0$ and $\Delta_{CC} > 0$. Both of these general predictions are markedly inconsistent with the data, which show clear distinct patterns for Δ_{CR}, Δ_{CC}, and Δ_{MX} across the parameter space. Panel A summarizes CR preferences: Δ_{CR} is largely invariant to changes in p but declines sharply in r, leading to $\Delta_{CR} \approx 0$ at higher r values. Panel B summarizes CC preferences: In contrast to Δ_{CR}, Δ_{CC} is largely invariant to changes in r but is increasing sharply in p, with $\Delta_{CC} < 0$ at lower p values. The structural connection between CR and CC preferences—and their distinct patterns throughout the parameter space—implies that people cannot have a neutral attitude to probabilistic mixtures. This again emerges as a distinct systematic pattern in Δ_{MX} shown in Panel C: Mean Δ_{MX} is positive for most parameters and becomes substantially larger as p and r fall. Appendix Tables A.4, A.5, and A.6 provide information on the statistical significance of the patterns in Figure 3 through mean and sign tests for the EU null of zero along with regression results for how Δ_{CR}, Δ_{CC}, and Δ_{MX} change with p and r.[26] These tables indicate that quantities in excess of roughly 1.5 in absolute

[25] Recall that for two randomly drawn (p, r) combinations that a participant sees, we elicit each valuation twice, generating observations $\{h_{AB}, h'_{AB}, h_{AB'}, h'_{AB'}, h_{CD}, h'_{CD}\}$ and allowing us to construct independent measures of each of the three main objects of study. For the remaining two (p, r) combinations, we only elicit the CD valuation twice, generating observations $\{h_{AB}, h_{AB'}, h_{CD}, h'_{CD}\}$ and allowing us to construct independent measures of Δ_{CR} and Δ_{CC} but not Δ_{MX}. This means that we have twice as many observations for Δ_{CR} and Δ_{CC} than for Δ_{MX}.

[26] In McGranaghan et al. (2024), we similarly tested for the existence of CRP using paired valuation tasks. While most of McGranaghan et al. (2024) presents results based on choose-m tasks in which participants report the middle value that makes them indifferent between Options A and B and C and D respectively, we also collected choose-h tasks

value in Figure 3 are statistically different from zero and that the noted sensitivities to p and r are statistically significant.[27]

Looking across the three panels in Figure 3, two striking regularities emerge. First, near the canonical parameterizations for CR and CC problems (i.e., at $p = 0.8$ or 0.9 and $r = 0.1$, 0.2, or 0.3), we find both $\Delta_{CR} > 0$ and $\Delta_{CC} > 0$. Thus, CRP and CCP appear at canonical parameter values, consistent with the findings from the paired-choice paradigm. At the same time, Δ_{MX} tends toward zero at these values such that the generally positive attitude toward mixtures seen in Panel C would be missed by focusing exclusively on the canonical parameterizations. Second, for small p and small r, we find a robust pattern of $\Delta_{CR} > 0$, $\Delta_{CC} < 0$, and $\Delta_{MX} > 0$, which contrasts sharply with the predictions of the leading parametrized non-EU models in Table 1.[28]

Figure 3: Stage 1 Valuations: Mean Δ_{CR}, Δ_{CC}, and Δ_{MX} by p for each r

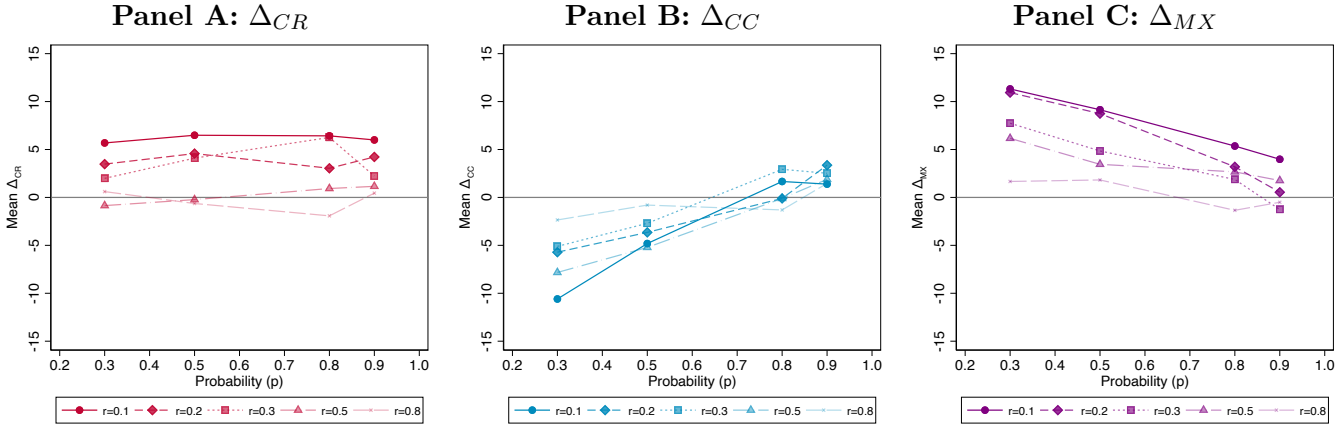

Notes: Figure depicts mean values of $\Delta_{CR} = h_{AB} - h_{CD}$, $\Delta_{CC} = h_{AB'} - h'_{CD}$, and $\Delta_{MX} = h'_{AB} - h'_{AB'}$. Panels A and B aggregate over 8,408 observations, with each point corresponding to roughly 420 observations. Panel C aggregates over the 4,204 observations for which we elicit h'_{AB} and $h'_{AB'}$, with each point corresponding to roughly 210 observations. Expected utility predicts $\Delta = 0$ in all three panels.

4.2 Aggregate Behavior in Choice Tasks

As a secondary analysis, we examine aggregate behavior using stage 2 choices. For each (p, r) combination, we pool data across all payment values for H to generate the measures $CRE - RCRE$,

for validation and robustness that are more directly comparable to the measures in this paper. McGranaghan et al. (2024) explored a smaller range of r ($r \in \{0.2, 0.4, 0.6\}$ compared to $r \in \{0.1, 0.2, 0.3, 0.5, 0.8\}$ in this paper) and also captures some lower values of p ($p \in \{0.1, 0.2, 0.5, 0.8, 0.9\}$ compared to $p \in \{0.3, 0.5, 0.8, 0.9\}$ in this paper). In both cases, we find no evidence of a systematic CRP as the direction and magnitude of the effects depend on experimental parameter choices, especially the choice of r. Relative to McGranaghan et al. (2024), the parameters considered in this paper yield slightly more instances of CRP, particularly for cases in which $r = 0.1$. This underscores the role low values of r play in generating evidence of CRP.

[27] An alternative, though less direct, measure of MXP is $\Delta_{CR} - \Delta_{CC}$. Appendix Tables A.4 and A.5 also provide results for this measure, which are qualitatively and quantitatively similar to the results for our direct measure Δ_{MX}.

[28] The aggregate patterns for Δ_{CR}, Δ_{CC}, and Δ_{MX} in Figure 3 are qualitatively reproduced when we construct corresponding mean measures using only each participant's first observation. Though noisier, similar sensitivities to problem parameters remain along with frequent observations of $\Delta_{CR} > 0$, $\Delta_{CC} < 0$, and $\Delta_{MX} > 0$.

$CCE - RCCE$, and $MXE - RMXE$. The first two measures are defined in Section 2.3, and the third is defined analogously.

Figure 4 is the analog of Figure 3 when we use choices instead of valuations. The same qualitative conclusions emerge for our three main preferences of interest: The CR pattern is largely invariant to p, with a CRE at small r but not at large r; the CC pattern is largely invariant to r, with a mild CCE at large p but a strong $RCCE$ at small p; and the MX pattern depends on both p and r, with a general MXE that is substantially stronger for smaller p and smaller r. Appendix Table A.9 is analogous to Table A.5 and confirms the statistical significance of these patterns.

Figure 4: Stage 2 Choices: Mean $CRE - RCRE$, $CCE - RCCE$, $MXE - RMXE$ by p for each r

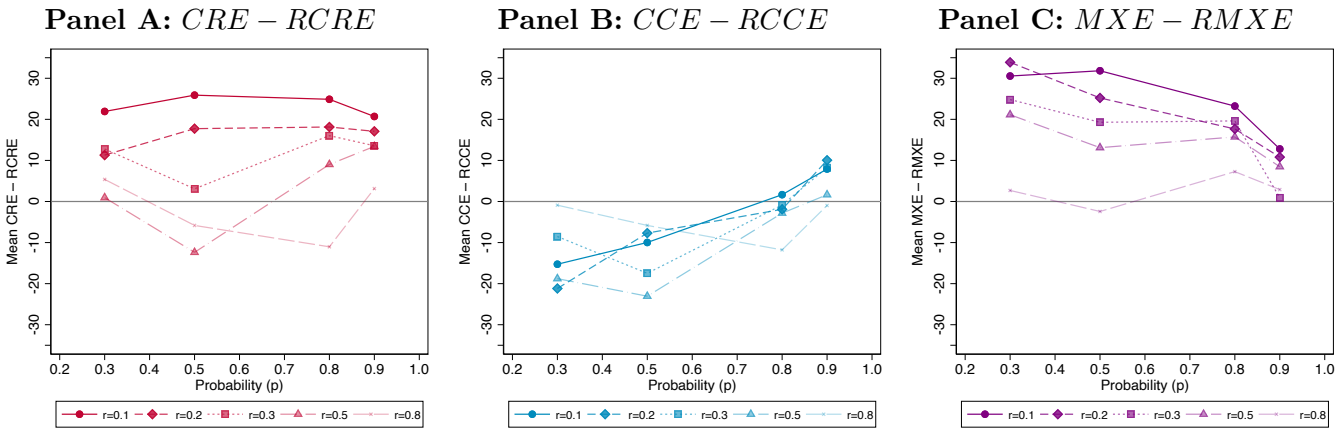

Notes: Figure depicts average values of $CRE - RCRE$, $CCE - RCCE$, and $MXE - RMXE$. Each panel aggregates over 8,408 observations. Each point in each panel aggregates over the six payment values for H noted in Table 3 and corresponds to approximately 420 observations. The line for zero choice difference is indicated in all three panels but only serves as a reference.

Although our stage 2 choices yield the same qualitative message as our stage 1 valuations, Section 2.5 highlights a drawback of using binary choice tasks: When comparing behavior across such tasks, conclusions can be biased if noise has a differential impact across decisions. In McGranaghan et al. (2024), we demonstrate the existence of differential noise within the context of the CRE, and in particular, that noise has a larger impact on the CD decision than on the AB decision. In Appendix C.3, we conduct a similar analysis using the data from the current experiment. We find evidence of differential noise in all three problems. For CR problems, we again find that noise has a larger impact on the CD decision than the AB decision. For CC problems, we find that noise has a larger impact on the AB' decision than the CD decision. For the MX problems, we find that noise has a larger impact on the AB' decision than the AB decision.[29] Given that we find evidence of differential noise for all three problems, it may seem surprising that our choice data yield the same aggregate conclusions as our valuations data. However, as noted in Section 2.5, this successful replication stems from our

[29]Interestingly, these conclusions differ from the predictions of EU with additive i.i.d utility noise, which predicts that noise has a smaller impact on the AB choices than either the AB' or CD choices, with equal impact on the latter two. See Appendix C.3 for more details.

deliberate selection of experimental parameters to induce offsetting biases in stage 2; specifically, it reflects our choice of a balanced set of H payment values at each (p, r, M).

4.3 Heterogeneity in Behavioral Patterns

Whereas Figures 3 and 4 characterize mean responses, it is also important to investigate behavior at the individual level.[30] To relate our data to the directional model predictions in Table 1, we focus on participants' directional responses in valuation tasks, which map directly to those predictions. For example, we create indicators for whether a person exhibits $\Delta_{CR} > 0$, $\Delta_{CR} = 0$ (denoted $\oslash$CR), or $\Delta_{CR} < 0$ in their valuations for CR problems. With three possible directional responses for each of the three measures of interest, there are 27 possible combinations. Figure 5 presents a histogram across these 27 combinations using the 4,204 observations for which we have independent measures of Δ_{CR}, Δ_{CC}, and Δ_{MX}. Note that the variation in Figure 5 is across (p, r) and both across and within participants.

Figure 5: Histogram of Response Patterns

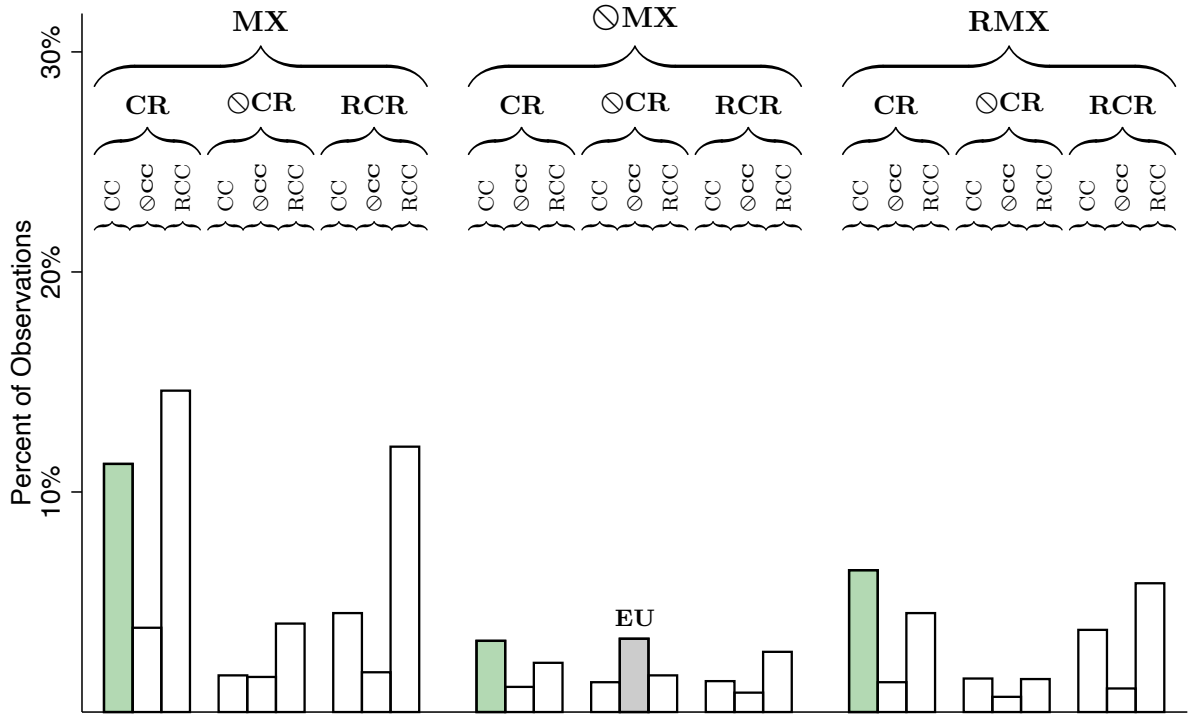

Notes: Figure presents histogram of $(sign(\Delta_{CR}), sign(\Delta_{CC}), sign(\Delta_{MX}))$ combinations, where $\Delta_{CR} = h_{AB} - h_{CD}$, $\Delta_{CC} = h_{AB'} - h'_{CD}$, and $\Delta_{MX} = h'_{AB} - h'_{AB'}$. The histogram covers the 4,204 observations for which we elicit h'_{AB} and $h'_{AB'}$, with each participant contributing two observations. Each variable can have three potential signs, leading to 27 possible patterns. These signs correspond to the named patterns (e.g., CR to $\Delta_{CR} > 0$, RCR to $\Delta_{CR} < 0$, and $\oslash$CR to $\Delta_{CR} = 0$). Patterns marked in light green are ones with both $\Delta_{CR} > 0$ and $\Delta_{CC} > 0$, a frequent prediction of leading parametrized behavioral models (see Table 1).

[30] We did not pre-register any specific hypotheses or analyses with regards to these individual preference patterns. This heterogeneity analysis is therefore exploratory.

Figure 5 reveals that the mean behavior in Figures 3 and 4 masks substantial heterogeneity. Patterns that are consistent with the standard behavioral hypothesis of $\Delta_{CR} > 0$ and $\Delta_{CC} > 0$ are highlighted in green. Such observations constitute only a small fraction of the observed patterns (21.0 percent). As foreshadowed by Figures 3 and 4, the most frequent single pattern is $\Delta_{CR} > 0$, $\Delta_{CC} < 0$, and $\Delta_{MX} > 0$, though even this modal pattern accounts for only 14.6 percent of observations.[31]

To the extent that some of the variability in responses reflects heterogeneous preferences, it will be important for models of risk preferences to accommodate this variability. Before reaching that conclusion, however, we must assess the extent to which the variability in responses reflects heterogeneous preferences versus noise.

4.4 Decomposing Variability in Responses into Preference and Noise

In this section, we estimate the population distribution of underlying preferences and the magnitude of decision noise.[32] We then use these estimates for two purposes. First, we assess how much of the variability in our data is due to preference heterogeneity versus noise. Second, we derive what the distribution of preference patterns from Figure 5 would look like in the absence of noise.

To disentangle noise from preferences, we leverage the fact that we collect repeat measures of participants' valuations. Intuitively, if the noise is independent across repeat elicitations, then the covariance between the two elicitations reflects only heterogeneity in preferences. We provide an overview of our approach here. Appendix D provides a more complete description of our decomposition.

We begin with some notation for the population distribution of the underlying indifference values for a fixed (p, r, M). We define the expectation $E(h^*_{AB}, h^*_{AB'}, h^*_{CD}) \equiv (\mu^*_{AB}, \mu^*_{AB'}, \mu^*_{CD})$, and the variance-covariance matrix

$$\mathbf{V}\begin{pmatrix} h^*_{AB} \\ h^*_{AB'} \\ h^*_{CD} \end{pmatrix} \equiv \begin{pmatrix} \theta^2_{AB} & \theta_{AB,AB'} & \theta_{AB,CD} \\ \theta_{AB,AB'} & \theta^2_{AB'} & \theta_{AB',CD} \\ \theta_{AB,CD} & \theta_{AB',CD} & \theta^2_{CD} \end{pmatrix}. \tag{1}$$

For $XY \in \{AB, AB', CD\}$, we assume an individual's repeated XY valuations are

$$h_{XY} = h^*_{XY} + \varepsilon_{XY} \qquad \text{and} \qquad h'_{XY} = h^*_{XY} + \varepsilon'_{XY},$$

[31] Appendix Figures A.1 to A.3 depict these distributions for various (p, r) subsets. Near the canonical parameterizations ($p = 0.8$ or 0.9 and $r = 0.1$, 0.2, or 0.3), the combination $\Delta_{CR} > 0$ and $\Delta_{CC} > 0$ is indeed more prevalent (28.9 percent). Nonetheless, there is still substantial variability, and the combination $\Delta_{CR} > 0$, $\Delta_{CC} < 0$, and $\Delta_{MX} > 0$ still accounts for 13.9 percent of observations. Alternatively, for parametrizations where Figure 3 suggests the $\Delta_{CR} > 0$, $\Delta_{CC} < 0$, and $\Delta_{MX} > 0$ combination should be strongest ($p = 0.3$ or 0.5 and $r = 0.1$, 0.2, or 0.3), that combination constitutes 21.4 percent. However, there is substantial variability at all problem parameters.

[32] Our pre-registration outlined a potential exploratory exercise to recover the distributions of preferences incorporating both valuations and choices. In this exercise we focus on only valuation data and discuss the connection between choices and valuations in Section 4.5.

where $E(\varepsilon_{XY}) = E(\varepsilon'_{XY}) = 0$, $var(\varepsilon_{XY}) = var(\varepsilon'_{XY}) = \sigma^2_{XY}$, and ε_{XY} and ε'_{XY} are independent of each other, underlying preferences, and all other noise draws.

Under these assumptions, we can derive theoretical predictions for the empirical moments:

$$\begin{aligned} var(h_{XY}) &= \theta^2_{XY} + \sigma^2_{XY}, \\ cov(h_{XY}, h'_{XY}) &= \theta^2_{XY}, \text{ and} \\ cov(h_{XY}, h_{WZ}) &= \theta_{XY,WZ}. \end{aligned}$$

The first equation highlights that with only a single elicitation of an XY valuation, we could not decompose its variance into the separate preference and noise components. The second equation captures our central intuition: If the noise draws for the two elicitations are independent, then their covariance identifies the variance of the preference heterogeneity.[33]

Given this formulation, there are twelve model parameters to estimate for each (p, r): three μ^*_{XY} terms capturing the population average preference, three θ^2_{XY} terms capturing preference heterogeneity, three $\theta_{XY,WZ}$ terms capturing the covariance between preferences, and three σ^2_{XY} terms capturing the impact of noise. We derive estimates of these terms by calculating the relevant sample moments. For example, $\hat{\theta}^2_{AB} = cov_s(h_{AB}, h'_{AB})$ and $\hat{\sigma}^2_{AB} = var_s(h_{AB}) - cov_s(h_{AB}, h'_{AB})$, where cov_s and var_s denote a sample covariance or variance (see Appendix D.1 for details on how we calculate these moments given the structure of our data). Appendix Table A.7 reports our estimates of the 12 calculated terms for each (p, r) combination.[34]

Given these estimates, we can quantify how much of the variability in our data is due to heterogeneity in preferences versus noise. Consider first the variability in the indifference values h_{AB}, $h_{AB'}$, and h_{CD}. The last three columns of Appendix Table A.7 report the proportion of the variability for each indifference value that is due to preferences; that is, the ratio $\widehat{var}(h^*_{XY})/\widehat{var}(h_{XY}) = \hat{\theta}^2_{XY}/(\hat{\theta}^2_{XY} + \hat{\sigma}^2_{XY})$ for each $XY \in \{AB, AB', CD\}$. Averaging across the 20 (p, r) combinations, preference heterogeneity accounts for 61 percent of the variation in h_{AB}, 58 percent of the variation in $h_{AB'}$, and 48 percent of the variation in h_{CD}.

Next we consider variability in the preference measures Δ_{CR}, Δ_{CC}, and Δ_{MX}. For $\Delta_{CR} \equiv$

[33] If, instead, ε_{XY} and ε'_{XY} were not independent from each other (but still independent from preferences), then $cov(h_{XY}, h'_{XY}) = \theta^2_{XY} + cov(\varepsilon_{XY}, \varepsilon'_{XY})$. In such a case, the covariance between the two elicitations provides a biased estimated of preference heterogeneity. Though the bias is theoretically unsigned, it would be natural to assume $cov(\varepsilon_{XY}, \varepsilon'_{XY}) > 0$, which would lead us to overestimate the extent of preference heterogeneity, attributing to preferences behavioral heterogeneity that should be attributed to noise. If features of our elicitations led to ε_{XY} and ε'_{XY} being independent from each other but not independent from preferences, perhaps due to substantial boundary effects, then $cov(h_{XY}, h'_{XY}) = \theta^2_{XY} + cov(\varepsilon_{XY}, h^*_{XY}) + cov(\varepsilon'_{XY}, h^*_{XY})$, again leading to a biased estimate of preference heterogeneity. Though this bias is also unsigned, it would be natural to assume negative correlations between errors and preferences if boundary effects caused small values of h^*_{XY} to be inflated and large values to be deflated. This would lead us to underestimate the extent of preference heterogeneity. While we cannot assess the magnitude of such effects, one piece of suggestive evidence is that only approximately 10% of observations lie at the boundaries of our price lists.

[34] Appendix D.5 describes a more sophisticated approach using maximum-likelihood estimation (MLE). Because that approach requires additional distributional and implementation assumptions, we prefer the moment-based approach in the text. However, the MLE approach yields virtually identical conclusions.

$h_{AB} - h_{CD}$, it is straightforward to derive that

$$\begin{aligned} var(\Delta_{CR}) &= var(\Delta^*_{CR}) + \sigma^2_{AB} + \sigma^2_{CD}, \quad \text{and} \\ var(\Delta^*_{CR}) &= \theta^2_{AB} + \theta^2_{CD} - 2\theta_{AB,CD}, \end{aligned}$$

along with the analogous expressions for Δ_{CC} and Δ_{MX}. Appendix Table A.8 uses the estimates in Appendix Table A.7 to calculate these six variance terms for each (p, r) combination.[35] The last three columns of Appendix Table A.8 report the proportion of the variability for each preference measure that is due to preferences; that is, the ratio $\widehat{var}(\Delta^*_Z)/\widehat{var}(\Delta_Z)$ for each $Z \in \{CR, CC, MX\}$. Averaging across the 20 (p, r) combinations, preference heterogeneity accounts for 31 percent of the variation in Δ_{CR}, 31 percent of the variation in Δ_{CC}, and 25 percent of the variation in Δ_{MX}.

We next construct what the distribution of response patterns from Figure 5 would look like in the absence of decision noise. To do so, we make the additional assumption that the underlying preferences $(h^*_{AB}, h^*_{AB'}, h^*_{CD})$ have a joint normal distribution. For each (p, r) combination, we use the parameter estimates in Appendix Table A.7 to simulate 100,000 draws from this joint normal distribution and then convert each draw to a Δ^*_{CR}, Δ^*_{CC}, and Δ^*_{MX}.[36] This approach allows us to isolate the preference patterns underlying the observed response patterns depicted in Figure 5.

Figure 6 reproduces the distribution of response patterns in Figure 5 but adds black dots to denote the simulated distribution of preference patterns generated using the approach above. Note that any pattern that implies an intransitivity in the underlying indifference values $(h^*_{AB}, h^*_{AB'}, h^*_{CD})$ cannot emerge from this simulation.[37] Of the 27 possible response patterns, 14 imply an intransitivity. Neither our decomposed preferences nor any transitive theory of preferences can accommodate such patterns, which are marked in gray in Figure 6.[38]

Of the remaining 13 possible preference patterns, six are "strict" in the sense that they do not include a $\Delta^*_{CR} = 0$, $\Delta^*_{CC} = 0$, or $\Delta^*_{MX} = 0$, while the other seven are "weak" in the sense that they include a null preference. Our simulation permits both strict and weak patterns, and indeed, all 13 patterns have a positive share of simulated preferences. Figure 6 shows that some patterns arise more frequently in preferences than in the raw responses while the reverse is true for others. The four most prominent strict patterns (marked P1, P2, P3, P4, and indicated in blue) account

[35] When using this approach, nothing guarantees that the calculated $var(\Delta^*_Z) > 0$, and indeed there is one instance in which we estimate a negative variance term (for Δ_{MX} when $(p, r) = (0.3, 0.5)$). We exclude this case from our analysis.

[36] Specifically, we round each h^* draw to the midpoint of its two closest integers (e.g., any draw strictly between \$2 and \$3 is converted to \$2.50). We then use these adjusted h^* terms to generate the Δ^* terms. This approach permits the simulated Δ^* terms to be zero. See Appendix D.3 for complete details.

[37] For example, pattern RCRP-CCP-MXP would require $h^*_{CD} > h^*_{AB}$, $h^*_{AB'} > h^*_{CD}$, and $h^*_{AB} > h^*_{AB'}$, which cannot occur from a single realization of $(h^*_{AB}, h^*_{AB'}, h^*_{CD})$.

[38] Such patterns are empirically possible in our experiment given that we use independent noisy measures of the three Δ terms. Moreover, the frequencies of such patterns give an indication of the prevalence of noise relative to preferences. In the extreme, if all patterns were equally likely, the majority (i.e., $14/27 = 52\%$) would have inconsistencies. Instead, we observe that intransitive patterns represent 26% of overall response patterns, averaging 1.9% of observations per pattern and exceeding 3% in only two cases.

for approximately 73 percent of simulated preferences, but only 44 percent of raw responses. In other words, our simulation shows that these patterns would be even more frequent in the absence of decision noise. The three most prominent weak patterns (marked P12, P23, and P34, to denote the strict preference patterns that they lie between and indicated in light blue) account for eight percent of simulated preferences and 11 percent of raw responses. These patterns would therefore be slightly less frequent in the absence of decision noise. Together, the seven marked patterns account for 81 percent of simulated preferences and 55 percent of raw responses, representing the majority of both. As we show in Section 5, these marked patterns emerge as the seven patterns permitted by the model of upside potential that we posit to capture the observed attraction to probabilistic mixtures between a certain payment and a binary lottery with a higher expected value.

Figure 6: Preference Patterns vs. Data Patterns

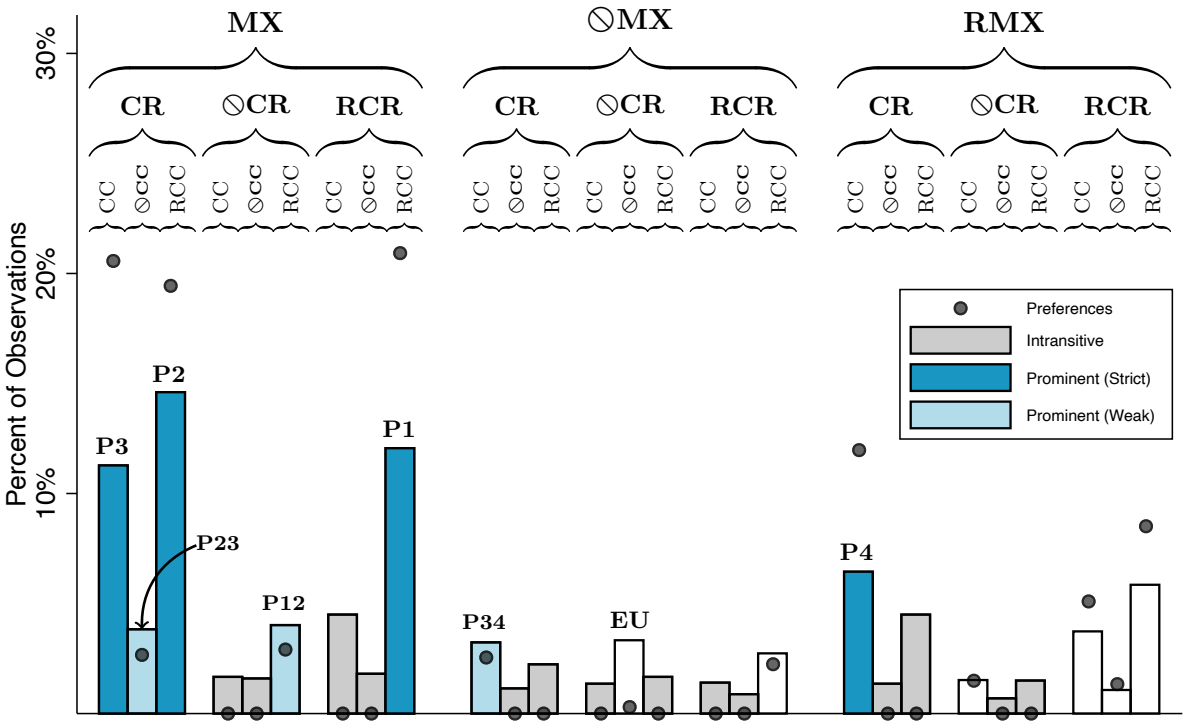

Note: Figure presents histograms of $(sign(\Delta_{CR}), sign(\Delta_{CC}), sign(\Delta_{MX}))$ combinations, where $\Delta_{CR} = h_{AB} - h_{CD}$, $\Delta_{CC} = h_{AB'} - h'_{CD}$, and $\Delta_{MX} = h'_{AB} - h'_{AB'}$, for the 4,204 observations for which we elicit h'_{AB} and $h'_{AB'}$. Each variable can have three potential signs, leading to 27 possible patterns. These signs correspond to the named patterns (e.g., CR to $\Delta_{CR} > 0$, RCR to $\Delta_{CR} < 0$, and ⦸CR to $\Delta_{CR} = 0$). Bars represent the share of raw responses and are identical to those in Figure 5. Black dots represent the share of simulated preferences following the decomposition and simulation described in Section 4.4. Patterns marked in gray denote patterns that would imply an intransitivity absent decision noise. Patterns marked in blue and denoted P1, P2, P3, and P4 are the four most frequent strict patterns. Patterns marked in light blue and denoted P12, P23, and P34 are weak patterns in between these frequent strict patterns. The strict and weak patterns labeled and marked in blue are those that are consistent with our theoretical development in Section 5.

4.5 Connecting Choices and Valuations

Before turning to our rationalization, we return to the connection between choices and valuations, but now we focus on connections at the *individual* level. Our design directly links each stage 2 binary choice to a corresponding stage 1 valuation. More precisely, if in stage 1 a participant provided valuations for a particular (p, r, M), then in stage 2 they made binary choices for a CR problem, a CC problem, and an MX problem for that same (p, r, M) and a randomly chosen payment value H. In other words, each stage 2 binary choice corresponds to a specific row from a corresponding stage 1 price list.

Panels A-C of Figure 7 illustrate that there is a strong connection between participants' stage 1 valuations and their stage 2 choices. In Panel A, the horizontal axis reflects participants' stage 1 Δ_{CR} measures grouped into percentile bins, and the vertical axis denotes the average stage 2 $CRE-RCRE$ within that bin for the corresponding stage 2 binary choice tasks. Panels B and C repeat this exercise for Δ_{CC} and Δ_{MX}. Across panels, stage 1 preference measures are highly predictive of stage 2 choice patterns. The correspondence is not perfect, and in particular, participants are more likely to exhibit the CRE pattern in choices than their Δ_{CR} measure predicts, less likely to exhibit the CCE pattern in choices than their Δ_{CC} measure predicts, and more likely to exhibit the MXE pattern in choices than their Δ_{MX} measure predicts. However, there is clearly a strong link between participants' valuations and their choices.

Panels D-F of Figure 7 shows that the link between stage 1 valuations and stage 2 choices becomes even tighter when we use our decomposition from Section 4.4 to reduce the noise in participants' stage 1 valuations. Specifically, we combine our estimate for the population distribution of preferences with each participant's stage 1 valuations to generate posterior expectations for each participant's $(h^*_{AB}, h^*_{AB'}, h^*_{CD})$ (see Appendix D.4 for details). We then convert those valuations into posterior expectations for each participant's $(\Delta^*_{CR}, \Delta^*_{CC}, \Delta^*_{MX})$, and use those in Panels D-F.[39]

Figure 7 highlights that valuations and carefully selected choices both capture common information about the underlying preferences. As such, it is not clear that either is more reliable for eliciting preferences—contrary to claims that choices are more reliable due to their simplicity and transparency (e.g., Brown and Healy, 2018 and Freeman et al., 2019). Indeed, our analysis demonstrates how using both choices and valuations in tandem can deliver stronger conclusions than either approach alone.

[39] Appendix Figure A.4 illustrates the link between stage 1 elicited indifference values and the corresponding stage 2 choice probabilities; specifically, how the likelihood of choosing A in an AB binary choice task depends on how the randomly selected H for that choice task compares to a participant's stage 1 indifference value h_{AB}. That link is also strong and provides further validation of our approach, but it is less directly related to our conclusions about CRP, CCP, and MXP.

Figure 7: Predicting Stage 2 Results using Stage 1 Valuations

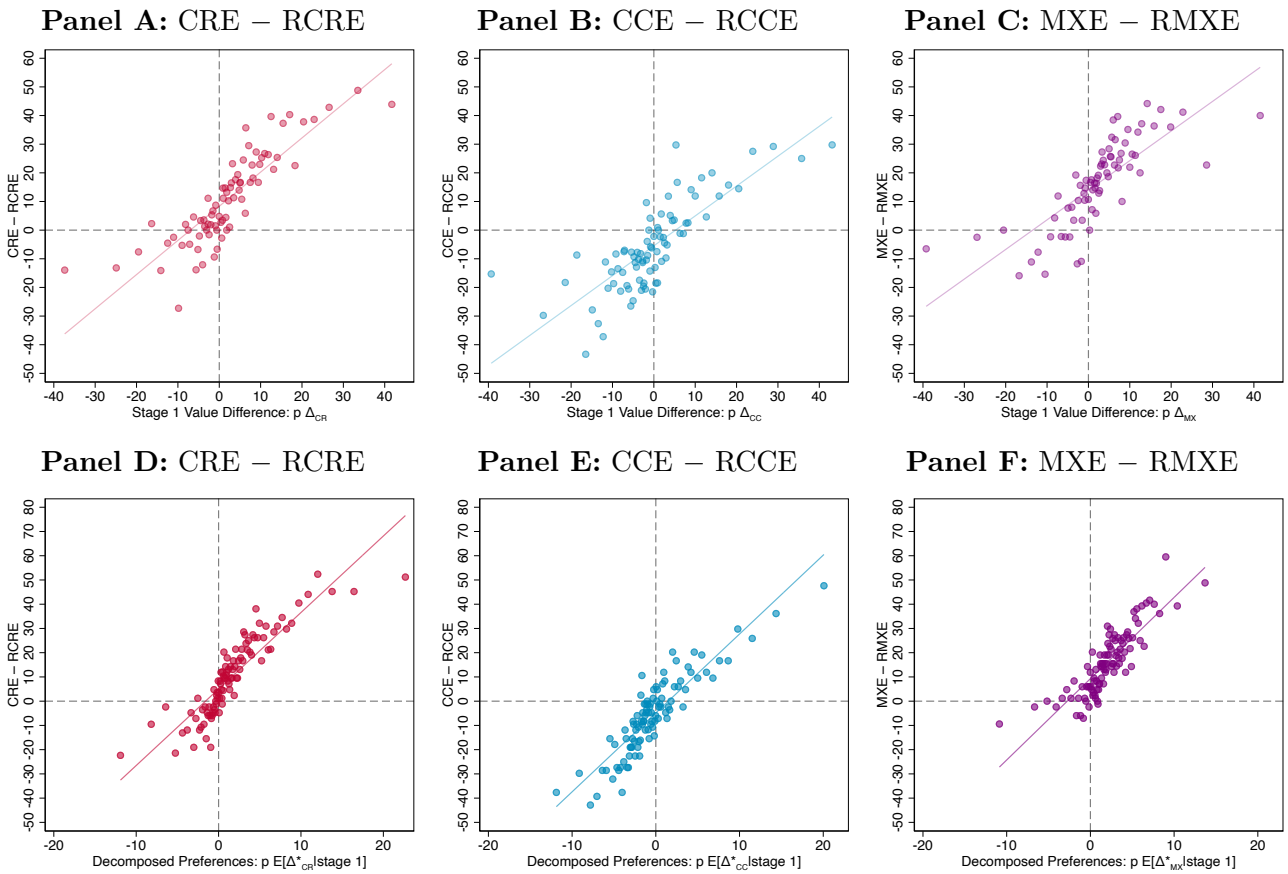

Notes: Figure relates individual measures of stage 1 Δ_{CR}, Δ_{CC}, and Δ_{MX} to stage 2 measures of $CRE - RCRE$, $CCE - RCCE$, and $MXE - RMXE$, respectively. Panels A-C use raw stage 1 responses. Panels D-F use the estimated population distribution of preferences from the decomposition in Section 4.4 combined with a participant's raw stage 1 valuations to generate posterior preference measures $E[\Delta^*_{CR}|\text{stage 1}]$, $E[\Delta^*_{CC}|\text{stage 1}]$, and $E[\Delta^*_{MX}|\text{stage 1}]$ for that participant. For each x-axis, one hundred equally sized bins are constructed, with approximately 84 observations per bin for CR and CC measures and 42 observations per bin for MX measures. Within each bin, the value of stage 2 choice differences is calculated to construct the y-axes. Due to a large number of observations at some values (particularly zero), there are 82, 78, and 74 unique bins in Panels A, B, and C, respectively. To make valuations comparable across (p, r), all stage 1 measures are scaled by p to control for the fact that a fixed value of the measure is predicted to yield a larger stage 2 effect the larger is p (see Appendix C.3 for details).

5 Proposed Rationalization: A Preference for Upside Potential

The modal pattern of CRP-RCCP-MXP and the broader prevalence of MXP violate both EU and the leading parameterized non-EU models in Table 1. Lacking an existing theory that accommodates these findings, we sketch a tentative model that might help to rationalize them; this model turns out to be a previously unstudied version of quadratic utility (Machina, 1982; Chew et al., 1991). While preliminary, we hope our analysis can spur the development of future models of risk preferences.

5.1 A Preference for Upside Potential

To motivate our approach, consider a concrete example from our data. When $p = 0.5$ (and hence $M = p \cdot 30 = 15$) and $r = 0.2$, the mean valuations are $h_{AB} = 38$, $h_{AB'} = 29$ and $h_{CD} = 33$. These valuations imply:

$$A = (15, 1) \sim (38, 0.5) = B, \text{ while } B' = (38, 0.1; 15, 0.8) \succ A, B.$$

The indifference $A \sim B$ reflects risk aversion: Relative to lottery A, lottery B offers higher expected value but also more risk. Now consider what it means to have an MXP where lottery B' is preferred to both A and B: Relative to A, the person wants some of the additional expected value in B at the cost of some of the additional risk, but not all of the additional expected value in B at the cost of all of the additional risk. At first glance, this intuition resembles the classic EU intuition from insurance and finance settings for a person deciding how much risk to accept. However, the EU logic does not hold in this example because the person is considering probabilistic mixtures between lotteries rather than hedging payoff amounts across states. Under EU, probabilistic mixtures between lotteries do not offer hedging benefits.

We consider an alternative psychology in which a person thinks in terms of *upside potential (UP)*: They first identify a set of outcomes that they consider to be "winning" outcomes, and then trade off (i) the total probability of winning versus (ii) an expected valuation of those winnings. Formally, if we let W denote the set of winning outcomes, then the person evaluates a lottery $X \equiv (x_1, q_1; ...; x_N, q_N)$ as

$$U(X) = \underbrace{\left(\sum_{i=1}^{N} q_i u(x_i)\right)}_{EU} + \underbrace{\left(\sum_{j=1}^{N} q_j I(x_j \in W)\right)}_{\substack{\text{probability of} \\ \text{winning something}}} \underbrace{\left(\sum_{k=1}^{N} q_k I(x_k \in W)\kappa(x_k)\right)}_{\substack{\text{expected valuation} \\ \text{of winnings}}}. \tag{2}$$

The first term is standard expected utility. The second term captures preferences for UP as the total probability of winning multiplied by the expected valuation of those winnings.[40] Returning to our motivating example, even when $A \sim B$, the UP model permits B' to improve on both. Relative to B, B' is attractive because it increases the total probability of winning something; relative to A, B' is attractive because it increases the expected valuation of the winnings.

The UP model falls within the broader class of "quadratic utility" models (Machina, 1982; Chew et al., 1991). For discrete lotteries of the form $X \equiv (x_1, q_1; ...; x_N, q_N)$, quadratic utility includes any model that can be written as $U(X) = \sum_{i=1}^{N} \sum_{j=1}^{N} \phi(x_i, x_j) q_i q_j$ for some symmetric function ϕ. For

[40] To keep this model well behaved, we assume that $\kappa(x) \geqslant 0$ for all $x \in W$.

$\phi(x,y) = (u(x)+u(y))/2 + (v(x)w(y)+v(y)w(x))/2$, quadratic utility yields

$$U(X) = \left(\sum_{i=1}^{N} q_i u(x_i)\right) + \left(\sum_{j=1}^{N} q_j v(x_j)\right)\left(\sum_{k=1}^{N} q_k w(x_k)\right),$$

and setting $v(z) = I(z \in W)$ and $w(z) = I(z \in W)\kappa(z)$ gives equation (2).

While this subcase of quadratic utility has not been studied before (to the best of our knowledge), it combines two previously proposed subcases, neither of which can explain our empirical patterns. Machina (1982) explores the case where $U(X) = \left(\sum_{i=1}^{N} q_i u(x_i)\right) + \left(\sum_{j=1}^{N} q_j v(x_j)\right)^2$; that is, the sum of an expected-utility functional and a second expected-utility functional squared (with $v(x) \geqslant 0$ for all x). Chew et al. (1991) discuss Machina's case and also $U(X) = \left(\sum_{i=1}^{N} q_i v(x_i)\right)\left(\sum_{j=1}^{N} q_j w(x_j)\right)$; that is, the product of two different expected-utility functionals (with $v(x) \geqslant 0$ and $w(x) \geqslant 0$ for all x). The former can generate a CRP and a CCP when $v(x) \neq u(x)$, but—as noted by Chew et al. (1991)—it also generates an aversion to mixtures of any two lotteries. Hence, in our context, the Machina specification would predict a global RMXP, which is inconsistent with our data. Chew et al. (1991) show that the latter generates preferences with an attraction to mixtures of any two lotteries, and thus in our context, it would predict a global MXP. We show it further generates a global ⃠CRP and RCCP. Because the vast majority of our data cover patterns other than ⃠CRP-RCCP-MXP, this case is also inconsistent with our data.[41]

Before deriving predictions for the UP model in equation (2), we must specify which outcomes the person considers "winning" outcomes. For our setting in which people face only binary and trinary lotteries that yield either zero or a positive amount, a natural assumption is that all strictly positive outcomes are in the set of winning outcomes W while zero is not (we discuss this assumption more in Section 5.3). Applying this assumption, and normalizing $u(0) = 0$,[42] equation (2) implies that the triplet $(h^*_{AB}, h^*_{AB'}, h^*_{CD})$ solves

$$u(M) + \kappa(M) = pu(h^*_{AB}) + p^2\kappa(h^*_{AB}) \tag{3}$$

$$u(M) + \kappa(M) = pru(h^*_{AB'}) + (1-r)u(M) + (pr + 1 - r)\left[pr\kappa(h^*_{AB'}) + (1-r)\kappa(M)\right] \tag{4}$$

$$ru(M) + r^2\kappa(M) = pru(h^*_{CD}) + (pr)^2\kappa(h^*_{CD}). \tag{5}$$

In Appendix E.1, we formally derive predictions from these equations, including the following proposition:

[41] See Appendix E.2 for details, including the ϕ functions that correspond to the two cases described in the text, and for a formal derivation of their predictions. Masatlioglu and Raymond (2016) show that the Kőszegi and Rabin (2007) model of loss aversion under CPE also falls within the class of quadratic utility models; its predictions (Table 1) also do not fit our data.

[42] This normalization merely simplifies these equations; in Appendix E.1, we present these equations and prove all results without making this normalization.

Proposition 1. Suppose that $(h^*_{AB}, h^*_{AB'}, h^*_{CD})$ is derived from equations (3), (4), and (5). For any $u(x)$ that is strictly increasing in x and $\kappa(x)$ that is strictly increasing in x and has $\kappa(x) \geqslant 0$ for all $x > 0$, a person must exhibit one of the following seven patterns of behavior:[43]

P1: $0 > \Delta^*_{CR} > \Delta^*_{CC}$ and $\Delta^*_{MX} > 0$ (RCRP−RCCP−MXP)

P12: $0 = \Delta^*_{CR} > \Delta^*_{CC}$ and $\Delta^*_{MX} > 0$ ($\oslash$CRP−RCCP−MXP)

P2: $\Delta^*_{CR} > 0 > \Delta^*_{CC}$ and $\Delta^*_{MX} > 0$ (CRP−RCCP−MXP)

P23: $\Delta^*_{CR} > \Delta^*_{CC} = 0$ and $\Delta^*_{MX} > 0$ (CRP−$\oslash$CCP−MXP)

P3: $\Delta^*_{CR} > \Delta^*_{CC} > 0$ and $\Delta^*_{MX} > 0$ (CRP−CCP−MXP)

P34: $\Delta^*_{CR} = \Delta^*_{CC} > 0$ and $\Delta^*_{MX} = 0$ (CRP−CCP− $\oslash$MXP)

P4: $\Delta^*_{CC} > \Delta^*_{CR} > 0$ and $\Delta^*_{MX} < 0$ (CRP−CCP−RMXP).

Proposition 1 establishes the empirical content of the UP model: Only seven of the 13 possible transitive patterns of behavior can occur. Recall that Figure 6 in Section 4.4 plots histograms of raw response patterns and decomposed preference patterns that emerge in our data, and we label the seven patterns in Proposition 1. In the histogram of decomposed preference patterns, the seven patterns from Proposition 1 account for 81 percent of observations, with the other six possible patterns accounting for only 19 percent. Moreover, in the histogram of raw response patterns—which also admits 14 additional intransitive patterns that can emerge only due to noise—the seven patterns from Proposition 1 still account for 55 percent, with the other six possible transitive patterns accounting for only 18 percent. Thus, the restrictions imposed by the UP model seem to accord well with the patterns we observe in our data.[44]

Proposition 2 refines Proposition 1 for the special case where $u(x) = x$, allowing us to isolate the role of the UP term in generating novel predictions.[45]

Proposition 2. Suppose that $(h^*_{AB}, h^*_{AB'}, h^*_{CD})$ is derived from equations (3), (4), and (5). If $u(x) = x$, then:

(1) If $\kappa(x)$ is strictly increasing in x and has $\kappa(x) \geqslant 0$ for all $x > 0$, then:

(a) If $ph^*_{AB} > M$ (i.e., if the person is risk averse in the AB decision), then $\Delta^*_{CR} > 0$ and thus

[43] Patterns including only strict preferences are denoted by single numbers, while patterns including a weak preference (e.g., $\oslash$CRP) are denoted by two numbers referring to the two corresponding strict-preference patterns.

[44] In the histogram of raw response patterns, five of the six transitive patterns that UP rules out occur at roughly the same rate as the intransitive patterns that arise only due to noise: The two strict transitive patterns each occur as often as each of the two strict intransitive preferences, and three of the four weak transitive preferences occur roughly as often as each of the 12 weak intransitive preferences. The exception is the (weak) EU pattern ruled out by the UP model, which occurs at a rate similar to the weak transitive patterns permitted by the model.

[45] For the reasons articulated in Rabin (2000) and Rabin and Thaler (2001), to the extent that $u(x)$ is meant to capture a standard EU motivation, it might be natural assume approximate linearity for u given the small stakes on our experiment. Such an assumption would be analogous to the suggestion in Kőszegi and Rabin (2007) to assume concave utility for large stakes but linear utility for small stakes, where the latter can be interpreted as a local approximation for the former.

the person must exhibit one of patterns P2, P23, P3, P34, or P4.

(b) If $ph^*_{AB} = M$ (i.e., if the person is risk neutral in the AB decision), then $\Delta^*_{CR} = 0$ and thus the person must exhibit pattern P12.

(c) If $ph^*_{AB} < M$ (i.e., if the person is risk loving in the AB decision), then $\Delta^*_{CR} < 0$ and thus the person must exhibit pattern P1.

(2) If $\kappa(x) = \phi x$ for some $\phi > 0$, then $ph^*_{AB} > M$ (i.e., the person is risk averse in the AB decision), $\Delta^*_{CR} > 0$, and $\Delta^*_{MX} > 0$, and thus the person must exhibit one of patterns P2, P23, or P3.

Part 1 of Proposition 2 provides additional testable predictions of the UP model that hold if the EU term is approximately linear. First, whether people exhibit risk aversion or risk tolerance in their AB decision is a sufficient statistic for whether they exhibit CRP or RCRP. Second, whether people exhibit risk aversion or risk tolerance in their AB decision also predicts a partial separation into preference patterns. We test these predictions using an approach analogous to that described in Section 4.5 (see in particular the notes for Figure 7) in which we use our posterior valuation estimates to construct an individual-level risk aversion measure in the AB task ($E[ph^*_{AB} - M|\text{stage 1}]$) and a corresponding CRP measure ($E[\Delta^*_{CR}|\text{stage 1}]$). We then analyze the relationship between the signs of these variables. Roughly 13 percent of observations exhibit risk tolerance, $E[ph^*_{AB} - M|\text{stage 1}] < 0$; of these, the majority (55 percent) exhibit RCRP. The remaining 87 percent of observations exhibit risk aversion; of these, the majority (69 percent) exhibit CRP. Thus, risk aversion is significantly correlated with CR preferences as the UP model predicts (Fisher's exact test $p < 0.001$). Extending this analysis to the posterior calculations for broader CR-CC-MX preference patterns, we find that for risk tolerant observations with $E[ph^*_{AB} - M|\text{stage 1}] < 0$, 48% exhibit P1 as predicted by Proposition 2, while 21% of risk averse observations exhibit P1 (Fisher's exact test $p < 0.001$). In contrast for risk averse observations, 69% exhibit P2, P3, or P4 as predicted by Proposition 2 (no posterior calculations indicate the intermediate P12, P23, or P34 patterns), while 45% of risk tolerant observations exhibit P2, P3, or P4 (Fisher's exact test $p < 0.001$). Thus, risk aversion is also significantly correlated with the nature of CR-CC-MX preferences as the UP model predicts.

For the interested reader, Proposition 2 also helps to clarify some of the mathematical mechanics in the UP model. In particular, Part 2 of Proposition 2 highlights that the basic structure of the UP model—specifically, how probabilities enter the UP term in equation (2)—creates a propensity to exhibit risk aversion in the AB decision and both a CRP and an MXP. The source of risk aversion in the AB decision is straightforward: A linear u means that the EU term argues for risk neutrality; when κ is also linear, the UP term argues for risk aversion in the AB choice, as the risky option B has its probability squared, thus making it less valuable. The combined impact of EU and UP terms is thus risk aversion in the AB problem.

The logic for why a person exhibits a CRP is related. Relative to the AB decision, scaling down the winning probabilities by a common ratio r scales down the EU term by r but scales down the UP term by r^2, and thus makes the UP term relatively less important. Since the UP term is the source of risk aversion, the net impact is that scaling down the winning probabilities by a common ratio r causes the person to become less risk averse—that is, they have a CRP.

The logic for why an MXP arises is more nuanced. Suppose $A \sim B$, recall $B' = (1-r)A + rB$, and consider how $U(B')$ varies with r. As r changes, there are two effects on the UP term. First, an increase in r leads to a reduction in the probability of winning, which creates a motive to make r small. Second, an increase in r leads to a change in the expected valuation of winnings. If there is risk aversion in the AB decision, increasing r leads to an increase in the expected valuation of winnings, which creates a motive to make r large. When κ is linear, the latter effect dominates for r small, while the former effect dominates for r large, hence why an intermediate r can be better than both $r = 0$ and $r = 1$—i.e., there is an MXP.

Of course, Part 1 of Proposition 2 highlights how, even if u is linear, nonlinearity in κ can generate all seven possible patterns from Proposition 1, and the logic for linear κ helps to explain when different patterns emerge for nonlinear κ. As long as there is risk aversion in the AB decision (which relies on κ not being too convex over the relevant range), the person will exhibit a CRP. But unlike for linear κ, Part 1a permits that there might be ⃠MXP or RMXP, which occur when κ is sufficiently concave over the relevant range. Parts 1b and 1c highlight that with a nonlinear κ there could be risk neutrality or risk loving in the AB decision (which occur when κ is sufficiently convex over the relevant range), in which case the person would exhibit ⃠CRP or RCRP, respectively. For these cases, the person must exhibit an MXP and a RCCP.

5.2 The Shape of the $\kappa(x)$ Function

We observe all seven response patterns predicted by Proposition 1 in our data, which, by Proposition 2, suggests a nonlinear κ function. To gain some initial insight into the possible shape of κ, we estimate it on our aggregate valuation data, identifying it from experimental variation in (p, r) combinations. Because our model is post-hoc and the experiment was not designed specifically to identify or estimate the shape of the κ function, we urge caution in interpreting this estimation. Nonetheless, we hope this analysis offers useful guidance for future modeling.

Our data include 60 aggregate valuations: the mean responses for h_{AB}, $h_{AB'}$, and h_{CD} for each of the 20 (p, r) combinations. Equations (3) to (5) implicitly define h^*_{AB}, $h^*_{AB'}$, and h^*_{CD} as a function of the experimental parameters (p, r, M) and the functions u and κ. To isolate the role of UP, we set $u(x) = x$, making the κ function the only object to estimate.

We parameterize the κ function as $\kappa(z; \theta)$ where θ is a vector of parameters to be estimated, and

estimate θ using non-linear least squares on the 60 observations assuming

$$h_{XY} = h^*_{XY}(p, r, M, \theta) + \epsilon \qquad \text{for } XY \in \{AB, AB', CD\}.$$

Appendix F describes the estimation details and provides the complete parameter estimates.

Lacking a strong a priori sense of the shape of κ, we begin with a flexible specification. In our 60 observations, $\kappa(z;\theta)$ is evaluated at $M = \{9, 15, 24, 27\}$ as well as values of h ranging from approximately 24 to 45. We therefore specify a five-parameter, continuous piecewise-linear form for κ with knots at 9, 15, 24, and 27.[46] The resulting estimate, shown in Panel A of Figure 8, exhibits an S-shape: convex for low values of z and concave for higher values. The estimated model captures a large share of the variation in h_{AB}, h'_{AB}, and h_{CD} across values of (p, r), yielding $R^2 = 0.76$ and an $MSE = 3.53$.[47] The correlation between predicted and observed h is 0.91, and the correlation for the corresponding Δ terms is 0.90 (see Appendix Figure A.5 Panel A). Figure 8 also clarifies the data limitations of our current design for estimation: κ is evaluated at only 4 points below $x = 30$ (the values of M fixed in the design) and then a cluster of points around $x = 35$.

Motivated by the S-shape in panel A of Figure 8, Appendix F.2 explores several parameterized functional forms for κ. Among these, the best fit is a three-parameter scaled logistic:

$$\kappa(z;\boldsymbol{\theta}) = \theta_1 \left[\frac{1}{1 + \exp(-\theta_2(z - \theta_3))} \right], \quad \theta_1, \theta_2, \theta_3 > 0. \tag{6}$$

Panel B of Figure 8 shows the estimated κ under this specification. Despite its parsimony, this parameterization retains substantial predictive accuracy with $R^2 = 0.52$, $MSE = 6.99$, a correlation between predicted and actual h of 0.84, and a correlation between predicted and actual Δ of 0.87 (see Appendix Figure A.5 panel B).

The three-parameter sigmoid performs reasonably well in-sample, suggesting that it could be used to generate predictions that shed light on the implications and limitations of the UP model. However, the fact that it is bounded above makes it ill-suited for global predictions. Moreover, because it substantially underperforms the piece-wise linear function in panel A, there is clear scope for identifying better parameterized functional forms. Such an exercise would be better pursued with alternative data that are intentionally designed to estimate κ.[48]

[46] In Appendix F, we report a version with an additional knot at 36. Since that model performs similarly, we retain the five-parameter version as our preferred specification.

[47] $R^2 = 1 - RSS/TSS$, where RSS is the sum of squared residuals between the estimated model and the data, and TSS is the sum of squared deviations to the average h across all 60 observations. Negative values indicate that predicting the mean for every observation would yield a better fit than the estimated model.

[48] In Appendix G.1, we estimate both original prospect theory (OPT) and cumulative prospect theory (CPT) with a flexible functional form for the probability weighting function $\pi(q)$ specified as a six-part piece-wise linear functional form that permits (but does not require) discontinuities at $q = 0$ and $q = 1$. Both models substantially underperform the UP estimates reported in the text.

Figure 8: Estimates for $\kappa(z;\theta)$ under Upside-Potential Model

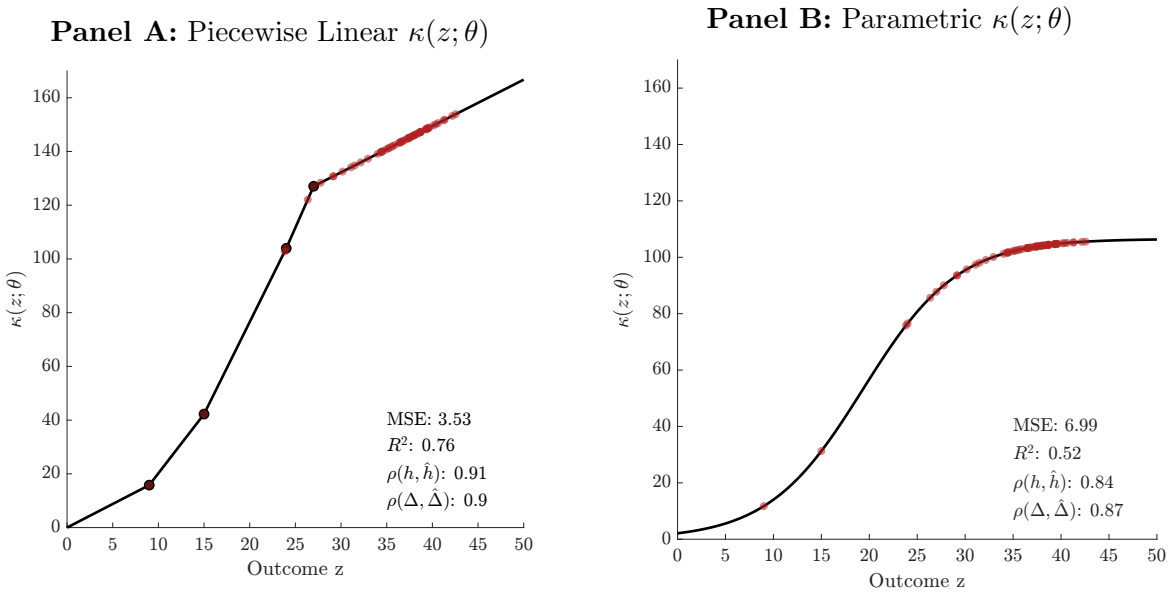

Notes: Figure presents estimates for $\kappa(z;\theta)$ under the UP model. The estimation is conducted using non-linear least squares with 60 observations of mean responses for h_{AB}, $h_{AB'}$, and h_{CD} (20 observations for each). Panel A presents estimates for $\kappa(z;\theta)$ when using a five-part piecewise linear formulation, and Panel B presents estimates for $\kappa(z;\theta)$ when using a three-parameter functional form for κ. Light red points in each panel correspond to locations where the function is evaluated in estimation. In panel A, black dots denote kinks in the piecewise linear formulation; in the estimation, the function is evaluated 15 times at each kink point. Each panel also presents fit values of mean squared error (MSE), in-sample R^2, correlation between predicted and actual h values, and correlation between predicted and actual Δ values. The in-sample R^2 is given by $1 - RSS/TSS$, where TSS is the sum of squared deviations to the average h among the 60 observations, and RSS is the sum of squared residuals between the estimated model to the data. See Appendix F.2 for details.

5.3 Other Implications and Limitations

Although several predictions of the UP model align well with our data, it is a post-hoc rationalization meant to stimulate future theorizing. To help inform such work, we outline some additional testable predictions of the model and discuss several of its limitations.

In Appendix E.3, we derive predictions of the UP model for indifference curves in a Marschak-Machina triangle. The model predicts that five patterns are possible, and these are presented in Figure 9.[49] In Panel A, a single linear indifference curve (shown in bold) separates convex (mixture-loving) indifference curves to the left and concave (mixture-averse) indifference curves to the right. In this case, the average slopes of the indifference curves must fan out everywhere.[50] Panel B shows the case where all indifference curves are concave, which also requires fanning out everywhere. Panels C,

[49] To help connect these five patterns of indifference curves to the seven patterns of behavior in Proposition 1, each panel in Figure 9 depicts a set of five points that would correspond to one (p, r) combination in our experiment (A, B, B', C and D), where we have chosen B such that $A \sim B$. See Appendix E.3 for details.

[50] We label an indifference curve as convex versus concave based on its shape in a Marschak-Machina triangle with q_L and q_H on the axes. Given this labeling, convex (concave) indifference curves correspond to locally quasi-concave (quasi-convex) preferences. Each indifference curve connects a point on either the horizontal axis or vertical axis to a point on the hypotenuse; "average slope" refers to the slope of the line segment that connects these two points. See Appendix E.3 for formal statements.

D, and E show cases where all indifference curves are convex: For all three cases, indifference curves fan out to the left of the AB indifference curve, but the cases differ in whether the average slopes of indifference curves to the right of the AB indifference curve fan out, remain constant, or fan in.

The indifference curves in Figure 9 suggest two testable predictions. First, although the UP model allows average slopes to fan out, remain constant, or fan in to the right of the AB indifference curve (permitting CRP, $\oslash$CRP, or RCRP), it requires fanning out to the left of the AB indifference curve. Hence, when comparing an AB decision to the EF decision depicted in each panel, the UP model predicts greater risk aversion in the latter.[51] Second, in any given triangle, indifference curves can transition from convex to concave at most once, and if there is a transition it must be from convex in the upper left to concave in the lower right. Hence, for instance, if a person exhibits an aversion to mixtures of lotteries A and B, then they must also exhibit an aversion to mixtures of any two lotteries to the right of A and B, such as mixtures of C and D. Analogously, if a person exhibits an attraction to mixtures of A and B, then they must also exhibit an attraction to mixtures of any two lotteries to the left of A and B, such as mixing lotteries E and F. Our data cannot speak to either of these predictions; collecting data along these lines might help guide future theorizing.

Beyond proposing new testable predictions, it is also useful to ask whether the UP model can accommodate established empirical regularities. For instance, one reliable empirical finding is that certainty equivalents for binary lotteries—i.e., an m such that $(m, 1) \sim (H, p)$—tend to exhibit risk aversion ($m < pH$) for larger p but risk tolerance ($m > pH$) for smaller p (see, e.g., Tversky and Kahneman, 1992). In Appendix E.4, we demonstrate that the UP model with an S-shaped κ function similar to the one we estimate can naturally generate this pattern.

While the UP model seems to perform well in some domains, it has some important limitations. First, not all prior empirical findings are well accommodated by the UP model. For example, some prior papers find a CRE for paired choice tasks when each choice task involves options with equal expected values.[52] The UP model can accommodate this pattern, but only if we assume that the expected-utility term in the model has a convex u (see Appendix E.5 for details). Because this is contrary to the more usual EU assumption that u is concave and (perhaps) approximately linear for small stakes, our formulation of the UP model may not accommodate this pattern.

Second, although we have developed the UP model to in principle be portable to other contexts,

[51] The asymmetry around the AB indifference curve arises because lotteries along the vertical axis (such as E) guarantee a winning outcome, whereas lotteries on the hypotenuse and along the horizontal axis have some possibility of not winning.

[52] In Table 1 in Blavatskyy et al. (2023), the 11 CR experiments with "Probability of highest outcome in risky lottery in the first question" equal to "Ratio of middle to highest outcome" involve choices between lotteries with equal expected values. Another prominent example is a more general form of common ratio effect, subproportionality, demonstrated in problems 7 and 8 in Kahneman and Tversky (1979); while this latter example is outside the domain of our study in that lottery A is not a certain lottery, an analogous result to that in Appendix E.5 still applies. While our discussion here assumes that these observed CRE patterns for equal-expected value lotteries have some preference component, we remind the reader that, because they are found using paired choice tasks, they could be due to choice noise (as discussed in Section 2.5).

Figure 9: Upside Potential Indifference Curves

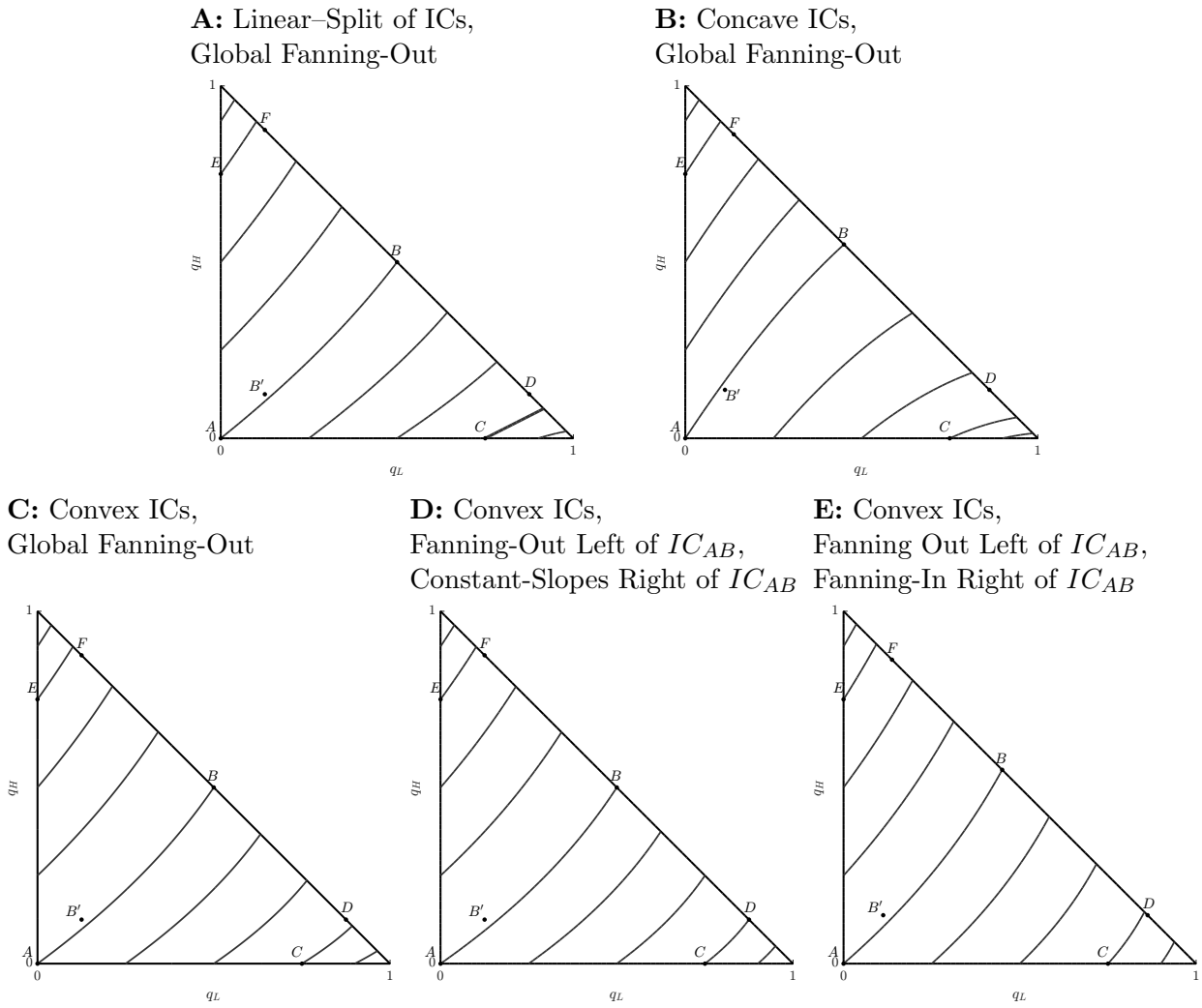

Notes: Figure depicts the five possible patterns of indifference curves (ICs) that can arise in a Marschak–Machina (MM) Triangle under the UP model (see Appendix E.3). Each triangle depicts lotteries with outcomes H, M, and 0 and associated probabilities q_H, q_M, and q_L. Lotteries $A = (M, 1)$, $B = (H, p)$, $C = (M, r)$, $D = (H, rp)$, and $B' = (H, rp; M, 1 - r)$ correspond to one (p, r) combination in our experiment, where we have chosen p such that $A \sim B$; lotteries $E = (H, s; M, 1 - s)$ and $F = (H, s + (1 - s)p)$ are the analogues to lotteries C and D but located in the upper-left corner. In Panel A, there is one linear indifference curve (shown in bold), where indifference curves are convex to its left and concave to its right, and where average slopes fan out throughout. The linear indifference curve could be anywhere in the triangle. In Panel B, all indifference curves are concave, and average slopes fan out throughout. In Panels C, D, and E, all indifference curves are convex, and average slopes fan out to the left of the AB indifference curve which we denote as IC_{AB} for convenience; the panels differ in that average slopes to the right of the AB indifference curve can fan out (Panel C), be constant (Panel D), or fan in (Panel E). See Appendix E.3 for a discussion of how these five patterns of indifference curves connect to the seven possible patterns of behavior in Proposition 1.

there are open questions in how to do so. Perhaps most notable is the question of what determines the set W of winning outcomes. In our setting, we adopt the natural assumption that positive outcomes are winning outcomes while zero is not. To apply the model more broadly, we need a more principled definition of this set—and data designed to assess it. This issue is analogous to the definition of the

reference point in prospect theory and other reference-dependent models. As in that literature, one might assume some exogenous rule, or allow a person's assessment of winning outcomes to depend on features of the choice set (in the spirit of Kőszegi and Rabin, 2007).

A related issue is that a person could have an analogous concern for *downside potential*. In other words, a person might also identify a set of outcomes that they consider to be "losing" outcomes, and then trade off the total probability of losing versus an expected (negative) valuation of those losses. A better understanding of when and how individuals focus on the upside or downside of a lottery is crucial for applying the UP model (or related models) more broadly.

Finally, and more speculatively, the κ function itself may be context dependent. In particular, it is not at all clear that a κ function estimated on small stakes would extrapolate well for making predictions on large stakes. Indeed, an outcome of \$30 might generate substantial "upside" utility in the context of our experiment, but if we re-ran our experiment with all stakes increased by a factor of 10, the same outcome of \$30 might generate very little "upside" utility.

The UP model that we develop is merely a first attempt to rationalize our data given that they are inconsistent with leading parameterized non-EU models. By delineating the ways in which it does well while also highlighting its limitations, we hope our analysis can spur the development of future models of risk preferences.

6 Discussion

In this paper, we study connected CR-CC-MX problems across a broad range of experimental parameters. While our empirical findings for mean preferences match the common wisdom of CRP, CCP, and near-zero MXP when using canonical experimental parameters, we find a robust pattern of CRP-RCCP-MXP at other experimental parameters. More generally, our empirical results highlight how mean preference patterns can be sensitive to experimental parameters and that there can be substantial heterogeneity in these patterns. Because these empirical results are inconsistent with both EU and leading non-EU models, we posit a theoretical model motivated by the prevalence of MXP in our data. Encouragingly, this approach to accommodating MXP also explains the modal CRP-RCCP-MXP pattern we observe, and successfully predicts some more nuanced patterns in our data, suggesting it might provide useful direction for future theoretical work. We conclude by discussing some broader implications of our analysis.

Our analysis highlights the benefits of studying connected phenomena over a broad range of the parameter space to deliver both a richer picture of preferences and sharper tests of existing theories. Many prominent non-standard models of preferences—in domains such as risk, ambiguity, intertemporal choice and beyond—are built on data from a few canonical examples, with limited empirical insights of how behavior might be sensitive to relevant features of the decision problem.

Moreover, the prior literature has often studied non-standard choice problems in isolation rather than together. A more comprehensive empirical foundation for evaluating theories emerges by jointly studying multiple preference features across a broad range of parameters.

Our analysis also reinforces a key methodological point from McGranaghan et al. (2024) that cautions against using only binary choice data when making comparisons across decisions and instead encourages also using valuation data for such comparisons. Many behavioral "effects" are based on evidence from comparisons of paired binary choice tasks. In our data, the CR, CC, and MX problems all show hallmarks of the confounds induced by differential noise, indicating that binary choice data could present a biased picture of the underlying preferences unless problem parameters are carefully chosen. Our binary choice data ultimately generate the same qualitative conclusions as our valuations data due to our deliberate selection of balanced problems with offsetting bias—a selection made possible by the fact that we had pilot data on valuations. In the future, researchers analyzing behavioral effects should consider the potential for bias in isolated choice problems, mitigate this bias through careful selection of offsetting problems where possible, and complement choice data with valuation data to deliver stronger conclusions than either approach alone.

Our analysis relates to a nascent literature that explores deliberate randomization (i.e., mixing) between lotteries (Agranov and Ortoleva, 2017; Dwenger et al., 2018; Feldman and Rehbeck, 2022; Agranov et al., 2023; Agranov and Ortoleva, 2023). These studies typically present individuals with the same decision problem multiple times, either mixed throughout the study or repeated explicitly in a row, and randomization manifests as making different choices across repetitions. A notable limitation of such designs is that they cannot reveal an RMXP. Nonetheless, deliberate randomization between two successive presentations of an AB choice is clearly consistent with exhibiting an MXP in our context. Future work could explore whether there is an empirical connection between these behaviors by testing whether the people who exhibit an MXP in paired decision tasks are the same as those who exhibit deliberate randomization in two successive presentations of an AB choice.[53] Exploring the empirical connection seems particularly apt given the different theoretical explanations for mixture preferences here and elsewhere. In particular, a common rationalization of purposeful randomization in the prior literature has been the theory of cautious expected utility (Cerreia-Vioglio et al., 2015) (CEU), but CEU maintains betweenness in comparisons with degenerate lotteries like lottery A in our study, and thus it cannot accommodate the type of mixture preferences we study and observe. Additionally, the UP model permits conditions under which individuals are averse to mixtures, rather than always exhibiting a systematic preference for them.

On the surface, our empirical finding of an MXP and the proposed rationalization in the form of our UP model may seem to contradict recent work suggesting that decisionmakers penalize lotteries

[53] In the spirit of such exercises, Feldman and Rehbeck (2022) link non-constant responses in successive presentations to preferences for mixtures elicited directly as a choice of convex combinations between lotteries.

with greater numbers of outcomes (Bernheim and Sprenger, 2020; Fudenberg and Puri, 2022; Puri, 2025). However, that work focuses on different types of lotteries and, therefore, could be consistent with our results. For example, Bernheim and Sprenger (2020) find that people prefer binary lotteries to nearby trinary lotteries that are constructed by splitting one of the binary lottery payments into two equally likely payments while retaining the same expected value. This comparison is very different from our MX problem. Moreover, the UP model can accommodate both phenomena. As we discuss in Section 5.1, our model generates an MXP even with a linear κ function. At the same time, whether a person is averse to the type of lottery splitting studied by Bernheim and Sprenger (2020) is related to the local concavity or convexity of κ around the split outcome, with local concavity implying an aversion to splits (see Appendix E.6 for details). Investigating these connections is a promising direction for future work.

Finally, and most importantly, our results call for the development of new models of risk preferences alongside the development of a more complete empirical foundation for risky choice. Our empirical findings are at odds with both EU and leading non-EU models. We have taken a first step in postulating a post-hoc model that performs well on the narrow domain of our data, but it is clearly not a complete account of risky choice. CR-CC-MX problems represent a tiny fraction of risky choices and extending the domain through principled exploration of problems away from this structure is a critical next step. We hope the psychology of upside potential, and its novel perspective on the potential source of risk attitudes, will prove useful for guiding such empirical explorations and the theories that will follow.

References

Agranov, M., Healy, P. J., and Nielsen, K. (2023). Stable randomisation. *Economic Journal*, 133(655):2553–2579.

Agranov, M. and Ortoleva, P. (2017). Stochastic choice and preferences for randomization. *Journal of Political Economy*, 125(1):40–68.

Agranov, M. and Ortoleva, P. (2023). Ranges of randomization. *Review of Economics and Statistics*.

Allais, M. (1953). Le comportement de l'homme rationnel devant le risque: critique des postulats et axiomes de l'école américaine. *Econometrica*, 21(4):503–546.

Bateman, I. and Munro, A. (2005). An experiment on risky choice amongst households. *The Economic Journal*, 115(502):C176–C189.

Bell, D. E. (1985). Disappointment in decision making under uncertainty. *Operations research*, 33(1):1–27.

Bernheim, B. D., Royer, R., and Sprenger, C. (2022). Robustness of rank independence in risky choice. *AEA Papers and Proceedings*, 112:415–420.

Bernheim, B. D. and Sprenger, C. (2020). On the empirical validity of cumulative prospect theory: Experimental evidence of rank-independent probability weighting. *Econometrica*, 88(4):1363–1409.

Blavatskyy, P., Ortmann, A., and Panchenko, V. (2022). On the experimental robustness of the Allais paradox. *American Economic Journal: Microeconomics*, 14(1):143–63.

Blavatskyy, P., Panchenko, V., and Ortmann, A. (2023). How common is the common-ratio effect? *Experimental Economics*, pages 253–272.

Blavatskyy, P. R. (2006). Violations of betweenness or random errors? *Economics Letters*, 91(1):34–38.

Blavatskyy, P. R. (2010). Reverse common ratio effect. *Journal of Risk and Uncertainty*, 40(3):219–241.

Brown, A. L. and Healy, P. J. (2018). Separated decisions. *European Economic Review*, 101:20–34.

Burke, M. S., Carter, J. R., Gominiak, R. D., and Ohl, D. F. (1996). An experimental note on the Allais paradox and monetary incentives. *Empirical Economics*, 21(4):617–632.

Camerer, C. F. and Ho, T.-H. (1994). Violations of the betweenness axiom and nonlinearity in probability. *Journal of Risk and Uncertainty*, 8(2):167–196.

Cerreia-Vioglio, S., Dillenberger, D., and Ortoleva, P. (2015). Cautious expected utility and the certainty effect. *Econometrica*, 83(2):693–728.

Chapman, J., Dean, M., Ortoleva, P., Snowberg, E., and Camerer, C. (2023). Econographics. *Journal of Political Economy Microeconomics*, 1(1):115–161.

Chew, S. H. (1983). A generalization of the quasi-linear mean with applications to the measurement of income inequality and decision theory resolving the Allais paradox. *Econometrica*, 51(4):1065–1092.

Chew, S. H., Epstein, L. G., and Segal, U. (1991). Mixture symmetry and quadratic utility. *Econometrica: Journal of the Econometric Society*, pages 139–163.

Chew, S. H. and MacCrimmon, K. (1979). Alpha utility theory, lottery composition, and the allais paradox. *Working paper*, 686.

Chew, S. H. and Waller, W. S. (1986). Empirical tests of weighted utility theory. *Journal of Mathematical Psychology*, 30(1):55–72.

Dean, M. and Ortoleva, P. (2019). The empirical relationship between nonstandard economic behaviors. *Proceedings of the National Academy of Sciences*, 116(33):16262–16267.

Dekel, E. (1986). An axiomatic characterization of preferences under uncertainty: Weakening the independence axiom. *Journal of Economic Theory*, 40(2):304–318.

Dwenger, N., Kübler, D., and Weizsäcker, G. (2018). Flipping a coin: Evidence from university applications. *Journal of Public Economics*, 167:240–250.

Feldman, P. and Rehbeck, J. (2022). Revealing a preference for mixtures: An experimental study of risk. *Quantitative Economics*, 13:761–786.

Freeman, D. J., Halevy, Y., and Kneeland, T. (2019). Eliciting risk preferences using choice lists. *Quantitative Economics*, 10(1):217–237.

Fudenberg, D. and Puri, I. (2022). Simplicity and probability weighting in choice under risk. *American Economic Review: Papers & Proceedings*, 122:421–425.

Gul, F. (1991). A theory of disappointment aversion. *Econometrica*, 59(3):667–686.

Huber, C., Dreber, A., Huber, J., Johannesson, M., Kirchler, M., Weitzel, U., Abellán, M., Adayeva, X., Ay, F. C., Barron, K., et al. (2023). Competition and moral behavior: A meta-analysis of forty-five crowd-sourced experimental designs. *Proceedings of the National Academy of Sciences*, 120(23):e2215572120.

Ingersoll, J. (2008). Non-monotonicity of the Tversky-Kahneman probability-weighting function: A cautionary note. *European Financial Management*, 14(3):385–390.

Jain, R. and Nielsen, K. (2024). A systematic test of the independence axiom near certainty. *Working Paper*.

Kahneman, D. and Tversky, A. (1979). Prospect theory: An analysis of decision under risk. *Econometrica*, 47(2):263–292.

Kobayashi, S. J. and Lucia, A. (2023). Robust estimation of risk preferences. *Working Paper*.

Kőszegi, B. and Rabin, M. (2007). Reference-dependent risk attitudes. *American Economic Review*, 97(4):1047–1073.

Lattimore, P. K., Baker, J. R., and Witte, A. D. (1992). The influence of probability on risky choice: A parametric examination. *Journal of Economic Behavior and Organization*, 17(3):377–400.

Loomes, G. and Sugden, R. (1986). Disappointment and dynamic consistency in choice under uncertainty. *The Review of Economic Studies*, 53(2):271–282.

Loomes, G. and Sugden, R. (1998). Testing different stochastic specifications of risky choice. *Economica*, 65(260):581–598.

Lucia, A. (2024). What drives violations of the independence axiom? the role of decision confidence. *Working Paper*.

Machina, M. J. (1982). "expected utility" analysis without the independence axiom. *Econometrica*, 50(2):277–323.

Masatlioglu, Y. and Raymond, C. (2016). A behavioral analysis of stochastic reference dependence. *American Economic Review*, 106(9):2760–2782.

McFadden, D. (1974). Conditional logit analysis of qualitative choice behavior. In Zarembka, P., editor, *Frontiers in Econometrics*, pages 105–142. Academic Press, New York.

McFadden, D. (1981). Econometric models of probabilistic choice behavior. In Manski, C. F. and McFadden, D., editors, *Structural Analysis of Discrete Data and Econometric Applications*, chapter 5, pages 198–272. MIT Press, Cambridge, MA.

McGranaghan, C., Nielsen, K., O'Donoghue, T., Somerville, J., and Sprenger, C. D. (2024). Distinguishing common ratio preferences from common ratio effects using paired valuation tasks. *American Economic Review*, 114(2):307–347.

Menkveld, A. J., Dreber, A., Holzmeister, F., Huber, J., Johannesson, M., Kirchler, M., Neusüss, S., Razen, M., Weitzel, U., Abad-Díaz, D., et al. (2024). Nonstandard errors. *The Journal of Finance*, 79(3):2339–2390.

Puri, I. (2025). Simplicity and risk. *Journal of Finance*, 80(2):1029–1080.

Rabin, M. (2000). Risk aversion and expected-utility theory: A calibration theorem. *Econometrica*, 68(5):1281–1292.

Rabin, M. and Thaler, R. H. (2001). Anomalies: risk aversion. *Journal of Economic perspectives*, 15(1):219–232.

Simonsohn, U., Simmons, J. P., and Nelson, L. D. (2020). Specification curve analysis. *Nature Human Behaviour*, 4(11):1208–1214.

Stango, V. and Zinman, J. (2023). We are all behavioural, more, or less: A taxonomy of consumer decision-making. *Review of Economic Studies*, 90(3):1470–1498.

Steegen, S., Tuerlinckx, F., Gelman, A., and Vanpaemel, W. (2016). Increasing transparency through a multiverse analysis. *Perspectives on Psychological Science*, 11(5):702–712.

Tversky, A. and Kahneman, D. (1992). Advances in prospect theory: Cumulative representation of uncertainty. *Journal of Risk and Uncertainty*, 5(4):297–323.

Connecting Common Ratio and Common Consequence Preferences

Christina McGranaghan Kirby Nielsen Ted O'Donoghue
Jason Somerville Charles D. Sprenger

February 13, 2026

Online Appendix

Table of Contents

A Additional Tables and Figures

Table A.1: Participant Demographics

	(1) Full Sample	(2) Any $r = 0.1$	(3) Any $r = 0.2$	(4) Any $r = 0.3$	(5) Any $r = 0.5$	(6) Any $r = 0.8$
Number of Participants	2,102	1,247	1,250	1,246	1,221	1,212
Time Taken (in minutes)	27.3	27.2	27.3	27.3	27.3	27.4
Age	25.2	25.1	25.1	25.4	25.2	25.2
Prolific Score	99.8	99.8	99.8	99.8	99.8	99.8
Number of Approvals	304.9	304.7	298.7	310.5	302.9	305.5
Female	50.0	50.6	50.2	49.9	49.5	50.3
Current Student	41.9	42.0	43.7	41.0	40.1	42.0
College Degree	62.1	62.4	61.8	62.5	62.7	62.5
Working (full- or part-time)	59.3	58.5	59.3	60.8	58.9	60.1
English First Language	57.9	58.9	57.2	59.1	58.9	56.8
Attention Checks						
Incentive Question Correct	95.5	95.4	95.8	95.7	95.8	95.6
Passed Attention Check	96.3	96.2	96.6	96.4	96.2	96.5
Comprehension Questions						
MPL Question Correct	85.2	84.5	85.5	84.5	85.9	84.7
Bin Question Correct	79.4	79.7	79.7	78.9	78.5	79.9
Both Questions Correct	69.4	69.5	69.7	67.7	69.4	69.3
Current Residency						
United States	24.6	25.3	23.2	25.2	26.0	24.6
United Kingdom	38.4	37.9	39.8	39.3	37.3	38.0
Portugal	21.8	21.7	22.5	20.5	21.5	22.9
Spain	5.5	5.3	5.0	5.6	5.2	5.8
Germany	3.1	3.4	2.9	3.0	3.1	2.7

Notes: Column (1): participant demographics for all 2,102 participants. Columns (2) to Column (6): participant demographics if ever assigned to a given value of r across four possible (p, r) pairs.

Table A.2: Mean Valuations by p and r

	h_{AB}	$h_{AB'}$	h_{CD}	h'_{CD}	N	h'_{AB}	$h'_{AB'}$	N
Panel A: $r = 0.1$								
$p = 0.3$	36.78	23.83	31.10	34.43	406	36.24	24.92	208
$p = 0.5$	37.99	27.77	31.50	32.59	421	37.62	28.47	203
$p = 0.8$	41.34	36.52	34.91	34.86	422	40.50	35.14	205
$p = 0.9$	40.37	35.20	34.37	33.81	430	40.36	36.38	219
Panel B: $r = 0.2$								
$p = 0.3$	35.63	26.35	32.16	32.07	425	34.89	23.95	212
$p = 0.5$	38.57	29.17	34.00	32.82	468	39.09	30.35	207
$p = 0.8$	39.56	36.36	36.52	36.46	419	38.79	35.59	216
$p = 0.9$	39.42	38.71	35.20	35.34	398	40.22	39.68	194
Panel C: $r = 0.3$								
$p = 0.3$	36.48	29.14	34.49	34.25	399	36.50	28.76	211
$p = 0.5$	39.65	32.95	35.55	35.65	389	38.74	33.89	194
$p = 0.8$	42.18	39.37	35.92	36.44	474	40.88	39.01	249
$p = 0.9$	39.32	40.14	37.09	37.62	435	39.00	40.26	213
Panel D: $r = 0.5$								
$p = 0.3$	37.38	30.17	38.23	38.00	426	37.64	31.48	207
$p = 0.5$	39.28	34.37	39.51	39.58	412	38.62	35.17	221
$p = 0.8$	38.75	37.61	37.82	37.71	388	38.87	36.21	191
$p = 0.9$	38.58	38.67	37.43	36.78	425	39.12	37.36	197
Panel E: $r = 0.8$								
$p = 0.3$	37.34	34.54	36.73	36.89	446	36.73	35.07	237
$p = 0.5$	38.04	37.45	38.67	38.25	412	38.81	36.98	193
$p = 0.8$	40.64	41.25	42.56	42.56	399	40.50	41.84	215
$p = 0.9$	38.32	39.48	37.87	38.01	414	38.21	38.71	212

Notes: Table presents mean valuations for each (p, r) combination. Each participant provides a valuation for four (p, r) combinations subject to the restriction that they see each p exactly once. For two (p, r) pairs, participants report all six valuations: h_{AB}, $h_{AB'}$, h_{CD}, h'_{AB}, $h'_{AB'}$, and h'_{CD}. For the remaining two (p, r) pairs, participants provide four valuations: h_{AB}, $h_{AB'}$, h_{CD}, and h'_{CD}. We randomly label multiple valuations h_{XY} or h'_{XY}, so that it was equally likely that either was presented first.

Table A.3: Correlations Between h_{XY} and h'_{XY} by p and r

	(1) $r = 0.1$	(2) $r = 0.2$	(3) $r = 0.3$	(4) $r = 0.5$	(5) $r = 0.8$
		Panel A: $\rho(h_{AB}, h'_{AB})$			
$p = 0.3$	0.600	0.600	0.581	0.552	0.610
$p = 0.5$	0.715	0.621	0.725	0.682	0.712
$p = 0.8$	0.619	0.596	0.645	0.526	0.731
$p = 0.9$	0.527	0.602	0.534	0.576	0.542
		Panel B: $\rho(h_{AB'}, h'_{AB'})$			
$p = 0.3$	0.497	0.596	0.590	0.416	0.652
$p = 0.5$	0.548	0.406	0.622	0.683	0.652
$p = 0.8$	0.596	0.711	0.558	0.634	0.654
$p = 0.9$	0.455	0.516	0.705	0.503	0.640
		Panel C: $\rho(h_{CD}, h'_{CD})$			
$p = 0.3$	0.452	0.453	0.570	0.538	0.541
$p = 0.5$	0.474	0.512	0.410	0.590	0.583
$p = 0.8$	0.435	0.484	0.461	0.389	0.529
$p = 0.9$	0.462	0.431	0.485	0.453	0.432

Notes: Table reports correlation coefficients calculated using all valuations for which there are multiple measures for a given individual and (p, r). Multiple measures of h_{CD} are available for all observations, and therefore an average sample of 420 observations is used to compute each $\rho(h_{CD}, h'_{CD})$. Multiple measures of h_{AB} and $h_{AB'}$ are available for only half of observations, and therefore an average sample of 210 observations is used to compute each $\rho(h_{AB}, h'_{AB})$ and $\rho(h_{AB'}, h'_{AB'})$. The exact sample sizes for each cell are listed in Appendix Table A.2.

Table A.4: Mean Δ_{CR}, Δ_{CC}, and Δ_{MX} by p and r

Panel A: Mean Δ_{CR}

	$p = 0.3$	$p = 0.5$	$p = 0.8$	$p = 0.9$
$r = 0.1$	$5.68^{*,\dagger}$	$6.49^{*,\dagger}$	$6.42^{*,\dagger}$	$6.00^{*,\dagger}$
$r = 0.2$	$3.48^{*,\dagger}$	$4.57^{*,\dagger}$	$3.04^{*,\dagger}$	$4.22^{*,\dagger}$
$r = 0.3$	$1.99^{*,\dagger}$	$4.10^{*,\dagger}$	$6.26^{*,\dagger}$	$2.23^{*,\dagger}$
$r = 0.5$	-0.85	-0.23	0.93	1.16
$r = 0.8$	0.61	-0.63	$-1.92^{*,\dagger}$	0.45

Panel B: Mean Δ_{CC}

	$p = 0.3$	$p = 0.5$	$p = 0.8$	$p = 0.9$
$r = 0.1$	$-10.60^{*,\dagger}$	$-4.81^{*,\dagger}$	1.66	1.39
$r = 0.2$	$-5.72^{*,\dagger}$	$-3.65^{*,\dagger}$	-0.10	$3.36^{*,\dagger}$
$r = 0.3$	$-5.11^{*,\dagger}$	$-2.70^{*,\dagger}$	2.93^{*}	2.52^{*}
$r = 0.5$	$-7.83^{*,\dagger}$	$-5.22^{*,\dagger}$	-0.11	1.89^{*}
$r = 0.8$	$-2.35^{*,\dagger}$	$-0.80^{\dagger}$	$-1.31^{\dagger}$	1.46^{*}

Panel C: Mean $\Delta_{CR} - \Delta_{CC}$

	$p = 0.3$	$p = 0.5$	$p = 0.8$	$p = 0.9$
$r = 0.1$	$16.28^{*,\dagger}$	$11.30^{*,\dagger}$	$4.76^{*,\dagger}$	$4.61^{*,\dagger}$
$r = 0.2$	$9.19^{*,\dagger}$	$8.22^{*,\dagger}$	$3.14^{*,\dagger}$	$0.86^{\dagger}$
$r = 0.3$	$7.10^{*,\dagger}$	$6.80^{*,\dagger}$	$3.32^{*,\dagger}$	$-0.29^{\ddagger}$
$r = 0.5$	$6.98^{*,\dagger}$	$4.99^{*,\dagger}$	1.04	-0.73
$r = 0.8$	$2.96^{*,\dagger}$	0.17	-0.62	-1.01

Panel D: Mean Δ_{MX}

	$p = 0.3$	$p = 0.5$	$p = 0.8$	$p = 0.9$
$r = 0.1$	$11.32^{*,\dagger}$	$9.15^{*,\dagger}$	$5.36^{*,\dagger}$	$3.98^{*,\dagger}$
$r = 0.2$	$10.94^{*,\dagger}$	$8.74^{*,\dagger}$	$3.19^{*,\dagger}$	0.54
$r = 0.3$	$7.74^{*,\dagger}$	$4.85^{*,\dagger}$	$1.87^{*,\dagger}$	-1.26
$r = 0.5$	$6.16^{*,\dagger}$	$3.45^{*,\dagger}$	$2.66^{*,\dagger}$	$1.76^{\dagger}$
$r = 0.8$	$1.67^{*,\dagger}$	$1.82^{*,\dagger}$	-1.34	-0.50

Notes: Table presents mean values along with corresponding hypothesis tests for $\Delta_{CR} = h_{AB} - h_{CD}$, $\Delta_{CC} = h_{AB'} - h'_{CD}$, $\Delta_{CR} - \Delta_{CC}$, and $\Delta_{MX} = h'_{AB} - h'_{AB'}$. Panels A, B, and C aggregate data across all 8,408 observations, with each entry corresponding to roughly 420 observations. Panel D aggregates across the 4,204 observations for which we elicit h'_{AB} and $h'_{AB'}$, with each entry corresponding to roughly 210 observations. Expected utility null hypothesis corresponds to zero mean or zero sign difference. * denotes that the value is significantly different from zero at the 5 percent level using a means test. † denotes a significant deviation in the direction of the reported sign at the 5 percent level using a sign test.

Table A.5: Predicting the Prevalence of CR, CC, and MX by p and r

Outcome:	(1) Δ_{CR}	(2) Δ_{CC}	(3) $\Delta_{CR} - \Delta_{CC}$	(4) Δ_{MX}
Probability (p)	1.00	13.96	−12.96	−10.95
	(0.67)	(0.71)	(0.92)	(0.95)
Common Ratio (r)	−9.16	1.82	−10.97	−9.24
	(0.66)	(0.74)	(0.84)	(0.86)
Outcome Mean	2.74	−1.72	4.46	4.07
Observations	8,408	8,408	8,408	4,204

Notes: Table presents ordinary least squares regressions of $\Delta_{CR} = h_{AB} - h_{CD}$, $\Delta_{CC} = h_{AB'} - h'_{CD}$, $\Delta_{CR} - \Delta_{CC}$, and $\Delta_{MX} = h'_{AB} - h'_{AB'}$ on experimental parameters (p, r). Columns (1)-(3) use all 8,408 observations from 2,102 participants, while column (4) uses 4,204 observations from 2,102 participants. Specification also includes a constant that is not reported. Standard errors clustered at individual level in parentheses.

Table A.6: Means and Sign Tests

Probability (p)	Common Ratio (r)	Δ (Mean)	Mean Test (p-value)	Number of Cases: $\Delta > 0$	Number of Cases: $\Delta = 0$	Number of Cases: $\Delta < 0$	Sign Test (p-value)	Δ (Median)
				Panel A: Test of $\Delta^*_{CR} = 0$				
0.3	0.1	5.68	0.000	224	65	117	0.000	4
0.3	0.2	3.48	0.000	208	60	157	0.009	0
0.3	0.3	1.99	0.016	186	72	141	0.015	0
0.3	0.5	−0.85	0.243	160	93	173	0.511	0
0.3	0.8	0.61	0.363	176	79	191	0.465	0
0.5	0.1	6.49	0.000	245	71	105	0.000	5
0.5	0.2	4.57	0.000	249	93	126	0.000	1
0.5	0.3	4.10	0.000	215	52	122	0.000	2
0.5	0.5	−0.23	0.722	153	97	162	0.652	0
0.5	0.8	−0.63	0.295	146	112	154	0.686	0
0.8	0.1	6.42	0.000	278	50	94	0.000	6
0.8	0.2	3.04	0.000	239	60	120	0.000	3
0.8	0.3	6.26	0.000	299	62	113	0.000	4
0.8	0.5	0.93	0.214	176	65	147	0.119	0
0.8	0.8	−1.92	0.004	121	76	202	0.000	−1
0.9	0.1	6.00	0.000	291	55	84	0.000	3
0.9	0.2	4.22	0.000	236	61	101	0.000	2
0.9	0.3	2.23	0.002	230	74	131	0.000	1
0.9	0.5	1.16	0.112	191	77	157	0.077	0
0.9	0.8	0.45	0.443	177	62	175	0.958	0
				Panel B: Test of $\Delta^*_{CC} = 0$				
0.3	0.1	−10.60	0.000	93	36	277	0.000	−8
0.3	0.2	−5.72	0.000	129	50	246	0.000	−3
0.3	0.3	−5.11	0.000	121	59	219	0.000	−2
0.3	0.5	−7.83	0.000	96	59	271	0.000	−6
0.3	0.8	−2.35	0.002	156	73	217	0.002	0
0.5	0.1	−4.81	0.000	127	54	240	0.000	−4
0.5	0.2	−3.65	0.000	128	69	271	0.000	−4
0.5	0.3	−2.70	0.002	119	64	206	0.000	−1
0.5	0.5	−5.22	0.000	106	67	239	0.000	−4
0.5	0.8	−0.80	0.240	136	85	191	0.003	0
0.8	0.1	1.66	0.062	171	86	165	0.785	0
0.8	0.2	−0.10	0.894	164	60	195	0.113	0
0.8	0.3	2.93	0.000	216	77	181	0.088	0
0.8	0.5	−0.11	0.887	155	76	157	0.955	0
0.8	0.8	−1.31	0.071	149	46	204	0.004	−1
0.9	0.1	1.39	0.059	170	111	149	0.263	0
0.9	0.2	3.36	0.000	182	81	135	0.010	0
0.9	0.3	2.52	0.002	193	70	172	0.295	0
0.9	0.5	1.89	0.009	170	73	182	0.558	0
0.9	0.8	1.46	0.026	170	72	172	0.957	0
				Panel C: Test of $\Delta^*_{MX} = 0$				
0.3	0.1	11.32	0.000	143	27	38	0.000	9
0.3	0.2	10.94	0.000	161	18	33	0.000	10
0.3	0.3	7.74	0.000	127	43	41	0.000	5
0.3	0.5	6.16	0.000	127	35	45	0.000	5
0.3	0.8	1.67	0.031	114	41	82	0.027	0
0.5	0.1	9.15	0.000	144	30	29	0.000	10
0.5	0.2	8.74	0.000	139	38	30	0.000	6
0.5	0.3	4.85	0.000	113	36	45	0.000	4
0.5	0.5	3.45	0.000	111	48	62	0.000	1
0.5	0.8	1.82	0.048	89	48	56	0.008	0
0.8	0.1	5.36	0.000	132	35	38	0.000	5
0.8	0.2	3.19	0.001	125	35	56	0.000	4
0.8	0.3	1.87	0.049	144	36	69	0.000	2
0.8	0.5	2.66	0.009	107	32	52	0.000	2
0.8	0.8	−1.34	0.117	70	53	92	0.099	0
0.9	0.1	3.98	0.001	134	37	48	0.000	3
0.9	0.2	0.54	0.634	87	37	70	0.201	0
0.9	0.3	−1.26	0.218	86	40	87	1.000	0
0.9	0.5	1.76	0.103	95	45	57	0.003	0
0.9	0.8	−0.50	0.519	79	42	91	0.399	0

Notes: Means test and sign test for Δ_{CR}, Δ_{CC}, and Δ_{MX} for each (p, r) combination. We conduct a two-sided t-test for the difference in means. We also conduct a two-sided sign test, where we exclude all ties (instances of $\Delta_Z = 0$). See Appendix C.1 for test descriptions.

Table A.7: Decomposition Estimates Using Sample Variances and Covariances

p	r	$\hat{\mu}^*_{AB}$	$\hat{\mu}^*_{AB'}$	$\hat{\mu}^*_{CD}$	$\hat{\theta}^2_{AB}$	$\hat{\theta}^2_{AB'}$	$\hat{\theta}^2_{CD}$	$\hat{\sigma}^2_{AB}$	$\hat{\sigma}^2_{AB'}$	$\hat{\sigma}^2_{CD}$	$\hat{\theta}_{AB,AB'}$	$\hat{\theta}_{AB,CD}$	$\hat{\theta}_{AB',CD}$	$\frac{\widehat{var}(h^*_{AB})}{\widehat{var}(h_{AB})}$	$\frac{\widehat{var}(h^*_{AB'})}{\widehat{var}(h_{AB'})}$	$\frac{\widehat{var}(h^*_{CD})}{\widehat{var}(h_{CD})}$
0.30	0.10	36.60	24.20	32.76	127.57	116.63	121.34	89.60	113.51	149.90	67.60	72.33	59.02	0.59	0.51	0.45
0.30	0.20	35.38	25.55	32.11	128.19	125.59	112.58	89.40	93.15	135.46	83.78	83.58	51.81	0.59	0.57	0.45
0.30	0.30	36.49	29.01	34.37	136.26	154.58	142.43	94.33	92.86	107.37	112.63	102.50	98.28	0.59	0.62	0.57
0.30	0.50	37.47	30.60	38.11	112.96	89.81	116.68	94.05	134.99	99.86	105.38	96.68	70.63	0.55	0.40	0.54
0.30	0.80	37.13	34.72	36.81	118.54	141.79	110.51	75.12	79.78	93.66	123.11	99.39	98.90	0.61	0.64	0.54
0.50	0.10	37.87	28.00	32.04	131.74	118.41	103.05	45.82	87.38	114.88	66.46	39.88	57.31	0.74	0.58	0.47
0.50	0.20	38.73	29.53	33.41	114.48	84.97	104.47	77.30	116.24	100.13	74.02	51.62	45.28	0.60	0.42	0.51
0.50	0.30	39.35	33.26	35.60	137.46	132.95	77.39	39.14	76.33	111.11	90.80	50.30	49.33	0.78	0.64	0.41
0.50	0.50	39.05	34.65	39.55	141.52	149.10	111.93	59.96	68.07	77.58	128.19	105.99	98.14	0.70	0.69	0.59
0.50	0.80	38.29	37.30	38.46	124.54	142.36	98.81	47.91	70.29	70.71	121.28	95.32	100.29	0.72	0.67	0.58
0.80	0.10	41.06	36.07	34.89	95.20	131.89	79.57	86.22	91.60	103.12	87.95	30.56	50.51	0.52	0.59	0.44
0.80	0.20	39.30	36.10	36.49	92.16	132.02	82.28	55.71	58.57	87.54	73.91	45.93	71.78	0.62	0.69	0.48
0.80	0.30	41.73	39.25	36.18	124.91	129.88	70.67	78.15	111.98	83.25	96.18	45.22	55.22	0.62	0.54	0.46
0.80	0.50	38.79	37.14	37.77	77.64	107.64	56.87	66.41	58.58	89.09	60.79	38.08	44.72	0.54	0.65	0.39
0.80	0.80	40.59	41.46	42.56	125.53	141.80	87.45	52.95	67.88	77.78	120.60	77.93	75.43	0.70	0.68	0.53
0.90	0.10	40.37	35.60	34.09	108.44	83.80	68.31	86.15	104.57	79.63	72.62	31.18	56.60	0.56	0.44	0.46
0.90	0.20	39.68	39.02	35.27	119.39	109.76	58.06	68.12	106.57	76.72	102.61	33.54	48.55	0.64	0.51	0.43
0.90	0.30	39.21	40.18	37.35	80.60	148.54	79.39	76.88	64.15	84.33	88.51	45.70	64.85	0.51	0.70	0.48
0.90	0.50	38.75	38.25	37.10	91.12	88.15	57.69	84.15	101.63	69.62	73.62	43.71	46.43	0.52	0.46	0.45
0.90	0.80	38.28	39.22	37.94	78.65	102.70	44.32	67.37	61.36	58.67	86.33	49.02	50.54	0.54	0.63	0.43
0.63	0.38	38.71	34.46	36.14	113.35	121.62	89.19	71.74	87.97	93.52	91.82	61.92	64.68	0.61	0.58	0.48

Notes: Table reports decomposition estimates calculated from relevant sample variances and covariances (see Section 4.4 and Appendix D.1 for details). The final line presents averages over all 20 rows.

Table A.8: Preference-Noise Decomposition Using Estimates from Appendix Table A.7

p	r	$\hat{\Delta}^{**}_{CR}$	$\hat{\Delta}^{**}_{CC}$	$\hat{\Delta}^{**}_{MX}$	$\widehat{var}(\Delta^{*}_{CR})$	$\widehat{var}(\Delta^{*}_{CC})$	$\widehat{var}(\Delta^{*}_{MX})$	$\widehat{var}(\Delta_{CR})$	$\widehat{var}(\Delta_{CC})$	$\widehat{var}(\Delta_{MX})$	$\frac{\widehat{var}(\Delta^{*}_{CR})}{\widehat{var}(\Delta_{CR})}$	$\frac{\widehat{var}(\Delta^{*}_{CC})}{\widehat{var}(\Delta_{CC})}$	$\frac{\widehat{var}(\Delta^{*}_{MX})}{\widehat{var}(\Delta_{MX})}$
0.30	0.10	3.83	−8.56	12.39	104.23	119.93	108.99	343.74	383.35	312.11	0.30	0.31	0.35
0.30	0.20	3.27	−6.56	9.83	73.62	134.56	86.22	298.48	363.17	268.77	0.25	0.37	0.32
0.30	0.30	2.12	−5.36	7.48	73.69	100.46	65.58	275.39	300.68	252.76	0.27	0.33	0.26
0.30	0.50	−0.65	−7.52	6.87	36.28	65.23	–	230.20	300.08	221.04	0.16	0.22	–
0.30	0.80	0.32	−2.09	2.41	30.27	54.50	14.12	199.05	227.95	169.01	0.15	0.24	0.08
0.50	0.10	5.82	−4.04	9.87	155.04	106.84	117.24	315.74	309.10	250.45	0.49	0.35	0.47
0.50	0.20	5.33	−3.88	9.20	115.72	98.88	51.41	293.15	315.25	244.95	0.39	0.31	0.21
0.50	0.30	3.75	−2.34	6.09	114.25	111.68	88.81	264.49	299.11	204.27	0.43	0.37	0.43
0.50	0.50	−0.50	−4.90	4.40	41.46	64.75	34.24	179.00	210.41	162.27	0.23	0.31	0.21
0.50	0.80	−0.18	−1.16	0.98	32.72	40.58	24.35	151.34	181.59	142.55	0.22	0.22	0.17
0.80	0.10	6.18	1.18	5.00	113.65	110.43	51.20	302.99	305.16	229.02	0.38	0.36	0.22
0.80	0.20	2.81	−0.39	3.20	82.58	70.74	76.35	225.84	216.85	190.64	0.37	0.33	0.40
0.80	0.30	5.55	3.07	2.48	105.13	90.11	62.43	266.53	285.35	252.56	0.39	0.32	0.25
0.80	0.50	1.02	−0.62	1.65	58.34	75.08	63.69	213.84	222.75	188.68	0.27	0.34	0.34
0.80	0.80	−1.97	−1.10	−0.87	57.12	78.38	26.13	187.86	224.04	146.96	0.30	0.35	0.18
0.90	0.10	6.27	1.51	4.77	114.38	38.91	46.99	280.17	223.11	237.71	0.41	0.17	0.20
0.90	0.20	4.41	3.75	0.66	110.37	70.73	23.93	255.21	254.02	198.62	0.43	0.28	0.12
0.90	0.30	1.86	2.83	−0.97	68.58	98.24	52.12	229.78	246.71	193.15	0.30	0.40	0.27
0.90	0.50	1.65	1.15	0.50	61.40	52.99	32.02	215.16	224.23	217.79	0.29	0.24	0.15
0.90	0.80	0.34	1.27	−0.93	24.93	45.94	8.68	150.98	165.97	137.42	0.17	0.28	0.06
0.63	0.38	2.56	−1.69	4.25	78.69	81.45	54.45	243.95	262.94	211.04	0.31	0.30	0.25

Notes: Table calculates model-implied variances of Δ_Z's and Δ^*_Z's using the decomposition estimates from Table A.7 (see Section 4.4 and Appendix D.2 for details). Absence of entry for $\widehat{var}(\Delta^*_{MX})$ when $p = 0.30$ and $r = 0.50$ due to fact that, when calculating $var(\Delta^*_Z)$ from sample variances and covariances, nothing guarantees that they are positive (see Appendix D.2). The final line presents averages over all 20 rows.

Table A.9: Sensitivity of Results to Experimental Parameters in our Stage 2 Experiments

Panel A. Experimental-Parameter Sensitivity

	(1) CR Study	(2) CC Study	(3) MX Study
Probability (p)	23.25	49.57	−28.62
	(6.16)	(6.14)	(5.89)
Common Ratio (r)	−35.19	−2.70	−29.88
	(2.47)	(2.52)	(2.30)
Outcome Mean	10.45	−5.77	16.00
Experiments	120	120	120
Observations	8,408	8,408	8,408

Panel B. Canonical vs. Non-Canonical Parameters

	(4) Canonical	(5) Non-Canonical	(6) Difference
	(i): KT Parameters		
CRE − RCRE	17.02	9.67	−7.35
	(8.36)	(13.76)	[−1.86]
Experiments	12	108	120
	(ii): Allais Parameters		
CCE − RCCE	7.91	−6.51	−14.41
	(5.93)	(12.96)	[−2.73]
Experiments	6	114	120

Notes: Panel A presents linear regressions that assess the sensitivity of experimental results from CR, CC, or MX studies from our stage 2 experiments. The specifications include the probability of the high outcome (p), the common ratio (r) linearly, and a constant. Column (1) presents the results for the 120 CR experiments that we conducted in stage 2 of our experiment, where the outcome is the net share of participants displaying a CRE relative to an RCRE, $CRE - RCRE$. Column (2) presents the results for the 120 CC experiments that we conducted in stage 2 of our experiment, where the outcome is the net share of participants displaying a CCE relative to an RCCE, $CCE - RCCE$. Column (3) presents the results for the 120 CC experiments that we conducted in stage 2 of our experiment, where the outcome is the net share of participants displaying a MXE relative to an RMXE, $MXE - RMXE$. Standard errors are in parentheses. Panel B presents the average of these outcomes based on whether our stage 2 experiments were conducted at the canonical parameters in Kahneman and Tversky (1979) ($p = 0.8$, $r \in \{0.2, 0.3\}$) or Allais (1953) ($p = 0.9$, $r = 0.1$). Standard deviations are in parentheses, and t-statistics are in brackets.

Figure A.1: Histogram of Response Patterns for $r \in \{0.1, 0.2, 0.3\}$ and $p \in \{0.8, 0.9\}$

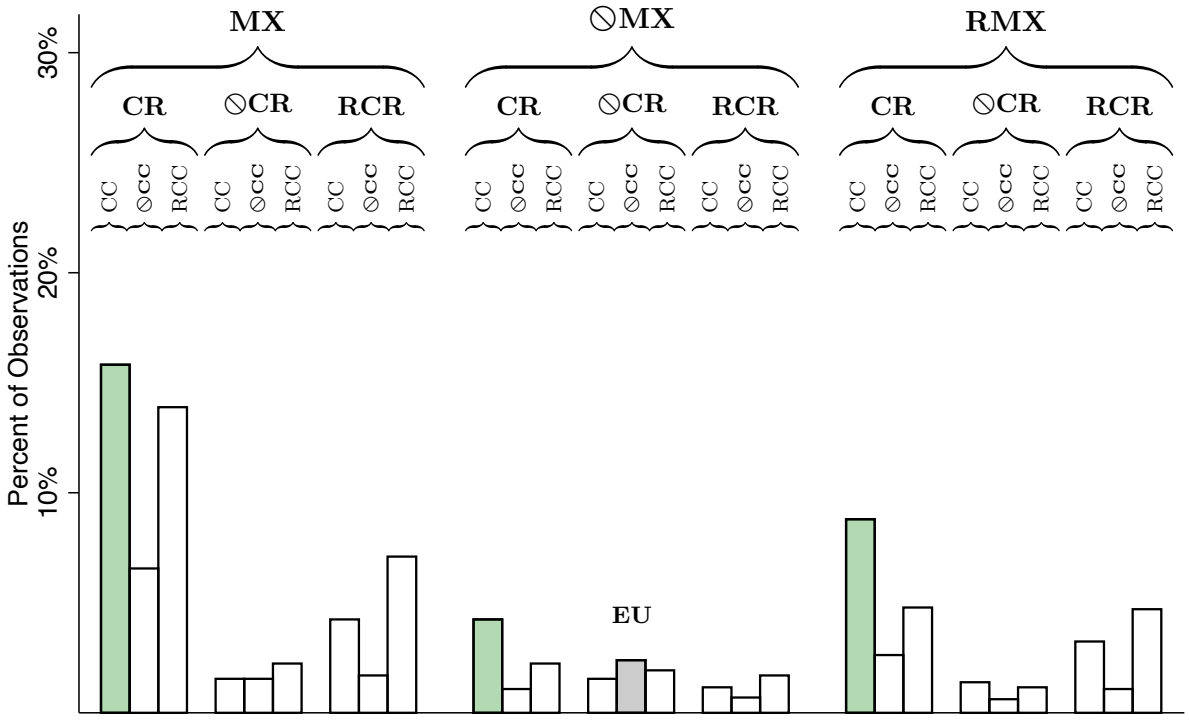

Notes: Figure presents histogram of $(sign(\Delta_{CR}), sign(\Delta_{CC}), sign(\Delta_{MX}))$ combinations, where $\Delta_{CR} = h_{AB} - h_{CD}$, $\Delta_{CC} = h_{AB'} - h'_{CD}$, and $\Delta_{MX} = h'_{AB} - h'_{AB'}$. Each variable can have three potential signs, leading to 27 possible patterns. These signs correspond to the named patterns (e.g., CR to $\Delta_{CR} > 0$, RCR to $\Delta_{CR} < 0$, and ⊘CR to $\Delta_{CR} = 0$). The histogram covers the 1,296 observations from the parameters $r \in \{0.1, 0.2, 0.3\}$ and $p \in \{0.8, 0.9\}$ for which we elicit h'_{AB} and $h'_{AB'}$. Patterns marked in light green are ones with $\Delta_{CR} > 0$ and $\Delta_{CC} > 0$.

Figure A.2: Histogram of Response Patterns for $r \notin \{0.1, 0.2, 0.3\}$ or $p \notin \{0.8, 0.9\}$

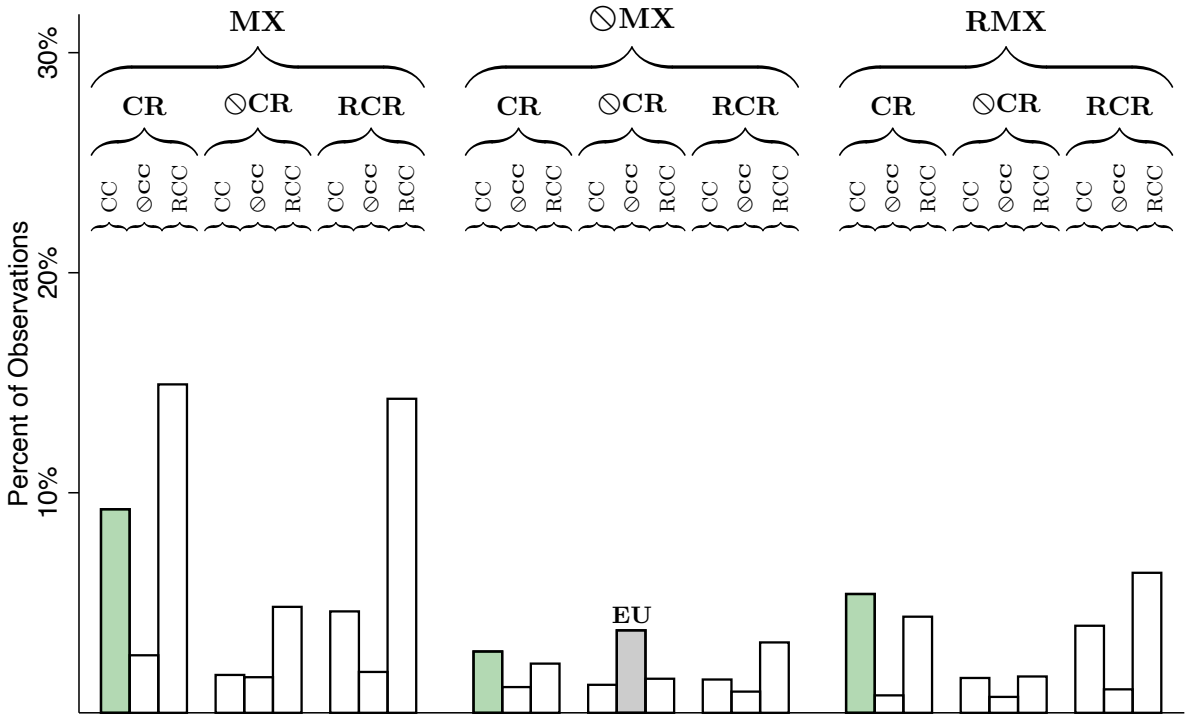

Notes: Figure presents histogram of $(sign(\Delta_{CR}), sign(\Delta_{CC}), sign(\Delta_{MX}))$ combinations, where $\Delta_{CR} = h_{AB} - h_{CD}$, $\Delta_{CC} = h_{AB'} - h'_{CD}$, and $\Delta_{MX} = h'_{AB} - h'_{AB'}$. Each variable can have three potential signs, leading to 27 possible patterns. These signs correspond to the named patterns (e.g., CR to $\Delta_{CR} > 0$, RCR to $\Delta_{CR} < 0$, and ⊘CR to $\Delta_{CR} = 0$). The histogram covers the 2,908 observations from the parameters $r \notin \{0.1, 0.2, 0.3\}$ or $p \notin \{0.8, 0.9\}$ for which we elicit h'_{AB} and $h'_{AB'}$. Patterns marked in light green are ones with $\Delta_{CR} > 0$ and $\Delta_{CC} > 0$.

Figure A.3: Histogram of Response Patterns for $r \in \{0.1, 0.2, 0.3\}$ and $p \in \{0.3, 0.5\}$

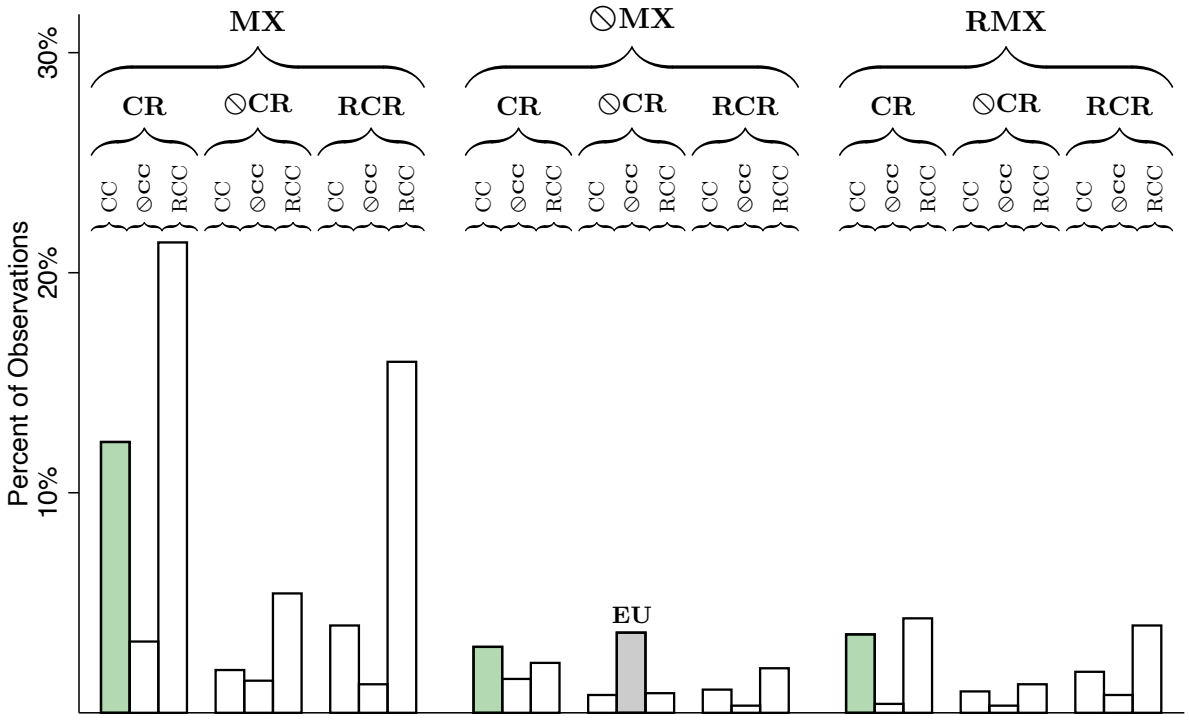

Notes: Figure presents histogram of $(sign(\Delta_{CR}), sign(\Delta_{CC}), sign(\Delta_{MX}))$ combinations, where $\Delta_{CR} = h_{AB} - h_{CD}$, $\Delta_{CC} = h_{AB'} - h'_{CD}$, and $\Delta_{MX} = h'_{AB} - h'_{AB'}$. Each variable can have three potential signs, leading to 27 possible patterns. These signs correspond to the named patterns (e.g., CR to $\Delta_{CR} > 0$, RCR to $\Delta_{CR} < 0$, and ⊘CR to $\Delta_{CR} = 0$). The histogram covers the 2,508 observations from the parameters $r \in \{0.1, 0.2, 0.3\}$ or $p \in \{0.3, 0.5\}$ for which we elicit h'_{AB} and $h'_{AB'}$. Patterns marked in light green are ones with $\Delta_{CR} > 0$ and $\Delta_{CC} > 0$.

Figure A.4: Predicting Stage 2 Choice Probabilities using Stage 1 Valuations

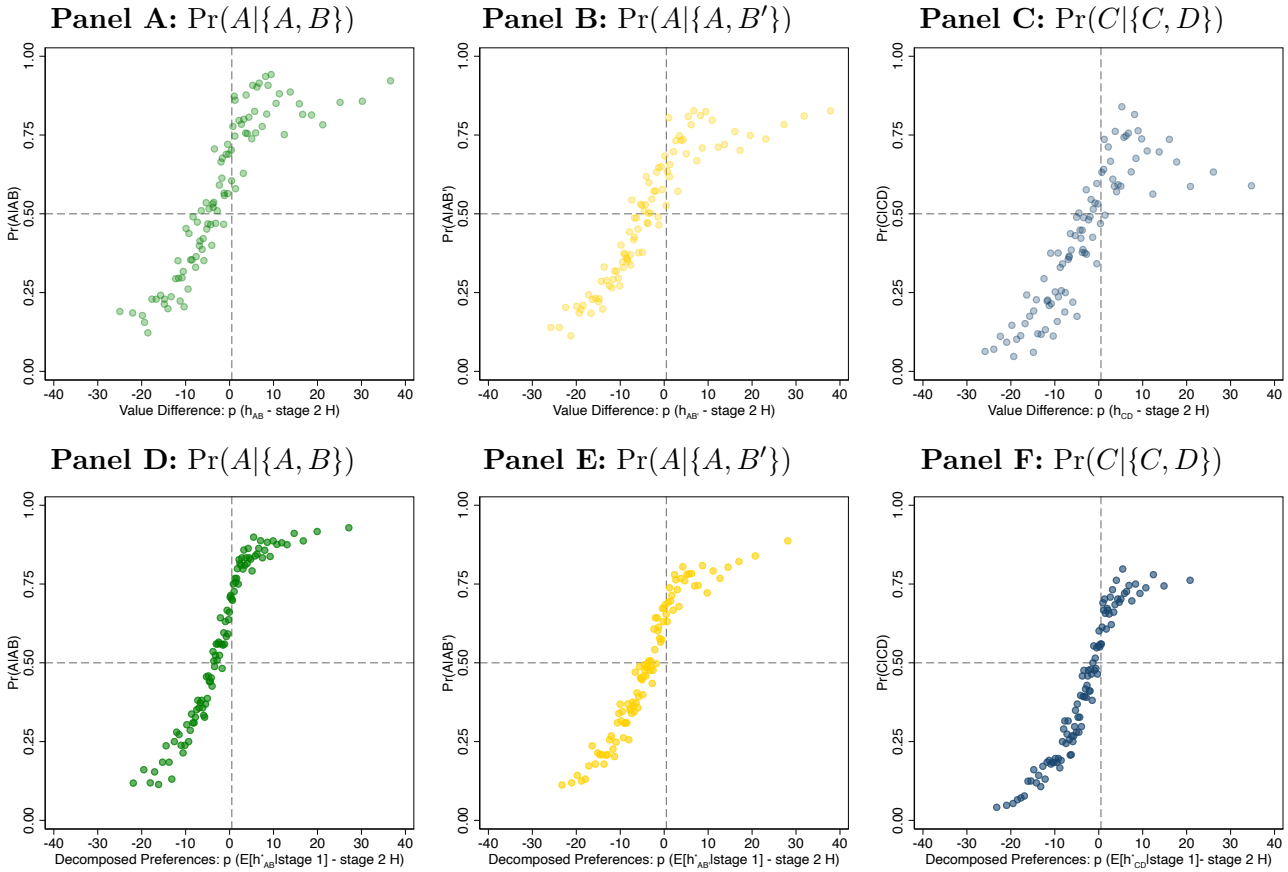

Notes: Figure relates individual stage 1 measures of $h_{XY} - H$ to stage 2 choice shares $\Pr(X|\{X, Y\})$. Panels A-C use raw stage 1 responses. Panels D-F use the estimated population distribution of preferences from the decomposition in Section 4.4 combined with a participant's raw stage 1 valuations to generate a posterior preference measure $E[h^*_{XY}|\text{stage 1}]$ for that participant. For each x-axis, one hundred equally sized bins are constructed with approximately 168 observations per bin. Within each bin, the stage 2 choice share is calculated to construct the y-axis. Due to a large number of observations at some values, there are 94, 93, and 91 unique bins in panels A, B, and C, respectively. To make valuations comparable across (p, r), all stage 1 measures are scaled by p to control for the fact that a fixed value of the measure is predicted to yield a larger stage 2 effect the larger is p (see Appendix C.3 for details).

Figure A.5: Structural Estimates and Model Fit

Panel A: Upside Potential Estimates – Flexible Five Parameter Model

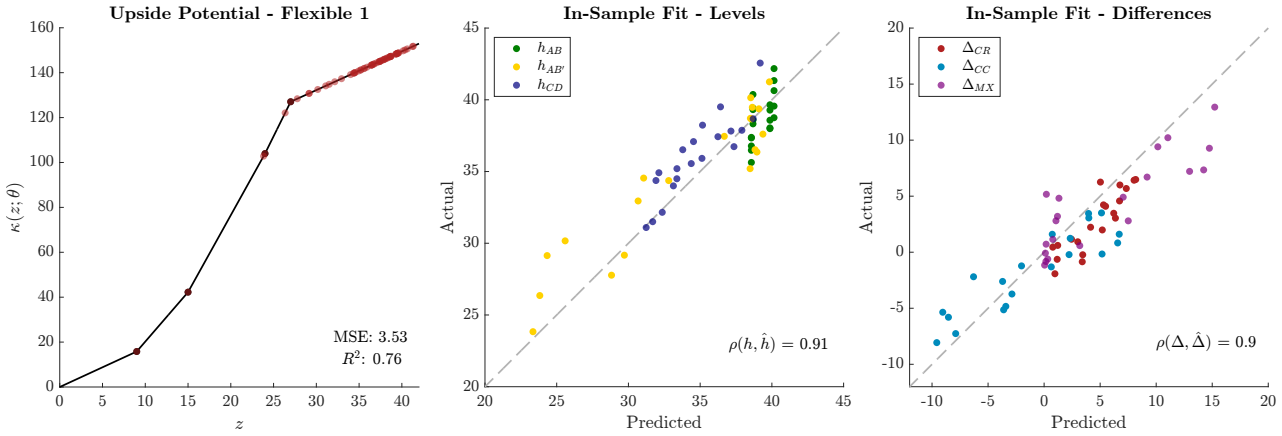

Panel B: Upside Potential Estimates – Parametric Functional Form

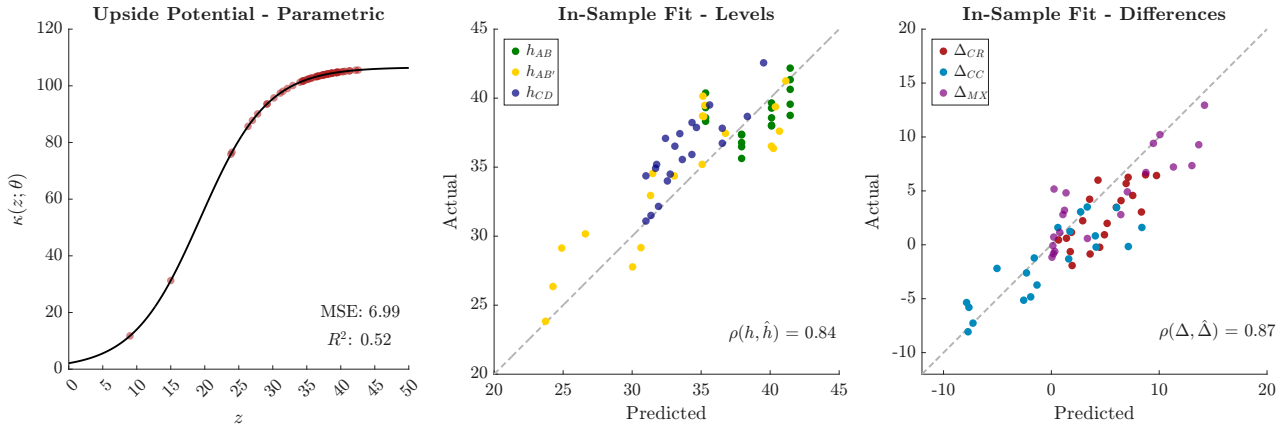

Panel C: CPT Probability Weighting Estimates – Flexible Functional Form

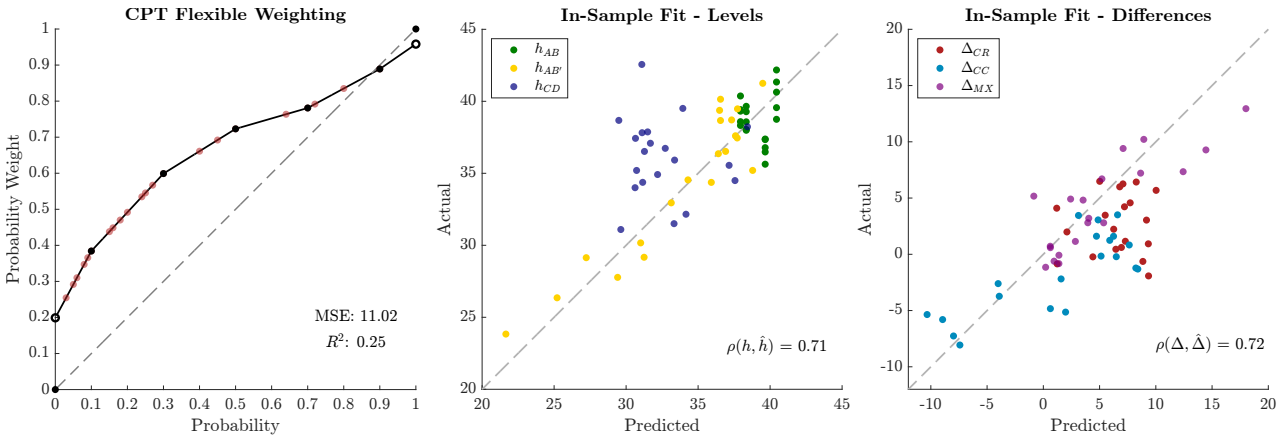

Notes: This figure presents the estimated parameter functions and model fit for our model of upside potential with a flexible (Panel A) and a parametric (Panel B) functional form, along with the best-fitting CPT model with a flexible form (Panel C). The left panels depict the estimated functions, κ or π. The middle panels depict the in-sample fit for our three valuations, h_{AB}, $h_{AB'}$, and h_{CD}. The right panels depict the in-sample fit for our three preference measures, Δ_{CR}, Δ_{CC}, and Δ_{MX}.

B Predictions of Existing Non-EU Models

In this appendix, we derive the predictions presented in Table 1. To review the structure, given parameters (M, p, r), h^*_{AB}, $h^*_{AB'}$, and h^*_{CD} are the *indifference values* that satisfy the following indifference conditions:

$$\begin{aligned}(M,1) &\sim (h^*_{AB}, p)\\ (M,1) &\sim (h^*_{AB'}, pr; M, 1-r)\\ (M,r) &\sim (h^*_{CD}, pr)\end{aligned}$$

The objects of interest are then:

$$\begin{aligned}\Delta^*_{CR} &\equiv h^*_{AB} - h^*_{CD}\\ \Delta^*_{CC} &\equiv h^*_{AB'} - h^*_{CD}\\ \Delta^*_{MX} &\equiv h^*_{AB} - h^*_{AB'}\end{aligned}$$

B.1 Original Prospect Theory (OPT)

Under original prospect theory (OPT) as in Kahneman and Tversky (1979), the indifference values are determined from:

$$\begin{aligned}v(M) &= \pi(p)v(h^*_{AB}) &&\iff h^*_{AB} = v^{-1}\left(\frac{1}{\pi(p)}v(M)\right)\\ v(M) &= \pi(pr)v(h^*_{AB'}) + \pi(1-r)v(M) &&\iff h^*_{AB'} = v^{-1}\left(\frac{1-\pi(1-r)}{\pi(pr)}v(M)\right)\\ \pi(r)v(M) &= \pi(pr)v(h^*_{CD}) &&\iff h^*_{CD} = v^{-1}\left(\frac{\pi(r)}{\pi(pr)}v(M)\right)\end{aligned}$$

Hence:

$$\begin{aligned}\Delta^*_{CR} > 0 &\iff h^*_{AB} > h^*_{CD} \iff \frac{1}{\pi(p)} > \frac{\pi(r)}{\pi(pr)}\\ \Delta^*_{CC} > 0 &\iff h^*_{AB'} > h^*_{CD} \iff 1-\pi(1-r) > \pi(r)\\ \Delta^*_{MX} > 0 &\iff h^*_{AB} > h^*_{AB'} \iff \frac{1}{\pi(p)} > \frac{1-\pi(1-r)}{\pi(pr)}\end{aligned}$$

In this formulation, $v(x)$ is a value function defined over experimental gains and losses, but note that as long as v is monotonically increasing, its form is irrelevant to OPT's predictions for the sign of Δ^*_{CR}, Δ^*_{CC}, and Δ^*_{MX}. In contrast, $\pi(q)$ is a probability weighting function that transforms

probabilities into decision weights, and its form fully determines those predictions. Here, we derive predictions using the functional form from Tversky and Kahneman (1992):

$$\pi(q) = \frac{q^\delta}{[q^\delta + (1-q)^\delta]^{1/\delta}}$$

This one-parameter functional form nests the EU case of $\pi(q) = q$ when $\delta = 1$. For $\delta \in (0.279, 1)$, it has the inverse-S shape emphasized by Tversky and Kahneman (1992) and the subsequent literature: It is initially concave and then convex, with overweighting ($\pi(q) > q$) for small q and then underweighting ($\pi(q) < q$) for larger q.[54] Tversky and Kahneman (1992) suggest a δ of roughly 0.6. For $\delta > 1$, this functional form initially yields an S-shape—initially convex and then concave with underweighting for small q and then overweighting for larger q—but eventually becomes convex with underweighting for all $q \in (0, 1)$.

OPT Result:

(1) $\delta \in (0.279, 1)$ implies $\Delta^*_{CR} > 0$ and $\Delta^*_{CC} > 0$; Δ^*_{MX} can be positive or negative depending on (p, r) combination.

(2) $\delta > 1$ implies $\Delta^*_{CR} < 0$, $\Delta^*_{CC} > 0$, and $\Delta^*_{MX} < 0$.

Proof: Consider first the Δ^*_{CR} results. Rearranging the condition above yields

$$\Delta^*_{CR} : 0 \quad \Longleftrightarrow \quad \frac{\pi(pr)}{\pi(r)} : \pi(p)$$

which we can write as

$$\frac{(pr)^\delta}{[(pr)^\delta + (1-pr)^\delta]^{1/\delta}} \frac{\left[(r)^\delta + (1-r)^\delta\right]^{1/\delta}}{(r)^\delta} : \frac{(p)^\delta}{[(p)^\delta + (1-p)^\delta]^{1/\delta}}.$$

Canceling terms and then taking both sides to the power δ yields

$$\frac{(r)^\delta + (1-r)^\delta}{(pr)^\delta + (1-pr)^\delta} : \frac{1}{(p)^\delta + (1-p)^\delta}$$

$$[(p)^\delta + (1-p)^\delta][(r)^\delta + (1-r)^\delta] : (pr)^\delta + (1-pr)^\delta$$

$$(pr)^\delta + (p(1-r))^\delta + (r(1-p))^\delta + ((1-p)(1-r))^\delta : (pr)^\delta + (1-pr)^\delta$$

$$(p(1-r))^\delta + (r(1-p))^\delta + ((1-p)(1-r))^\delta : (1-pr)^\delta$$

Note that we can rewrite this as

$$a^\delta + b^\delta + c^\delta : d^\delta$$

[54] For $\delta \in (0, 0.279)$, $\pi(q)$ is nonmonotonic (Ingersoll, 2008).

where $a = p(1-r)$, $b = r(1-p)$, $c = (1-p)(1-r)$, and $d = 1-pr$, and note that $a+b+c = d$. Then because the function $f(x) = x^\delta$ is concave when $\delta < 1$, it follows that $a+b+c = d$ implies $f(a)+f(b)+f(c) > f(d)$, and thus $\delta < 1$ implies $\Delta^*_{CR} > 0$. Analogously, $f(x)$ is convex when $\delta > 1$, so $a+b+c = d$ implies $f(a)+f(b)+f(c) < f(d)$, and thus $\delta > 1$ implies $\Delta^*_{CR} < 0$.

Next consider the Δ^*_{CC} results. Rearranging the condition above yields

$$\Delta^*_{CC} : 0 \quad \Longleftrightarrow \quad 1 : \pi(r) + \pi(1-r)$$

which we can write as

$$1 : \frac{(r)^\delta}{\left[(r)^\delta + (1-r)^\delta\right]^{1/\delta}} + \frac{(1-r)^\delta}{\left[(r)^\delta + (1-r)^\delta\right]^{1/\delta}}$$

$$1 : \left[(r)^\delta + (1-r)^\delta\right]^{1-1/\delta}$$

When $\delta < 1$: $r < 1$ and $\delta < 1$ implies $r^\delta > r$ and $(1-r)^\delta > 1-r$ and thus $(r)^\delta + (1-r)^\delta > 1$. In addition, $\delta < 1$ implies $1 - 1/\delta < 0$, and thus $\left[(r)^\delta + (1-r)^\delta\right]^{1-1/\delta} < 1$ and therefore $\Delta^*_{CC} > 0$.

When $\delta > 1$: $r < 1$ and $\delta > 1$ implies $r^\delta < r$ and $(1-r)^\delta < 1-r$ and thus $(r)^\delta + (1-r)^\delta < 1$. In addition, $\delta > 1$ implies $1 - 1/\delta > 0$, and thus $\left[(r)^\delta + (1-r)^\delta\right]^{1-1/\delta} < 1$ and therefore again $\Delta^*_{CC} > 0$.

Finally, when $\delta > 1$, the combination of $\Delta^*_{CR} < 0$ and $\Delta^*_{CC} > 0$ implies $\Delta^*_{MX} = \Delta^*_{CR} - \Delta^*_{CC} < 0$. In contrast, for $\delta < 1$, it is possible for Δ^*_{MX} to be positive or negative.

■

B.2 Cumulative Prospect Theory (CPT)

Cumulative prospect theory (CPT) as in Tversky and Kahneman (1992) differs from OPT only for gambles with more than one non-zero outcome. In our context, this means they differ only in the evaluation of lottery B'. Hence, the h^*_{AB} and h^*_{CD} indifference values are as in OPT, but the $h^*_{AB'}$ indifference value is now determined from:

$$v(M) = \pi(pr)v(h^*_{AB'}) + (\pi(pr+1-r) - \pi(pr))v(M)$$

$$\Longleftrightarrow \quad h^*_{AB'} = v^{-1}\left(\frac{1 - (\pi(pr+1-r) - \pi(pr))}{\pi(pr)} v(M)\right)$$

Hence, we now have:

$$\begin{aligned}
\Delta^*_{CR} > 0 &\iff h^*_{AB} > h^*_{CD} \iff \frac{1}{\pi(p)} > \frac{\pi(r)}{\pi(pr)} \\
\Delta^*_{CC} > 0 &\iff h^*_{AB'} > h^*_{CD} \iff 1 - (\pi(pr + 1 - r) - \pi(pr)) > \pi(r) \\
\Delta^*_{MX} > 0 &\iff h^*_{AB} > h^*_{AB'} \iff \frac{1}{\pi(p)} > \frac{1 - (\pi(pr + 1 - r) - \pi(pr))}{\pi(pr)}
\end{aligned}$$

As in OPT, the value function v is irrelevant for the model's predictions for the sign of Δ^*_{CR}, Δ^*_{CC}, and Δ^*_{MX}, which are fully determined by the form of the probability weighting function π. Here, we again derive predictions using the functional form from Tversky and Kahneman (1992).

CPT Result:

(1) $\delta \in (0.279, 1)$ implies $\Delta^*_{CR} > 0$ and $\Delta^*_{CC} > 0$; Δ^*_{MX} can be positive or negative.

(2) $\delta > 1$ implies $\Delta^*_{CR} < 0$; Δ^*_{CC} and Δ^*_{MX} can be positive or negative.

Proof: The Δ^*_{CR} equations are the same as in OPT, and thus the proof from the OPT Result still holds. So we just need to prove that $\delta \in (0.279, 1)$ implies $\Delta^*_{CC} > 0$.

We begin with two preliminary results. First, note that for all $\delta > 0.279$,

$$\pi(1/2) = \frac{(1/2)^\delta}{[2(1/2)^\delta]^{1/\delta}} = \left(\frac{1}{2}\right)^{\delta - \frac{\delta-1}{\delta}} < \frac{1}{2} \quad \text{because } \delta - \frac{\delta - 1}{\delta} > 1.$$

Second, we prove that

$$\pi(1-a) - \pi(1-b) > \pi(b) - \pi(a) \qquad \text{for any } 0 \leqslant a < b \leqslant 1/2 \tag{B.1}$$

In words, equation (B.1) says that $\pi(q)$ is steeper for q above $1/2$ than for q below $1/2$. To prove this, we rewrite the inequality in equation (B.1) as $\pi(a) + \pi(1-a) > \pi(b) + \pi(1-b)$, which yields

$$\frac{(a)^\delta + (1-a)^\delta}{[(a)^\delta + (1-a)^\delta]^{(1/\delta)}} > \frac{(b)^\delta + (1-b)^\delta}{[(b)^\delta + (1-b)^\delta]^{(1/\delta)}}$$

$$\left[(a)^\delta + (1-a)^\delta\right]^{1-(1/\delta)} > \left[(b)^\delta + (1-b)^\delta\right]^{1-(1/\delta)}$$

Then because

$$\frac{d\left[(x)^\delta + (1-x)^\delta\right]^{1-(1/\delta)}}{dx} = (1 - (1/\delta))\left[(x)^\delta + (1-x)^\delta\right]^{-(1/\delta)} \delta(x^{\delta-1} - (1-x)^{\delta-1})$$

is negative as long as $\delta < 1$ and $x < 1/2$, equation (B.1) follows.

We now prove that $\delta \in (0.279, 1)$ implies $\Delta^*_{CC} > 0$. The Δ^*_{CC} condition can be written as

$$\Delta^*_{CC} > 0 \quad \Longleftrightarrow \quad \frac{1 + \pi(pr)}{2} > \frac{\pi(pr + 1 - r) + \pi(r)}{2}$$

Let's define z such that $\min\{r, pr+1-r\} \equiv pr+z$, and note that this implies that $\max\{r, pr+1-r\} = 1-z$ (so that $(r)+(pr+1-r) = (pr+z)+(1-z) = 1+pr$). We can then rewrite the Δ^*_{CC} condition as

$$\Delta^*_{CC} > 0 \quad \Longleftrightarrow \quad \frac{1 + \pi(pr)}{2} > \frac{\pi(pr + z) + \pi(1 - z)}{2}$$

The LHS is the y-value for the midpoint of the line segment that connects the points $(pr, \pi(pr))$ and $(1, 1)$, while the RHS is the y-value for the midpoint of the line segment that connects the points $(pr+z, \pi(pr+z))$ and $(1-z, \pi(1-z))$, where the x-value for both midpoints is $(1+pr)/2$. Given the inverse-S shape of $\pi(q)$ for $\delta \in (0.279, 1)$ and the fact that $\pi(1/2) < 1/2$, the LHS line segment can intersect $\pi(q)$ for at most one $\bar{q} \in (pr, 1)$. Moreover, if such a $\bar{q}$ exists, then $pr < \bar{q} < 1/2$, $\pi(pr) > pr$ and $\pi(\bar{q}) > \bar{q}$.

If such a $\bar{q}$ does not exist, then the LHS line segment must be everywhere above the RHS line segment, and thus the Δ^*_{CC} condition holds.

If such a $\bar{q}$ exists but $pr + z > \bar{q}$, then again the LHS line segment must be everywhere above the RHS line segment, and thus the Δ^*_{CC} condition holds.

Finally, suppose such a $\bar{q}$ exists but $pr + z < \bar{q} < 1/2$. If π is concave at $\bar{q}$ and thus concave for all $q < \bar{q}$, then $\pi(pr + z) - \pi(pr) < \pi(z) < 1 - \pi(1 - z)$ (where the first inequality follows from the concavity of π for $q < \bar{q}$ and the second inequality follows from equation (B.1) with $a = 0$ and $b = z < 1/2$), and thus the Δ^*_{CC} condition holds. Suppose instead π is convex at $\bar{q}$ and thus convex for all $q > \bar{q}$. Because $pr + z < \bar{q} < 1/2$ and thus $1 - pr - z > 1/2$, we have $\pi(pr + z) - \pi(pr) < \pi(1 - pr) - \pi(1 - pr - z) < 1 - \pi(1 - z)$ (where the first inequality follows from equation (B.1) and the second inequality follows from the fact that π is convex for all $q > \bar{q}$). Hence, again the Δ^*_{CC} condition holds.

This covers all cases, and hence $\delta \in (0.279, 1)$ implies $\Delta^*_{CC} > 0$.

Finally, we note that a symmetric argument does not work for $\delta > 1$ because equation (B.1) does not flip to maintain the symmetry. More precisely, if $pr + z > \bar{q}$, an analogous argument implies that $\Delta^*_{CC} < 0$. But when $pr+z < \bar{q}$, equation (B.1) still implies $\pi(pr+z)-\pi(pr) < \pi(1-pr)-\pi(1-pr-z)$, and this creates the possibility that $\Delta^*_{CC} > 0$—in fact, it is easy to generate such examples.

■

B.3 Kőszegi-Rabin Loss Aversion Under CPE

We next consider predictions from the Kőszegi-Rabin (2007) model of loss aversion when we apply choice-acclimating personal equilibrium (CPE). Under CPE, the utility from a lottery $X \equiv (x, q_H; 0, q_L)$ where $x > 0$ and $q_H + q_L = 1$ is

$$U(X) = q_H u(x) - \Lambda q_H q_L u(x)$$

and the utility from a lottery $Y \equiv (x, q_H; y, q_M; 0, q_L)$ where $x > y > 0$ and $q_H + q_M + q_L = 1$ is

$$U(Y) = q_H u(x) + q_M u(y) - \Lambda q_H (q_M + q_L) u(x) - \Lambda q_M (q_L - q_H) u(y).$$

where the parameter Λ is a measure of loss aversion.[55] $\Lambda > 0$ implies loss aversion (losses loom larger than gains), and $\Lambda < 0$ implies gain attraction (gains loom larger than losses). In this formulation, u is the person's intrinsic utility over outcomes (e.g., that might be used under EU), where we have normalized $u(0) = 0$.

Applied to our context, the indifference values are determined from:

$$\begin{aligned} u(M) &= pu(h^*_{AB}) - \Lambda p(1-p)u(h^*_{AB}) \\ u(M) &= pru(h^*_{AB'}) + (1-r)u(M) - \Lambda pr(1-pr)u(h^*_{AB'}) - \Lambda(1-r)r(1-2p)u(M) \\ ru(M) - \Lambda r(1-r)u(M) &= pru(h^*_{CD}) - \Lambda pr(1-pr)u(h^*_{CD}) \end{aligned}$$

from which we can derive:

$$\begin{aligned} h^*_{AB} &= u^{-1}\left(\frac{1}{p(1-\Lambda(1-p))}u(M)\right) \\ h^*_{AB'} &= u^{-1}\left(\frac{1+\Lambda(1-r)(1-2p)}{p(1-\Lambda(1-pr))}u(M)\right) \\ h^*_{CD} &= u^{-1}\left(\frac{1-\Lambda(1-r)}{p(1-\Lambda(1-pr))}u(M)\right). \end{aligned}$$

To ensure this model is well-behaved, we put two restrictions on the range of Λ. First, if Λ becomes too positive, utility can be *decreasing* in h. For instance, the utility from lottery D can be written as $[pr - \Lambda pr(1-pr)]u(h)$, and this is increasing in h only if $\Lambda < 1/(1-pr)$. To rule out these perverse cases, we restrict $\Lambda \leqslant 1$. Second, if Λ becomes too negative, the indifference values can be smaller than M. For instance, $h^*_{AB} > M$ requires $1/(p(1-\Lambda(1-p))) > 1$ or $\Lambda > -1/p$. To rule out these perverse cases, we restrict $\Lambda \geqslant -1$.

[55] The Kőszegi and Rabin (2007) model has two parameters, a parameter η which captures the relative importance of gain-loss utility versus intrinsic utility, and a parameter λ that captures loss aversion. However, under CPE these parameters always appear as the product $\eta(\lambda - 1)$ and thus cannot be distinguished, so we define $\Lambda \equiv \eta(\lambda - 1)$.

With these restrictions in place:

$$\begin{array}{lllll}
\Delta^*_{CR} > 0 & \iff & h^*_{AB} > h^*_{CD} & \iff & \dfrac{1}{p(1-\Lambda(1-p))} > \dfrac{1-\Lambda(1-r)}{p(1-\Lambda(1-pr))} \\
\Delta^*_{CC} > 0 & \iff & h^*_{AB'} > h^*_{CD} & \iff & 1+\Lambda(1-r)(1-2p) > 1-\Lambda(1-r) \\
\Delta^*_{MX} > 0 & \iff & h^*_{AB} > h^*_{AB'} & \iff & \dfrac{1}{p(1-\Lambda(1-p))} > \dfrac{1+\Lambda(1-r)(1-2p)}{p(1-\Lambda(1-pr))}
\end{array}$$

Note that, much as for the value function under OPT and CPT, the utility function u is irrelevant for the model's predictions for the sign of Δ^*_{CR}, Δ^*_{CC}, and Δ^*_{MX}, where in this model these are fully determined by the value of the parameter Λ.

Kőszegi-Rabin CPE Result:

(1) $\Lambda \in (0,1]$ implies $\Delta^*_{CR} > 0$, $\Delta^*_{CC} > 0$, and $\Delta^*_{MX} < 0$.

(2) $\Lambda \in [-1,0)$ implies $\Delta^*_{CR} < 0$, $\Delta^*_{CC} < 0$, and $\Delta^*_{MX} > 0$.

Proof: Consider first the Δ^*_{CR} condition, which we can write as:

$$\Delta^*_{CR} : 0 \iff \frac{1}{1-\Lambda(1-p)} : \frac{1-\Lambda(1-r)}{1-\Lambda(1-pr)}$$

The LHS is independent of r. The RHS is equal to the LHS when $r = 1$, and moreover

$$\frac{dRHS}{dr} = \frac{(1-\Lambda(1-pr))\Lambda - (1-\Lambda(1-r))\Lambda p}{(1-\Lambda(1-pr))^2} = \frac{(1-p)(\Lambda-\Lambda^2)}{(1-\Lambda(1-pr))^2}$$

If $\Lambda \in (0,1]$, then $\Lambda - \Lambda^2 > 0$ and thus $dRHS/dr > 0$, from which it follows that $\Delta^*_{CR} > 0$ for all $r < 1$.

If $\Lambda \in [-1,0)$, then $\Lambda - \Lambda^2 < 0$ and thus $dRHS/dr < 0$, from which it follows that $\Delta^*_{CR} < 0$ for all $r < 1$.

Next consider the Δ^*_{CC} condition, which we can write as:

$$\Delta^*_{CC} : 0 \iff 1+\Lambda(1-r)(1-2p) \;:\; 1-\Lambda(1-r)$$

$$\iff \qquad 2\Lambda(1-r)(1-p) \;:\; 0$$

Since the LHS is positive for $\Lambda \in (0,1]$ and negative for $\Lambda \in [-1,0)$, $\Delta^*_{CC} > 0$ for any $\Lambda \in (0,1]$ and $\Delta^*_{CC} < 0$ for any $\Lambda \in [-1,0)$.

Finally consider the Δ^*_{MX} condition, which we can write as:

$$\Delta^*_{MX} : 0 \iff \frac{1}{1-\Lambda(1-p)} : \frac{1+\Lambda(1-r)(1-2p)}{1-\Lambda(1-pr)}$$

The LHS is independent of r. The RHS is equal to the LHS when $r = 1$, and moreover

$$\frac{dRHS}{dr} = \frac{(1-\Lambda(1-pr))(-\Lambda(1-2p)) - (1+\Lambda(1-r)(1-2p))\Lambda p}{(1-\Lambda(1-pr))^2}$$

$$= \frac{\Lambda(p-1) + \Lambda^2(1-2p)(1-p)}{(1-\Lambda(1-pr))^2} = \frac{(1-p)\Lambda\left[-1+\Lambda(1-2p)\right]}{(1-\Lambda(1-pr))^2}$$

For $\Lambda \in (0,1]$, $p > 1/2$ clearly implies $dRHS/dr < 0$, and when $p < 1/2$ then $\Lambda \leqslant 1$ implies $-1+\Lambda(1-2p) < 0$ and thus again $dRHS/dr < 0$. It follows that $\Delta^*_{MX} < 0$ for any $\Lambda \in (0,1]$.

For $\Lambda \in [-1,0)$, $p < 1/2$ clearly implies $dRHS/dr > 0$, and when $p > 1/2$ then $\Lambda \geqslant -1$ implies $-1+\Lambda(1-2p) < 0$ and thus again $dRHS/dr > 0$. It follows that $\Delta^*_{MX} > 0$ for any $\Lambda \in [-1,0)$.

■

B.4 Bell Disappointment Aversion (Bell DA)

Next, we consider predictions from Bell's (1985) model of disappointment aversion. Under this model, the utility from a lottery $X \equiv (x_1, p_1; ...; x_N, p_N)$ is

$$U(X) = \left(\sum_{n=1}^{N} p_n u(x_n)\right) - \beta\left(\sum_{n=1}^{N} p_n I\left(u(x_n) < \bar{U}\right)\left(\bar{U} - u(x_n)\right)\right),$$

where $u(\cdot)$ is an intrinsic utility function, and $\bar{U} \equiv \sum_{i=1}^{N} p_i u(x_i)$ is the expected intrinsic utility. When the parameter $\beta > 0$, it reflects a (constant) marginal disutility of disappointment experienced when one's realized intrinsic utility is below the expected intrinsic utility. If $\beta < 0$, then $-\beta$ effectively reflects a (constant) marginal utility of elation experienced when one's realized intrinsic utility is above the expected intrinsic utility.[56]

Applied to our context, the indifference values for h^*_{AB} and h^*_{CD} are determined from:

$$u(M) = pu(h^*_{AB}) - \beta(1-p)(pu(h^*_{AB}) - 0)$$

$$ru(M) - \beta(1-r)(ru(M) - 0) = pru(h^*_{CD}) - \beta(1-pr)(pru(h^*_{CD}) - 0)$$

and thus

$$h^*_{AB} = u^{-1}\left(\frac{1}{p(1-\beta(1-p))}u(M)\right) \qquad \text{and} \qquad h^*_{CD} = u^{-1}\left(\frac{1-\beta(1-r)}{p(1-\beta(1-pr))}u(M)\right).$$

[56] Bell (1985) further assumes that $u(x) = x$ and has separate parameters for disappointment (d) and elation (e). His model is equivalent to the version in the text with $\beta = d - e$. Loomes and Sugden (1986) also use this formulation, but they consider nonlinear disappointment and elation.

Note that for two-outcome lotteries such as our lotteries B, C, and D, the utilities under Bell DA are equivalent to those under Kőszegi-Rabin CPE, where β replaces Λ. Hence, we need an analogous restriction that the range of β is $[-1, 1]$.

For the $h^*_{AB'}$ indifference value, we must carefully assess whether, at the indifference value, $u(M)$ is larger or smaller than the expected intrinsic utility $pru(h^*_{AB'}) + (1-r)u(M)$ because that matters for the utility from lottery B'. We can write $pru(h^*_{AB'}) + (1-r)u(M) > u(M)$ as $u(h^*_{AB'}) > u(M)/p$. If we assume that $u(h^*_{AB'}) > u(M)/p$, then the $h^*_{AB'}$ is determined from:

$$\begin{aligned} u(M) = \quad & pru(h^{*(1)}_{AB'}) + (1-r)u(M) - \beta(1-r)(pru(h^{*(1)}_{AB'}) + (1-r)u(M) - u(M)) \\ & -\beta r(1-p)(pru(h^{*(1)}_{AB'}) + (1-r)u(M) - 0) \end{aligned}$$

$$\iff \quad h^{*(1)}_{AB'} = u^{-1}\left(\frac{1-\beta p(1-r)}{p(1-\beta(1-pr))}u(M)\right)$$

Note that as long as $1-\beta(1-pr) > 0$, $u(h^*_{AB'}) > u(M)/p$ when $1-\beta p(1-r) > 1-\beta(1-pr)$, or $\beta(1-p) > 0$, which holds as long as $\beta > 0$. Since $1-\beta(1-pr) > 0$ for all $\beta \in [0, 1]$, it follows that $h^*_{AB'} = h^{*(1)}_{AB'}$ for all $\beta \in [0, 1]$.

If we instead assume that $u(h^*_{AB'}) < u(M)/p$, then the $h^*_{AB'}$ is determined from:

$$u(M) = pru(h^{*(2)}_{AB'}) + (1-r)u(M) - \beta r(1-p)(pru(h^{*(2)}_{AB'}) + (1-r)u(M) - 0)$$

$$\iff \quad h^{*(2)}_{AB'} = u^{-1}\left(\frac{1+\beta(1-p)(1-r)}{p(1-\beta r(1-p))}u(M)\right)$$

Note that as long as $1-\beta r(1-p) > 0$, $u(h^*_{AB'}) < u(M)/p$ when $1+\beta(1-p)(1-r) < 1-\beta r(1-p)$, or $\beta(1-p) < 0$, which holds as long as $\beta < 0$. Since $1-\beta r(1-p) > 0$ for all $\beta \in [-1, 0]$, it follows that $h^*_{AB'} = h^{*(2)}_{AB'}$ for all $\beta \in [-1, 0]$.

Given these indifference values:

$$\begin{array}{lllll} \Delta^*_{CR} > 0 & \iff & h^*_{AB} > h^*_{CD} & \iff & \dfrac{1}{1-\beta(1-p)} > \dfrac{1-\beta(1-r)}{1-\beta(1-pr)} \\ \Delta^*_{CC} > 0 & \iff & h^*_{AB'} > h^*_{CD} & \iff & 1-\beta p(1-r) > 1-\beta(1-r) \quad \text{if } \beta \in [0,1] \\ & & & & \dfrac{1+\beta(1-p)(1-r)}{1-\beta r(1-p)} > \dfrac{1-\beta(1-r)}{1-\beta(1-pr)} \quad \text{if } \beta \in [-1,0] \\ \Delta^*_{MX} > 0 & \iff & h^*_{AB} > h^*_{AB'} & \iff & \dfrac{1}{1-\beta(1-p)} > \dfrac{1-\beta p(1-r)}{1-\beta(1-pr)} \quad \text{if } \beta \in [0,1] \\ & & & & \dfrac{1}{1-\beta(1-p)} > \dfrac{1+\beta(1-p)(1-r)}{1-\beta r(1-p)} \quad \text{if } \beta \in [-1,0] \end{array}$$

Hence, under Bell DA, the model's predictions for the sign of Δ^*_{CR}, Δ^*_{CC}, and Δ^*_{MX} are determined by the value of the parameter β.

Bell DA Result:

(1) $\beta \in (0,1)$ implies $\Delta^*_{CR} > 0$, $\Delta^*_{CC} > 0$, and $\Delta^*_{MX} < 0$.

(2) $\beta \in (-1,0)$ implies $\Delta^*_{CR} < 0$, $\Delta^*_{CC} < 0$, and $\Delta^*_{MX} > 0$.

Proof: For Δ^*_{CR}, the condition is equivalent to that under Kőszegi-Rabin CPE, and thus the proof is the same.

Next consider the Δ^*_{CC} condition.

For $\beta \in [0,1]$, $\Delta^*_{CC} > 0$ if $1 - \beta p(1-r) > 1 - \beta(1-r)$ or $\beta(1-r)(1-p) > 0$, which holds for any $\beta \in [0,1]$.

For $\beta \in [-1,0]$, $\Delta^*_{CC} < 0$ if

$$\begin{aligned}
\frac{1+\beta(1-p)(1-r)}{1-\beta r(1-p)} &< \frac{1-\beta(1-r)}{1-\beta(1-pr)} \\
(1+\beta(1-p)(1-r))(1-\beta(1-pr)) &< (1-\beta(1-r))(1-\beta r(1-p)) \\
\beta((1-p)(1-r)-(1-pr)) - \beta^2(1-p)(1-r)(1-pr) &< -\beta(1-pr) + \beta^2(1-p)(1-r)r \\
\beta(1-p)(1-r)(1-\beta(1-pr+r)) &< 0
\end{aligned}$$

which holds for any $\beta \in [-1,0]$.

Finally consider the Δ^*_{MX} condition.

For $\beta \in [0,1]$:

$$\Delta^*_{MX} : 0 \iff \frac{1}{1-\beta(1-p)} > \frac{1-\beta p(1-r)}{1-\beta(1-pr)}$$

The LHS is independent of r. The RHS is equal to the LHS when $r = 1$, and moreover

$$\frac{dRHS}{dr} = \frac{(1-\beta(1-pr))(\beta p) - (1-\beta p(1-r))(\beta p)}{(1-\beta(1-pr))^2} = \frac{-\beta^2 p(1-p)}{(1-\beta(1-pr))^2}$$

Hence, $\beta \in [0,1]$ implies $dRHS/dr < 0$, and thus $\Delta^*_{MX} < 0$ for any $r < 1$.

For $\beta \in [-1,0]$:

$$\Delta^*_{MX} : 0 \iff \frac{1}{1-\beta(1-p)} > \frac{1+\beta(1-p)(1-r)}{1-\beta r(1-p)}$$

The LHS is independent of r. The RHS is equal to the LHS when $r = 1$, and moreover

$$\frac{dRHS}{dr} = \frac{(1-\beta r(1-p))(-\beta(1-p)) - (1-\beta(1-p)(1-r))(-\beta(1-p))}{(1-\beta r(1-p))^2} = \frac{\beta^2(1-p)^2}{(1-\beta(1-pr))^2}$$

Hence, $\beta \in [-1,0]$ implies $dRHS/dr > 0$, and thus $\Delta^*_{MX} > 0$ for any $r < 1$.

■

B.5 Gul Disappointment Aversion (Gul DA)

We next consider predictions from the Gul (1991) model of disappointment aversion. Under this model, the utility from a lottery $X \equiv (x_1, p_1; ...; x_N, p_N)$ is the $U(X)$ that satisfies

$$U(X) = \left(\sum_{n=1}^{N} p_n u(x_n) \right) - \beta \left(\sum_{n=1}^{N} p_n I\left(u(x_n) < U(X)\right) \left(U(X) - u(x_n)\right) \right),$$

where $u(x)$ is an intrinsic utility function, and a person experiences disappointment when their realized intrinsic utility is below the overall utility of the lottery $U(X)$. As in Bell DA, $\beta > 0$ is disappointment aversion while $\beta < 0$ is elation-loving. Applying this to binary gambles of the form $X \equiv (x, q_H; 0, q_L)$, this becomes

$$U(X) = q_H u(x) - \beta q_L (U(X) - 0)) \quad \Longleftrightarrow \quad U(X) = \frac{q_H}{1 + \beta q_L} u(x).$$

Gul imposes $\beta > -1$, which guarantees that $U(X)$ is increasing in the payoff x for any q_L. This model does not require an upper bound for β. The indifference values h^*_{AB} and h^*_{CD} are given by:

$$u(M) = \frac{p}{1 + \beta(1-p)} u(h^*_{AB}) \iff h^*_{AB} = u^{-1}\left(\frac{1 + \beta(1-p)}{p} u(M) \right)$$

$$\tfrac{r}{1+\beta(1-r)} u(M) = \tfrac{pr}{1+\beta(1-pr)} u(h^*_{CD}) \iff h^*_{CD} = u^{-1}\left(\frac{1 + \beta(1-pr)}{p(1 + \beta(1-r))} u(M) \right)$$

For the $h^*_{AB'}$ indifference value, in principle, we must carefully assess whether, at the indifference value, $u(M)$ is larger or smaller than $U(B')$ (analogous to what we did for Bell DA). However, because $h^*_{AB'}$ is determined by the condition $u(M) = U(B')$, we know that $u(M) = U(B')$ at $H = h^*_{AB'}$. It follows that, at $H = h^*_{AB'}$, we have:

$$U(B') = pru(H) + (1-r)u(M) - \beta r(1-p)(U(B') - 0)$$

or

$$U(B') = \frac{pr}{1 + \beta r(1-p)} u(H) + \frac{1-r}{1 + \beta r(1-p)} u(M).$$

Then $h^*_{AB'}$ is derived from

$$u(M) = \frac{pr}{1 + \beta r(1-p)} u(h^*_{AB'}) + \frac{1-r}{1 + \beta r(1-p)} u(M) \quad \Longleftrightarrow \quad h^*_{AB'} = u^{-1}\left(\frac{1 + \beta(1-p)}{p} u(M) \right).$$

Notice that $h^*_{AB'} = h^*_{AB}$ and thus $\Delta^*_{MX} = 0$ (a well known property of Gul DA) and thus $\Delta^*_{CR} = \Delta^*_{CC}$.

Hence, there is only one remaining condition to consider:

$$\Delta^*_{CR} = \Delta^*_{CC} > 0 \iff h^*_{AB} = h^*_{AB'} > h^*_{CD} \iff 1 + \beta(1-p) > \tfrac{1+\beta(1-pr)}{1+\beta(1-r)}$$

Hence, under Gul DA, the model's predictions for the sign of Δ^*_{CR}, Δ^*_{CC}, and Δ^*_{MX} are determined by the value of the parameter β.

Gul DA Result:

(1) $\beta > 0$ implies $\Delta^*_{CR} = \Delta^*_{CC} > 0$ and $\Delta^*_{MX} = 0$.

(2) $\beta \in (-1, 0)$ implies $\Delta^*_{CR} = \Delta^*_{CC} < 0$, and $\Delta^*_{MX} = 0$.

Proof: The Δ^*_{CR} condition is:

$$\Delta^*_{CR} : 0 \iff 1 + \beta(1-p) : \frac{1+\beta(1-pr)}{1+\beta(1-r)}$$

The LHS is independent of r. The RHS is equal to the LHS when $r = 1$, and moreover

$$\frac{dRHS}{dr} = \frac{(1+\beta(1-r))(-\beta p) - (1+\beta(1-pr))(-\beta)}{(1+\beta(1-r))^2} = \frac{(\beta+\beta^2)(1-p)}{(1+\beta(1-r))^2}$$

Hence, $\beta > 0$ implies $dRHS/dr > 0$ and thus $\Delta^*_{CR} = \Delta^*_{CC} > 0$, while $\beta \in (-1, 0)$ implies $dRHS/dr < 0$ and thus $\Delta^*_{CR} = \Delta^*_{CC} < 0$.

■

B.6 Cautious Expected Utility (CEU)

We next consider the implications of the *cautious expected utility (CEU)* model introduced by Cerreia-Vioglio et al. (2015). Unlike the models above, their focus is a representation theorem and not a parameterized model, but firm predictions for our context follow from their axioms.

To illustrate, suppose we fix $H = h^*_{AB}$ so that $B \sim A$. Because lottery A is a sure amount, their key axiom of *negative certainty independence (NCI)* implies that $rB + (1-r)0 \gtrsim rA + (1-r)0$ for any $r \in (0, 1)$. Because $rB + (1-r)0 = D$ and $rA + (1-r)0 = C$, CEU permits a CRP (i.e., $\Delta^*_{CR} > 0$) but not an RCRP. NCI also implies (see page 697 of Cerreia-Vioglio et al., 2015) that $rB + (1-r)A \sim B$ for any $r \in (0, 1)$. Because $rB + (1-r)A = B'$, CEU implies $A \sim B \sim B'$ and thus $\Delta^*_{MX} = 0$. Finally, $\Delta^*_{MX} = 0$ implies $\Delta^*_{CC} = \Delta^*_{CR}$.

To summarize, when the predictions of CEU differ from EU, those predictions are $\Delta^*_{CC} = \Delta^*_{CR} > 0$ and $\Delta^*_{MX} = 0$, i.e., the CRP-CCP-⃠MXP pattern.

B.7 Puri Simplicity Preferences

Finally, we consider the implications of the model of *simplicity preferences* introduced by Puri (2025). Under this model, the utility from a lottery $X \equiv (x_1, p_1; ...; x_N, p_N)$ is

$$U(X) = \sum_{n=1}^{N} p_n u(x_n) - \omega(N).$$

The first term is a standard EU term, and $\omega(N)$ is a complexity cost term that is increasing in N—i.e., lotteries with more possible outcomes have a larger complexity cost. Here, we derive predictions for our context under the assumption that $\omega(1) < \omega(2) < \omega(3)$.

To derive predictions, it is convenient to fix the parameters (M, p, r) and then define $EU(X|h)$ to be the expected utility of lottery $X \in \{B, B', D\}$ as a function of h. Also, recall that, for any h, $EU(C) - EU(D|h) = EU(A) - EU(B'|h) = r(EU(A) - EU(B|h))$.

Under this model, h^*_{CD} must satisfy $EU(C) - \omega(2) = EU(D|h^*_{CD}) - \omega(2)$ and therefore $EU(C) = EU(D|h^*_{CD})$. This in turn implies $EU(A) = EU(B|h^*_{CD})$ and thus $EU(A) - \omega(1) > EU(B|h^*_{CD}) - \omega(2)$. It follows that $h^*_{AB} > h^*_{CD}$ and thus $\Delta^*_{CR} > 0$. Similarly, it also implies $EU(A) = EU(B'|h^*_{CD})$ and thus $EU(A) - \omega(1) > EU(B'|h^*_{CD}) - \omega(3)$. It follows that $h^*_{AB'} > h^*_{CD}$ and thus $\Delta^*_{CC} > 0$.

Under this model, h^*_{AB} must satisfy $EU(A) - \omega(1) = EU(B|h^*_{AB}) - \omega(2)$ and therefore $EU(A) < EU(B|h^*_{AB})$. Since B' is a mixture of A and B, we must have $EU(A) < EU(B'|h^*_{AB}) < EU(B|h^*_{AB})$ and thus $EU(B'|h^*_{AB}) - \omega(3) < EU(B|h^*_{AB}) - \omega(2)$. It follows that $EU(A) - \omega(1) > EU(B'|h^*_{AB}) - \omega(3)$ and thus $h^*_{AB'} > h^*_{AB}$ and $\Delta^*_{MX} < 0$.

To summarize, if $\omega(1) < \omega(2) < \omega(3)$, then Puri simplicity preferences predict $\Delta^*_{CR} > 0$, $\Delta^*_{CC} > 0$, and $\Delta^*_{MX} < 0$, i.e., the CRP-CCP-RMXP pattern.

C The Impact of Noise on Valuations and Choices

In Section 2.5, we discuss the impact of noise on valuation tasks and binary choice tasks, and the inferential challenges that arise as a result. This appendix formalizes the intuition in that section by replicating and expanding on the theoretical results in McGranaghan et al. (2024).

We assume that the same underlying preferences drive behavior for both valuation tasks and binary choice tasks. Using the notation from Section 2.2, a person will have three underlying indifference values h^*_{AB}, $h^*_{AB'}$, and h^*_{CD} for a fixed (p, r, M) that satisfy:

- Prefer A over B if and only if $H < h^*_{AB}$,
- Prefer A over B' if and only if $H < h^*_{AB'}$, and
- Prefer C over D if and only if $H < h^*_{CD}$.

We can then characterize that person's CR, CC, and MX preferences by $\Delta^*_{CR} \equiv h^*_{AB} - h^*_{CD}$, $\Delta^*_{CC} \equiv h^*_{AB'} - h^*_{CD}$, and $\Delta^*_{MX} \equiv h^*_{AB} - h^*_{AB'}$. EU implies $\Delta^*_{CC} = \Delta^*_{CR} = \Delta^*_{MX} = 0$.

C.1 The Impact of Noise on Valuations

In Section 2.5, we provide an intuitive argument for how paired valuation tasks might yield unbiased inference even in the presence of noise. Here, we provide a formal argument.

To combine a participant's underlying preferences with noise to generate their stated valuations, we begin with an assumption that is more general than the one used in Section 2.5:

Assumption C1v: Impact of Noise on Valuations

A person's *stated valuations* $(h_{AB}, h_{AB'}, h_{CD})$ are $h_{AB} \equiv \Gamma(h^*_{AB}, \varepsilon_{AB})$, $h_{AB'} \equiv \Gamma(h^*_{AB'}, \varepsilon_{AB'})$, and $h_{CD} \equiv \Gamma(h^*_{CD}, \varepsilon_{CD})$, where $(\varepsilon_{AB}, \varepsilon_{AB'}, \varepsilon_{CD})$ are noise draws from a continuous joint distribution with convex support, and Γ is increasing in both arguments with $\Gamma(h, 0) = h$ for all h.

In Assumption C1v, the function Γ permits a variety of models for how a person's underlying indifference points combine with choice noise to generate their stated valuations. We highlight two special cases of Assumption C1v:

Assumption C2a: $\Gamma(h, \varepsilon) = h + \varepsilon$, and $E(\varepsilon_{AB}) = E(\varepsilon_{AB'}) = E(\varepsilon_{CD}) = 0$.

Assumption C2b: $\Gamma(h, \varepsilon)$ is potentially nonlinear in h and ε, but $\varepsilon_{AB} \overset{d}{=} k_{AB}\varepsilon_{CD}$ for some $k_{AB} > 0$, $\varepsilon_{AB'} \overset{d}{=} k_{AB'}\varepsilon_{CD}$ for some $k_{AB'} > 0$, and ε_{CD} is symmetric about 0.

Assumption C2a is the assumption we use in Section 2.5 and represents the simple case in which stated valuations are given by the true underlying preference plus a mean-zero error term. Assumption C2b is less straightforward at first glance, but it is consistent with assumptions researchers frequently use when analyzing choice data, where they model noise as a symmetric additive perturbation of utility in the spirit of McFadden (1974, 1981). To illustrate, consider the following example:

Example: Expected Utility and Prospect Theory

Suppose that a person evaluates a lottery (x, q) with $x > 0$ as $\pi(q)u(x)$, and evaluates a lottery $(x, q; y, s)$ with $x > y > 0$ as $\pi(q)u(x) + w(q, s)u(y)$. This formulation reduces to EU when $\pi(q) = q$, $w(q, s) = s$, and $u(x)$ is a Bernoulli utility function. This formulation reduces to CPT when $\pi(q)$ is a probability weighting function, $w(q, s) = \pi(q + s) - \pi(q)$, and $u(x)$ is a value function defined over gains and losses. Finally, this formulation reduces to OPT when $\pi(q)$ is a probability weighting function, $w(q, s) = \pi(s)$, and $u(x)$ is a value function defined over gains and losses.

With this formulation, the underlying indifference points satisfy

$$\begin{aligned}
u(M) = \pi(p)u(h^*_{AB}) \qquad &\Leftrightarrow \qquad h^*_{AB} = u^{-1}\left(\frac{1}{\pi(p)}u(M)\right) \\
u(M) = \pi(pr)u(h^*_{AB'}) + w(pr, 1-r)u(M) \qquad &\Leftrightarrow \qquad h^*_{AB'} = u^{-1}\left(\frac{1 - w(pr, 1-r)}{\pi(pr)}u(M)\right) \\
\pi(r)u(M) = \pi(pr)u(h^*_{CD}) \qquad &\Leftrightarrow \qquad h^*_{CD} = u^{-1}\left(\frac{\pi(r)}{\pi(pr)}u(M)\right)
\end{aligned}$$

Now suppose we incorporate additive utility noise in the spirit of McFadden (1974, 1981) by assuming that the stated valuations satisfy

$$\begin{aligned}
u(M) = \pi(p)u(h_{AB}) + \epsilon_{AB} \qquad &\Leftrightarrow \qquad h_{AB} = u^{-1}\left(u(h^*_{AB}) - \frac{\epsilon_{AB}}{\pi(p)}\right) \\
u(M) = \pi(pr)u(h_{AB'}) + w(pr, 1-r)u(M) + \epsilon_{AB'} \qquad &\Leftrightarrow \qquad h_{AB'} = u^{-1}\left(u(h^*_{AB'}) - \frac{\epsilon_{AB'}}{\pi(pr)}\right) \\
\pi(r)u(M) = \pi(pr)u(h_{CD}) + \epsilon_{CD} \qquad &\Leftrightarrow \qquad h_{CD} = u^{-1}\left(u(h^*_{CD}) - \frac{\epsilon_{CD}}{\pi(pr)}\right)
\end{aligned}$$

where ϵ_{AB}, $\epsilon_{AB'}$, and ϵ_{CD} reflect additive utility noise.[57] When applying this approach, it is common to further assume that ϵ_{CD} has some distribution that is symmetric about 0 (e.g., a mean-zero normal or logistic distribution), and that $\epsilon_{AB} \stackrel{d}{=} k'_{AB}\epsilon_{CD}$ and $\epsilon_{AB'} \stackrel{d}{=} k'_{AB'}\epsilon_{CD}$ for some $k'_{AB} > 0$ and $k'_{AB'} > 0$ (e.g., when the error terms all have the same distributional form but are permitted to have different variances). If so, then this formulation fits Assumption

[57] The latter equations use $(1/\pi(p))u(M) = u(h^*_{AB})$, $((1 - w(pr, 1 - r))/\pi(pr))u(M) = u(h^*_{AB'})$, and $(\pi(r)/\pi(pr))u(M) = u(h^*_{CD})$.

C2b with $\Gamma(h, \varepsilon) = u^{-1}(u(h) - \varepsilon)$, where $\varepsilon_{AB} = k'_{AB}\epsilon_{CD}/\pi(p)$, $\varepsilon_{AB'} = k'_{AB'}\epsilon_{CD}/\pi(pr)$, and $\varepsilon_{CD} = \epsilon_{CD}/\pi(pr)$. Finally, EU with additive utility noise that is i.i.d. across the AB, AB', and CD choices (so $k'_{AB} = k'_{AB'} = 1$) implies $\varepsilon_{AB} = r\varepsilon_{CD}$ and $\varepsilon_{AB'} = \varepsilon_{CD}$.

Proposition C1v describes when unbiased tests of the null of $\Delta^*_Z = 0$, $Z \in \{CR, CC, MX\}$, are possible using paired valuation tasks and Assumption C2a or C2b.

Proposition C1v *(Paired Valuation Tasks Can Yield Unbiased Tests):* Consider a person who provides stated valuations $(h_{AB}, h_{AB'}, h_{CD})$.

(1) Under Assumption C2a, $E(\Delta_Z) = \Delta^*_Z$ for all $Z \in \{CR, CC, MX\}$.

(2) Under Assumption C2b, $\Pr(\Delta_Z > 0) = \Pr(\Delta_Z < 0) = 1/2$ for all $Z \in \{CR, CC, MX\}$.

The proof and intuition for Proposition C1v are virtually the same as those for Proposition 2 in McGranaghan et al. (2024), and thus we omit them here. Part (1) establishes that we can test the null of $\Delta^*_Z = 0$ under Assumption C2a using a means test. Part (2) establishes that we can test the null of $\Delta^*_Z = 0$ under Assumption C2b using a sign test that tests whether the observed proportions of $\Delta_Z > 0$ and $\Delta_Z < 0$ are the same.[58] These are the two tests reported in Table A.4.

C.2 The Impact of Noise on Choices

In Section 2.5, we describe how noise can make it problematic to infer preferences when comparing behavior across binary choice tasks. We provide a formal argument here. To model how a participant's underlying preferences combine with noise to generate their choices in the three binary choice tasks, we use the following alternative to Assumption C1v:

Assumption C1c: Impact of Noise on Choices

A person's *realized indifference points* are the $(h_{AB}, h_{AB'}, h_{CD})$ described in Assumption C1v. Then:

- In an AB choice task, the person chooses $A \equiv (M, 1)$ over $B \equiv (H, p)$ if and only if $H \leqslant h_{AB} \equiv \Gamma(h^*_{AB}, \varepsilon_{AB})$,

[58] Our formal test uses the following logic. If $\Pr(\Delta_Z > 0) = \Pr(\Delta_Z < 0) = 1/2$ for every observation, the likelihood of observing at most n instances of $\Delta_Z > 0$ out of N observations is equal to $G(n, N)$, where G denotes the cumulative distribution function for a binomial distribution with a 50 percent success rate. Hence, if we observe n_+ instances of $\Delta_Z > 0$ and n_- instances of $\Delta_Z < 0$, the p-value for a two-sided sign test under the null of $\Delta^*_Z = 0$ is $2 * G(\min\{n_+, n_-\}, n_+ + n_-)$.

- In an AB' choice task, the person chooses $A \equiv (M, 1)$ over $B' \equiv (H, p; M, 1-r)$ if and only if $H \leqslant h_{AB'} \equiv \Gamma(h^*_{AB'}, \varepsilon_{AB'})$,
- In a CD choice task, the person chooses $C \equiv (M, r)$ over $D \equiv (H, pr)$ if and only if $H \leqslant h_{CD} \equiv \Gamma(h^*_{CD}, \varepsilon_{CD})$.

In a choice task, the observed data comes in the form of the proportion of participants who choose each option. Under Assumption C1c, the relevant proportions are:

$$\Pr(A|AB) = \Pr(H < h_{AB}),\ \Pr(A|AB') = \Pr(H < h_{AB'}), \text{ and } \Pr(C|CD) = \Pr(H < h_{CD}).$$

Proposition C2c establishes conditions under which paired choice tasks yield biased tests of the null of $\Delta^*_Z = 0$, $Z \in \{CR, CC, MX\}$.

Proposition C2c *(Paired Choice Tasks Can Yield Biased Tests)*: Consider a person who has $h^*_{AB} = h^*_{AB'} = h^*_{CD} \equiv h^*$ and thus $\Delta^*_{CR} = \Delta^*_{CC} = \Delta^*_{MX} = 0$. Suppose that $\varepsilon_{AB} \overset{d}{=} k_{AB}\varepsilon_{CD}$ and $\varepsilon_{AB'} \overset{d}{=} k_{AB'}\varepsilon_{CD}$ for some $k_{AB} > 0$ and $k_{AB'} > 0$, and define $\chi \equiv \Pr(\varepsilon_{AB} < 0) = \Pr(\varepsilon_{AB'} < 0) = \Pr(\varepsilon_{CD} < 0)$.

(1) If $h^* - H > 0$ and thus the person has $A \succ B$, $A \succ B'$, and $C \succ D$, then:
   (a) $k_{AB} < 1$ implies $\Pr(A|AB) > \Pr(C|CD) > \chi$ (CRE); $k_{AB} > 1$ implies $\Pr(C|CD) > \Pr(A|AB) > \chi$ (RCRE); and $k_{AB} = 1$ implies $\Pr(A|AB) = \Pr(C|CD) = \chi$ ($\oslash$CRE);
   (b) $k_{AB'} < 1$ implies $\Pr(A|AB') > \Pr(C|CD) > \chi$ (CCE); $k_{AB'} > 1$ implies $\Pr(C|CD) > \Pr(A|AB') > \chi$ (RCCE); and $k_{AB'} = 1$ implies $\Pr(A|AB') = \Pr(C|CD) = \chi$ ($\oslash$CCE); and
   (c) $k_{AB} < k_{AB'}$ implies $\Pr(A|AB) > \Pr(A|AB') > \chi$ (MXE); $k_{AB} > k_{AB'}$ implies $\Pr(A|AB') > \Pr(A|AB) > \chi$ (RMXE); and $k_{AB} = k_{AB'}$ implies $\Pr(A|AB) = \Pr(A|AB') = \chi$ ($\oslash$MXE).

(2) If $h^* - H < 0$ and thus the person has $B \succ A$, $B' \succ A$, and $D \succ C$, then:
   (a) $k_{AB} < 1$ implies $\Pr(A|AB) < \Pr(C|CD) < \chi$ (RCRE); $k_{AB} > 1$ implies $\Pr(C|CD) < \Pr(A|AB) < \chi$ (CRE); and $k_{AB} = 1$ implies $\Pr(A|AB) = \Pr(C|CD) = \chi$ ($\oslash$CRE);
   (b) $k_{AB'} < 1$ implies $\Pr(A|AB') < \Pr(C|CD) < \chi$ (RCCE); $k_{AB'} > 1$ implies $\Pr(C|CD) < \Pr(A|AB') < \chi$ (CCE); and $k_{AB'} = 1$ implies $\Pr(A|AB') = \Pr(C|CD) = \chi$ ($\oslash$CCE); and
   (c) $k_{AB} < k_{AB'}$ implies $\Pr(A|AB) < \Pr(A|AB') < \chi$ (RMXE); $k_{AB} > k_{AB'}$ implies $\Pr(A|AB') < \Pr(A|AB) < \chi$ (MXE); and $k_{AB} = k_{AB'}$ implies $\Pr(A|AB) = \Pr(A|AB') = \chi$ ($\oslash$MXE).

(3) If $h^* - H = 0$ and thus the person has $A \sim B \sim B'$ and $C \sim D$, then $\Pr(A|AB) = \Pr(A|AB') = \Pr(C|CD) = \chi$ for all k_{AB} and $k_{AB'}$.

Again, the proof and intuition for Proposition C2c are virtually the same as the proof and intuition for Proposition 1 in McGranaghan et al. (2024), and thus we omit them here. Also, note that Proposition C2c holds under Assumption C2b, and it would also hold under Assumption C2a if in addition to $E(\varepsilon_{AB}) = E(\varepsilon_{AB'}) = E(\varepsilon_{CD}) = 0$ we also have $\varepsilon_{AB} \stackrel{d}{=} k_{AB}\varepsilon_{CD}$ and $\varepsilon_{AB'} \stackrel{d}{=} k_{AB'}\varepsilon_{CD}$ for some $k_{AB} > 0$ and $k_{AB'} > 0$. Hence, paralleling Corollary 1 in McGranaghan et al., paired choice tasks can yield biased tests while paired valuation tasks yield unbiased tests under the same assumptions about noise.

Beyond replicating the CRE result from Proposition 1 in McGranaghan et al. (2024) and extending it the CCE and MXE experiments, Proposition C2c also illustrates that the potential for misleading conclusions is even greater when attempting to identify preference patterns by comparing behavior across three binary choices. In particular, even when the true underlying preferences involve ⃠CRP, ⃠CCP, and ⃠MXP, many different patterns can emerge across the three choice tasks depending on the values for k_{AB} and $k_{AB'}$ and the experimenter-chosen parameter H. For instance, if $k_{AB'} < k_{AB} < 1$, then $H < h^*$ would lead to pattern CRE-CCE-RMXE, while $H > h^*$ would lead to pattern RCRE-RCCE-MXE. Alternatively, if $k_{AB} < 1 < k_{AB'}$, then $H < h^*$ would lead to pattern CRE-RCCE-MXE, while $H > h^*$ would lead to pattern RCRE-CCE-RMXE. Many other patterns are possible, and the only cases where the prediction would be the pattern ⃠CRE-⃠CCE-⃠MXE that corresponds to underlying preferences are the knife-edge cases where either distance to indifference is zero, $h^* - H = 0$, or differential noise is absent, $k_{AB} = k_{AB'} = 1$.

Proposition C2c establishes that choice tasks can yield a wide set of patterns when the true underlying preferences are ⃠CRP-⃠CCP-⃠MXP. The same can hold even when people have different underlying preferences. To illustrate, consider behavior under Assumption C2a with the additional assumption of $\varepsilon_{AB} \stackrel{d}{=} k_{AB}\varepsilon_{CD}$ and $\varepsilon_{AB'} \stackrel{d}{=} k_{AB'}\varepsilon_{CD}$ for some $k_{AB} > 0$ and $k_{AB'} > 0$. Under these assumptions, we can write the choice proportions as follows:

$$\begin{array}{rcccc} \Pr(A|AB) & = & \Pr(H < h^*_{AB} + \varepsilon_{AB}) & = & \Pr\left(-\varepsilon_{CD} < \frac{1}{k_{AB}}(h^*_{AB} - H)\right) \\ \Pr(A|AB') & = & \Pr(H < h^*_{AB'} + \varepsilon_{AB'}) & = & \Pr\left(-\varepsilon_{CD} < \frac{1}{k_{AB'}}(h^*_{AB'} - H)\right) \\ \Pr(C|CD) & = & \Pr(H < h^*_{CD} + \varepsilon_{CD}) & = & \Pr\left(-\varepsilon_{CD} < h^*_{CD} - H\right) \end{array}$$

We next define $\bar{h}^*_{CR} \equiv (h^*_{AB} + h^*_{CD})/2$, $\bar{h}^*_{CC} \equiv (h^*_{AB'} + h^*_{CD})/2$, and $\bar{h}^*_{MX} \equiv (h^*_{AB} + h^*_{AB'})/2$, which are the average indifference values for the three paired valuations. Using these, and recalling for choices that $CRE - RCRE = \Pr(A|AB) - \Pr(C|CD)$, $CCE - RCCE = \Pr(A|AB') - \Pr(C|CD)$, and $MXE - RMXE = \Pr(A|AB) - \Pr(A|AB')$, we can derive predicted behavior in choice tasks:

$$\begin{array}{rcl} CRE - RCRE & = & \Pr\left(-\varepsilon_{CD} < h^*_{CD} - H + \Psi_{CR}\right) - \Pr\left(-\varepsilon_{CD} < h^*_{CD} - H\right) \\ CCE - RCCE & = & \Pr\left(-\varepsilon_{CD} < h^*_{CD} - H + \Psi_{CC}\right) - \Pr\left(-\varepsilon_{CD} < h^*_{CD} - H\right) \\ MXE - RMXE & = & \Pr\left(-\varepsilon_{AB'} < h^*_{AB'} - H + \Psi_{MX}\right) - \Pr\left(-\varepsilon_{AB'} < h^*_{AB'} - H\right) \end{array} \tag{C.1}$$

where

$$\begin{aligned}\Psi_{CR} &= 0.5\left(\tfrac{1}{k_{AB}}+1\right)\Delta^*_{CR}+\left(\tfrac{1}{k_{AB}}-1\right)(\bar{h}^*_{CR}-H)\\ \Psi_{CC} &= 0.5\left(\tfrac{1}{k_{AB'}}+1\right)\Delta^*_{CC}+\left(\tfrac{1}{k_{AB'}}-1\right)(\bar{h}^*_{CC}-H)\\ \Psi_{MX} &= 0.5\left(\tfrac{k_{AB'}}{k_{AB}}+1\right)\Delta^*_{MX}+\left(\tfrac{k_{AB'}}{k_{AB}}-1\right)(\bar{h}^*_{MX}-H)\end{aligned} \tag{C.2}$$

Hence, whether one's choices exhibit a CRE, CCE, or MXE depends on whether Ψ_{CR}, Ψ_{CC}, or Ψ_{MX} are positive or negative. In the the knife-edge cases where $\bar{h}^*_Z - H = 0$ for $Z \in \{CR, CC, MX\}$ or $k_{AB} = k_{AB'} = 1$, $\Psi_{CR} \propto \Delta^*_{CR}$, $\Psi_{CC} \propto \Delta^*_{CC}$, and $\Psi_{MX} \propto \Delta^*_{MX}$. Generalizing our earlier conclusion, in these knife-edge cases, choices will reveal the qualitative direction of underlying preferences.

In contrast, when $\bar{h}^*_Z - H \neq 0$ for $Z \in \{CR, CC, MX\}$ and k_{AB} and $k_{AB'}$ are not equal to one, then we have differential noise, and whether one exhibits a CRE, CCE, or MXE also depends on the relevant *distance to indifference*, i.e., $\bar{h}^*_{CR} - H$, $\bar{h}^*_{CC} - H$, or $\bar{h}^*_{MX} - H$. Indeed, if we fix the experimental parameters (M, p, r) and the associated underlying preferences $(h^*_{AB}, h^*_{AB'}, h^*_{CD})$, we can use equation (C.2) to derive predicted behavior as a function of the experimenter-chosen parameter H:

$$CRE - RCRE > 0 \Leftrightarrow \Psi_{CR} > 0 \Leftrightarrow \begin{cases} H > \bar{h}^*_{CR} - \dfrac{k_{AB}+1}{2(k_{AB}-1)}\Delta^*_{CR} & \text{if } k_{AB} > 1 \\ H < \bar{h}^*_{CR} + \dfrac{k_{AB}+1}{2(1-k_{AB})}\Delta^*_{CR} & \text{if } k_{AB} < 1 \\ \Delta^*_{CR} > 0 & \text{if } k_{AB} = 1 \end{cases}$$

$$CCE - RCCE > 0 \Leftrightarrow \Psi_{CC} > 0 \Leftrightarrow \begin{cases} H > \bar{h}^*_{CC} - \dfrac{k_{AB'}+1}{2(k_{AB'}-1)}\Delta^*_{CC} & \text{if } k_{AB'} > 1 \\ H < \bar{h}^*_{CC} + \dfrac{k_{AB'}+1}{2(1-k_{AB'})}\Delta^*_{CC} & \text{if } k_{AB'} < 1 \\ \Delta^*_{CC} > 0 & \text{if } k_{AB'} = 1 \end{cases}$$

$$MXE - RMXE > 0 \Leftrightarrow \Psi_{MX} > 0 \Leftrightarrow \begin{cases} H < \bar{h}^*_{MX} + \dfrac{k_{AB'}+k_{AB}}{2(k_{AB'}-k_{AB})}\Delta^*_{MX} & \text{if } k_{AB} < k_{AB'} \\ H > \bar{h}^*_{MX} - \dfrac{k_{AB'}+k_{AB}}{2(k_{AB}-k_{AB'})}\Delta^*_{MX} & \text{if } k_{AB} > k_{AB'} \\ \Delta^*_{MX} > 0 & \text{if } k_{AB} = k_{AB'} \end{cases}$$

Note that if the experimenter chooses $H = \bar{h}^*_{CR}$, then participants' $CRE - RCRE$ will reveal the sign of their underlying Δ^*_{CR}. An analogous point holds when the experimenter chooses $H = \bar{h}^*_{CC}$ or $H = \bar{h}^*_{MX}$. However, without observing valuations, it is hard for the experimenter to select these H's. Moreover, if the experimenter is trying to use choices to identify patterns across the three preferences, a single H may not be sufficient to accurately infer all three preferences.

Finally, we highlight how, as the experimenter varies the experimental parameter H, a variety of biased patterns can emerge. For example, suppose $h^*_{AB} = 36$, $h^*_{AB'} = 34$, and $h^*_{CD} = 30$, in which case underlying preferences have the pattern CRP, CCP, MXP. If in addition $k_{AB} = 0.5$ while

$k_{AB'} = 1.5$, participants would exhibit a CRE for $H < 42$, a CCE for $H > 22$, and an MXE for $H < 37$. Hence, for $H \in (22, 37)$, participants would exhibit the CRE-CCE-MXE pattern consistent with their underlying preferences. However, for H outside of this range we might observe the patterns CRE-RCCE-MXE, CRE-CCE-RMXE, or RCRE-CCE-RMXE.

The message is clear: If one wants to learn about patterns of CR-CC-MX preferences so as to be able to assess models of risk preferences, then using choice tasks will be problematic. In contrast, under the same assumptions as the analysis here, valuation tasks can be used to get unbiased measures of the underlying preferences Δ^*_{CR}, Δ^*_{CC}, and Δ^*_{MX}.

C.3 Connecting Stage 1 Valuations and Stage 2 Choices

Our discussion in Appendix C.1 and C.2 assumes that the same underlying preferences drive behavior for both valuation tasks and choice tasks, and thus there should be a strong connection between the two. In Section 4.5 of the main paper, we provide some evidence on that connection. Here, we provide the underlying theory on which that evidence is based. Again, this follows a similar treatment in McGranaghan et al. (2024).

Specifically, we consider Assumption C2a with the additional assumptions that $\varepsilon_{AB} \overset{d}{=} k_{AB}\varepsilon_{CD}$ and $\varepsilon_{AB'} \overset{d}{=} k_{AB'}\varepsilon_{CD}$ for some $k_{AB} > 0$ and $k_{AB'} > 0$. In this case, equations C.1 and C.2 characterize the predictions for stage 2 choices as a function of underlying indifference values h^*_{AB}, $h^*_{AB'}$, and h^*_{CD}. At the same time, Proposition C1v part 1 establishes that a participant's stage 1 valuations h_{AB}, $h_{AB'}$, and h_{CD} are unbiased measures of those underlying indifference values.

Hence, we conduct the following empirical analyses. First, we either (i) use each participant's stage 1 stated valuations h_{AB}, $h_{AB'}$, and h_{CD} to directly generate (noisy) empirical measures Δ_{CR}, Δ_{CC}, Δ_{MX}, $\bar{h}_{CR}$, $\bar{h}_{CC}$, and $\bar{h}_{MX}$, or (ii) use each participant's stage 1 stated valuations h_{AB}, $h_{AB'}$, and h_{CD} combined with our decomposition from Section 4.4 to generate posterior measures of an individual's underlying preferences $E[\Delta^*_{CR}|stage1]$, $E[\Delta^*_{CC}|stage1]$, $E[\Delta^*_{MX}|stage1]$, $E[\bar{h}^*_{CR}|\text{stage 1}]$, $E[\bar{h}^*_{CC}|\text{stage 1}]$, and $E[\bar{h}^*_{MX}|\text{stage 1}]$ (see Appendix D.4 for details). We then test the following predictions from equations C.1 and C.2:

(1) A person's observed $CRE - RCRE$, $CCE - RCCE$, and $MXE - RMXE$ at stage 2 should depend positively on their associated stage 1 value difference Δ_{CR}, Δ_{CC}, Δ_{MX}.

(2) With one caveat, a person's observed $CRE - RCRE$, $CCE - RCCE$, and $MXE - RMXE$ at stage 2 should depend positively on their associated distance to indifference $\bar{h}_{CR} - H$, $\bar{h}_{CC} - H$, $\bar{h}_{MX} - H$ when the noise is more impactful for the second choice (the CD choice for CRE and CCE, the AB' choice for MXE), and should depend negatively on their associated distance to indifference when the noise is more impactful for the first choice. The caveat is that, while this

prediction holds when the magnitude of the relevant distance to indifference is not too large, when that magnitude gets large enough (positive or negative), the relationship reverses because $\Pr(-\varepsilon_Z < h_Z^* - H)$ approaches zero (as in Figure 7 of McGranaghan et al. (2024)).

When we test these predictions, we increase power by combining data across different combinations of (p, r). Because for each preference the impact of the value difference or the distance to indifference is larger for larger p, in our empirical analyses we multiply these terms by p to make them more comparable across different values for p.

We visually assess prediction (1) in Figure 7 and we visually assess prediction (2) in Appendix Figure C.1. Panels A-C of Appendix Table C.1 provide corresponding formal tests via regressions of $CRE-RCRE$, $CCE-RCCE$, and $MXE-RMXE$ from stage 2 on the corresponding values of Δ_Z and $\bar{h}_Z - H$ from stage 1 (in both cases normalized by p). In each panel, four different specifications are provided: (1) ordinary least squares using the full sample of 8408 stage 2 observations; (2) ordinary least squares using samples of 4204 stage 2 observations for which multiple elicitations of relevant h valuations were conducted at stage 1; (3) two-stage least squares using samples of 4204 stage 2 observations for which multiple elicitations of relevant h valuations were conducted at stage 1 and instrumenting for Δ_Z and $\bar{h}_Z - H$ with the alternate elicitation's values, which accounts for potential measurement error in Δ_Z and $\bar{h}_Z - H$; (4) ordinary least squares using the full sample of 8408 stage 2 observations, but replacing Δ_Z and $\bar{h}_Z - H$ with the posterior expectations of preference given stage 1 behavior (i.e., $E[\Delta_Z^*|\text{stage 1}]$ $E[\bar{h}_Z^* - H|\text{stage 1}]$.

Figure 7 and Appendix Table C.1 show substantial support for prediction (1) with significant linkages between values of Δ_Z and corresponding differences in choice probabilities for CR, CC, and MX problems across all specifications. Appendix Figure C.1 and Appendix Table C.1 also document the relevance of prediction (2) for all three problems. For CR problems, the data show a significant positive relationship between $\bar{h}_{CR} - H$ and $CRE - RCRE$ across all specifications, indicating that noise is more impactful for the CD choice than the AB choice. For CC problems the data using raw valuations in columns (1) through (3) show limited relationship between $\bar{h}_{CC} - H$ and $CCE - RCCE$. However, when using the posterior expectation of preferences in column (4), the data show a significant negative relationship between $E[\bar{h}_{CC}^*|\text{stage 1}] - H$ and $CCE - RCCE$, indicating that noise is more impactful for the AB' choice than the CD choice. For MX problems the data show a significant positive relationship between $\bar{h}_{MX} - H$ and $MXE - RMXE$ across all specifications, indicating that noise is more impactful for the AB' choice than the AB choice. All three problems show the hallmarks of differential noise and the combined data suggest that noise has the most impact on AB' choices, followed by CD choices, followed by AB choices.

Interestingly, these conclusions differ from the predictions of EU with additive i.i.d utility noise. In particular, Example 1 from Appendix C.1 derives that, under EU with additive i.i.d. utility noise,

$\varepsilon_{AB} = r\varepsilon_{CD}$ and $\varepsilon_{AB'} = \varepsilon_{CD}$. In words, under EU with additive i.i.d utility noise, the impact of noise on the AB' and CD choices should be the same, and both should be larger than the impact of noise on the AB choice.

Figure C.1: Predicting Stage 2 Results using Stage 1 Distance to Indifference

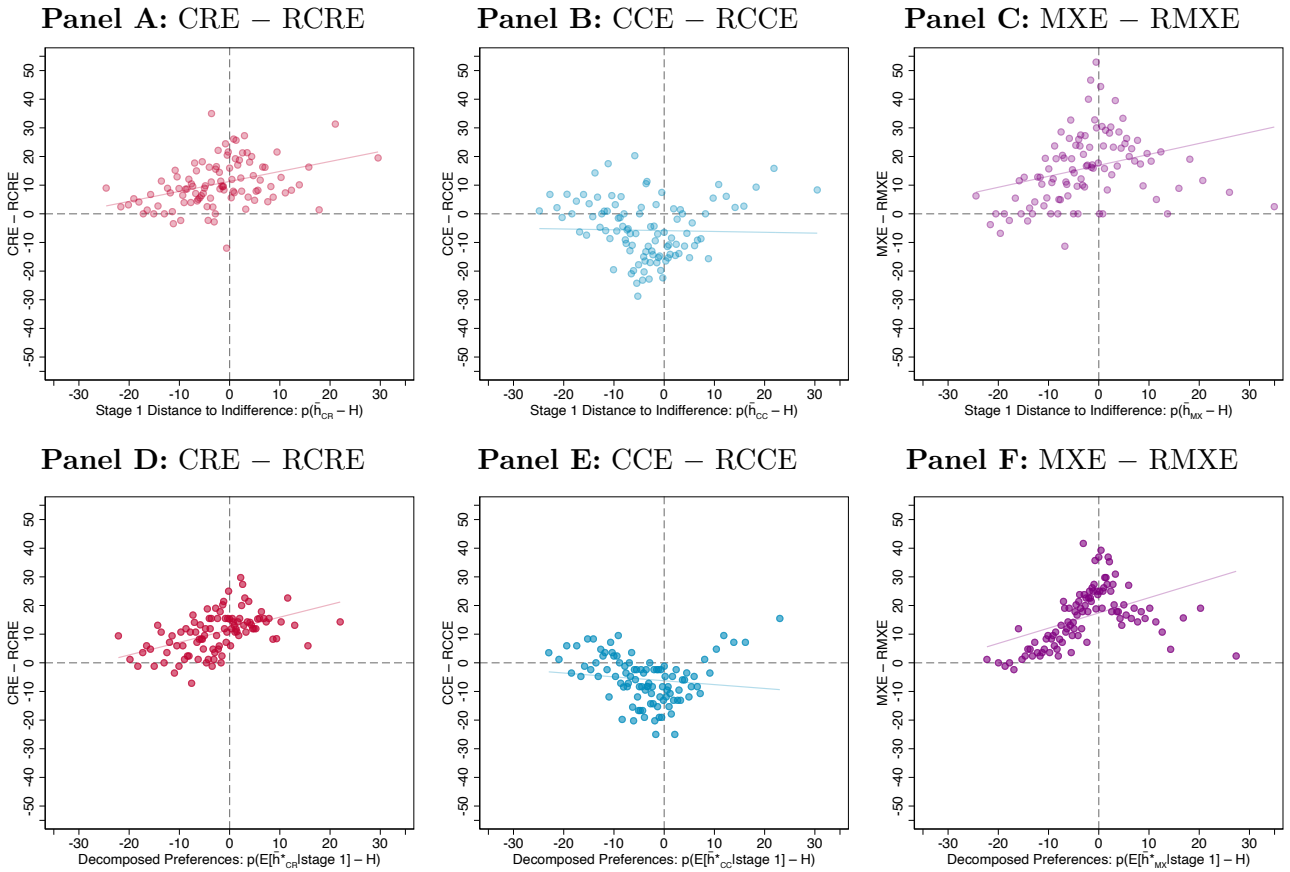

Notes: Figure relates individual stage 1 measures of $\bar{h}_{CR} - H$, $\bar{h}_{CC} - H$, and $\bar{h}_{MX} - H$ to stage 2 measures of $CRE - RCRE$, $CCE - RCCE$, and $MXE - RMXE$, respectively. Panels A-C use raw stage 1 responses. Panels D-F use the estimated population distribution of preferences from the decomposition in Section 4.4 combined with a participant's raw stage 1 valuations to generate posterior preference measures $E[\bar{h}^*_{CR}|\text{stage 1}]$, $E[\bar{h}^*_{CC}|\text{stage 1}]$, and $E[\bar{h}^*_{MX}|\text{stage 1}]$ for that participant. For each x-axis, one hundred equally sized bins are constructed with approximately 84 observations per bin for the CR and CC panels and approximately 42 observations for the MX panels. Within each bin, the value of stage 2 choice differences is calculated to construct the y-axes. Due to a large of observations at some values, there are 94, 93, and 91 unique bins in panels A, B, and C, respectively. To make valuations comparable across (p, r), all stage 1 measures are scaled by p to control for the fact that a fixed value of the measure is predicted to yield a larger stage 2 effect the larger is p (see Appendix C.3 for details).

Table C.1: Regressions Predicting Stage 2 Binary Choices Using Stage 1 Valuations

	(1) Full Sample	(2) Multiple Observations Available	(3) 2SLS	(4) Decomposed Preferences
	Panel A. $CRE - RCRE \in \{-1, 0, 1\}$			
$p\Delta_{CR}$	1.07	1.08	2.60	2.77
	(0.07)	(0.09)	(0.26)	(0.16)
$p(\bar{h}_{CR} - H)$	0.40	0.30	0.20	0.32
	(0.07)	(0.09)	(0.12)	(0.08)
Outcome Mean	10.45	10.04	10.04	10.45
	Panel B. $CCE - RCCE \in \{-1, 0, 1\}$			
$p\Delta_{CC}$	0.96	0.87	2.92	3.26
	(0.07)	(0.09)	(0.36)	(0.18)
$p(\bar{h}_{CC} - H)$	−0.03	−0.01	−0.16	−0.46
	(0.07)	(0.09)	(0.14)	(0.08)
Outcome Mean	−5.77	−4.69	−4.69	−5.77
	Panel C. $MXE - RMXE \in \{-1, 0, 1\}$			
$p\Delta_{MX}$	0.80	0.93	3.17	3.00
	(0.07)	(0.10)	(0.44)	(0.23)
$p(\bar{h}_{MX} - H)$	0.39	0.43	0.62	0.65
	(0.06)	(0.07)	(0.11)	(0.07)
Outcome Mean	16.00	15.91	15.91	16.00
Individuals	2102	1051	1051	2102
Observations	8,408	4,204	4,204	8,408

Notes: Table presents linear regressions of individuals' stage 2 decisions on stage 1 measures of their Δ_Z and $\bar{h}_Z - H$ for $Z \in \{CR, CC, MX\}$. Panel A presents results for CR experiments, where the outcome is 1 if the participant chose A and D (CRE), -1 if they chose B and C (RCRE), and zero otherwise. Panel B presents results for CC experiments, where the outcome is 1 if the participant chose A and D (CCE), -1 if they chose B' and C (RCRE), and zero otherwise. Panel C presents results for MX experiments, where the outcome is 1 if the participant chose A and B' (MXE), -1 if they chose B and A (RMXE), and zero otherwise. Columns (1)-(3) use raw stage 1 responses. Column (1) presents the full sample results for all four (p, r) combinations that participants saw. For panel C, we use the valuations h'_{AB} or $h'_{AB'}$ for the half of (p, r) that they exist for, and h_{AB} or $h_{AB'}$ otherwise. Column (2) restricts the sample to only the half of (p, r) conditions for which which we have multiple measures of all three valuations. Column (3) leverages these multiple observations to implement instrumental variable regressions using two-stage least squares, where we instrument for $p\Delta$ and $p(\bar{h} - H)$ with their duplicate measures. For Column (4), we use the estimated population distribution of preferences from the decomposition in Section 4.4 combined with a participant's raw stage 1 valuations to generate posterior preference measures $E[\Delta^*_Z|\text{stage 1}]$ and $E[\bar{h}^*_Z|\text{stage 1}]$. To make valuations comparable across (p, r), all stage 1 measures are scaled by p to control for the fact that a fixed value of the measure is predicted to yield a larger stage 2 effect the larger is p (see Appendix C.3 for details).

D Further Details on Decomposing Preference and Noise

In this appendix, we provide further details for the decomposition exercise in Section 4.4. In this exercise, we derive an estimate for the population distribution of underlying preferences along with the magnitude of decision noise. We then use these estimates for three purposes. First, we assess how much of the variability in our data is due to heterogeneity in preferences versus noise. Second, we derive what the histogram of response patterns from Figure 5 would look like if we were to remove the decision noise. Third, we construct refined measures of individual preferences that attempt to remove some of the noise.

D.1 Underlying Model and Estimating Its Parameters

For a fixed (p, r, M), let $\boldsymbol{h}^* \equiv (h^*_{AB}, h^*_{AB'}, h^*_{CD})$ be a vector of underlying indifference values. The population distribution of $\boldsymbol{h}^*$ has expectation $E(\boldsymbol{h}^*) \equiv (\mu^*_{AB}, \mu^*_{AB'}, \mu^*_{CD}) \equiv \boldsymbol{\mu}^*$ and variance-covariance matrix

$$\mathbf{V}\begin{pmatrix} h^*_{AB} \\ h^*_{AB'} \\ h^*_{CD} \end{pmatrix} \equiv \begin{pmatrix} \theta^2_{AB} & \theta_{AB,AB'} & \theta_{AB,CD} \\ \theta_{AB,AB'} & \theta^2_{AB'} & \theta_{AB',CD} \\ \theta_{AB,CD} & \theta_{AB',CD} & \theta^2_{CD} \end{pmatrix} \equiv \boldsymbol{\Sigma}^*. \tag{D.1}$$

For $XY \in \{AB, AB', CD\}$, we assume a person's two elicited XY valuations are

$$h_{XY} = h^*_{XY} + \varepsilon_{XY} \qquad \text{and} \qquad h'_{XY} = h^*_{XY} + \varepsilon'_{XY},$$

where $E(\varepsilon_{XY}) = E(\varepsilon'_{XY}) = 0$, $var(\varepsilon_{XY}) = var(\varepsilon'_{XY}) = \sigma^2_{XY}$, and ε_{XY} and ε'_{XY} are independent of each other, of the underlying preferences, and of all other noise draws. Note that this model has twelve parameters: three μ^*_{XY} terms, three θ^2_{XY} terms, three $\theta_{XY,WZ}$ terms, and three σ^2_{XY} terms.

Now let $\boldsymbol{h} \equiv (h_{AB}, h_{AB'}, h_{CD}, h'_{AB}, h'_{AB'}, h'_{CD})$ denote a vector of observed valuations. Under these assumptions, we can derive the predicted mean and variance-covariance matrix for the observed $\boldsymbol{h}$ as a function of the 12 parameters of the underlying model:

$$E(\boldsymbol{h}) = (\mu^*_{AB}, \mu^*_{AB'}, \mu^*_{CD}, \mu^*_{AB}, \mu^*_{AB'}, \mu^*_{CD}) \equiv \boldsymbol{\mu}$$

$$\mathbf{V}(\boldsymbol{h}) = \begin{pmatrix} \theta^2_{AB} + \sigma^2_{AB} & \theta_{AB,AB'} & \theta_{AB,CD} & \theta^2_{AB} & \theta_{AB,AB'} & \theta_{AB,CD} \\ \theta_{AB,AB'} & \theta^2_{AB'} + \sigma^2_{AB'} & \theta_{AB',CD} & \theta_{AB,AB'} & \theta^2_{AB'} & \theta_{AB',CD} \\ \theta_{AB,CD} & \theta_{AB',CD} & \theta^2_{CD} + \sigma^2_{CD} & \theta_{AB,CD} & \theta_{AB',CD} & \theta^2_{CD} \\ \theta^2_{AB} & \theta_{AB,AB'} & \theta_{AB,CD} & \theta^2_{AB} + \sigma^2_{AB} & \theta_{AB,AB'} & \theta_{AB,CD} \\ \theta_{AB,AB'} & \theta^2_{AB'} & \theta_{AB',CD} & \theta_{AB,AB'} & \theta^2_{AB'} + \sigma^2_{AB'} & \theta_{AB',CD} \\ \theta_{AB,CD} & \theta_{AB',CD} & \theta^2_{CD} & \theta_{AB,CD} & \theta_{AB',CD} & \theta^2_{CD} + \sigma^2_{CD} \end{pmatrix} \equiv \boldsymbol{\Sigma}$$

Each entry in $\mathbf{V}(\boldsymbol{h})$ is a theoretical prediction for an empirical moment. For instance, $var(h_{AB}) = \theta^2_{AB} + \sigma^2_{AB}$, and $cov(h_{AB}, h'_{AB}) = \theta^2_{AB}$. Hence, we can obtain estimates for the 12 model parameters by calculating the relevant sample moments or combination of sample moments. Specifically, using "hats" to denote estimates and the subscript s to denote sample moments, we can derive estimates for the model's 12 parameters using:

$$\begin{aligned} \widehat{\mu}^*_{XY} &= E_s(h_{XY}) \\ \widehat{\theta}^2_{XY} &= cov_s(h_{XY}, h'_{XY}) \\ \widehat{\theta}_{XY,WZ} &= cov_s(h_{XY}, h_{WZ}) \\ \widehat{\sigma}^2_{XY} &= var_s(h_{XY}) - cov_s(h_{XY}, h'_{XY}) \end{aligned}$$

To calculate the sample moments, we proceed as follows. Recall that roughly 420 participants provide valuations for each (p, r), but only half of those (roughly 210) provide all six valuations $(h_{AB}, h_{AB'}, h_{CD}, h'_{AB}, h'_{AB'}, h'_{CD})$, while the other half (again roughly 210) provide only four valuations $(h_{AB}, h_{AB'}, h_{CD}, h'_{CD})$. Given this, for each (p, r):

- To calculate $E_s(h_{XY})$ and $var_s(h_{XY})$, we include all observations of h_{XY} including repeats. Hence, for $XY \in \{AB, AB'\}$, these moments are calculated using roughly 630 observations, and for $XY \in \{CD\}$, these moments are calculated using roughly 840 observations.

- To calculate $cov_s(h_{XY}, h'_{XY})$, we include all pairs that we have (which is always 0 or 1 per participant who faced that (p, r)). Hence, for $XY \in \{AB, AB'\}$, this moment is calculated using roughly 210 observations, and for $XY \in \{CD\}$, this moment is calculated using roughly 420 observations.

- To calculate $cov_s(h_{XY}, h_{WZ})$, we include all (h_{XY}, h_{WZ}) pairs (which we have for every participant who faced that (p, r)), and we also include the (h'_{XY}, h'_{WZ}) pairs for the participants who provided all six valuations for that (p, r). Hence, all three of these moments are calculated using roughly 630 observations.

Using this approach to calculate the sample moments, Appendix Table A.7 reports estimates for the model's 12 parameters for each of the 20 (p, r) combinations.

Appendix D.5 describes a more sophisticated estimation approach using MLE. Because that approach requires additional distributional assumptions, is more time-consuming, and is sensitive to starting values and other estimation details, we prefer the approach described here. We note, however, that the MLE approach yields very similar estimates.

D.2 Assessing the Role of Heterogeneity versus Noise

Given these estimates, we can assess how much of the variability in our data is due to heterogeneity in preferences versus noise. Consider first variability in the elicited indifference values h_{AB}, $h_{AB'}$, and h_{CD}. The last three columns of Appendix Table A.7 report the estimated proportion of the variability for each elicited indifference value that is due to preferences—i.e., the ratio $\widehat{var}(h^*_{XY})/\widehat{var}(h_{XY}) = \hat{\theta}^2_{XY}/(\hat{\theta}^2_{XY} + \hat{\sigma}^2_{XY})$ for each $XY \in \{AB, AB', CD\}$. Averaging across the 20 (p, r) combinations, preference heterogeneity accounts for 61 percent of the variation in h_{AB}, 58 percent of the variation in $h_{AB'}$, and 48 percent of the variation in h_{CD}.

Next consider variability in the preference measures Δ_{CR}, Δ_{CC}, and Δ_{MX}. For $\Delta_{CR} \equiv h_{AB} - h_{CD}$, it is straightforward to derive that

$$\begin{aligned} & var(\Delta_{CR}) = var(\Delta^*_{CR}) + \sigma^2_{AB} + \sigma^2_{CD} \\ \text{and} \quad & var(\Delta^*_{CR}) = \theta^2_{AB} + \theta^2_{CD} - 2\theta_{AB,CD}. \end{aligned}$$

One can perform analogous derivations for Δ_{CC} and Δ_{MX}. Appendix Table A.8 uses the estimates in Appendix Table A.7 to calculate these six variances for each (p, r) combination.[59] The last three columns of Appendix Table A.8 report the proportion of the variability for each preference measure that is due to preferences—i.e., the ratio $\widehat{var}(\Delta^*_Z)/\widehat{var}(\Delta_Z)$ for each $Z \in \{CR, CC, MX\}$. Averaging across the 20 (p, r) combinations, preference heterogeneity accounts for 31 percent of the variation in Δ_{CR}, 31 percent of the variation in Δ_{CC}, and 25 percent of the variation in Δ_{MX}.

D.3 Simulating Preference Patterns

We next investigate what the histogram of response patterns from Figure 5 would look like if we were to remove the decision noise. To do so, we make the additional assumption that the underlying preferences have a joint normal distribution:

$$\boldsymbol{h}^* \sim N\left(\boldsymbol{\mu}^*, \boldsymbol{\Sigma}^*\right).$$

[59] When calculating things in this way, nothing guarantees that the calculated $var(\Delta^*_Z) > 0$, and indeed there is one instance where this problem arises (for Δ_{MX} when $(p, r) = (0.3, 0.5)$). We ignore this case and focus on the other 59 cases.

For each (p, r) combination, we use the estimated parameters in Appendix Table A.7 to generate 100,000 draws from a joint normal distribution for $\boldsymbol{h}^*$. We then convert each h^*_{XY} draw into the midpoint of its two closest integers (e.g., any draw strictly between \$2 and \$3 is converted to \$2.50). This approach is consistent with the valuations response scales in our experiment, since the switching rows for anyone with an underlying h^*_{XY} strictly between \$2 and \$3 would be the \$2 and \$3 rows, in which case we would assign them a valuation of \$2.50. We then use these converted h^*_{XY} terms to generate the Δ^*_Z terms.[60] Figure 6 presents the distribution of preference patterns when we aggregate across all 20 (p, r) combinations.

Note that this approach permits null preference patterns, including EU consistency. However, it does not permit preference patterns which would imply intransitivities between h^*_{AB}, $h^*_{AB'}$, and h^*_{CD}. Of the 27 possible preference patterns in Figures 5 and 6, only 13 can therefore emerge from our simulation of preferences. The remaining 14 patterns can still emerge in the data due to decision noise (and the fact that we have independent measures of the three preferences).

D.4 Using the Decomposition to Refine Measures of Individual Preferences

In Section 4.5 and Appendix C.3, we link an individual's stage 1 valuations to their stage 2 choices. Specifically, we create measures of individual preferences using stage 1 valuations, and then use those measures to predict stage 2 choice patterns. The simplest way to create measures of individual preferences is to take their stage 1 valuations at face value; for example, a measure of their underlying Δ^*_{CR} is simply $\Delta_{CR} = h_{AB} - h_{CD}$. An alternative approach is to combine a participant's stage 1 valuations with our decomposition estimates to generate refined measures of their individual preferences. Intuitively, the decomposition provides us with a prior for each participant's $(h^*_{AB}, h^*_{AB'}, h^*_{CD})$, and a participant's valuations provide a signal that we can use to generate the corresponding posterior.

If $\boldsymbol{h}^*$, the ε_{XY} terms, and the ε'_{XY} terms are all jointly normally distributed, then $(\boldsymbol{h}^*, \boldsymbol{h})$ is also jointly normally distributed, specifically:

$$\begin{pmatrix} \boldsymbol{h}^* \\ \boldsymbol{h} \end{pmatrix} \sim N\left(\begin{pmatrix} \boldsymbol{\mu}^* \\ \boldsymbol{\mu} \end{pmatrix}, \begin{pmatrix} \boldsymbol{\Sigma}^* & \boldsymbol{\Sigma_{12}} \\ \boldsymbol{\Sigma_{21}} & \boldsymbol{\Sigma} \end{pmatrix} \right),$$

where

$$\boldsymbol{\Sigma_{12}} = \begin{pmatrix} \theta^2_{AB} & \theta_{AB,AB'} & \theta_{AB,CD} & \theta^2_{AB} & \theta_{AB,AB'} & \theta_{AB,CD} \\ \theta_{AB,AB'} & \theta^2_{AB'} & \theta_{AB',CD} & \theta_{AB,AB'} & \theta^2_{AB'} & \theta_{AB',CD} \\ \theta_{AB,CD} & \theta_{AB',CD} & \theta^2_{CD} & \theta_{AB,CD} & \theta_{AB',CD} & \theta^2_{CD} \end{pmatrix}.$$

[60] When carrying out this exercise, we do not impose the upper and lower bounds of our experimental price lists.

Hence, if participant i provides a set of valuations $\boldsymbol{h}_i$, the conditional distribution of $\boldsymbol{h}^*$ given $\boldsymbol{h} = \boldsymbol{h}_i$ is $\boldsymbol{h}^*|_{\boldsymbol{h}=\boldsymbol{h}_i} \sim N(\boldsymbol{\mu}^*_{\text{post}}, \boldsymbol{\Sigma}^*_{\text{post}})$ where

$$\boldsymbol{\mu}^*_{\text{post}} = \boldsymbol{\mu}^* + \boldsymbol{\Sigma_{12}}\boldsymbol{\Sigma}^{-1}(\boldsymbol{h}_i - \boldsymbol{\mu})$$
$$\boldsymbol{\Sigma}^*_{\text{post}} = \boldsymbol{\Sigma}^* - \boldsymbol{\Sigma_{12}}\boldsymbol{\Sigma}^{-1}\boldsymbol{\Sigma_{21}}.$$

Again, our goal is to obtain more precise measures of a participant's Δ^*_Z terms (for Figure 7) and $\bar{h}^*_Z$ terms (for Appendix Figure C.1). It is straightforward to use the parameter estimates in Appendix Table A.7 to generate $\boldsymbol{\mu}^*_{\text{post}}$ for each participant.[61] We denote the components of $\boldsymbol{\mu}^*_{\text{post}}$ by $E[h^*_{AB}|\text{stage 1}]$, $E[h^*_{AB'}|\text{stage 1}]$, and $E[h^*_{CD}|\text{stage 1}]$. These represent our more refined measure of the participant's h^* terms. We then use these define the following more refined measures for the Δ^*_Z terms and $\bar{h}^*_{XY}$ terms.

$$\begin{aligned}
E[\Delta^*_{CR}|\text{stage 1}] &\equiv E[h^*_{AB}|\text{stage 1}] - E[h^*_{CD}|\text{stage 1}] \\
E[\Delta^*_{CC}|\text{stage 1}] &\equiv E[h^*_{AB'}|\text{stage 1}] - E[h^*_{CD}|\text{stage 1}] \\
E[\Delta^*_{MX}|\text{stage 1}] &\equiv E[h^*_{AB}|\text{stage 1}] - E[h^*_{AB'}|\text{stage 1}] \\
E[\bar{h}^*_{CR}|\text{stage 1}] &\equiv (E[h^*_{AB}|\text{stage 1}] + E[h^*_{CD}|\text{stage 1}])/2 \\
E[\bar{h}^*_{CC}|\text{stage 1}] &\equiv (E[h^*_{AB'}|\text{stage 1}] + E[h^*_{CD}|\text{stage 1}])/2 \\
E[\bar{h}^*_{MX}|\text{stage 1}] &\equiv (E[h^*_{AB}|\text{stage 1}] + E[h^*_{AB'}|\text{stage 1}])/2
\end{aligned}$$

The refined measures $E[h^*_{AB}|\text{stage 1}]$, $E[h^*_{AB'}|\text{stage 1}]$, and $E[h^*_{CD}|\text{stage 1}]$ are all tightly correlated with their respective raw measures h_{AB}, $h_{AB'}$, and h_{CD}, with correlations of 0.89, 0.88, 0.83, respectively. Similarly, $E[\Delta^*_{CR}|\text{stage 1}]$, $E[\Delta^*_{CC}|\text{stage 1}]$, and $E[\Delta^*_{MX}|\text{stage 1}]$ are tightly correlated with Δ_{CR}, Δ_{CC}, and Δ_{MX}, with correlations of 0.79, 0.79, 0.69, respectively. Finally, $E[\bar{h}^*_{CR}|\text{stage 1}]$, $E[\bar{h}^*_{CC}|\text{stage 1}]$, and $E[\bar{h}^*_{MX}|\text{stage 1}]$ are tightly correlated with $\bar{h}_{CR}$, $\bar{h}_{CC}$, and $\bar{h}_{MX}$, with correlations of 0.91, 0.91, 0.92, respectively. In Figure 7 and Appendix Figure C.1, we predict stage 2 choices using both the raw measures and the refined measures. The qualitative conclusions are much the same, although the refined measures make the link between stages more precise.

D.5 Decomposition Using MLE

Our analysis in Appendix D.1 through D.4 estimates the model parameters using the relevant sample moments or combination of sample moments. The advantage of this approach is that it requires fewer distributional assumptions and implementation assumptions. For example, our assessment of the relative contributions of preference heterogeneity versus noise in Appendix D.2 does not require

[61] Recall that each participant provides all six valuations for two of their (p, r) combinations, but only four valuations for their remaining two (p, r) combinations. For the latter instances, everything above is adjusted appropriately.

any distributional assumptions.

Here we describe an alternative approach to estimate the parameters via MLE. We assume as in Appendix D.4 that $\boldsymbol{h}^*$, the ε_{XY} terms, and the ε'_{XY} terms are all jointly normally distributed, and therefore, $\boldsymbol{h} \sim N(\boldsymbol{\mu}, \boldsymbol{\Sigma})$. Recognizing the interval nature of our valuation tasks, an observation provides both a lower bound (ζ) and an upper bound (υ) on the participant's $\boldsymbol{h}$ valuations:

$$\zeta(\boldsymbol{h}) = \begin{pmatrix} \zeta(h_{AB}) \\ \zeta(h_{AB'}) \\ \zeta(h_{CD}) \\ \zeta(h'_{AB}) \\ \zeta(h'_{AB'}) \\ \zeta(h'_{CD}) \end{pmatrix} \qquad \textbf{and} \qquad \upsilon(\boldsymbol{h}) = \begin{pmatrix} \upsilon(h_{AB}) \\ \upsilon(h_{AB'}) \\ \upsilon(h_{CD}) \\ \upsilon(h'_{AB}) \\ \upsilon(h'_{AB'}) \\ \upsilon(h'_{CD}) \end{pmatrix}.$$

For instance, if for an h_{XY} valuation task the person switches between the row with $H = \$32$ and $H = \$33$, then $\zeta(h_{XY}) = 32$ and $\upsilon(h_{XY}) = 33$. For observations censored at the lower bound (i.e., the person always chooses the right-hand option, even when $H = p \cdot \$30$), we set $\zeta(h_{XY}) = -\infty$ and $\upsilon(h_{XY}) = p \cdot \$30$, whereas for observations censored at the upper bound (i.e., the person always chooses the left-hand option even when $H = p \cdot \$30 + \$50$), we set $\zeta(h_{XY}) = p \cdot \$30 + \$50$ and $\upsilon(h_{XY}) = \infty$. Finally, recall that we only collect h'_{AB} and $h'_{AB'}$ for half of observations; all missing valuations are treated as uninformative and assigned $\zeta(h_{XY}) = -\infty$ and $\upsilon(h_{XY}) = \infty$. Missing valuations therefore play no role in the estimation of the parameters as they have a likelihood of 1 (and log-likelihood zero) for all $(\boldsymbol{\mu}, \boldsymbol{\Sigma})$.

Given a participant's observed $\zeta(\boldsymbol{h})$ and $\upsilon(\boldsymbol{h})$, the model-implied likelihood of that observation as a function of the parameters in $(\boldsymbol{\mu}, \boldsymbol{\Sigma})$ is $F(\upsilon(\boldsymbol{h}); \boldsymbol{\mu}, \boldsymbol{\Sigma}) - F(\zeta(\boldsymbol{h}); \boldsymbol{\mu}, \boldsymbol{\Sigma})$, where $F(\cdot; \boldsymbol{\mu}, \boldsymbol{\Sigma})$ is the CDF for $\boldsymbol{h}$ given parameters $(\boldsymbol{\mu}, \boldsymbol{\Sigma})$. From here, it is straightforward to set up the sample log-likelihood summing over all participants.

We run this estimation separately for each of the 20 (p, r) combinations. Appendix Tables D.1 and D.2 provide MLE results analogous to those of Appendix Tables A.7 and A.8, where Appendix Table D.2 is constructed from Appendix Table D.1 in exactly the same way that Appendix Table A.8 is constructed from Appendix Table A.7 (see Appendix D.2).

The message from the MLE estimation is much the same as that for our simpler estimation based on sample moments. Appendix Figure D.1 compares the MLE estimates from Appendix Table D.1 to the estimates from Appendix Table A.7. For the most part, the estimated parameters are close to each other, although the MLE approach yields slightly more variability for both noise and preference heterogeneity, which reflects that the MLE approach recognizes the interval nature of the data and the noise implications of censoring. The central conclusion that preference heterogeneity accounts for

roughly half of the variation in the h_{XY} measures and one third of the variation in the Δ_Z measures remains the same.

Table D.1: Decomposition Calculations (Levels)

p	r	$\hat{\mu}^*_{AB}$	$\hat{\mu}^*_{AB'}$	$\hat{\mu}^*_{CD}$	$\hat{\theta}^2_{AB}$	$\hat{\theta}^2_{AB'}$	$\hat{\theta}^2_{CD}$	$\hat{\sigma}^2_{AB}$	$\hat{\sigma}^2_{AB'}$	$\hat{\sigma}^2_{CD}$	$\hat{\theta}_{AB,AB'}$	$\hat{\theta}_{AB,CD}$	$\hat{\theta}_{AB',CD}$	$\frac{\widehat{var(h^*_{AB})}}{var(h_{AB})}$	$\frac{\widehat{var(h^*_{AB'})}}{var(h_{AB'})}$	$\frac{\widehat{var(h^*_{CI}}}{var(h_{CI}}$
0.30	0.10	36.32	23.89	32.96	165.72	142.30	171.21	87.27	129.38	187.73	65.22	75.75	50.90	0.66	0.52	0.4
0.30	0.20	35.68	26.01	32.37	147.88	148.81	132.19	111.17	109.70	150.86	86.45	74.29	52.92	0.57	0.58	0.4
0.30	0.30	36.55	29.08	35.59	154.91	173.54	158.78	110.22	108.48	130.01	114.77	99.71	84.06	0.58	0.62	0.5
0.30	0.50	38.12	30.79	38.27	131.12	100.42	123.34	98.47	167.92	120.87	107.12	101.86	83.57	0.57	0.37	0.5
0.30	0.80	38.55	34.93	37.08	123.18	125.81	112.63	79.66	89.28	120.25	108.92	97.83	92.47	0.61	0.58	0.4
0.50	0.10	37.13	27.20	32.21	144.02	128.73	111.15	56.11	102.89	129.35	60.59	30.98	52.74	0.72	0.56	0.4
0.50	0.20	39.09	29.91	33.36	141.93	84.57	120.34	76.70	142.77	112.80	73.01	52.22	43.15	0.65	0.37	0.5
0.50	0.30	38.99	33.78	35.43	138.49	146.69	75.83	62.08	77.64	124.71	84.85	41.46	43.56	0.69	0.65	0.3
0.50	0.50	38.97	34.15	40.02	158.14	157.17	122.18	61.86	73.42	84.33	124.47	109.29	101.97	0.72	0.68	0.5
0.50	0.80	38.65	37.31	38.24	133.73	150.45	98.27	44.89	84.00	77.84	123.83	92.35	99.00	0.75	0.64	0.5
0.80	0.10	41.73	35.66	34.30	122.38	148.05	91.53	73.99	122.34	127.81	82.03	33.24	55.65	0.62	0.55	0.4
0.80	0.20	39.46	36.02	36.23	85.48	154.69	94.78	65.08	62.81	103.52	77.09	45.94	72.38	0.57	0.71	0.4
0.80	0.30	41.96	39.24	35.81	142.87	157.14	78.15	81.71	122.15	95.29	93.58	54.73	53.78	0.64	0.56	0.4
0.80	0.50	39.01	36.96	37.95	80.20	109.95	59.97	72.98	69.23	98.05	65.54	38.58	38.32	0.52	0.61	0.3
0.80	0.80	40.88	41.40	42.78	129.48	153.71	81.27	54.50	73.24	90.39	124.83	77.86	69.38	0.70	0.68	0.4
0.90	0.10	40.02	35.44	34.10	117.75	103.71	83.53	108.62	119.50	98.60	83.33	30.79	56.43	0.52	0.46	0.4
0.90	0.20	39.83	38.93	34.90	122.09	143.76	75.25	86.71	97.02	95.03	106.11	44.12	48.54	0.58	0.60	0.4
0.90	0.30	38.33	38.95	36.92	92.02	187.01	92.09	82.05	68.90	95.55	94.46	52.51	67.51	0.53	0.73	0.4
0.90	0.50	39.39	38.74	37.72	99.10	110.57	63.43	93.54	113.06	78.71	86.81	43.83	53.60	0.51	0.49	0.4
0.90	0.80	38.39	39.50	38.11	85.16	115.05	49.05	69.71	66.60	61.51	87.58	48.53	52.27	0.55	0.63	0.4
0.62	0.38	38.85	34.39	36.22	125.78	137.11	99.75	78.87	100.02	109.16	92.53	62.29	63.61	0.61	0.58	0.4

Note: Decomposition estimates from MLE exercise. Final line presents averages over all 20 rows.

Table D.2: Decomposition Calculations (Differences)

p	r	$\hat{\Delta}^{**}_{CR}$	$\hat{\Delta}^{**}_{CC}$	$\hat{\Delta}^{**}_{MX}$	$\widehat{var(\Delta^{*}_{CR})}$	$\widehat{var(\Delta^{*}_{CC})}$	$\widehat{var(\Delta^{*}_{MX})}$	$\widehat{var(\Delta_{CR})}$	$\widehat{var(\Delta_{CC})}$	$\widehat{var(\Delta_{MX})}$	$\frac{\widehat{var(\Delta^{*}_{CR})}}{\widehat{var(\Delta_{CR})}}$	$\frac{\widehat{var(\Delta^{*}_{CC})}}{\widehat{var(\Delta_{CC})}}$	$\frac{\widehat{var(\Delta^{*}_{MX})}}{\widehat{var(\Delta_{MX})}}$
0.30	0.10	3.36	-9.07	12.43	185.44	211.71	177.59	460.44	528.82	394.23	0.40	0.40	0.45
0.30	0.20	3.31	-6.36	9.67	131.49	175.15	123.79	393.52	435.72	344.67	0.33	0.40	0.36
0.30	0.30	0.96	-6.51	7.47	114.26	164.18	98.90	354.49	402.68	317.60	0.32	0.41	0.31
0.30	0.50	-0.14	-7.48	7.34	50.74	56.61	17.30	270.08	345.40	283.69	0.19	0.16	0.06
0.30	0.80	1.47	-2.16	3.62	40.16	53.50	31.15	240.06	263.03	200.09	0.17	0.20	0.16
0.50	0.10	4.93	-5.01	9.93	193.21	134.40	151.56	378.67	366.64	310.57	0.51	0.37	0.49
0.50	0.20	5.73	-3.45	9.18	157.85	118.61	80.49	347.34	374.18	299.96	0.45	0.32	0.27
0.50	0.30	3.56	-1.65	5.21	131.40	135.41	115.48	318.19	337.75	255.20	0.41	0.40	0.45
0.50	0.50	-1.05	-5.87	4.82	61.74	75.41	66.37	207.93	233.17	201.65	0.30	0.32	0.33
0.50	0.80	0.41	-0.93	1.34	47.30	50.71	36.51	170.03	212.55	165.40	0.28	0.24	0.22
0.80	0.10	7.44	1.36	6.07	147.44	128.28	106.38	349.24	378.43	302.70	0.42	0.34	0.35
0.80	0.20	3.23	-0.21	3.44	88.38	104.71	86.00	256.97	271.03	213.89	0.34	0.39	0.40
0.80	0.30	6.15	3.43	2.72	111.56	127.73	112.85	288.56	345.16	316.71	0.39	0.37	0.36
0.80	0.50	1.06	-0.99	2.05	63.01	93.28	59.06	234.05	260.56	201.27	0.27	0.36	0.29
0.80	0.80	-1.90	-1.38	-0.52	55.03	96.23	33.52	199.91	259.85	161.26	0.28	0.37	0.21
0.90	0.10	5.92	1.34	4.58	139.70	74.38	54.81	346.92	292.48	282.93	0.40	0.25	0.19
0.90	0.20	4.93	4.03	0.90	109.09	121.93	53.62	290.83	313.98	237.35	0.38	0.39	0.23
0.90	0.30	1.41	2.02	-0.62	79.09	144.08	90.12	256.69	308.54	241.07	0.31	0.47	0.37
0.90	0.50	1.68	1.02	0.66	74.86	66.80	36.06	247.12	258.57	242.67	0.30	0.26	0.15
0.90	0.80	0.28	1.39	-1.10	37.15	59.56	25.06	168.37	187.67	161.37	0.22	0.32	0.16
0.62	0.38	2.64	-1.82	4.46	100.94	109.63	77.83	288.97	318.81	256.71	0.33	0.34	0.29

Note: Decomposition estimates calculated from from MLE exercise. Final line presents averages over all 20 rows.

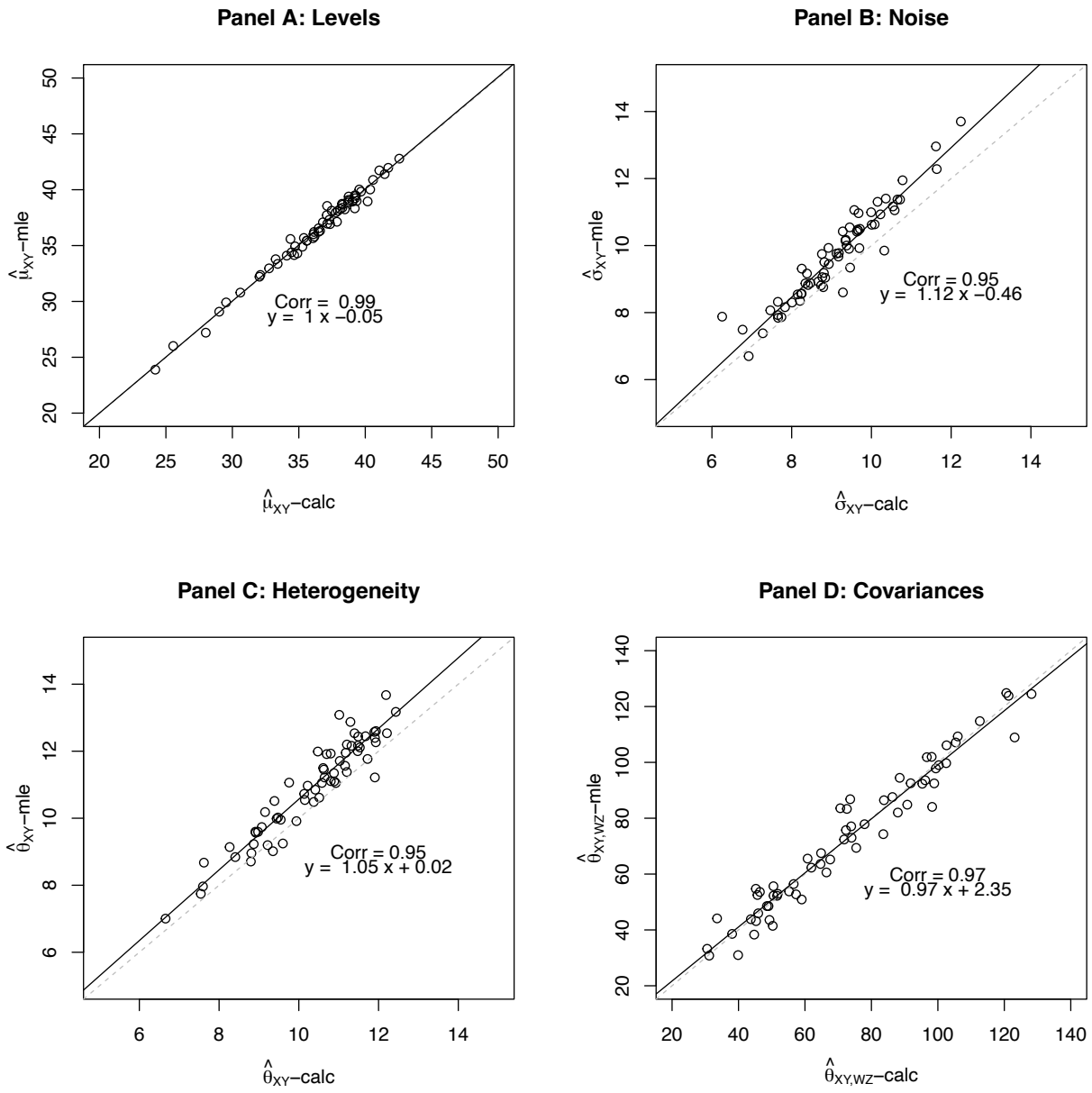

Figure D.1: Comparison of Decomposition Results (Direct Calculation vs. MLE)

Notes: Figure relates calculated quantities from Table A.7 to MLE estimates from Appendix Table D.1. Correlation reported for all observations in each panel.

E Upside-Potential Model: Analysis

E.1 Main Predictions of the Upside-Potential Model

In this section, we provide proofs for Propositions 1 and 2 from Section 5.1 of the main text. For completeness, we replicate the model assumptions here.

Suppose that a person has in mind a set W of outcomes that they consider "winning" outcomes, and then that person evaluates a lottery $X \equiv (x_1, q_1; ...; x_N, q_N)$ as

$$U(X) = \left(\sum_{i=1}^{N} q_i u(x_i)\right) \quad + \left(\sum_{j=1}^{N} q_j I(x_j \in W)\right)\left(\sum_{k=1}^{N} q_k I(x_k \in W)\kappa(x_k)\right). \tag{E.1}$$

To ensure that the model is well-behaved, we assume that u and κ are both strictly increasing in x, and that $\kappa(x) \geqslant 0$ for all $x \in W$.

It will be useful for intuitions and proofs to define $Ef(X) \equiv \sum_{i=1}^{N} q_i f(x_i)$, which is an expected utility from lottery X given utility function f. If we then define $v(x) \equiv I(x \in W)$ and $w(x) \equiv I(x \in W)\kappa(x)$, we can rewrite $U(X)$ as

$$U(X) = Eu(X) + (Ev(X))\,(Ew(X))\,.$$

We first note that, as long as the winning set W satisfies $x \in W$ implies $x' \in W$ for all $x' > x$, the UP model respects first-order stochastic dominance: If lottery X' FOSD lottery X, standard results imply $Eu(X') > Eu(X)$, $Ev(X') \geqslant Ev(X) \geqslant 0$, and $Ew(X') \geqslant Ew(X) \geqslant 0$, from which it immediately follows that $U(X') > U(X)$.[1]

Before we can derive predictions for the upside potential model in equation (E.1), we must make an assumption on what outcomes are included in the set W of winning outcomes. For our experiment in which people face only binary and trinary lotteries that yield either zero or a positive amount, a natural assumption is that all positive outcomes are included in the set of winning outcomes while zero is not (again, we discuss this assumption more in Section 5.3). We apply this assumption throughout the analysis below.

For parameters (M, p, r), lotteries $A \equiv (M, 1)$ and $C \equiv (M, r)$ are independent of h, but lotteries $B(h) \equiv (h, p)$, $B'(h) \equiv (h, pr; M, 1-r)$, and $D(h) \equiv (h, pr)$ are functions of h. Note that $C = rA$ and thus $Eu(C) = rEu(A)$, $D(h) = rB(h)$ and thus $Eu(D(h)) = rEu(B(h))$ for any h, and $B'(h) = (1-r)A + rB$ and thus $Eu(B'(h)) = (1-r)Eu(A) + rEu(B(h))$ for any h.

It is straightforward to show that, in the UP model, $U(B(h))$, $U(B'(h))$, and $U(D(h))$ are all continuous and increasing in h for all $h \geqslant M$, which implies that h^*_{AB}, $h^*_{AB'}$, and h^*_{CD} all exist and

[1] The inequalities $Ev(X') \geqslant Ev(X)$ and $Ew(X') \geqslant Ew(X)$ are weak because it could be that both X' and X contain no outcomes in the winning set W, in which case $Ev(X') = Ev(X) = 0$, and $Ew(X') = Ew(X) = 0$.

are unique. The value h^*_{AB} satisfies $U(A) = U(B(h^*_{AB}))$, which we can write as

$$Eu(A) + \kappa(M) = Eu(B(h^*_{AB})) + p^2\kappa(h^*_{AB}). \tag{E.2}$$

The value $h^*_{AB'}$ satisfies $U(A) = U(B'(h^*_{AB'}))$, which we can write as

$$Eu(A) + \kappa(M) = Eu(B'(h^*_{AB'})) + (pr + 1 - r)\left[pr\kappa(h^*_{AB'}) + (1 - r)\kappa(M)\right]. \tag{E.3}$$

The value h^*_{CD} satisfies $U(C) = U(D(h^*_{CD}))$, which we can write as

$$Eu(C) + r^2\kappa(M) = Eu(D(h^*_{CD})) + (pr)^2\kappa(h^*_{CD}). \tag{E.4}$$

Proposition A1 derives predictions from these equations (Part 1 is Proposition 1 in the text):

Proposition A1. Suppose that $(h^*_{AB}, h^*_{AB'}, h^*_{CD})$ is derived from equations (E.2), (E.3), and (E.4). For any $u(x)$ that is strictly increasing in x and $\kappa(x)$ that is strictly increasing in x and has $\kappa(x) \geqslant 0$ for all $x > 0$:

(1) A person must exhibit one of the following seven patterns of behavior:

P1:	$0 > \Delta^*_{CR} > \Delta^*_{CC}$ and $\Delta^*_{MX} > 0$	(RCRP−RCCP−MXP)
P12:	$0 = \Delta^*_{CR} > \Delta^*_{CC}$ and $\Delta^*_{MX} > 0$	($\oslash$CRP−RCCP−MXP)
P2:	$\Delta^*_{CR} > 0 > \Delta^*_{CC}$ and $\Delta^*_{MX} > 0$	(CRP−RCCP−MXP)
P23:	$\Delta^*_{CR} > \Delta^*_{CC} = 0$ and $\Delta^*_{MX} > 0$	(CRP−$\oslash$CCP−MXP)
P3:	$\Delta^*_{CR} > \Delta^*_{CC} > 0$ and $\Delta^*_{MX} > 0$	(CRP−CCP−MXP)
P34:	$\Delta^*_{CR} = \Delta^*_{CC} > 0$ and $\Delta^*_{MX} = 0$	(CRP−CCP− $\oslash$MXP)
P4:	$\Delta^*_{CC} > \Delta^*_{CR} > 0$ and $\Delta^*_{MX} < 0$	(CRP−CCP−RMXP).

(2) More precisely:

(a) Whether a person exhibits a CRP, $\oslash$CRP, or an RCRP depends on whether h^*_{AB} is such that $\kappa(M)$ is greater than, equal to, or less than $p^2\kappa(h^*_{AB})$, or equivalently on whether $Eu(B(h^*_{AB}))$ is greater than, equal to, or less than $Eu(A)$.

(b) Whether a person exhibits an MXP, $\oslash$MXP, or an RMXP depends on whether h^*_{AB} is such that $\kappa(M)$ is less than, equal to, or greater than $p\kappa(h^*_{AB})$.

(c) Whether a person exhibits a CCP, a $\oslash$CCP, or an RCCP depends on whether $h^*_{AB'}$ is such that $\kappa(M)$ is greater than, equal to, or less than $\left(\frac{p}{2-p}\right)\kappa(h^*_{AB'})$.

(d) If h^*_{AB} is such that $\kappa(M) < p^2\kappa(h^*_{AB})$ and thus the person has an RCRP, then the person must also exhibit an MXP and an RCCP. Hence, the person must exhibit pattern P1.

(e) If h^*_{AB} is such that $\kappa(M) = p^2\kappa(h^*_{AB})$ and thus the person has $\oslash$CRP, then the person must also exhibit an MXP and an RCCP. Hence, the person must exhibit pattern P12.

(f) If h^*_{AB} is such that $\kappa(M) > p^2\kappa(h^*_{AB})$ and thus the person has CRP, then the person could exhibit an MXP, $\oslash$MXP, or an RMXP. If the person exhibits either $\oslash$MXP or an RMXP, then they must exhibit CCP; otherwise, they could have CCP, $\oslash$CCP, or an RCCP. Hence, the person must exhibit one of patterns P2, P23, P3, P34, or P4.

Proof: The statement in part (1) follows directly from parts (2d), (2e), and (2f), so we only need to prove each of the statements in part (2).

Proof of part (2a): We can rewrite equation (E.2) as

$$\kappa(M) - p^2\kappa(h^*_{AB}) = Eu(B(h^*_{AB})) - Eu(A).$$

Hence, whether h^*_{AB} is such that $\kappa(M)$ is greater than, equal to, or less than $p^2\kappa(h^*_{AB})$ is equivalent to whether $Eu(B(h^*_{AB}))$ is greater than, equal to, or less than $Eu(A)$.

Because $Eu(C) = rEu(A)$ and $Eu(D(h)) = rEu(B(h))$ for all h, the comparison between $U(C)$ and $U(D(h^*_{AB}))$ can be written as

$$\begin{aligned} Eu(C) + r^2\kappa(M) &: Eu(D(h^*_{AB})) + (pr)^2\kappa(h^*_{AB}) \\ rEu(A) + r^2\kappa(M) &: rEu(B(h^*_{AB})) + (pr)^2\kappa(h^*_{AB}) \\ r(\kappa(M) - p^2\kappa(h^*_{AB})) &: Eu(B(h^*_{AB})) - Eu(A) \end{aligned}$$

If h^*_{AB} is such that $\kappa(M) > p^2\kappa(h^*_{AB})$, which implies $\kappa(M) - p^2\kappa(h^*_{AB}) = Eu(B(h^*_{AB})) - Eu(A) > 0$, then $r(\kappa(M) - p^2\kappa(h^*_{AB})) < Eu(B(h^*_{AB})) - Eu(A)$. It follows that $U(C) < U(D(h^*_{AB}))$ and thus $h^*_{CD} < h^*_{AB}$, that is, CRP. Analogously, if h^*_{AB} is such that $\kappa(M) < p^2\kappa(h^*_{AB})$, then the person exhibits RCRP, and if h^*_{AB} is such that $\kappa(M) = p^2\kappa(h^*_{AB})$, then the person exhibits $\oslash$CRP.

Proof of part (2b): Because, for any h, $Eu(B'(h)) = (1-r)Eu(A) + rEu(B(h))$, we have

$$U(B'(h)) = (1-r)Eu(A) + rEu(B(h)) + (1-r+pr)((1-r)\kappa(M) + pr\kappa(h)).$$

Since $Eu(A)$ and $Eu(B(h))$ are independent of r,

$$\frac{d[U(B'(h))]}{dr} = Eu(B(h)) - Eu(A) + (-(1-p))((1-r)\kappa(M) + pr\kappa(h)) + (1-r+pr)(p\kappa(h) - \kappa(M))$$

and thus

$$\frac{d^2[U(B'(h))]}{dr^2} = -2(1-p)(p\kappa(h) - \kappa(M)).$$

If h^*_{AB} is such that $\kappa(M) < p\kappa(h^*_{AB})$, then $\frac{d^2[U(B'(h))]}{dr^2} < 0$ for all $r \in [0,1]$. Because $U(A) = U(B(h^*_{AB}))$ (by the definition of h^*_{AB}), $\frac{d^2[U(B'(h))]}{dr^2} < 0$ implies $U(B'(h^*_{AB})) > U(A) = U(B(h^*_{AB}))$ for any $r \in (0,1)$, and thus $h^*_{AB'} < h^*_{AB}$, that is the person exhibits a MXP. Analogously, if h^*_{AB} is such that $\kappa(M) > p\kappa(h^*_{AB})$, then the person exhibits RMXP, and if h^*_{AB} is such that $\kappa(M) = p\kappa(h^*_{AB})$, then the person exhibits $\oslash$MXP.

Proof of part (2c): Because, for any h, $Eu(B'(h)) = (1-r)Eu(A) + rEu(B(h))$, we can rewrite equation E.3 as

$$rEu(A) + \kappa(M) = rEu(B(h^*_{AB'})) + (pr + 1 - r)\left[pr\kappa(h^*_{AB'}) + (1-r)\kappa(M)\right].$$

Substituting $Eu(C) = rEu(A)$ and $Eu(D(h^*_{AB'})) = rEu(B(h^*_{AB'}))$ and rearranging the other terms, this becomes

$$Eu(C) + r^2\kappa(M) = Eu(D(h^*_{AB'})) + (pr)^2\kappa(h^*_{AB'}) + (1-r)r\left(p\kappa(h^*_{AB'}) - (2-p)\kappa(M)\right).$$

If $h^*_{AB'}$ is such that $\kappa(M) > \left(\frac{p}{2-p}\right)\kappa(h^*_{AB'})$, it follows that $Eu(C) + r^2\kappa(M) < Eu(D(h^*_{AB'})) + (pr)^2\kappa(h^*_{AB'})$, and thus $h^*_{CD} < h^*_{AB'}$, that is the person exhibits a CCP. Analogously, if $h^*_{AB'}$ is such that $\kappa(M) < \left(\frac{p}{2-p}\right)\kappa(h^*_{AB'})$, then the person exhibits RCCP, and if $h^*_{AB'}$ is such that $\kappa(M) = \left(\frac{p}{2-p}\right)\kappa(h^*_{AB'})$, then the person exhibits $\oslash$CCP.

Proof of parts (2d) and (2e): If h^*_{AB} is such that $\kappa(M) \leqslant p^2\kappa(h^*_{AB})$, so that the person exhibits RCRP or $\oslash$CRP, then we must have $\kappa(M) < p\kappa(h^*_{AB})$. Thus from part (2b) the person must exhibit an MXP. Finally, because $\Delta^*_{CC} = \Delta^*_{CR} - \Delta^*_{MX}$, the combination of $\Delta^*_{CR} \leqslant 0$ and $\Delta^*_{MX} > 0$ implies $\Delta^*_{CC} < 0$, that is, an RCCP.

Proof of part (2f): If h^*_{AB} is such that $\kappa(M) > p^2\kappa(h^*_{AB})$, so that the person exhibits CRP, it is possible that $\kappa(M)$ is less than, greater than, or equal to $p\kappa(h^*_{AB})$, and thus from part (2b) the person could exhibit an MXP, $\oslash$MXP, or an RMXP. If the person exhibits either $\oslash$MXP or an RMXP, because $\Delta^*_{CC} = \Delta^*_{CR} - \Delta^*_{MX}$, the combination of $\Delta^*_{CR} > 0$ and $\Delta^*_{MX} \leqslant 0$ implies $\Delta^*_{CC} > 0$, that is, a CCP. Finally, if the person exhibits CRP and MXP, it is straightforward to generate examples in which the person exhibits CCP, $\oslash$CCP, or RCCP.

■

Proposition A2, which is equivalent to Proposition 2 in the text, considers the special cases $u(x) = x$ and possibly also $\kappa(x) = \phi x$ for some $\phi > 0$.

Proposition A2. Suppose that $(h^*_{AB}, h^*_{AB'}, h^*_{CD})$ is derived from equations (E.2), (E.3), and (E.4). If $u(x) = x$, then:

(1) If $\kappa(x)$ is strictly increasing in x and has $\kappa(x) \geqslant 0$ for all $x > 0$, then:

(a) If $ph^*_{AB} > M$ (i.e., if the person is risk averse in the AB decision), then $\Delta^*_{CR} > 0$ and thus the person must exhibit one of patterns P2, P23, P3, P34, or P4.

(b) If $ph^*_{AB} = M$ (i.e., if the person is risk neutral in the AB decision), then $\Delta^*_{CR} = 0$ and thus the person must exhibit pattern P12.

(c) If $ph^*_{AB} < M$ (i.e., if the person is risk loving in the AB decision), then then $\Delta^*_{CR} > 0$ and thus the person must exhibit pattern P1.

(2) If $\kappa(x) = \phi x$ for some $\phi > 0$, then $ph^*_{AB} > M$ (i.e., the person is risk averse in the AB decision), $\Delta^*_{CR} > 0$, and $\Delta^*_{MX} > 0$, and thus the person must exhibit one of patterns P2, P23, or P3.

Proof: Proof of part (1): When $u(x) = x$, whether $Eu(B(h^*_{AB}))$ is greater than, equal to, or less than $Eu(A)$ is equivalent to whether ph^*_{AB} is greater than, equal to, or less than M. In addition, from the proof of Proposition A1 part (2a), whether $Eu(B(h^*_{AB}))$ is greater than, equal to, or less than $Eu(A)$ is equivalent to whether h^*_{AB} is such that $\kappa(M)$ is greater than, equal to, or less than $p^2\kappa(h^*_{AB})$.

It follows that $ph^*_{AB} > M$ implies $Eu(B(h^*_{AB})) > Eu(A)$ and thus $\kappa(M) > p^2\kappa(h^*_{AB})$, and then part (2f) from Proposition A1 implies that the person must exhibit one of patterns P2, P23, P3, P34, or P4. Analogously, $ph^*_{AB} = M$ implies $\kappa(M) = p^2\kappa(h^*_{AB})$, and thus part (2e) from Proposition A1 implies that the person must exhibit pattern P12; and $ph^*_{AB} < M$ implies $\kappa(M) < p^2\kappa(h^*_{AB})$, and thus part (2d) from Proposition A1 implies that the person must exhibit pattern P1.

Proof of part (2): When $u(x) = x$ and $\kappa(x) = \phi x$, equation (E.2) becomes $M + \phi M = ph^*_{AB} + p^2\phi h^*_{AB}$ or $\phi(M - p^2h^*_{AB}) = ph^*_{AB} - M$. Because $ph^*_{AB} > p^2h^*_{AB}$, this condition can hold only if $ph^*_{AB} > M > p^2h^*_{AB}$, and thus $p\kappa(h^*_{AB}) > \kappa(M) > p^2\kappa(h^*_{AB})$ (since $\kappa(x) = \phi x$). Applying the conditions from parts (2a) and (2b) of Proposition A1, $\kappa(M) > p^2\kappa(h^*_{AB})$ implies CRP, while $\kappa(M) < p\kappa(h^*_{AB})$ implies MXP. It is straightforward to generate examples in which the person exhibits CCP, $\oslash$CCP, or RCCP, and thus patterns P2, P23, and P3 are all possible.

■

E.2 Relationship to Quadratic Utility

The material in this section draws heavily from Chew et al. (1991), where we present everything in terms of discrete lotteries of the form $X \equiv (x_1, q_1; ...; x_N, q_N)$. We begin with the definition of quadratic utility (Machina, 1982; Chew et al., 1991):

Definition: A person has *quadratic utility* if their utility functional U can be expressed as

$$U(X) = \sum_{i=1}^{N} \sum_{j=1}^{N} \phi(x_i, x_j) q_i q_j$$

for some symmetric function ϕ.

Quadratic utility is a broad class that includes a number of sub-cases—indeed, it includes standard expected utility as a special case: $\phi(x, y) = (u(x) + u(y))/2$ yields $U(X) = \sum_{i=1}^{N} u(x_i) q_i$.

The UP model in equation (E.1) is also a special case of quadratic utility. In particular, if $\phi(x, y) = (u(x) + u(y))/2 + (v(x)w(y) + v(y)w(x))/2$, quadratic utility yields the functional

$$U(X) = \left(\sum_{i=1}^{N} q_i u(x_i) \right) + \left(\sum_{j=1}^{N} q_j v(x_j) \right) \left(\sum_{k=1}^{N} q_k w(x_k) \right). \tag{E.5}$$

If we further use $v(z) = I(z \in W)$ and $w(z) = I(z \in W)\kappa(z)$, then we obtain equation (E.1). While this sub-case of quadratic utility has not been studied before (to the best of our knowledge), it in fact combines together two sub-cases that have been studied before but neither of which can explain well our empirical patterns.

Machina (1982) studies the utility functional

$$U(X) = \left(\sum_{i=1}^{N} q_i u(x_i) \right) + \left(\sum_{j=1}^{N} q_j v(x_j) \right)^2. \tag{E.6}$$

This functional is the sum of an expected-utility functional and a second expected-utility functional squared, where $v(x) \geqslant 0$ for all x to keep the model well behaved.[2] This functional corresponds to quadratic utility with $\phi(x, y) = (u(x) + u(y))/2 + v(x)v(y)$. Machina (1982) highlights how this functional can generate a CRP and a CCP. However, it also generates preferences with an aversion to mixtures of any two lotteries, as pointed out by Chew et al. (1991), and thus a global RMXP in our context (except for two knife-edge cases). Hence, it will be not able to accommodate the dominant patterns in our data that involve an MXP.

[2] In particular, if $v(x) < 0$ for some range of x, then $(v(x))^2$ would be decreasing in x over that range, and thus the model could generate violations of monotonicity.

To be more precise, Proposition A3 in Section E.2.1 fully characterizes the implications of the Machina functional in equation (E.6) for the patterns that could emerge in our context. If $v(x)$ is a positive affine transformation of $u(x)$, then this functional is equivalent to expected utility with utility function $u(x)$, and thus the person exhibits $\oslash$CRP-$\oslash$CCP-$\oslash$MXP. In addition, even if $v(x)$ reflects different expected-utility preferences from $u(x)$, there could be a knife-edge case in which the $\bar{h}$ that makes $u(M) = pu(\bar{h}) + (1-p)u(0)$ just happens to also make $v(M) = pv(\bar{h}) + (1-p)v(0)$, in which case again the person exhibits $\oslash$CRP-$\oslash$CCP-$\oslash$MXP. Otherwise, the person must exhibit one of four patterns: CRP-CCP-RMXP, RCRP-CCP-RMXP, RCRP-$\oslash$CCP-RMXP, or RCRP-RCCP-RMXP. The first of these is a pattern that could emerge from the UP model that we labeled P4. The remaining three are patterns that cannot emerge from the UP model, and that also show up with limited frequency in our data.

Chew et al. (1991) discuss several sub-cases of quadratic utility, for each highlighting the connection between a utility functional and a specific ϕ function. In addition to the expected-utility and the Machina cases described above, they also discuss the case where $\phi(x,y) = (v(x)w(y) + v(y)w(x))/2$, which leads to the utility functional

$$U(X) = \left(\sum_{i=1}^{N} q_i v(x_i)\right)\left(\sum_{j=1}^{N} q_j w(x_j)\right). \tag{E.7}$$

This functional is the product of two expected-utility functionals, where $v(x) \geqslant 0$ and $w(x) \geqslant 0$ for all x to keep the model well behaved. Chew et al. point out how this case generates preferences with an attraction to mixtures of any two lotteries, and thus a global MXP in our context (except for two knife-edge cases). However, it also generates a global $\oslash$CRP and RCCP and thus also will not work for our purposes.

To be more precise, Proposition A4 in Section E.2.1 fully characterizes the implications of the Chew et al. functional in equation (E.7) for the patterns that could emerge in our context. Much as for the Machina functional, if $w(x)$ is a positive affine transformation of $v(x)$, then this functional is equivalent to expected utility with utility function $v(x)$, and even if $w(x)$ reflects different expected-utility preferences from $v(x)$, there could be a knife-edge case in which the $\bar{h}$ that makes $v(M) = pv(\bar{h}) + (1-p)v(0)$ just happens to also make $w(M) = pw(\bar{h}) + (1-p)w(0)$, in which case again the person exhibits $\oslash$CRP-$\oslash$CCP-$\oslash$MXP. Otherwise, the person must exhibit the pattern $\oslash$CRP-RCCP-MXP. This is a pattern that could emerge from the UP model that we labeled P12. However, because much of our data cover other patterns, this case is too restrictive for our purposes.

Finally, note that the utility functional in equation (E.5) reflects a combination of the utility functionals in equations (E.6) and (E.7). However, without any further assumptions on u, v, or w, equation (E.5) would be overly permissive—e.g., by continuity as w approaches v, it would permit the three additional patterns that can emerge from the Machina specification but not from the UP

model. Hence, the additional assumptions that $v(x) = I(x \in W)$ and $w(x) = I(x \in W)\kappa(x)$ have bite in that they shrink the set of permitted patterns down to the seven patterns in Proposition 1, which again are the more prominent patterns in our data.

E.2.1 Propositions and Proofs for Other Quadratic Utility Specifications

In this section, we present the propositions referenced in Section E.2 along with their proofs. We again use the notation from Section E.1. We define $Eu(X) \equiv \sum_{i=1}^{N} q_i u(x_i)$, and define $Ev(X)$ and $Ew(X)$ analogously. And for parameters (M, p, r), we define lotteries $A \equiv (M, 1)$, $B(h) \equiv (h, p)$, $B'(h) \equiv (h, pr; M, 1-r)$, $C \equiv (M, r)$, and $D(h) \equiv (h, pr)$.

Proposition A3: Suppose a person evaluates lotteries according to the Machina functional in equation (E.6). Then:

(1) If there exists $\bar{h}$ such that both $u(M) = pu(\bar{h}) + (1-p)u(0)$ and $v(M) = pv(\bar{h}) + (1-p)v(0)$, then $h^*_{AB} = h^*_{AB'} = h^*_{CD} = \bar{h}$ and thus the person will have ⃠CRP-⃠CCP-⃠MXP.

(2) Otherwise, the person must have RMXP combined with either CRP-CCP, RCRP-CCP, RCRP-⃠CCP, or RCRP-RCCP. More precisely:

   (a) The person must exhibit an RMXP.

   (b) Whether a person exhibits a CRP or an RCRP depends on whether h^*_{AB} is such that $pu(h^*_{AB}) + (1-p)u(0)$ is greater than or less than $u(M)$. (If $pu(h^*_{AB}) + (1-p)u(0) = u(M)$, the condition in part 1 must hold and the person will have ⃠CRP-⃠CCP-⃠MXP.)

   (c) Suppose h^*_{AB} is such that $pu(h^*_{AB}) + (1-p)u(0) > u(M)$ and thus the person has CRP. The combination of CRP and RMXP implies CCP, and thus the person will exhibit CRP-CCP-RMXP.

   (d) Suppose h^*_{AB} is such that $pu(h^*_{AB}) + (1-p)u(0) < u(M)$ and thus the person has RCRP. The combination of RCRP and RMXP permits any CCP preference, and thus the person could exhibit RCRP-CCP, RCRP-⃠CCP, or RCRP-RCCP.

Proof: For any h, $U(B'(h)) = Eu(B'(h)) + (Ev(B'(h)))^2$. Because $B'(h) = (1-r)A + rB(h)$, we can rewrite this as

$$U(B'(h)) = [(1-r)Eu(A) + rEu(B(h))] + [(1-r)Ev(A) + rEv(B(h))]^2.$$

Since $Eu(A)$, $Eu(B(h))$, $Ev(A)$, and $Ev(B(h))$ are all independent of r, it is straightforward to derive that for all h

$$\frac{dU(B'(h))}{dr} = Eu(B(h)) - Eu(A) + 2[(1-r)Ev(A) + rEv(B(h))][Ev(B(h)) - Ev(A)]$$

and

$$\frac{d^2U(B'(h))}{dr^2} = 2[Ev(B(h)) - Ev(A)]^2.$$

Proof of part (1): Suppose there exists $\bar{h}$ such that both $u(M) = pu(\bar{h}) + (1-p)u(0)$ and $v(M) = pv(\bar{h}) + (1-p)v(0)$, which is necessarily true if v is a positive affine transformation of u, and could happen to be true even if u and v reflect different expected-utility preferences. Because these are equivalent to $Eu(A) = Eu(B(\bar{h}))$ and $Ev(A) = Ev(B(\bar{h}))$, it immediately follows that $h^*_{AB} = \bar{h}$. In addition, these conditions also imply that $rEu(A) = rEu(B(\bar{h}))$ and $r^2Ev(A) = r^2Ev(B(\bar{h}))$, from which it immediately follows that $h^*_{CD} = \bar{h}$. Finally, these conditions further imply that $\frac{dU(B'(\bar{h}))}{dr} = 0$, which implies $h^*_{AB'} = \bar{h}$. The result follows.

Proof of part (2): The statement in part (2) follows directly from parts (2c) and (2d), so we merely prove each of the parts.

Proof of part (2a): If there does not exist $\bar{h}$ such that both $u(M) = pu(\bar{h}) + (1-p)u(0)$ and $v(M) = pv(\bar{h}) + (1-p)v(0)$, then h^*_{AB} must be such that either $Eu(A) > Eu(B(h^*_{AB}))$ and $(Ev(A))^2 < (Ev(B(h^*_{AB})))^2$ or $Eu(A) < Eu(B(h^*_{AB}))$ and $(Ev(A))^2 > (Ev(B(h^*_{AB})))^2$. For either case, $Ev(B(h^*_{AB})) - Ev(A)$ is not equal to zero and thus $\frac{d^2U(B'(h^*_{AB}))}{dr^2} > 0$. Because $U(A) = U(B(h^*_{AB}))$ (by the definition of h^*_{AB}), $\frac{d^2U(B'(h^*_{AB}))}{dr^2} > 0$ implies $U(B'(h^*_{AB})) < U(A) = U(B(h^*_{AB})$ for any $r \in (0,1)$, and thus $h^*_{AB'} > h^*_{AB}$, that is, the person exhibits a RMXP.

Proof of part (2b): First note that the critical condition can be rewritten as whether h^*_{AB} is such that $Eu(B(h^*_{AB}))$ is greater than or less than $Eu(A)$. Next note that the comparison between $U(C)$ and $U(D(h^*_{AB}))$ can be written as

$$\begin{aligned} Eu(C) + (Ev(C))^2 &: Eu(D(h^*_{AB})) + (Ev(D(h^*_{AB})))^2 \\ rEu(A) + (rEv(A))^2 &: rEu(B(h^*_{AB})) + (rEv(B(h^*_{AB})))^2 \\ Eu(A) - Eu(B(h^*_{AB})) &: r[(Ev(B(h^*_{AB})))^2 - (Ev(A))^2] \end{aligned}$$

Because h^*_{AB} must be such that

$$Eu(A) + (Ev(A))^2 = Eu(B(h^*_{AB})) + (Ev(B(h^*_{AB})))^2,$$

we must have

$$Eu(A) - Eu(B(h^*_{AB})) = (Ev(B(h^*_{AB})))^2 - (Ev(A))^2.$$

Hence, if h^*_{AB} is such that $Eu(B(h^*_{AB})) > Eu(A)$, then

$$Eu(A) - Eu(B(h^*_{AB})) < r[(Ev(B(h^*_{AB})))^2 - (Ev(A))^2] < 0$$

and thus $U(C) < U(D(h^*_{AB}))$. Thus, $h^*_{CD} < h^*_{AB}$, that is, the person exhibits a CRP. Analogously, if h^*_{AB} is such that $Eu(B(h^*_{AB})) < Eu(A)$, the person exhibits an RCRP.

Proof of part (2c) and (2d): These follow directly from parts (2a) and (2b) combined with the fact that $\Delta^*_{CC} = \Delta^*_{CR} - \Delta^*_{MX}$.

■

Proposition A4: Suppose a person evaluates lotteries according to the Chew et al. functional in equation (E.7). Then:

(1) If there exists $\bar{h}$ such that both $v(M) = pv(\bar{h}) + (1-p)v(0)$ and $w(M) = pw(\bar{h}) + (1-p)w(0)$, then $h^*_{AB} = h^*_{AB'} = h^*_{CD} = \bar{h}$ and thus the person will have ⊘CRP-⊘CCP-⊘MXP.

(2) Otherwise, the person must exhibit the pattern ⊘CRP-RCCP-MXP.

Proof: For any h, $U(B'(h)) = Ev(B'(h))Ew(B'(h))$. Because $B'(h) = (1-r)A + rB$, we can rewrite this as

$$U(B'(h)) = [(1-r)Ev(A) + rEv(B(h))][(1-r)Ew(A) + rEw(B(h))].$$

Since $Ev(A)$, $Ev(B(h))$, $Ew(A)$, and $Ew(B(h))$ are all independent of r,

$$\frac{dU(B'(h))}{dr} = [Ev(B(h)) - Ev(A)][(1-r)Ew(A) + rEw(B(h))] + [(1-r)Ev(A) + rEv(B(h))][Ew(B(h)) - Ew(A)]$$

and

$$\frac{d^2U(B'(h))}{dr^2} = 2[Ev(B(h)) - Ev(A)][Ew(B(h)) - Ew(A)].$$

Proof of part (1): Suppose there exists $\bar{h}$ such that both $v(M) = pv(\bar{h}) + (1-p)v(0)$ and $w(M) = pw(\bar{h}) + (1-p)w(0)$. Because these are equivalent to $Ev(A) = Ev(B(\bar{h}))$ and $Ew(A) = Ew(B(\bar{h}))$, it immediately follows that $h^*_{AB} = \bar{h}$. In addition, these conditions also imply that $rEv(A) = rEv(B(\bar{h}))$ and $rEw(A) = rEw(B(\bar{h}))$, from which it follows that $h^*_{CD} = \bar{h}$. Finally, these conditions further imply that $\frac{dU(B'(\bar{h}))}{dr} = 0$, which implies $h^*_{AB'} = \bar{h}$. The result follows.

Proof of part (2): h^*_{AB} must satisfy $Ev(A)Ew(A) = Ev(B(h^*_{AB}))Ew(B(h^*_{AB}))$. Because $Ev(C) = rEv(A)$, $Ew(C) = rEw(A)$, $Ev(D(h^*_{AB})) = rEv(B(h^*_{AB}))$, and $Ew(D(h^*_{AB})) = rEw(B(h^*_{AB}))$, it follows that $h^*_{CD} = h^*_{AB}$ and thus the person exhibits ⊘CRP.

Given $v(x) \geqslant 0$ and $w(x) \geqslant 0$ for all x, the h^*_{AB} condition can be rewritten as

$$\frac{Ev(A)}{Ev(B(h^*_{AB}))} = \frac{Ew(B(h^*_{AB}))}{Ew(A)}.$$

If there does not exist $\bar{h}$ such that $Ev(A) = Ev(B(\bar{h}))$ and $Ew(A) = Ew(B(\bar{h}))$, then either $\frac{Ev(A)}{Ev(B(h^*_{AB}))} = \frac{Ew(B(h^*_{AB}))}{Ew(A)} > 1$ or $1 > \frac{Ev(A)}{Ev(B(h^*_{AB}))} = \frac{Ew(B(h^*_{AB}))}{Ew(A)} > 0$. In the former case, $[Ev(B(h^*_{AB})) - Ev(A)] < 0$ while $[Ew(B(h^*_{AB})) - Ew(A)] > 0$, and thus $\frac{d^2U(B'(h))}{dr^2} < 0$. In the latter case, $[Ev(B(h^*_{AB})) - Ev(A)] > 0$ while $[Ew(B(h^*_{AB})) - Ew(A)] < 0$, and thus again $\frac{d^2U(B'(h))}{dr^2} < 0$. Because $U(A) = U(B(h^*_{AB}))$ (by the definition of h^*_{AB}), $\frac{d^2U(B'(h^*_{AB}))}{dr^2} < 0$ implies $U(B'(h^*_{AB})) > U(A) = U(B(h^*_{AB}))$ for any $r \in (0,1)$, and thus $h^*_{AB'} < h^*_{AB}$, that is, the person exhibit an MXP.

Finally, because $\Delta^*_{CC} = \Delta^*_{CR} - \Delta^*_{MX}$, the combination of $\bigcirc\!\!\!\!\backslash$CRP and MXP implies RCCP.

■

E.3 Implications for Indifference Curves in a Marschak-Machina Triangle

In Section 5.3, we describe some implications of the UP model for indifference curves in a Marschak-Machina triangle. In this subsection, we derive those implications. A Marschak-Machina triangle reflects preferences over lotteries of the form $(H, q_H; M, q_M; 0, q_L)$ for fixed amounts $M > 0$ and $H > M$. To simplify notation, we sometimes denote this lottery by (q_L, q_M, q_H).

Below, we prove the following proposition:[3]

Proposition A5: Suppose a person behaves according to the utility functional in equation (E.1). For any Marschak-Machina triangle, indifference curves must show one of the following five patterns:

I1: Exactly one indifference curve is linear, with convex (mixture-loving) indifference curves to the left and concave (mixture-averse) indifference curves to the right of the linear indifference curve, and global fanning out of average slopes.

I2: All indifference curves are concave (mixture-averse), with global fanning out of average slopes.

I3: All indifference curves are convex (mixture-loving), with global fanning out of average slopes.

[3]Chew et al. (1991) describe how quadratic utility can generate three regions of indifference curves, which they label regions I, II, and III. Proposition A5 characterizes the specific ways in which these regions can appear in the UP model, which again is a special case of quadratic utility. Proposition A5 further characterizes how, under the UP model, the average slopes of indifference curves change as we move through a Marschak-Machina triangle (where average slopes are defined below between Lemmas C2 and C3).

I4: All indifference curves are convex (mixture-loving), with fanning out of average slopes to the left and constant average slopes to the right of the indifference curve that contains lottery $A \equiv (0, 1, 0)$.

I5: All indifference curves are convex (mixture-loving), with fanning out of average slopes to the left and fanning in of average slopes to the right of the indifference curve that contains lottery $A \equiv (0, 1, 0)$ (which thus has the flattest average slope).

Figure 9 in Section 5.3 depicts these five patterns of indifference curves. To help connect these five patterns of indifference curves to the seven possible patterns of behavior in Proposition 1, each panel in Figure 9 depicts the five points from our experiment (A, B, B', C, and D), where we have chosen B such that $A \sim B$. For indifference-curve patterns I2, I4, and I5, the behavioral patterns are clear from Figure 9: I2 must yield CRP-CCP-RMXP (P4), I4 must yield ⃠CRP-RCCP-MXP (P12), and I5 must yield RCRP-RCCP-MXP (P1). For indifference-curve pattern I3, it is clear that the person must have CRP and MXP, but any CC preference is possible (so behavioral patterns P2, P23, and P3 are possible). For indifference-pattern I1, the person must have CRP; but any MX preference is possible depending on whether the linear indifference curve is to the right of (as shown), is to the left of, or is the indifference containing A; and when the person has CRP and MXP (as shown), any CC preference is possible (so all behavioral patterns are possible except P1 and P12).

We prove Proposition A5 through a series of lemmas. Lemma A1 establishes that, for the more general functional in equation (E.5) for which the UP model is a special case, each indifference curve in a Marschak-Machina triangle must be linear, concave, or convex (although this lemma does not say that that all indifference curves within a given triangle must have the same shape).[4]

Lemma A1: Suppose a person behaves according to the utility functional in equation (E.5). Then each indifference curve must be linear, concave, or convex.

Proof: Suppose that X and Y are two lotteries that satisfy $U(X) = U(Y)$, and consider lottery $Z \equiv (1 - \alpha)X + \alpha Y$. Note that $\alpha \in (0, 1)$ would make Z yield a point on the line segment $\overline{XY}$, whereas $\alpha < 0$ or $\alpha > 1$ would make Z a point on the line that contains X and Y but outside the line segment $\overline{XY}$.

Given $U(Z) = Eu(Z) + (Ev(Z))(Ew(Z))$, applying usual rules for expected-utility functionals,

[4]We label an indifference curve as convex versus concave based on its shape in a Marschak-Machina triangle with q_L and q_H on the axes; given this labeling, convex (concave) indifference curves are associated with preferences being locally quasi-concave (quasi-convex). Lemma A1 is analogous to Lemma A2.1 in Chew et al. (1991).

we can rewrite this as

$$U(Z) = [(1-\alpha)Eu(X) + \alpha Eu(Y)] + [(1-\alpha)Ev(X) + \alpha Ev(Y)][(1-\alpha)Ew(X) + \alpha Ew(Y)].$$

Differentiating this twice with respect to α yields

$$\frac{d^2[U(Z)]}{d\alpha^2} = 2[Ev(Y) - Ev(X)][Ew(Y) - Ew(X)].$$

Note that $\frac{d^2[U(Z)]}{d\alpha^2}$ is independent of α, and thus there are three cases: (i) It could be that $\frac{d^2[U(Z)]}{d\alpha^2} = 0$, in which case $U(Z) = U(X) = U(Y)$ for all α. (ii) It could be that $\frac{d^2[U(Z)]}{d\alpha^2} < 0$, in which case $U(Z) > U(X) = U(Y)$ for all $\alpha \in (0,1)$ and $U(Z) < U(X) = U(Y)$ for all $\alpha < 0$ and $\alpha > 1$. (iii) It could be that $\frac{d^2[U(Z)]}{d\alpha^2} > 0$, in which case $U(Z) < U(X) = U(Y)$ for all $\alpha \in (0,1)$ and $U(Z) > U(X) = U(Y)$ for all $\alpha < 0$ and $\alpha > 1$.

If case (i) holds, it immediately follows that the indifference curve containing X and Y is linear. Moreover, from case (i), it also follows that if an indifference curve is anywhere linear, then it must be everywhere linear. Given this latter point, the combination of cases (ii) and (iii) imply that all nonlinear indifference curves must be concave or convex. To see this, note that if an indifference curve had both convex and concave regions, then there must be an X and Y that does not satisfy any of cases (i), (ii), and (iii) (given that indifference curves are continuous), which would be a contradiction.

While the above completes the proof of Lemma A1, note that it further follows that if an X and Y satisfy case (i), then the indifference curve that contains X and Y is linear; if an X and Y satisfy case (ii), then the indifference curve that contains X and Y is convex; and (iii) if an X and Y satisfy case (iii), then the indifference curve that contains X and Y is concave.

■

Lemma A2 establishes that for the UP model in equation (E.1), there is a simple condition to check the shape of an indifference curve:

Lemma A2: Suppose a person behaves according to the utility functional in equation (E.1). If lottery $X \equiv (q_L, q_M, q_H)$ and lottery $Y \equiv (p_L, p_M, p_H)$ have $U(X) = U(Y)$, $p_H > q_H$ and $q_M + q_H > p_M + p_H$,[5] then:

(1) If $\frac{\kappa(M)}{\kappa(H)} = \frac{p_H - q_H}{q_M - p_M}$, the indifference curve through X and Y is linear.

[5]Note that $U(X) = U(Y)$ and $p_H > q_H$ together imply $q_M + q_H > p_M + p_H$, because otherwise X would FOSD Y, and the UP model respects FOSD.

(2) If $\dfrac{\kappa(M)}{\kappa(H)} < \dfrac{p_H - q_H}{q_M - p_M}$, the indifference curve through X and Y is convex.

(3) If $\dfrac{\kappa(M)}{\kappa(H)} > \dfrac{p_H - q_H}{q_M - p_M}$, the indifference curve through X and Y is concave.

Proof: If $v(x) = I(x > 0)$ and $w(x) = I(x > 0)\kappa(x)$, then $Ev(X) = q_M + q_H$, $Ev(Y) = p_M + p_H$, $Ew(X) = q_M\kappa(M) + q_H\kappa(H)$, and $Ew(Y) = p_M\kappa(M) + p_H\kappa(H)$. Applying the equation from the proof of Lemma A1,

$$\begin{aligned}\frac{d^2[U(Z)]}{d\alpha^2} &= 2[Ev(Y) - Ev(X)][Ew(Y) - Ew(X)] \\ &= 2[(p_M + p_H) - (q_M + q_H)][(p_M - q_M)\kappa(M) + (p_H - q_H)\kappa(H)].\end{aligned}$$

Because $[(p_M + p_H) - (q_M + q_H)] < 0$, $p_H > q_H$, and $q_M > p_M$, it follows that the sign of $\frac{d^2[U(Z)]}{d\alpha^2} > 0$ depends on how $\frac{\kappa(M)}{\kappa(H)}$ compares to $\frac{p_H - q_H}{q_M - p_M}$. Specifically:

- If $\frac{\kappa(M)}{\kappa(H)} = \frac{p_H - q_H}{q_M - p_M}$, then $\frac{d^2[U(Z)]}{d\alpha^2} = 0$ and we are in case (i) from the proof of Lemma A1, and thus the indifference curve through X and Y is linear.
- If $\frac{\kappa(M)}{\kappa(H)} < \frac{p_H - q_H}{q_M - p_M}$, then $\frac{d^2[U(Z)]}{d\alpha^2} < 0$ and we are in case (ii) from the proof of Lemma A1, and thus the indifference curve through X and Y is convex.
- If $\frac{\kappa(M)}{\kappa(H)} > \frac{p_H - q_H}{q_M - p_M}$, then $\frac{d^2[U(Z)]}{d\alpha^2} > 0$ and we are in case (iii) from the proof of Lemma A1, and thus the indifference curve through X and Y is concave.

■

We next introduce notation to talk about the slope of the line segment that connects two lotteries in a Marschak-Machina triangle, which will be useful for evaluating the criterion in Lemma A2, and also for evaluating whether the average slopes of indifference curves are fanning in versus fanning out.

Consider two lotteries $X \equiv (q_L, q_M, q_H)$ and $Y \equiv (p_L, p_M, p_H)$ with $p_H > q_H$ and $q_M + q_H > p_M + p_H$ (and thus $q_M > p_M$ and $p_L > q_L$). Denote the slope of the line segment $\overline{XY}$ by $m(\overline{XY})$, and note that

$$m(\overline{XY}) = \frac{p_H - q_H}{p_L - q_L} = \frac{p_H - q_H}{(q_M - p_M) - (p_H - q_H)}.$$

The critical value in Lemma A2 can then be written as $(p_H - q_H)/(q_M - p_M) = m(\overline{XY})/(m(\overline{XY}) + 1)$, which is increasing in $m(\overline{XY})$. It follows that the steeper (flatter) the line segment $\overline{XY}$, the more likely it is that the indifference curve containing X and Y is convex (concave).

Hence, a natural way to characterize the shape of indifference curves as we move through a Marschak-Machina triangle is to evaluate the slopes of line segments connecting indifferent points on

the edges of the triangle, which reflect the average slopes of indifference curves. Hence, we introduce notation for such lotteries. For a fixed M and H (i.e., for a particular Marschak-Machina triangle):

- Define $A \equiv (0, 1, 0)$, and then define p_0 and B such that $B = (1 - p_0, 0, p_0)$ and $B \sim A$. In other words, A is the vertex, and B is the indifferent point on the hypotenuse.
- For any $s \in [0, 1]$, define $C(s) \equiv (1 - s, s, 0)$, and then define $p_1(s)$ and $D(s)$ such that $D(s) = (1 - p_1(s), 0, p_1(s))$ and $D(s) \sim C(s)$. In other words, $C(s)$ is a point on the x-axis, and $D(s)$ is the indifferent point on the hypotenuse. Note that for $s = 1$, $C(s) = A$ and thus $D(s) = B$, and as $s \to 0$, both $C(s) \to (1, 0, 0)$ and $D(s) \to (1, 0, 0)$.
- For any $s \in [0, 1]$, define $E(s) \equiv (0, s, 1 - s)$, and then define $p_2(s)$ and $F(s)$ such that $F(s) \equiv (1 - p_2(s), 0, p_2(s))$ and $F(s) \sim E(s)$. In other words, $E(s)$ is a point on the y-axis, and $F(s)$ is the indifferent point on the hypotenuse. Note that for $s = 1$, $E(s) = A$ and thus $F(s) = B$, and as $s \to 0$, both $E(s) \to (0, 0, 1)$ and $F(s) \to (0, 0, 1)$.

Using this notation, Lemma A3 characterizes the slopes of line segments connecting indifferent points on the edges of the triangle.

Lemma A3: Suppose a person behaves according to the utility functional in equation (E.1). Then:

(1) For any $s' < s \leqslant 1$:

   (a) If $\kappa(M) > (p_0)^2\kappa(H)$, then for any $s' < s \leqslant 1$, $m(\overline{C(s')D(s')}) < m(\overline{C(s)D(s)})$, that is, indifference curves fan out as we move through the triangle from $\overline{AB}$ toward the lower right.

   (b) If $\kappa(M) = (p_0)^2\kappa(H)$, then for any $s' < s \leqslant 1$, $m(\overline{C(s')D(s')}) = m(\overline{C(s)D(s)})$, that is, indifference curves have the same average slope as we move through the triangle from $\overline{AB}$ toward the lower right.

   (c) If $\kappa(M) < (p_0)^2\kappa(H)$, then for any $s' < s \leqslant 1$, $m(\overline{C(s')D(s')}) > m(\overline{C(s)D(s)})$, that is, indifference curves fan in as we move through the triangle from $\overline{AB}$ toward the lower right.

(2) For any $s' < s \leqslant 1$, $m(\overline{E(s')F(s')}) > m(\overline{E(s)F(s)})$, that is, indifference curves fan out as we move through the triangle from $\overline{AB}$ toward the upper left.

Proof:

Proof of Part (1): Fix an $s \in (0, 1]$, and recall that $p_1(s)$ is the p in lottery $D(s)$. Under the UP model, $C(s) \sim D(s)$ implies $Eu(C(s)) + s^2\kappa(M) = Eu(D(s)) + (p_1(s))^2\kappa(H)$ or

$$Eu(C(s)) - Eu(D(s)) = (p_1(s))^2\kappa(H) - s^2\kappa(M).$$

Define $\alpha = s'/s$ so that $C(s') = \alpha C(s) + (1-\alpha)(1,0,0) = (1-\alpha s, \alpha s, 0)$. Also define $\tilde{D}(s'|s) = \alpha D(s) + (1-\alpha)(1,0,0) = (1-\alpha p_1(s), 0, \alpha p_1(s))$, which is the point on the hypotenuse such that $m(\overline{C(s')\tilde{D}(s'|s)}) = m(\overline{C(s)D(s)})$. Hence, if $C(s') \succ \tilde{D}(s'|s)$, then $D(s')$ must be up the hypotenuse from $\tilde{D}(s'|s)$, and thus $m(\overline{C(s')D(s')}) > m(\overline{C(s)D(s)})$. Analogously, $C(s') \prec \tilde{D}(s'|s)$ implies $m(\overline{C(s')D(s')}) < m(\overline{C(s)D(s)})$, and $C(s') \sim \tilde{D}(s'|s)$ implies $m(\overline{C(s')D(s')}) = m(\overline{C(s)D(s)})$. The comparison between $C(s')$ and $\tilde{D}(s'|s)$ is

$$\begin{aligned} Eu(C(s')) + (\alpha s)^2\kappa(M) &: Eu(\tilde{D}(s'|s)) + (\alpha p_1(s))^2\kappa(H) \\ Eu(C(s')) - Eu(\tilde{D}(s'|s)) &: \alpha^2[(p_1(s))^2\kappa(H) - s^2\kappa(M)] \\ Eu(C(s)) - Eu(D(s)) &: \alpha[(p_1(s))^2\kappa(H) - s^2\kappa(M)] \end{aligned} \tag{E.8}$$

where the last step follows from $Eu(C(s')) - Eu(\tilde{D}(s'|s)) = \alpha[Eu(C(s)) - Eu(D(s))]$.

Proof of part (1a): Suppose $\kappa(M) > (p_0)^2\kappa(H)$. Then $A \sim B$ implies

$$Eu(A) - Eu(B) = (p_0)^2\kappa(H) - \kappa(M) < 0.$$

Applying condition (E.8) for $s = 1$ and thus $p_1(s) = p_0$ and $\alpha = s'$, and recalling $C(1) = A$ and $D(1) = B$, for any $s' \in (0,1)$, the comparison between $C(s')$ and $\tilde{D}(s'|1)$ is

$$Eu(A) - Eu(B) : s'[(p_0)^2\kappa(H) - \kappa(M)].$$

Because $Eu(A) - Eu(B) = (p_0)^2\kappa(H) - \kappa(M) < 0$, $s' \in (0,1)$ implies $C(s') \prec \tilde{D}(s'|1)$ and thus $m(\overline{C(s')D(s')}) < m(\overline{AB})$. Also, because the probability of the high outcome in $\tilde{D}(s'|1)$ is $s'p_0$, the combination of equation (E.4) and $C(s') \prec \tilde{D}(s'|1)$ implies

$$Eu(C(s')) - Eu(\tilde{D}(s'|1)) < (s'p_0)^2\kappa(H) - (s')^2\kappa(M) < 0,$$

where the first inequality follows from $C(s') \prec \tilde{D}(s'|1)$ and the second follows from $(p_0)^2\kappa(H) - \kappa(M) < 0$. Because it further must be that $p_1(s') < s'p_0$ in order to make $D(s') \sim C(s')$, it must also be that $(p_1(s'))^2\kappa(H) - (s')^2\kappa(M) < 0$. It follows that for any $s' \in (0,1)$,

$$Eu(C(s')) - Eu(D(s')) = (p_1(s'))^2\kappa(H) - (s')^2\kappa(M) < 0.$$

Finally, swapping s' for s in the prior statement, given that each of these terms is negative, the result follows directly from applying condition (E.8) to any pair $s \in (0,1]$ and $s' \in (0,s)$.

Proof of part (1b): If $\kappa(M) = (p_0)^2\kappa(H)$, then $Eu(A) - Eu(B) = (p_0)^2\kappa(H) - \kappa(M) = 0$. Because $A = C(1)$ and $B = D(1)$, condition (E.8) implies that, for any $s' \in (0,1)$, we have $C(s') \sim \tilde{D}(s'|1)$,

and thus $m(\overline{C(s')D(s')}) = m(\overline{AB})$. The result follows.

Proof of part (1c): The proof is analogous to the proof for part (1a). Specifically, $\kappa(M) < (p_0)^2\kappa(H)$ implies that $Eu(A) - Eu(B) = (p_0)^2\kappa(H) - \kappa(M) > 0$, which in turn implies that, for all $s' \in (0,1)$, we must have $m(\overline{C(s')D(s')}) > m(\overline{AB})$ and also $Eu(C(s')) - Eu(D(s')) = (p_1(s'))^2\kappa(H) - (s')^2\kappa(M) > 0$. Finally, given that each of these terms is positive, the result follows directly from applying condition (E.8) to any pair $s \in (0,1]$ and $s' \in (0,s)$.

Proof of part (2): Fix an $s \in (0,1]$, and recall that $p_2(s)$ is the p in lottery $F(s)$. Under the UP model, $E(s) \sim F(s)$ implies $Eu(E(s)) + (1)(s\kappa(M) + (1-s)\kappa(H)) = Eu(F(s)) + (p_2(s))^2\kappa(H)$ or

$$Eu(E(s)) - Eu(F(s)) = (p_2(s))^2\kappa(H) - s\kappa(M) - (1-s)\kappa(H).$$

Define $\alpha = s'/s$ so that $E(s') = \alpha E(s) + (1-\alpha)(0,0,1) = (0, \alpha s, \alpha(1-s) + (1-\alpha))$. Also define $\tilde{F}(s'|s) = \alpha F(s) + (1-\alpha)(0,0,1) = (\alpha(1-p_2(s)), 0, \alpha p_2(s) + (1-\alpha))$, which is the point on the hypotenuse such that $m(\overline{E(s')\tilde{F}(s'|s)}) = m(\overline{E(s)F(s)})$. Hence, if $E(s') \succ \tilde{F}(s'|s)$, then $F(s')$ must be up the hypotenuse from $\tilde{F}(s'|s)$, and thus $m(\overline{E(s')F(s')}) > m(\overline{E(s)F(s)})$. We have

$$\begin{aligned} U(E(s')) &= \alpha Eu(E(s)) + (1-\alpha)u(H) + \alpha s\kappa(M) + \alpha(1-s)\kappa(H) + (1-\alpha)\kappa(H) \\ U(\tilde{F}(s'|s)) &= \alpha Eu(F(s)) + (1-\alpha)u(H) + (\alpha p_2(s) + (1-\alpha))^2\kappa(H) \end{aligned}$$

Hence, substituting $\alpha[Eu(E(s)) - Eu(F(s))] = \alpha[(p_2(s))^2\kappa(H) - s\kappa(M) - (1-s)\kappa(H)]$,

$$\begin{aligned} U(E(s')) - U(\tilde{F}(s'|s)) &= (1-\alpha)\kappa(H) - (\alpha p_2(s) + (1-\alpha))^2\kappa(H) + \alpha(p_2(s))^2\kappa(H) \\ &= [1 - \alpha - \alpha^2(p_2(s))^2 - 2\alpha p_2(s)(1-\alpha) - (1-\alpha)^2 + \alpha(p_2(s))^2]\kappa(H) \\ &= (1-\alpha)\alpha(1-p_2(s))^2 > 0. \end{aligned}$$

Hence, for any $s' < s \leqslant 1$, $E(s') \succ \tilde{F}(s'|s)$, and thus $m(\overline{E(s')F(s')}) > m(\overline{E(s)F(s)})$.

■

Finally, we can put it all together to prove Proposition A5:

Proof of Proposition A5: For a fixed (M,H) (i.e., for a specific Marschak-Machina triangle), find p_0 such that $A \equiv (M,1) \sim B \equiv (H,p_0)$.

If $\kappa(M) > (p_0)^2\kappa(H)$, then by Lemma A3 the average slopes of the indifference curves globally fan out, that is, get steeper as we move from the lower right to the upper left. If any indifference curve has average slope m such that $m/(m+1) = \kappa(M)/\kappa(H)$, then applying Lemma A2, that indifference curve is linear, while every indifference curve to its left must be convex and every indifference curve

to its right must be concave (pattern I1). Alternatively, if all indifference curves have slopes such that $m/(m+1) < \kappa(M)/\kappa(H)$, then by Lemma A2 all indifference curves are concave (pattern I2); and if all indifference curves have slopes such that $m/(m+1) > \kappa(M)/\kappa(H)$, then by Lemma A2 all indifference curves are convex (pattern I3).

If instead $\kappa(M) = (p_0)^2\kappa(H)$, then by Lemma A3 average slopes of the indifference curves fan out to the left and are constant to the right of the indifference curve that contains lottery A. Moreover, because $\kappa(M) = (p_0)^2\kappa(H)$ implies $\kappa(M) < p_0\kappa(H)$, it follows from Proposition A1 part (2b) that the indifference curve that contains lottery A is convex. Since all other indifference curves have average slopes that are at least as large as that for this indifference curve, and by Lemma A2 steeper average slopes are more likely to be convex, it follows that every indifference curve must be convex.

Finally, $\kappa(M) < (p_0)^2\kappa(H)$, then by Lemma A3 average slopes of the indifference curves fan out to the left and are fan in to the right of the indifference curve that contains lottery A, and thus this indifference curve has the flattest slope. Moreover, because $\kappa(M) < (p_0)^2\kappa(H)$ implies $\kappa(M) < p_0\kappa(H)$, it follows from Proposition A1 part (2b) that the indifference curve that contains lottery A is convex. Since all other indifference curves with larger average slopes, it again follows from Lemma A2 that every indifference curve must be convex.

■

E.4 Explaining Certainty Equivalents for Binary Gambles

A reliable empirical finding in the experimental literature on risky choice is that, when eliciting certainty equivalents for binary lotteries—i.e., an m such that $(m, 1) \sim (H, p)$—mean certainty equivalents indicate risk aversion ($m < pH$) for larger p but risk tolerance ($m > pH$) for smaller p (see, e.g., Tversky and Kahneman, 1992). In this appendix, we demonstrate that the UP model with an S-shaped κ function similar to the one we estimate can naturally generate this pattern.[6]

Under equation (2) with $u(x) = x$, the certainty equivalent C for a binary lottery (X, q) solves

$$C + \kappa(C) = qX + q^2\kappa(X).$$

[6]Note that our experiment did not consider probabilities below 0.3, which is the typical domain in which risk seeking is observed. Indeed, none of our aggregate results for a given (p, r) combination show risk tolerance. As a result, the specific estimates of our κ functions are not calibrated to capture the changing pattern of risk attitudes across probabilities that is typically observed in the literature. Instead, we consider whether functions with similar shapes could generate the behavioral patterns generally.

Figure E.1: Comparing $\kappa(qX)$ to $q^2\kappa(X)$

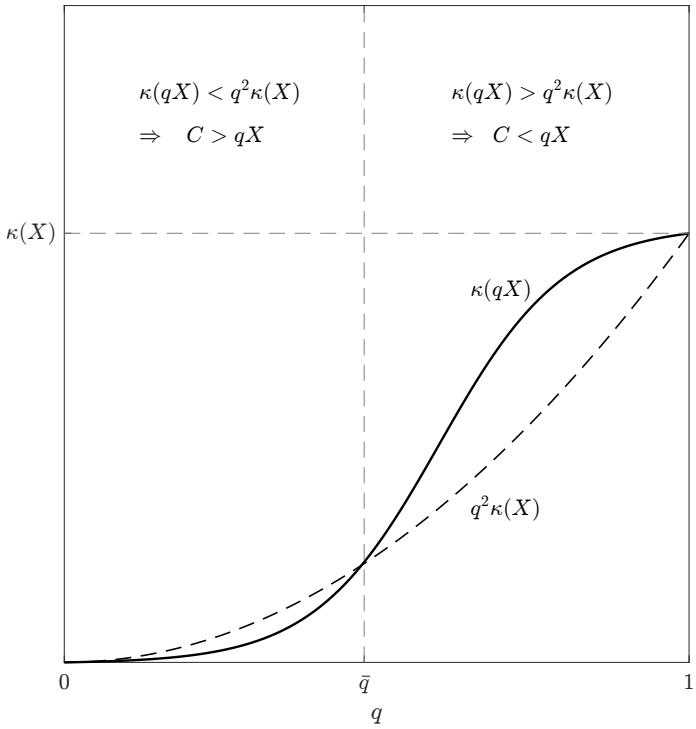

Notes: Figure plots $\kappa(qX)$ and $q^2\kappa(X)$ as a function of q (for a fixed X) given an S-shaped upside potential function $\kappa(x)$ for which the initial slope of $\kappa(qX)$ is flatter than that of $q^2\kappa(X)$. Under the UP model, the certainty equivalent C will exhibit risk tolerance ($C > qX$) when $\kappa(qX) < q^2\kappa(X)$, which occurs for probabilities $q < \bar{q}$, and risk aversion ($C < qX$) when $\kappa(qX) > q^2\kappa(X)$, which occurs for probabilities $q > \bar{q}$.

Thus, an individual will be risk tolerant, $C > qX$, if and only if[7]

$$\kappa(qX) < q^2\kappa(X).$$

If κ is S-shaped, with initial convexity followed by concavity, and if the initial slope is flatter than that of $q^2\kappa(X)$, there can naturally emerge a $\bar{q}$ such that $\kappa(qX) < q^2\kappa(X)$ for $q < \bar{q}$, and $\kappa(qX) > q^2\kappa(X)$ for $q > \bar{q}$ (as illustrated in Figure E.1). If so, then the model would indeed generate risk tolerance for small q ($q < \bar{q}$) and risk aversion for large q ($q > \bar{q}$). Therefore, an S-shaped κ function as suggested by Figure 8 can naturally generate the changing patterns of risk tolerance in certainty equivalents across the probability spectrum.

E.5 CRE and Equal-Expected-Value Lotteries

In Section 5.3, we describe how the UP model can generate a (noise-free) CRE for equal-expected-value lotteries only if the EU utility function u within the UP model is convex, which runs counter

[7] If $\kappa(qX) < q^2\kappa(X)$ then $qX + \kappa(qX) < qX + q^2\kappa(X)$, and thus C must be larger than qX. The only-if argument is analogous.

to usual assumptions on u. Here, we provide a proof of that result.

For any (p, r, M), if we create a CR paired-choice-task problem using $H = M/p$, then lotteries A and B have the same expected value (M), and lotteries C and D also have the same expected value (rM). A person would exhibit a (noise-free) CRE in that problem when, for that (p, r, M), their $h^*_{AB} > M/p$ (so they prefer lottery A over lottery B) and their $h^*_{CD} < M/p$ (so they prefer lottery D over lottery C).

The following proposition establishes that, in order for a person to have $h^*_{AB} > \frac{M}{p} > h^*_{CD}$, their function u must be locally convex.

Proposition A6. Suppose that h^*_{AB} and h^*_{CD} are derived from equations (E.2) and (E.4); that $u(x)$ is strictly increasing in x; and that $\kappa(x)$ is strictly increasing in x and has $\kappa(x) \geqslant 0$ for all $x > 0$. If $h^*_{AB} > \frac{M}{p} > h^*_{CD}$, then u must be locally convex, and specifically must satisfy $p(u(M/p) - u(0)) > u(M) - u(0)$.

Proof: From the proof of Proposition A.1, the h^*_{AB} condition in equation (E.2) can be rewritten as

$$\kappa(M) - p^2\kappa(h^*_{AB}) = Eu(B(h^*_{AB})) - Eu(A).$$

Analogously, the h^*_{CD} condition in equation (E.4) can be rewritten as

$$r^2\left(\kappa(M) - p^2\kappa(h^*_{CD})\right) = Eu(D(h^*_{CD})) - Eu(C).$$

If $h^*_{AB} > \frac{M}{p} > h^*_{CD}$, the person exhibits a CRP (i.e., $h^*_{AB} > h^*_{CD}$), and thus by Proposition A1 $\kappa(M) > p^2\kappa(h^*_{AB})$. Because κ is increasing, $h^*_{AB} > h^*_{CD}$ implies $\kappa(M) > p^2\kappa(h^*_{CD})$, and thus $Eu(D(h^*_{CD})) > Eu(C)$. Writing out these expected utilities yields $pru(h^*_{CD}) + (1 - pr)u(0) > rU(M) + (1-r)u(0)$. Because u is increasing and $\frac{M}{p} > h^*_{CD}$, it follows that $pru(M/p) + (1-pr)u(0) > rU(M) + (1 - r)u(0)$, and rearranging yields $p(u(M/p) - u(0)) > u(M) - u(0)$.

■

E.6 Event Splitting

In Section 6, we discuss the implications of our model for event splits—that is, how people feel when choosing between a lottery (H, p) versus a lottery $(H+z, p/2; H-z, p/2)$. Note that the second lottery is obtained from the first by splitting the "event" of a probability p of winning H into two "events", each with probability $p/2$, that maintain the expected value of the lottery. Several recent papers

(e.g., Bernheim and Sprenger (2020)) have found evidence that people dislike such splits, and one might wonder whether such evidence is inconsistent with our finding of mixture-loving preferences.

In our model, a person's preferences for or against event splitting can be determined separately from their preferences for or against mixtures. In particular, Proposition 2 demonstrated that an MXP emerges in our model due to the way that probabilities enter our model. In contrast, the following proposition establishes that preferences for or against event splitting depend on the local curvature of the function κ.

Proposition A7. Suppose a person is presented with a choice between lottery (H, p) and lottery $(H + z, p/2; H - z, p/2)$, and the person chooses based on the decision utility in equation (E.1) with $u(x) = x$. For any $(p, r) \in (0, 1)^2$:

(1) If κ is linear on domain $[H - z, H + z]$, then $(H, p) \sim (H + z, p/2; H - z, p/2)$;

(2) If κ is concave on domain $[H - z, H + z]$, then $(H, p) \succ (H + z, p/2; H - z, p/2)$; and

(3) If κ is convex on domain $[H - z, H + z]$, then $(H, p) \prec (H + z, p/2; H - z, p/2)$.

Proof: Applying equation (E.1) with $u(x) = x$, the decision-utility comparison is

$$pH + p^2\kappa(H) \quad : \quad \frac{p}{2}(H + z) + \frac{p}{2}(H - z) + p\left[\frac{p}{2}\kappa(H + z) + \frac{p}{2}\kappa(H - z)\right]$$

or

$$pH + p^2\left[\kappa(H)\right] \quad : \quad pH + p^2\left[\frac{1}{2}\kappa(H + z) + \frac{1}{2}\kappa(H - z)\right]$$

or

$$\kappa(H) \quad : \quad \frac{1}{2}\kappa(H + z) + \frac{1}{2}\kappa(H - z).$$

The result follows directly.

■

F Upside Potential Model: Estimation

This appendix presents the details of the structural estimation described in Section 5.2 for the UP model. For comparison, Appendix G.1 provides estimates of several prospect-theory specifications.

F.1 Data and General Approach

We evaluate how well alternative models can explain the observed preference patterns and their sensitivity to experimental parameters (p, r, M). As described in Section 5.2, the estimation sample contains 60 aggregate valuations: the mean responses for h_{AB}, $h_{AB'}$, and h_{CD} for each of 20 (p, r) cells (see the first three columns of Appendix Table A.2). We parameterize κ as $\kappa(x; \boldsymbol{\theta})$ and estimate $\boldsymbol{\theta}$ by nonlinear least squares using the 60 observations in the data. For each $XY \in \{AB, AB', CD\}$ and each (p, r, M) experimental parameterization, the model yields $h^*_{XY}(p, r, M; \boldsymbol{\theta})$, and we then use non-linear least squares to estimate

$$h_{XY} = h^*_{XY}(p, r, M; \boldsymbol{\theta}) + \varepsilon.$$

We assess the performance of each model using (i) its mean-squared error (MSE), (ii) its internal R^2, (iii) the correlation between the model-predicted h^*_{XY} and the observed h_{XY}, and (iv) the correlation between the model-predicted Δ^* and the observed Δ.

F.2 Estimating the Upside-Potential Model

We estimate the UP model in equation (2), where the model-implied valuations h^*_{AB}, $h^*_{AB'}$, and h^*_{CD} are defined by equations (3), (4), and (5) in the main text. To isolate the role of UP, we set $u(x) = x$, making the κ function the only object to estimate.[8]

Lacking an a priori sense of the shape of κ, we begin with a flexible functional form. In our experiment, $M \in \{9, 15, 24, 27\}$, and the observed means h range from 23.83 to 42.56 (Appendix Table A.2). Hence, we use a continuous piecewise-linear form with parameter vector $\boldsymbol{\theta} \equiv (\theta_1, \theta_2, \theta_3, \theta_4, \theta_5, \theta_6)$:

$$\kappa(x; \boldsymbol{\theta}) \equiv \begin{cases} \theta_1 x & \text{if } x \in [0, 9] \\ \kappa(9; \boldsymbol{\theta}) + \theta_2(x - 9) & \text{if } x \in [9, 15] \\ \kappa(15; \boldsymbol{\theta}) + \theta_3(x - 15) & \text{if } x \in [15, 24] \\ \kappa(24; \boldsymbol{\theta}) + \theta_4(x - 24) & \text{if } x \in [24, 27] \\ \kappa(27; \boldsymbol{\theta}) + \theta_5(x - 27) & \text{if } x \in [27, 36] \\ \kappa(36; \boldsymbol{\theta}) + \theta_6(x - 36) & \text{if } x \geqslant 36 \end{cases}$$

[8] As noted in Section 5.2, the UP model is post hoc and the experiment was not designed to identify κ. Therefore, identification relies on limited variation in (p, r) over a narrow support of values, and we urge caution in interpreting these estimates.

In our data, κ is evaluated at $x \in \{9, 15, 24, 27\}$ exactly 15 times each (i.e., for each of the four values of M). In contrast, the mean valuations we observe contain no observations in $(0, 9)$ or $(9, 15)$, only one in $(15, 24)$ and one in $(24, 27)$, and the remaining 58 in $(27, 43)$. Thus $\theta_1 - \theta_4$ primarily pin down $\kappa(9)$, $\kappa(15)$, $\kappa(24)$, and $\kappa(27)$. For $x \geqslant 27$, we permit κ to be either linear (i.e., $\theta_5 = \theta_6$) or two-part-linear with a kink at $x = 36$, where this point was chosen to roughly balance observations above and below the kink.

Appendix Table F.1 reports these two specifications: Column (1) allows a two-segment linear κ for $x \geqslant 27$, while column (2) imposes a single linear segment over this range. Appendix Figures F.1 and F.2 show, for each specification, (i) the estimated κ function, (ii) observed versus fitted h_{XY}, and (iii) observed versus fitted Δ.

Both the six- and five-parameter κ specifications fit the data well in-sample, with R^2 values above 0.75, correlations between predicted and actual h_{XY} valuations around 0.9, and correlations between predicted and actual Δ measures also around 0.9. Though the six-parameter model provides a slightly better in-sample fit for the levels of response, the five-parameter model performs slightly better in terms of correlation with the key preference measures, Δ_{CR}, Δ_{CC}, and Δ_{MX}. The six-parameter model also exhibits a slight non-monotonicity between 27 and 36 (i.e., $\hat{\theta}_5 < 0$), which we suspect is due to overfitting given limited variation across h_{XY} in this region. As Panel B of Figure F.1 shows, most observations over the range $x \in (27, 36)$ are h_{CD} responses, while for $x > 36$ we also observe h_{AB} and $h_{AB'}$. The six-parameter model can thus dedicate a parameter to fit a single type of data in the $x \in (27, 36)$ region, yielding a slightly better fit of the levels at the expense of differences. Due to this possibility of overfitting, we adopt the five-parameter model as our preferred specification.

Motivated by the S-shape in Panel A of Figure F.2, we set out to find a parsimonious and analytically tractable three-parameter functional form that could capture this essential feature of the κ function. Of those, the best-fitting version we found was the following three-parameter scaled logistic,[9] $\kappa(x; \boldsymbol{\theta})$ with $\boldsymbol{\theta} = (\theta_1, \theta_2, \theta_3)$:

$$\kappa(x; \boldsymbol{\theta}) = \theta_1 \left[\frac{1}{1 + \exp(-\theta_2(x - \theta_3))} \right], \quad \theta_1, \theta_2, \theta_3 > 0. \tag{F.1}$$

The term in brackets represents a classic two-parameter sigmoid function that goes from zero (as $x \to -\infty$) to 1 (as $x \to \infty$). θ_2 controls the steepness and θ_3 determines the inflection point, such that $\kappa(x; \boldsymbol{\theta})$ will be convex for any $x < \theta_3$ and concave for any $x > \theta_3$. Finally, θ_1 is a scale term that sets the upper asymptote.

Column (3) of Table F.1 reports estimates for the logistic specification in (F.1), while Appendix

[9] In addition to the cases described in the main text, we also explored several simple alternatives: (i) a log-over-linear shape $\theta_1\, x \log(1+\theta_2 x)/(1+\theta_3 x)$; (ii) a simple log form $\theta_1\, \log\big(1+(x/\theta_2)^{\theta_3}\big)$; (iii) a ratio of powers $(\theta_1\, x\theta_3 + 1)/(\theta_2^{\theta_3} + x^{\theta_3})$; and (iv) a double log $\theta_1\, \log\big(1 + \log(1 + (x/\theta_2)^{\theta_3})\big)$. While these alternatives can capture an S-shape, they produced a worse model fit.

Table F.1: Upside Potential Estimates

	(1) Flexible 1	(2) Flexible 2	(3) Parametric 1	(4) Parametric 2	(5) Parametric 3
θ_1	1.58	1.75	106.53	105.16	135.30
	(0.26)	(0.32)	(22.62)	(32.52)	(37.58)
θ_2	3.73	4.40	0.20	0.20	0.19
	(0.67)	(0.88)	(0.00)	(0.00)	(0.00)
θ_3	6.43	6.85	19.35	19.30	19.36
	(1.04)	(1.36)	(0.35)	(0.73)	(0.39)
θ_4	6.68	7.70		0.01	
	(1.63)	(1.63)		(0.11)	
θ_5	-0.25	1.72			
	(0.41)	(0.54)			
θ_6	6.95				
	(1.68)				
Observations	60	60	60	60	60
Degrees of Freedom	54	55	57	56	57
MSE – h_{XY} levels	2.71	3.53	6.99	6.99	7.72
R^2 – h_{XY} levels	0.82	0.76	0.52	0.52	0.47
$\rho(h_{XY}, \hat{h}_{XY})$	0.92	0.91	0.84	0.84	0.83
MSE – Δ Differences	6.15	7.58	8.20	8.15	7.51
R^2 – Δ Differences	0.66	0.58	0.55	0.55	0.59
$\rho(\Delta, \hat{\Delta})$ – Δ Differences	0.88	0.90	0.87	0.87	0.89

Notes: Non-linear least squares regressions using 60 mean values of $h_{AB}, h_{AB'}, h_{CD}$ as observations. Standard errors in parentheses. Flexible 1 is a continuous six-parameter piecewise-linear κ with knots at $x \in \{9, 15, 24, 27, 36\}$. Flexible 2 is the five-parameter version with a single linear segment for $x \geqslant 27$ (knots at $9, 15, 24, 27$). Parametric 1 is the three-parameter scaled logistic $\kappa(x; \boldsymbol{\theta}) = \theta_1 \big[1 + \exp\{-\theta_2(x - \theta_3)\}\big]^{-1}$. Parametric 2 augments Parametric 1 with a multiplicative term x^{θ_4}, yielding an unbounded specification with $\kappa(0) = 0$. Parametric 3 is a zero-anchored logistic that subtracts the value at $x = 0$ so that $\kappa(0) = 0$. R^2 values calculated as $1 - RSS/TSS$, where TSS is sum of squared deviations to the average value among the 60 observations, and RSS is the sum of squared residuals between the estimated model and the data. MSE values, R^2 values, and correlation between predicted and actual values, ρ, provided for both valuation levels (h terms) and differences (Δ terms).

Figure F.3 illustrates in-sample fit. The estimates imply substantial nonlinearity in the κ function with this simple parametric form and a reasonable overall fit (MSE = 6.99, $R^2 = 0.52$). However, imposing this functional form leads to a reduction in explanatory power for the levels of h_{XY} relative to the five-parameter piecewise model. In contrast, the correlation for the difference terms is comparable to the five-parameter model and exceeds those of the six-parameter alternative. Panel C of Figure F.3 shows that the three-parameter model tracks Δ_{CR}, Δ_{CC}, and Δ_{MX} closely across all 60 differences.

A drawback of the three-parameter scaled logistic in (F.1) is that it is bounded above by θ_1, which makes it ill-suited for global predictions and inconsistent with our non-parametric estimates.

To address this, we consider an unbounded four-parameter alternative with $\boldsymbol{\theta} \equiv (\theta_1, \theta_2, \theta_3, \theta_4)$:

$$\kappa(x; \boldsymbol{\theta}) = \theta_1 \left[\frac{x^{\theta_4}}{1 + \exp(-\theta_2(x - \theta_3))} \right], \quad \theta_1, \theta_2, \theta_3, \theta_4 > 0.$$

The multiplicative term x^{θ_4} ensures $\kappa(x) \to \infty$ as $x \to \infty$ and implies $\kappa(0) = 0$. The parameter θ_4 governs the asymptotic growth rate in the limit. We present the estimates of this specification in column (4). Despite permitting κ to be unbounded, we estimate $\theta_4 \approx 0$, which collapses to the prior specification in column (3). In other words, allowing for this additional flexibility does not improve the model fit.[10]

We also consider a zero-anchored κ function that sets $\kappa(0) = 0$. This specification captures the intuition that, in the limit, a person may regard a very small prize as effectively equivalent to no prize:

$$\kappa(x; \boldsymbol{\theta}) = \theta_1 \left[\frac{1}{1 + \exp\{-\theta_2(x - \theta_3)\}} \right] - \theta_1 \left[\frac{1}{1 + \exp\{-\theta_2(0 - \theta_3)\}} \right].$$

In this formulation, the first bracketed term is our specification from column (3). The second term subtracts off the value of the first term when it is evaluated at $x = 0$ to ensure that $\kappa(0) = 0$. Column (5) of Appendix Table F.1 presents estimates for this functional form, while Appendix Figure F.3 illustrates model fit. While this model performs reasonably well in matching the data, it underperforms the version in column (3) along all fit dimensions.

[10] We reiterate that while we find that a bounded function provides the best fit for the narrow domain that our data cover, it is unlikely to hold out-of-sample.

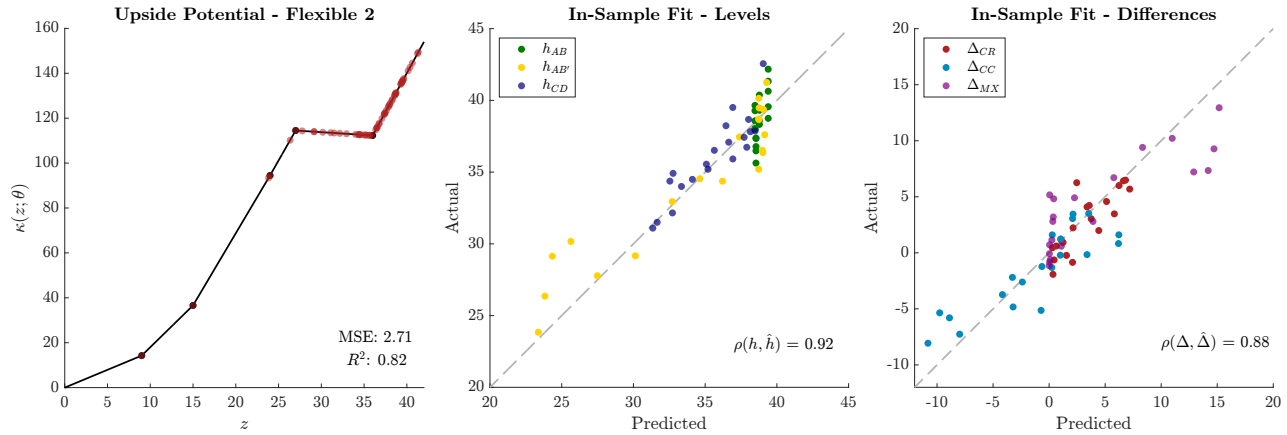

Figure F.1: Upside Potential Estimates - Flexible Six Parameter Model

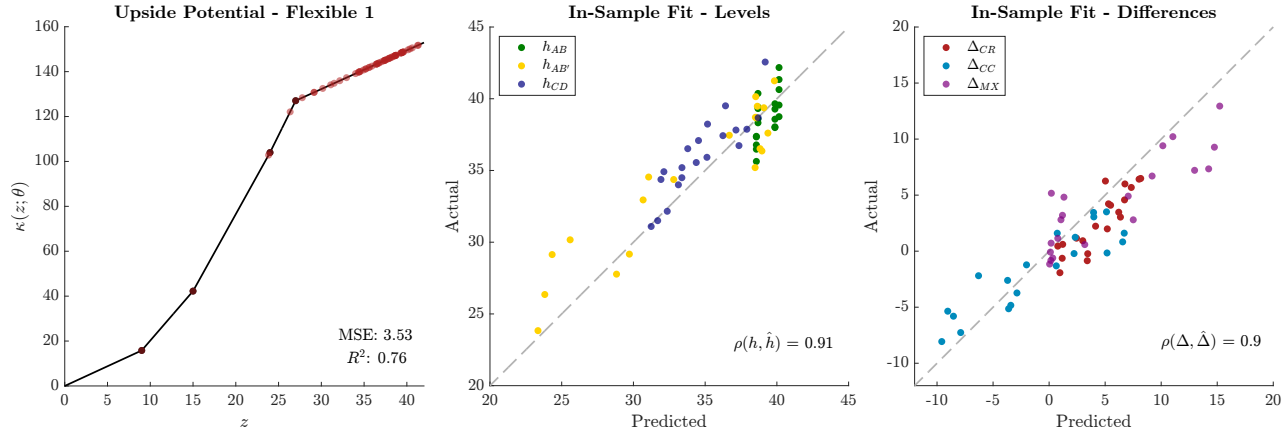

Figure F.2: Upside Potential Estimates - Flexible Five Parameter Model

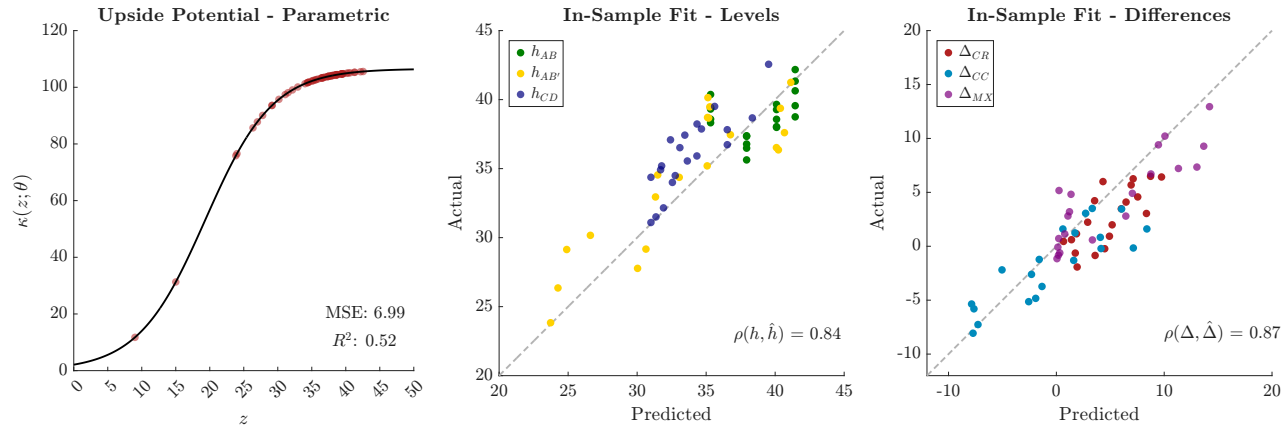

Figure F.3: Upside Potential Estimates - Parametric Functional Form

G Connections and Comparison to Prospect Theory Probability Weighting

In this appendix we provide in-sample comparison of the estimated fits between the UP model and various prospect theory formulations. Appendix G.1 shows that prospect theory fits substantially worse than upside potential even when endowed with more degrees of freedom. Appendix G.2 provides theoretical analysis establishing the distinction between the UP model and probability weighting that generates the differential fit.

G.1 Estimating Prospect-Theory Models

As a benchmark for the UP model, we also estimate several variants of prospect-theory models using the same 60 observations as used in the estimates of Appendix F.2. As in Appendix B.1, under original prospect theory (OPT) from Kahneman and Tversky (1979), a person's valuations are given by

$$h_{AB} = v^{-1}\left(\frac{1}{\pi(p)}v(M)\right), \quad h_{AB'} = v^{-1}\left(\frac{1-\pi(1-r)}{\pi(pr)}v(M)\right), \text{ and } \quad h_{CD} = v^{-1}\left(\frac{\pi(r)}{\pi(pr)}v(M)\right).$$

As in Appendix B.2, under cumulative prospect theory (CPT) as in Tversky and Kahneman (1992), a person's h_{AB} and h_{CD} valuations are as above, while their $h_{AB'}$ valuation is:

$$h_{AB'} = v^{-1}\left(\frac{1-(\pi(pr+1-r)-\pi(pr))}{\pi(pr)}v(M)\right).$$

For either version, the objects to estimate are the probability weighting function $\pi(q)$ and the value function $v(x)$.

We begin with some canonical functional forms. Specifically, we assume the value function is $v(x) = x^{\alpha}$, and we consider both the one-parameter probability weighting function from Tversky and Kahneman (1992),

$$\pi(q) = \frac{q^{\delta}}{[q^{\delta}+(1-q)^{\delta}]^{1/\delta}},$$

and the two-parameter specification from Lattimore et al. (1992),

$$\pi(q) = \frac{\gamma q^{\delta}}{\gamma q^{\delta}+(1-q)^{\delta}}.$$

Columns (1) and (2) of Appendix Table G.1 report CPT estimates for these two functional forms for $\pi(q)$, and columns (4) and (5) report the corresponding OPT estimates. Appendix Figures G.1, G.2, G.4, and G.5 depict for each specification: (i) the estimated probability weighting function; (ii)

observed versus model-predicted h_{XY}; and (iii) observed versus model-predicted Δ .

All four prospect-theory specifications have poor in-sample fit and substantially underperform the three-parameter UP model. The best fitting variant of prospect theory is CPT with the two-parameter $\pi(q)$ which has an MSE of 18.03, an R-squared of -0.23, a correlation between predicted and actual h_{XY} valuations of 0.55, and a correlation between predicted and actual Δ measures of 0.7. A negative R^2 value implies that predicting the sample mean for every response would outperform the model.

Although the PT estimates do not fit our data well overall, the estimated parameters for the one-parameter function are similar to those reported in previous studies. For example, using data on certainty equivalents for binary lotteries, Tversky and Kahneman (1992) report median estimates of $\alpha = 0.88$ and $\theta_1 = 0.61$. Likewise, Bernheim and Sprenger (2020) find $\alpha = 0.94$ and $\theta_1 = 0.72$ using similar data. In Appendix Table G.1, our estimates are $\alpha = 0.80$ and $\theta_1 = 0.84$ for CPT, and $\alpha = 0.75$ and $\theta_1 = 0.79$ for OPT.

It is perhaps not surprising that these canonical probability-weighting forms perform poorly on our data, as they were designed to generate a global CRP and CCP. We therefore assess how much better CPT and OPT perform with a more flexible specification. Specifically, we consider the following six-part piecewise-linear functional form for probability weighting:

$$\pi(q;\boldsymbol{\theta}) \equiv \begin{cases} 0 & \text{if } q = 0 \\ \theta_0 + \theta_1 q & \text{if } q \in (0, \bar{q}_1] \\ \pi(\bar{q}_1;\boldsymbol{\theta}) + \theta_2(q - \bar{q}_1) & \text{if } q \in [\bar{q}_1, \bar{q}_2] \\ \pi(\bar{q}_2;\boldsymbol{\theta}) + \theta_3(q - \bar{q}_2) & \text{if } q \in [\bar{q}_2, \bar{q}_3] \\ \pi(\bar{q}_3;\boldsymbol{\theta}) + \theta_4(q - \bar{q}_3) & \text{if } q \in [\bar{q}_3, \bar{q}_4] \\ \pi(\bar{q}_4;\boldsymbol{\theta}) + \theta_5(q - \bar{q}_4) & \text{if } q \in [\bar{q}_4, \bar{q}_5] \\ \pi(\bar{q}_5;\boldsymbol{\theta}) + \theta_6(q - \bar{q}_5) & \text{if } q \in [\bar{q}_5, 1) \\ 1 & \text{if } q = 1 \end{cases}$$

To give OPT and CPT additional flexibility, this piecewise-linear function permits (but does not require) discontinuities at $q = 0$ and $q = 1$. We select five interior knots $\{\bar{q}_i\}_{i=1}^5$ ex ante at probabilities where $\pi(\cdot)$ is most frequently evaluated, while roughly balancing observations per segment. For OPT we use $(\bar{q}_1, \ldots, \bar{q}_5) = (0.15, 0.30, 0.50, 0.70, 0.80)$ and for CPT we use $(0.15, 0.30, 0.50, 0.80, 0.90)$. This specification nests EU as a special case $\pi(q) = q$ when $\boldsymbol{\theta} = (0, 1, 1, 1, 1, 1, 1)$.

Columns (3) and (6) of Appendix Table G.1 report the flexible CPT and OPT estimates, respectively. Appendix Figures G.3 and G.6 depict the estimated probability weighting function and corresponding fit measures. For OPT, this added flexibility yields little improvement in fit—predicting the sample for every observation still outperforms the model. For CPT, this added flexibility improves

Table G.1: CPT and OPT Probability Weighting Estimates

	(1)	(2)	(3)	(4)	(5)	(6)
		CPT			**OPT**	
	Parametric 1	Parametric 2	Flexible	Parametric 1	Parametric 2	Flexible
Utility Curvature						
α	0.80	0.43	0.35	0.75	0.73	0.70
	(0.02)	(0.05)	(0.04)	(0.02)	(0.03)	(0.03)
Weighting Parameters						
θ_1	0.84	1.84	0.20	0.79	0.93	0.04
	(0.03)	(0.22)	(0.04)	(0.02)	(0.02)	(0.01)
θ_2		0.63	1.85		0.75	1.17
		(0.03)	(0.13)		(0.03)	(0.13)
θ_3			1.07			0.94
			(0.05)			(0.06)
θ_4			0.62			0.73
			(0.07)			(0.09)
θ_5			0.29			0.51
			(0.10)			(0.13)
θ_6			0.54			1.32
			(0.11)			(0.21)
θ_7			0.69			0.98
			(0.16)			(0.16)
Observations	60	60	60	60	60	60
Degrees of Freedom	58	57	52	58	57	52
h_{XY}-MSE	33.88	18.03	11.02	26.85	26.17	21.71
h_{XY}-R^2	−1.31	−0.23	0.25	−0.83	−0.78	−0.48
$\rho(h_{XY}, \hat{h}_{XY})$	−0.20	0.55	0.71	0.22	0.30	0.45
Δ-MSE	41.48	24.01	19.92	32.51	31.39	29.30
Δ-R^2	−1.28	−0.32	−0.10	−0.79	−0.73	−0.61
$\rho(\Delta, \hat{\Delta})$	−0.51	0.70	0.72	0.22	0.39	0.49

Notes: Non-linear least squares regressions for CPT and OPT using 60 mean values of $h_{AB}, h_{AB'}, h_{CD}$. Standard errors in parentheses. Parametric 1 corresponds to the one-parameter ($\theta_1 = \delta$) probability-weighting function in Tversky and Kahneman (1992). Parametric 2 corresponds to the two-parameter ($(\theta_1, \theta_2) = (\gamma, \delta)$) probability-weighting function in Lattimore et al. (1992). Flexible refers to the six-part piecewise-linear functional form, with knots at {0.15,0.3,0.5,0.8,0.9} for CPT and {0.15,0.3,0.5,0.7,0.8} for OPT. R^2 values calculated as $1 - RSS/TSS$, where TSS is sum of squared deviations to the average value among the 60 observations, and RSS is the sum of squared residuals between the estimated model and the data. Negative values indicate that predicting the mean for every observation would yield better fit than the estimated model. MSE values, R^2 values, and correlation between predicted and actual values, ρ, provided for both valuation levels, h_{XY}, and differences, Δ.

fit, roughly halving the MSE to 11.02 and producing a positive R^2 value. Nonetheless, the MSE for the best-performing CPT model is still around three times larger than our preferred UP model (which has three fewer degrees of freedom), while the R^2 is approximately three times smaller. Indeed, its

MSE is about 60 percent larger and its R^2 is about half as large as even our three-parameter UP model.

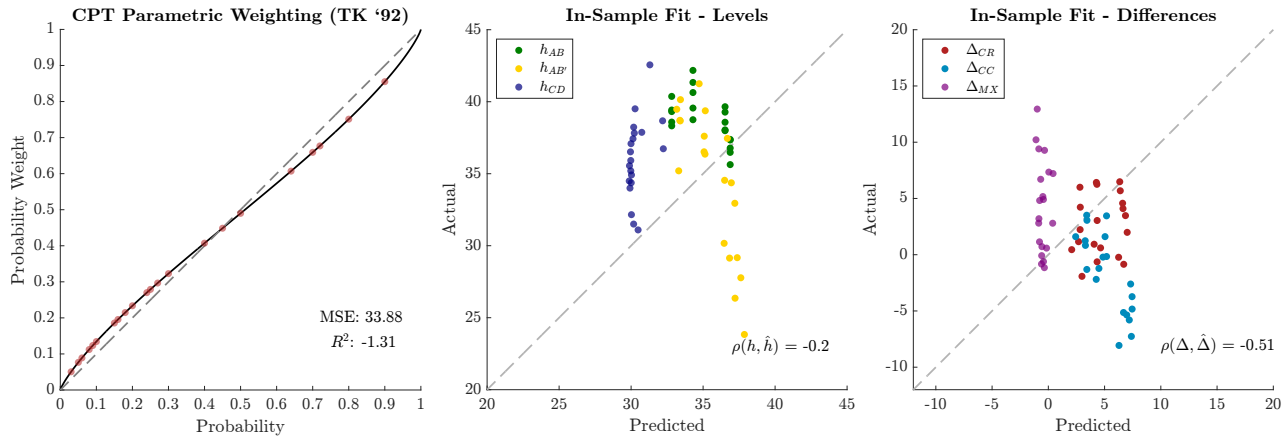

Figure G.1: CPT Probability Weighting Estimates - Parametric One Parameter Weighting Function

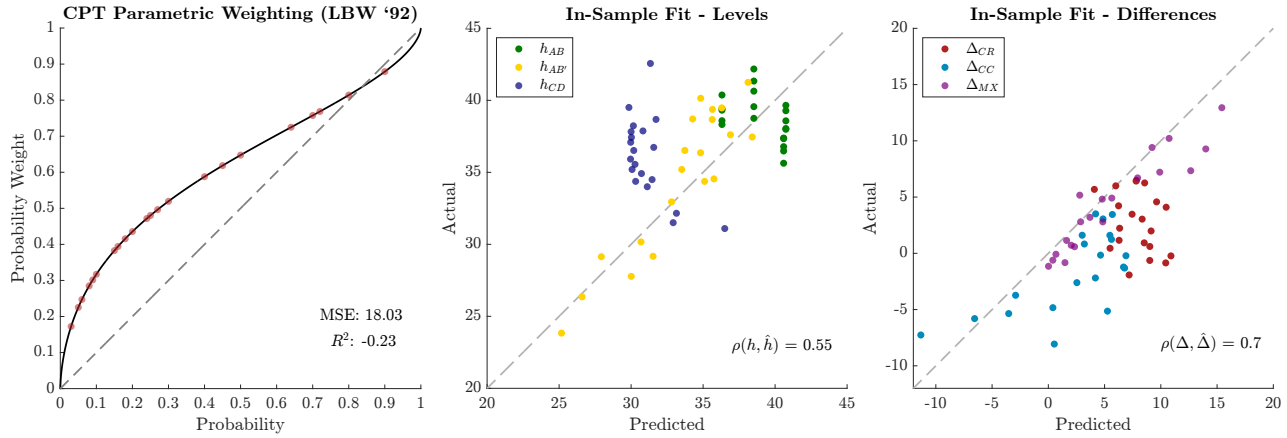

Figure G.2: CPT Probability Weighting Estimates - Parametric Two Parameter Weighting Function

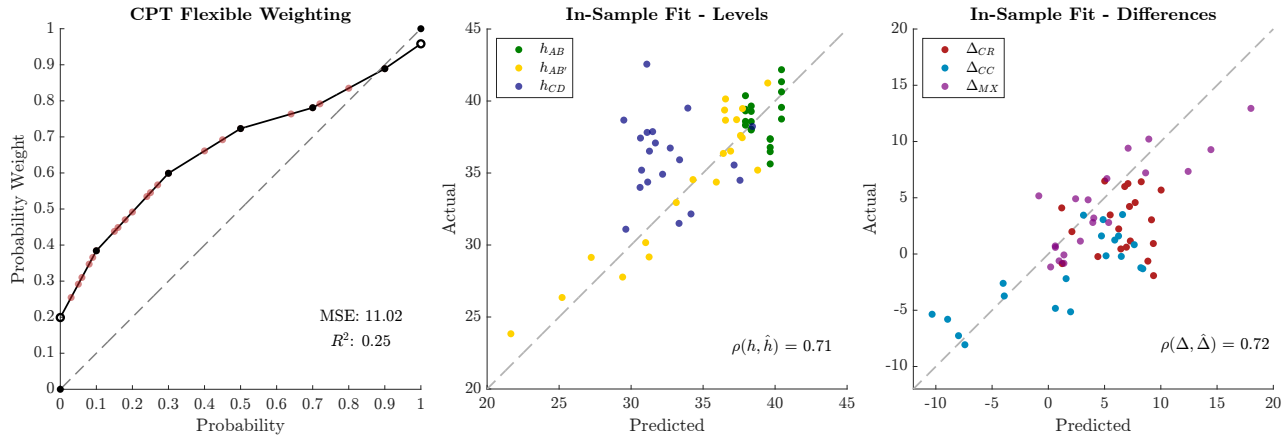

Figure G.3: CPT Probability Weighting Estimates - Flexible Functional Form

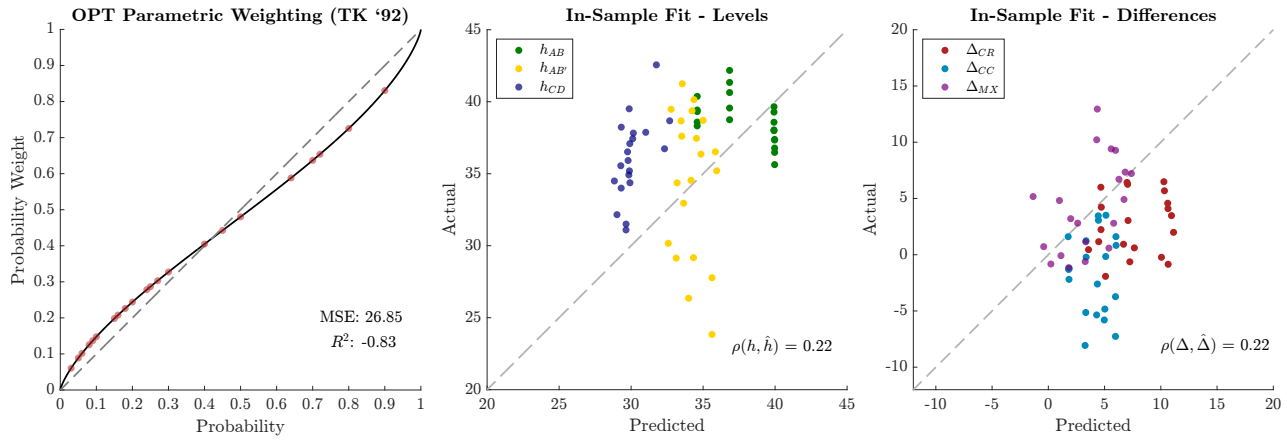

Figure G.4: OPT Probability Weighting Estimates - Parametric One Parameter Weighting Function

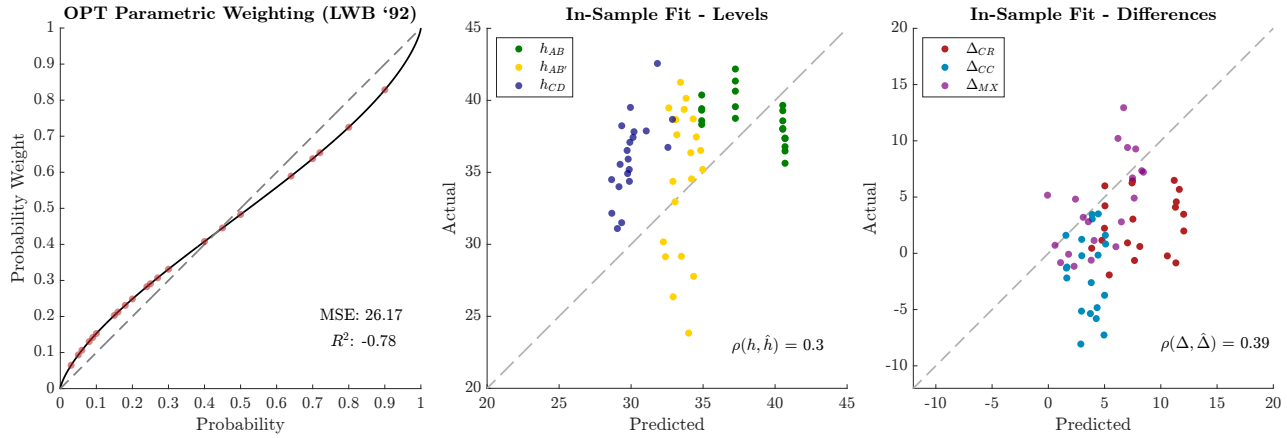

Figure G.5: OPT Probability Weighting Estimates - Parametric Two Parameter Weighting Function

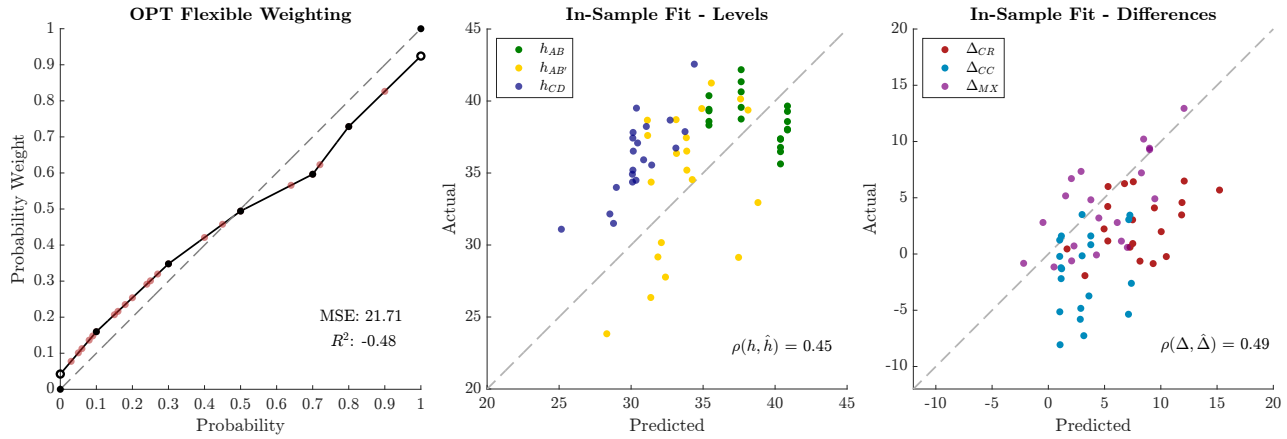

Figure G.6: OPT Probability Weighting Estimates - Flexible Functional Form

G.2 Distinguishing Upside Potential from Probability Weighting

Through Appendices F and G.1, we show that our model of upside potential provides a substantially better quantitative fit of our aggregate data than either CPT or OPT even when permitting flexible functional forms for probability weighting. In this section, we consider what properties of our model are fundamentally distinct from formulations of probability weighting which permit this improved fit.[11]

We focus on the different ways that probabilities enter into the models. Hence, throughout this section, we assume a linear κ function for our model (i.e., $\kappa(z) = \phi z$) and a linear value function for CPT or OPT (i.e., $v(z) = z$).[12]

We first assess whether either OPT or CPT with a flexible functional form for π could replicate the predictions from our UP model. Under OPT with a linear value function, the indifference values $(h^*_{AB}, h^*_{AB'}, h^*_{CD})$ are determined from:

$$\begin{aligned} M &= \pi(p)h^*_{AB} \\ M &= \pi(pr)h^*_{AB'} + \pi(1-r)M \\ \pi(r)M &= \pi(pr)h^*_{CD} \end{aligned}$$

Under CPT with a linear value function, the indifference values are determined from:

$$\begin{aligned} M &= \pi(p)h^*_{AB} \\ M &= \pi(pr)h^*_{AB'} + [\pi(pr+1-r) - \pi(pr)]M \\ \pi(r)M &= \pi(pr)h^*_{CD} \end{aligned}$$

As discussed above, OPT and CPT coincide for binary lotteries, but not for the trinary lottery B'.

Under the UP model, when $u(x) = x$ and $\kappa(z) = \phi z$, the indifference values are determined from

$$M = \frac{p + p^2\phi}{1+\phi} h^*_{AB} \tag{G.2}$$

$$M = \frac{pr + (pr+1-r)(pr)\phi}{1+\phi} h^*_{AB'} + \frac{(1-r) + (pr+1-r)(1-r)\phi}{1+\phi} M \tag{G.3}$$

$$\frac{r + r^2\phi}{1+\phi} M = \frac{pr + (pr)^2\phi}{1+\phi} h^*_{CD} \tag{G.4}$$

If we were making predictions for decisions that involve only sure amounts or binary lotteries with one winning outcome, then either OPT or CPT with probability weighting function $\pi(q) = (q + q^2\phi)/(1+\phi)$ will generate the same predictions as our UP model. This general point is reflected in the equations above by the fact that the h^*_{AB} and h^*_{CD} conditions would be the same in all three

[11] We emphasize that a comparison of prospect theory to our model on our data is apt in the sense that the probability weighting function in prospect theory was developed specifically to speak to anomalies in CR and CC problems.

[12] For CPT or OPT, adding a slope parameter to the value function would not change predictions.

models. Hence, for decisions that involve only sure amounts or binary lotteries with one winning outcome, our UP model is a special case of either OPT or CPT, and thus if we had data on only such decisions, our model could not outperform OPT or CPT.

It is for decisions that involve trinary lotteries with two winning outcomes that neither OPT nor CPT can replicate the predictions of our model. To see this under OPT, note that it would need to be the case that the weight on $h^*_{AB'}$ in equation (G.3) can be expressed purely as a function of pr, the weight on M in equation (G.3) can be expressed purely as a function of $(1-r)$, and those two functions would need to be the same. Neither of the first two conditions holds, and thus clearly the third does not as well.

To see this under CPT, note that we can rewrite the CPT condition for $h^*_{AB'}$ as

$$M = \pi(pr)\left[h^*_{AB'} - M\right] + \pi(pr + 1 - r)M$$

and the UP condition for $h^*_{AB'}$ as

$$M = \frac{pr + (pr + 1 - r)(pr)\phi}{1 + \phi}\left[h^*_{AB'} - M\right] + \frac{(pr + 1 - r) + (pr + 1 - r)^2\phi}{1 + \phi}M.$$

Here, we can match the weight on M if we use $\pi(q) = (q + q^2\phi)/(1 + \phi)$, but there is no way to express the weight on $(h^*_{AB'} - M)$ purely as a function of pr. For decisions that involve trinary lotteries, our UP model is therefore distinct from OPT and CPT even when we assume a linear κ function.

This analysis highlights a key difference between our model and OPT or CPT. For trinary lotteries, both CPT and OPT require that the weight applied to each outcome depend only on that outcome's probability (or cumulative probability in the case of CPT). For lottery B' this means the weight on the highest outcome $h^*_{AB'}$ must be a function solely of that outcome's probability, in this case pr. In contrast, under the UP model, the weight applied to outcome $h^*_{AB'}$ is a function both of pr and the total probability of winning, in this case $pr + 1 - r$. This fundamental distinction derives from the central psychology of the upside potential model: that winning probabilities can matter more the greater is the total chance of winning.

We can obtain further insights on the differences between the models by comparing the qualitative predictions for our experimental tasks of the UP model to the those of OPT or CPT when we assume probability weighting function $\pi(q) = (q + q^2\phi)/(1 + \phi)$.

Proposition 2 establishes that for linear κ, the upside potential model predicts both CRP and MXP, with no prediction for the CC preference. As described above, with probability weighting function $\pi(q) = (q + q^2\phi)/(1 + \phi)$, OPT and CPT both replicate the predictions of the UP model for the AB and CD tasks and thus both predict a CRP. Proposition A8 below establishes that OPT and CPT with this weighting function both further predict a CCP and an RMXP. In other words,

the two models would disagree on the MX preference, and might disagree on the CC preference.

Proposition A8. Suppose that $(h^*_{AB}, h^*_{AB'}, h^*_{CD})$ is derived from OPT or CPT with a linear value function and probability weighting function $\pi(q) = \frac{q+q^2\phi}{1+\phi}$. For any $(p,r) \in (0,1)^2$, we must have:

(1) $\Delta^*_{CR} > 0$;

(2) $\Delta^*_{CC} > 0$; and

(3) $\Delta^*_{MX} < 0$.

Proof: First note that part (1) follows from part (1) of Proposition 2 combined with the logic in the text that, when using $\pi(q) = \frac{q+q^2\phi}{1+\phi}$, both OPT and CPT replicate the predictions from the UP model for the AB task and the CD task.

Next, note that under both OPT and CPT, the condition for h^*_{AB} is $M = \frac{p+p^2\phi}{1+\phi} h^*_{AB}$, and thus for any $r \in (0,1)$,

$$M = r\left(\frac{p+p^2\phi}{1+\phi}\right) h^*_{AB} + (1-r)(M) = \left(\frac{pr+p^2r\phi}{1+\phi}\right)(h^*_{AB} - M) + \left(\frac{(1-r+pr)+(1-r+p^2r)\phi}{1+\phi}\right) M.$$

Consider the condition for $h^*_{AB'}$ under OPT. Define $f(h) \equiv \frac{pr+(pr)^2\phi}{1+\phi} h + \frac{(1-r)+(1-r)^2\phi}{1+\phi} M$, so under OPT, $h^*_{AB'}$ is defined by $M = f(h^*_{AB'})$. Because for any $r \in (0,1)$, $r\left(\frac{p+p^2\phi}{1+\phi}\right) > \frac{pr+(pr)^2\phi}{1+\phi}$ and $(1-r) > \frac{(1-r)+(1-r)^2\phi}{1+\phi}$, we must have $M > f(h^*_{AB})$. Since f is increasing in h, it follows that $h^*_{AB'} > h^*_{AB}$ and thus $\Delta^*_{MX} < 0$. Finally, the combination of $\Delta^*_{CR} > 0$ and $\Delta^*_{MX} < 0$ implies $\Delta^*_{CC} > 0$.

Now consider the condition for $h^*_{AB'}$ under CPT. Define

$$g(h) \equiv \left(\frac{pr+(pr)^2\phi}{1+\phi}\right)(h - M) + \left(\frac{(1-r+pr)+(1-r+pr)^2\phi}{1+\phi}\right) M,$$

so under CPT, $h^*_{AB'}$ is defined by $M = g(h^*_{AB'})$. Because for any $r \in (0,1)$, $\left(\frac{pr+p^2r\phi}{1+\phi}\right) > \frac{pr+(pr)^2\phi}{1+\phi}$ and $\left(\frac{(1-r+pr)+(1-r+p^2r)\phi}{1+\phi}\right) > \left(\frac{(1-r+pr)+(1-r+pr)^2\phi}{1+\phi}\right)$, we must have $M > g(h^*_{AB})$. Since g is increasing in h, it follows that $h^*_{AB'} > h^*_{AB}$ and thus $\Delta^*_{MX} < 0$. Finally, the combination of $\Delta^*_{CR} > 0$ and $\Delta^*_{MX} < 0$ implies $\Delta^*_{CC} > 0$.

■

Although it is not relevant for our analysis in this paper, we highlight one further distinction between our UP model and CPT. Under CPT, the weights attached to outcomes depend on their relative ranks, whereas under our UP model, they do not. To illustrate, consider a trinary lottery

$(x_1, q_1; x_2, q_2)$. Under CPT, if $x_1 > x_2 > 0$, this lottery is evaluated using $\pi(q_1)x_1 + [\pi(q_1 + q_2) - \pi(q_1)]x_2$, whereas if $x_2 > x_1 > 0$, it is evaluated using $\pi(q_2)x_2 + [\pi(q_1 + q_2) - \pi(q_2)]x_1$. Under our model with a linear κ function, for any $x_1 > 0$ and $x_2 > 0$, it is evaluated using $[1 + (q_1 + q_2)\phi]q_1x_1 + [1 + (q_1 + q_2)\phi]q_2x_2$. The weights that are applied to outcomes x_1 and x_2 under upside potential are symmetric—depending only on each outcome's probability and the total probability of winning—regardless of whether $x_1 > x_2$ or $x_2 > x_1$. This symmetry may be a valuable feature of the upside potential model given recent evidence of rank-independence in choice (Bernheim and Sprenger, 2020; Bernheim et al., 2022).

H Screenshots from the Online Experiment

OPTION A:		OPTION B:
100% CHANCE OF $24	OR	2% CHANCE OF $0 90% CHANCE OF $24 8% CHANCE OF **$24**
100% CHANCE OF $24	OR	2% CHANCE OF $0 90% CHANCE OF $24 8% CHANCE OF **$25**
100% CHANCE OF $24	OR	2% CHANCE OF $0 90% CHANCE OF $24 8% CHANCE OF **$26**
100% CHANCE OF $24	OR	2% CHANCE OF $0 90% CHANCE OF $24 8% CHANCE OF **$27**
100% CHANCE OF $24	OR	2% CHANCE OF $0 90% CHANCE OF $24 8% CHANCE OF **$28**
100% CHANCE OF $24	OR	2% CHANCE OF $0 90% CHANCE OF $24 8% CHANCE OF **$29**
100% CHANCE OF $24	OR	2% CHANCE OF $0 90% CHANCE OF $24 8% CHANCE OF **$30**
100% CHANCE OF $24	OR	2% CHANCE OF $0 90% CHANCE OF $24 8% CHANCE OF **$31**
100% CHANCE OF $24	OR	2% CHANCE OF $0 90% CHANCE OF $24 8% CHANCE OF **$32**
100% CHANCE OF $24	OR	2% CHANCE OF $0 90% CHANCE OF $24 8% CHANCE OF **$33**
100% CHANCE OF $24	OR	2% CHANCE OF $0 90% CHANCE OF $24 8% CHANCE OF **$34**

Figure H.1: Example Price List for Stage 1 AB' Valuation Task with $p = 0.8$ and $r = 0.1$

OPTION A:		OPTION B:
100% CHANCE OF $24	OR	20% CHANCE OF $0 80% CHANCE OF **$24**
100% CHANCE OF $24	OR	20% CHANCE OF $0 80% CHANCE OF **$25**
100% CHANCE OF $24	OR	20% CHANCE OF $0 80% CHANCE OF **$26**
100% CHANCE OF $24	OR	20% CHANCE OF $0 80% CHANCE OF **$27**
100% CHANCE OF $24	OR	20% CHANCE OF $0 80% CHANCE OF **$28**
100% CHANCE OF $24	OR	20% CHANCE OF $0 80% CHANCE OF **$29**
100% CHANCE OF $24	OR	20% CHANCE OF $0 80% CHANCE OF **$30**
100% CHANCE OF $24	OR	20% CHANCE OF $0 80% CHANCE OF **$31**
100% CHANCE OF $24	OR	20% CHANCE OF $0 80% CHANCE OF **$32**
100% CHANCE OF $24	OR	20% CHANCE OF $0 80% CHANCE OF **$33**
100% CHANCE OF $24	OR	20% CHANCE OF $0 80% CHANCE OF **$34**
100% CHANCE OF $24	OR	20% CHANCE OF $0 80% CHANCE OF **$35**
100% CHANCE OF $24	OR	20% CHANCE OF $0 80% CHANCE OF **$36**
100% CHANCE OF $24	OR	20% CHANCE OF $0 80% CHANCE OF **$37**

Figure H.2: Example Price List for Stage 1 AB Valuation Task with $p = 0.8$ and $r = 0.1$

OPTION A:		OPTION B:
90% CHANCE OF $0 10% CHANCE OF $24	OR	92% CHANCE OF $0 8% CHANCE OF **$24**
90% CHANCE OF $0 10% CHANCE OF $24	OR	92% CHANCE OF $0 8% CHANCE OF **$25**
90% CHANCE OF $0 10% CHANCE OF $24	OR	92% CHANCE OF $0 8% CHANCE OF **$26**
90% CHANCE OF $0 10% CHANCE OF $24	OR	92% CHANCE OF $0 8% CHANCE OF **$27**
90% CHANCE OF $0 10% CHANCE OF $24	OR	92% CHANCE OF $0 8% CHANCE OF **$28**
90% CHANCE OF $0 10% CHANCE OF $24	OR	92% CHANCE OF $0 8% CHANCE OF **$29**
90% CHANCE OF $0 10% CHANCE OF $24	OR	92% CHANCE OF $0 8% CHANCE OF **$30**
90% CHANCE OF $0 10% CHANCE OF $24	OR	92% CHANCE OF $0 8% CHANCE OF **$31**
90% CHANCE OF $0 10% CHANCE OF $24	OR	92% CHANCE OF $0 8% CHANCE OF **$32**
90% CHANCE OF $0 10% CHANCE OF $24	OR	92% CHANCE OF $0 8% CHANCE OF **$33**
90% CHANCE OF $0 10% CHANCE OF $24	OR	92% CHANCE OF $0 8% CHANCE OF **$34**
90% CHANCE OF $0 10% CHANCE OF $24	OR	92% CHANCE OF $0 8% CHANCE OF **$35**
90% CHANCE OF $0 10% CHANCE OF $24	OR	92% CHANCE OF $0 8% CHANCE OF **$36**
90% CHANCE OF $0 10% CHANCE OF $24	OR	92% CHANCE OF $0 8% CHANCE OF **$37**

Figure H.3: Example Price List for Stage 1 CD Valuation Task with $p = 0.8$ and $r = 0.1$

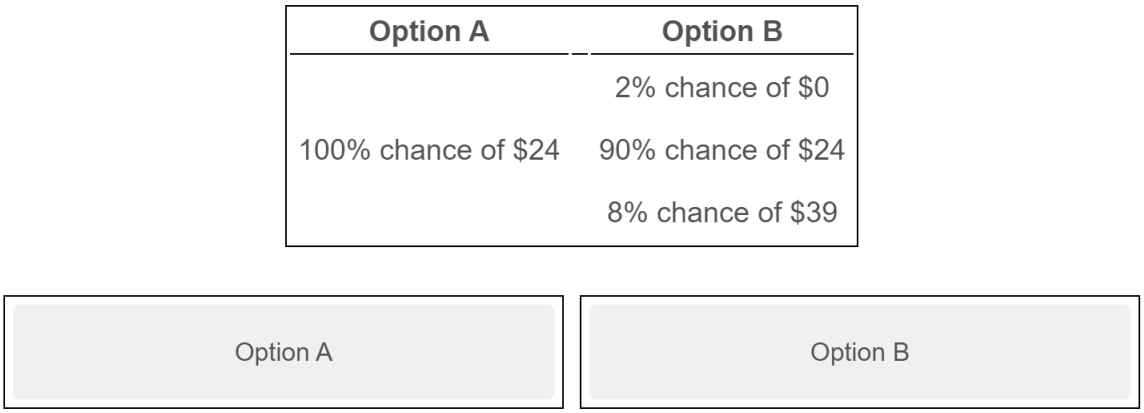

Figure H.4: Example AB' Binary Choice from Stage 2 with $p = 0.8$, $r = 0.1$, and $H = 39$

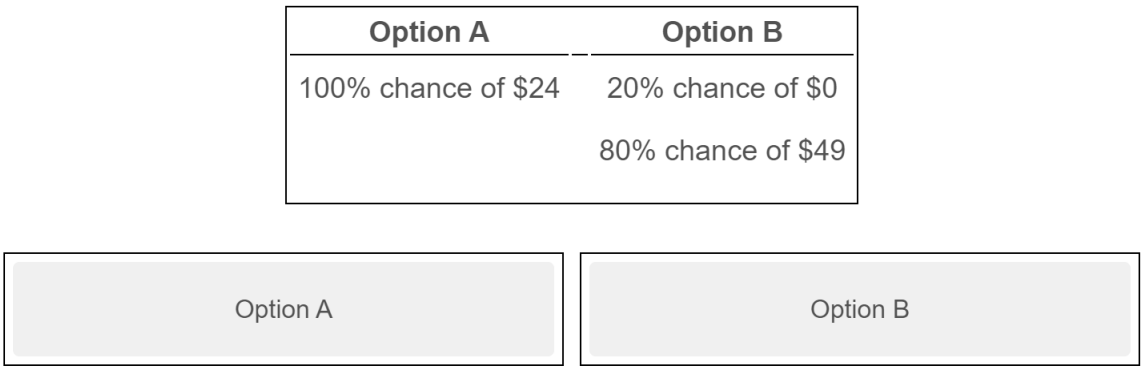

Figure H.5: Example AB Binary Choice from Stage 2 with $p = 0.8$, $r = 0.1$, and $H = 49$

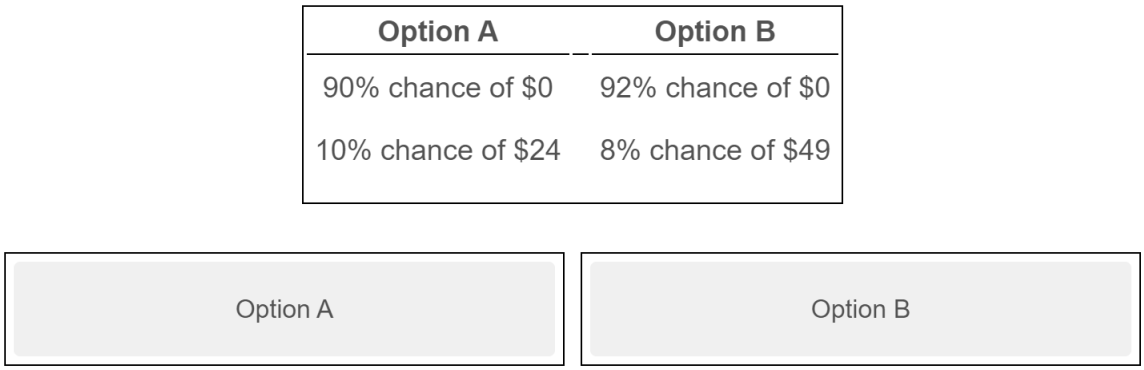

Figure H.6: Example CD Binary Choice from Stage 2 with $p = 0.8$, $r = 0.1$, and $H = 49$

Quiz Question #1:

Imagine a person who values the lottery shown in Option A below at exactly $24.50. That is, he would rather have the lottery than any sure amount less than $24.50, but would rather have the sure amount for any amount greater than $24.50.

How would this person fill out the list below?

OPTION A:		OPTION B:
25% CHANCE OF $0, 75% CHANCE OF $30	OR	100% CHANCE OF **$0**
25% CHANCE OF $0, 75% CHANCE OF $30	OR	100% CHANCE OF **$1**
25% CHANCE OF $0, 75% CHANCE OF $30	OR	100% CHANCE OF **$2**
25% CHANCE OF $0, 75% CHANCE OF $30	OR	100% CHANCE OF **$3**
25% CHANCE OF $0, 75% CHANCE OF $30	OR	100% CHANCE OF **$4**
	...	
25% CHANCE OF $0, 75% CHANCE OF $30	OR	100% CHANCE OF **$22**
25% CHANCE OF $0, 75% CHANCE OF $30	OR	100% CHANCE OF **$23**
25% CHANCE OF $0, 75% CHANCE OF $30	OR	100% CHANCE OF **$24**
25% CHANCE OF $0, 75% CHANCE OF $30	OR	100% CHANCE OF **$25**
25% CHANCE OF $0, 75% CHANCE OF $30	OR	100% CHANCE OF **$26**
25% CHANCE OF $0, 75% CHANCE OF $30	OR	100% CHANCE OF **$27**
25% CHANCE OF $0, 75% CHANCE OF $30	OR	100% CHANCE OF **$28**
25% CHANCE OF $0, 75% CHANCE OF $30	OR	100% CHANCE OF **$29**
25% CHANCE OF $0, 75% CHANCE OF $30	OR	100% CHANCE OF **$30**

Figure H.7: Incentivized Comprehension Check #1

Quiz Question #2:

Imagine a person who filled out the list like shown below.

60% CHANCE OF $0, 40% CHANCE OF $30	OR	50% CHANCE OF $0 50% CHANCE OF **$10**
60% CHANCE OF $0, 40% CHANCE OF $30	OR	50% CHANCE OF $0 50% CHANCE OF **$11**
60% CHANCE OF $0, 40% CHANCE OF $30	OR	50% CHANCE OF $0 50% CHANCE OF **$12**
60% CHANCE OF $0, 40% CHANCE OF $30	OR	50% CHANCE OF $0 50% CHANCE OF **$13**
60% CHANCE OF $0, 40% CHANCE OF $30	OR	50% CHANCE OF $0 50% CHANCE OF **$14**
60% CHANCE OF $0, 40% CHANCE OF $30	OR	50% CHANCE OF $0 50% CHANCE OF **$15**
60% CHANCE OF $0, 40% CHANCE OF $30	OR	50% CHANCE OF $0 50% CHANCE OF **$16**
60% CHANCE OF $0, 40% CHANCE OF $30	OR	50% CHANCE OF $0 50% CHANCE OF **$17**
60% CHANCE OF $0, 40% CHANCE OF $30	OR	50% CHANCE OF $0 50% CHANCE OF **$18**
60% CHANCE OF $0, 40% CHANCE OF $30	OR	50% CHANCE OF $0 50% CHANCE OF **$19**
60% CHANCE OF $0, 40% CHANCE OF $30	OR	50% CHANCE OF $0 50% CHANCE OF **$20**
60% CHANCE OF $0, 40% CHANCE OF $30	OR	50% CHANCE OF $0 50% CHANCE OF **$21**
60% CHANCE OF $0, 40% CHANCE OF $30	OR	50% CHANCE OF $0 50% CHANCE OF **$22**
60% CHANCE OF $0, 40% CHANCE OF $30	OR	50% CHANCE OF $0 50% CHANCE OF **$23**

Given these responses in the list, what would this person choose in the single decision below?

50% chance of $0 50% chance of $27	60% chance of $0 40% chance of $30

>>

Figure H.8: Incentivized Comprehension Check #2

Just for fun to take a little break: Can you spot the animal camouflaged below? Please click on the image where you think the animal is.

>>

Figure H.9: Example Visual Search Task